université PARIS-SACLAY

NNT : 2017SACLA041

Thèse de doctorat

AgroParisTech
INSTITUT DES SCIENCES ET INDUSTRIES DU VIVANT ET DE L'ENVIRONNEMENT
PARIS INSTITUTE OF TECHNOLOGY FOR LIFE, FOOD AND ENVIRONMENTAL SCIENCES

Modélisation des équilibres entre phases et simulation de la distillation des eaux-de-vie en vue d'une meilleure compréhension du comportement des composés volatils d'arôme

Thèse de doctorat de l'Université Paris-Saclay
préparée à AgroParisTech

École doctorale n°581 Agriculture, alimentation, biologie, environnement et santé (ABIES)
Spécialité de doctorat : Génie des procédés

Soutenue à Massy, le 13 décembre 2017, par

Cristian Felipe PUENTES MANCIPE

Composition du Jury :

François PUEL Professeur, CentraleSupélec	Président
Christophe COQUELET Professeur, Mines ParisTech	Rapporteur
Michel MEYER Professeur, INP-ENSIACET	Rapporteur
Martine ESTEBAN-DECLOUX Professeur, AgroParisTech	Directeur de thèse
Xavier JOULIA Professeur, INP-ENSIACET	Co-directeur de thèse
Jean-Paul VIDAL Docteur, Directeur UNGDA	Invité

A ma mère,

Qui a toujours cru en moi et m'a soutenu malgré la distance.
Elle m'a inspiré pour réaliser ce doctorat mais n'a pas pu voir son aboutissement.

REMERCIEMENTS

Cette thèse est le fruit d'une collaboration étroite entre différents acteurs académiques et industriels. Son bon déroulement au quotidien a été possible grâce à la participation d'un grand nombre de personnes. Ces lignes leur sont dédiées.

En tout premier lieu je voudrais exprimer ma gratitude à ma directrice de thèse, Martine Esteban-Decloux. Merci pour la confiance qu'elle a su placer en moi depuis la défense du projet auprès de l'école doctorale et pour m'avoir fait découvrir le domaine des eaux-de-vie. Sa rigueur, sa présence et ses qualités humaines ont été indispensables pour mener à bien cette thèse que nous tient à cœur. Merci infiniment.

Mes sincères remerciements vont à Xavier Joulia, pour avoir été un directeur de thèse *percutant*, comme dirait Martine. Merci pour son éclairage, ses remarques toujours pertinentes et sa sérénité. Pour trouver l'erreur là où je pensais que tout allait bien. Son regard externe ainsi que ses solides connaissances scientifiques nous ont permis d'exploiter les travaux de cette recherche de la meilleure manière.

Je remercie vivement les membres du jury de thèse. Christophe Coquelet et Michel Meyer, en qualité de rapporteurs, pour le temps qu'ils vont consacrer à l'évaluation de mon travail, et François Puel pour avoir accepté de présider ce jury.

Je me dois de remercier les membres du comité de thèse, Violaine Athès, Pierre Giampaoli, Patrice Paricaud et Jean-Paul Vidal. L'intérêt qu'ils ont porté au projet et leurs précieux conseils ont été d'importance capitale pour l'amener à son terme. De même, je remercie les membres du groupe distillation du RMT FIDELE, pour m'avoir fait bénéficier de leur expertise dans le domaine des eaux-de-vie.

Je tiens à remercier chaleureusement Patrice Paricaud pour m'avoir accueilli au sein de l'ENSTA ParisTech et pour avoir partagé avec moi ses connaissances en thermodynamique, reine des sciences. J'ai beaucoup appris grâce à notre collaboration et espère que nos chemins professionnels se recroiseront.

Je suis particulièrement reconnaissant à Jean-Paul Vidal, pour m'avoir ouvert les portes de l'UNGDA. Ce partenariat a été indispensable pour le bon déroulement du projet. Je remercie toute l'équipe du laboratoire pour sa gentillesse et sa bonne humeur, et tout particulièrement Stéphane Couturier, qui a suivi de près les analyses de mes échantillons. Merci pour sa disponibilité.

Ce travail n'aurait jamais été possible sans l'ouverture et la disponibilité des directeurs et en général du personnel des ateliers de distillation partenaires. Qu'ils en soient ici remerciés. Un grand merci à Marie-Claude Segur pour ses conseils et son accompagnent lors des campagnes expérimentales en Armagnac.

Bien sûr je n'oublie pas les stagiaires que j'ai encadrées de près ou de loin tout au long de ces trois années. Merci donc à Kelly, Elodie, Xuefan, Luciana et Miriam pour leur soutien dans l'analyse des

échantillons et dans l'acquisition des données d'équilibre. Leur contribution a été essentielle pour l'avancement de mes travaux.

Je souhaite aussi adresser mes remerciements à l'Ecole Doctorale ABIES, pour avoir financé ce doctorat. Ses directeurs, Alexandre Pery et Irina Vassileva, mènent tous les jours un travail exceptionnel d'accompagnement et de formation des doctorants.

Je remercie également tous les membres l'équipe CaliPro. Bien que l'on n'ait pas pu partager beaucoup de moments ensemble, je suis reconnaissant de votre accueil chaleureux et de vos gentilles paroles au quotidien. Un remerciement tout particulier à Nicolas Descharles, pour son aide précieuse lors des analyses, et à Colette pour sa gentillesse et son aide dans les démarches administratives.

Je ne peux oublier de mentionner mes professeurs de mon *alma mater*, l'Université Nationale de Colombie. Ils ont grandement contribué à ma formation académique, sans laquelle je n'aurais pu arriver à cette étape. Une pensée particulière pour Pedro Bejarano et pour Kristian Rios, deux hommes avec une fine connaissance des opérations de séparation. Ils m'auront appris les premiers notions sur la distillation (*the workhorse* des industies chimiques, comme ils avaient l'habitude de l'appeler) et m'auront transmis leur passion pour le génie chimique. J'espère avoir été à la hauteur avec ce doctorat.

Merci à mes amis de Paris, pour leurs encouragements et tous les bons moments que l'on a partagés ensemble. Venant d'horizons différents, j'ai pu découvrir grâce à eux une autre facette de la vie dans cette ville que j'aime tant.

Toute ma gratitude va à Yannick pour son amitié inconditionnelle depuis déjà cinq ans. Je ne pourrais jamais le remercier assez. Merci pour son soutien dans les moments difficiles, pour les bons repas qui ont rendu plus agréables mes longues journées de rédaction. Pour m'avoir accueilli quand j'avais envie de retourner en Normandie et changer un peu d'air. Ça y est, j'ai fini de rédiger ma thèse, on pourra aller se promener à Varengeville.

Pour finir, je remercie ma petite famille et mes amis en Colombie. Merci à eux pour leur soutien immuable et pour l'amour qu'ils m'ont toujours accordé dans la distance.

Gracias de todo corazón

VALORISATION DES TRAVAUX DE RECHERCHE

ARTICLES

1. **Puentes C.,** Paricaud P., Joulia X., Giampaoli P., Athès V., Esteban-Decloux M. Vapor-liquid equilibrium (VLE) of ethyl lactate highly diluted in ethanol -water mixtures at 101.3 kPa. Experimental measurements and thermodynamic modeling using semi-empirical models. Journal of Chemical Data. *Soumise en août 2017*.
2. **Puentes C**., Joulia X., Athès V., Esteban-Decloux M. Review and thermodynamic modeling with NRTL model of vapor-liquid equilibria (VLE) of aroma compounds highly diluted in ethanol - water mixtures at 101.3 kPa. Industrial & Engineering Chemistry Research. *Soumise en septembre 2017*.
3. **Puentes C.**, Joulia X., Vidal J.-P, Esteban-Decloux M. Simulation of continuous distillation of Spirits for a better understanding of aroma compounds behavior: Application to Armagnac production. Food and Bioproducts Processing. *A soumettre avant fin 2017.*
4. **Puentes C**., Paricaud P., Joulia X., Esteban-Decloux M. Predictive thermodynamic modeling of vapor-liquid equilibria (VLE) for aroma compounds highly diluted in ethanol-water mixtures at 101.33 kPa using COSMO and UNIFAC models. Fluid Phase Equilibria. *A soumettre avant fin 2017*.

COMMUNICATIONS ORALES OU PAR POSTER DANS DES CONGRÈS

1. **Puentes C.,** Esteban-Decloux M., Paricaud P. Génération et cohérence de données d'équilibre thermodynamique en vue de la simulation des unités de distillation des eaux-de-vie. Journée technique de la Société Française de Génie des Procédés (SFGP). Sujet : Données thermodynamiques, production, cohérence et impact sur la conception des procédés industriels. IFP Energies nouvelles. 1 avril 2016. Rueil-Malmaison, France. (Poster).
2. **Puentes C.**, Esteban-Decloux M., Paricaud P. 2016. Generation and thermodynamic modelling of vapor-liquid equilibria data for aroma compounds in hydroalcoholic mixtures - Application to the simulation of spirits distillation units. 14th PPEPPD. International conference on properties and phase equilibria for product and process design (Conférence internationale sur les propriétés thermodynamiques et les équilibres entre phases pour la conception des produits et des procédés). 22-26 mai 2016. Porto, Portugal. (Poster).
3. **Puentes C.**, Joulia X., Paricaud P., Giampaoli P., Athès V., Guichard H., Ségur M.-C., Vidal J.-P, Esteban-Decloux M. Simulation of aroma compound behaviour during Spirits distillation. Symposium on sensory evaluation of wine and spirits (Colloque sur l'évaluation sensorielle de vins et eaux-de-vie). 20 octobre 2016. Massy, France. (Oral).
4. **Puentes C.**, Joulia X., Paricaud P., Giampaoli P., Athès V., Ségur M.-C., Vidal J.-P, Esteban-Decloux M. Le génie des procédés peut-il dévoiler les secrets de la distillation des eaux-de-vie traditionnelles ? Colloque RMT-ACTIA. L'agroalimentaire durable. 26 janvier 2017. Paris, France. (Oral).

5. **Puentes C.**, Joulia X., Paricaud P., Athès V., Giampaoli P., Esteban-Decloux M. Distillation of spirits: from thermodynamic modelling to process simulation. 16ème congrès de la Société Française de Génie des Procédés (SFGP). 11-13 juillet 2017. Nancy, France. (Oral)
6. **Puentes C.**, Joulia X., Paricaud P., Athès V., Giampaoli P., Douady A., Esteban-Decloux M. 2017. Process engineering applied to distillation of fruit brandies. 10th World Congress of Chemical Engineering (10ème Congrès Mondial de Génie Chimique). 1-5 octobre 2017. Barcelone, Espagne. (Poster).

TABLE DES MATIÈRES

INTRODUCTION GENERALE

La filière des spiritueux englobe toutes les boissons alcoolisées produites par distillation, par macération ou par infusion de matières premières agricoles. Les activités économiques de production et distribution au sein de cette filière sont génératrices d'emploi et constituent une source importante de recettes fiscales pour de nombreux gouvernements [International Center for Alcohol Policies, 2006 ; Institute of Alcohols Studies, 2016]. En France, la production annuelle de spiritueux est de 6 millions d'hectolitres. Cette filière participe favorablement à la balance commerciale du pays, avec un chiffre d'affaires correspondant à environ 2% du chiffre du secteur agro-alimentaire français et à 8% des exportations de ce secteur [FSS, 2017].

Parmi les produits de cette filière, les eaux-de-vie sont des boissons issues d'un procédé comportant la fermentation alcoolique de différentes matières premières puis la distillation des moûts fermentés. Des étapes de vieillissement et d'assemblage complètent l'élaboration des produits commercialisés. La qualité des eaux-de-vie est un paramètre essentiel dans la conduite et la maîtrise de leur fabrication. La définition de cette qualité est complexe car elle est intimement liée à la composition de l'eau-de-vie, mais également à son évolution tout au long de la chaîne de production, depuis la sélection de terroirs et le travail du sol jusqu'à la mise en bouteille [Cantagrel et al., 1990].

Du point du vue chimique, une eau-de-vie est constituée d'une matrice hydroalcoolique avec un très grand nombre de composés volatils d'arôme à faibles concentrations. Ces espèces peuvent avoir un impact positif ou négatif sur les propriétés organoleptiques du produit selon leur concentration et leur seuil de perception, mais également en fonction de la présence d'autres composés. Il s'agit d'un phénomène complexe, à tel point que les composés à l'état de traces, avec les plus bas seuils de perception, peuvent avoir un impact plus important que les composés à forte concentration. D'autre part, tandis que certains composés peuvent avoir un effet positif à basses teneurs, leur comportement peut devenir opposé lorsque leurs concentrations dépassent certains niveaux, ajoutant des notes d'arôme non désirables [MacNamara et al., 2010 ; Welcker et al., 2014]. Des études analytiques ont démontré que les eaux-de-vie françaises, dont l'Armagnac, le Calvados et le Cognac, ont globalement des compositions très proches. Toutefois, leurs propriétés organoleptiques sont très différentes en raison des légères variations de concentration des composés volatils [Ledauphin et al., 2010]. La composition en composés volatils d'arôme résulte de la combinaison de différents facteurs dont la nature et le traitement des matières premières, mais surtout des transformations ayant lieu lors des phases de fermentation, distillation et vieillissement [Ng, 2002 ; Dragone et al., 2009 ; MacNamara et al., 2010].

L'étape de distillation joue un rôle important sur la composition finale en composés volatils d'arôme. Outre la concentration en éthanol dans le distillat, un triple but concernant les composés volatils d'arôme est recherché : (i) extraction des espèces favorables ou marqueurs de qualité, (ii) élimination des espèces indésirables ou marqueurs de défaut et enfin (iii) génération de nouveaux composés volatils d'arôme, avec un impact sur la qualité, par le biais de réactions chimiques [Cantagrel et al., 1990]. Malgré le fait que cette opération soit pratiquée depuis plusieurs siècles, sa conduite s'appuie essentiellement sur des connaissances empiriques, sans qu'il existe une véritable compréhension du comportement des composés volatils d'arôme. Ceci empêche la mise en place d'adaptations ou d'améliorations pour faire face aux enjeux de qualité et de durabilité imposés par l'industrie du XXI^{ème} siècle.

En France, la production des eaux-de-vie traditionnelles est basée sur deux méthodes de distillation : (i) distillation continue avec reflux dans des colonnes multiétagées et (ii) distillation discontinue dans des alambics simples ou multiétagés. Toutes les unités opèrent à pression atmosphérique. Le **tableau 0-1** présente les caractéristiques de distillation pour les eaux-de-vie françaises labélisées avec l'Appellation d'Origine Contrôlée (AOC), à savoir, Armagnac, Calvados, Cognac et Rhum Martinique [Decloux et Joulia, 2009].

Dans ce domaine, il convient de souligner que l'unité légale pour quantifier la concentration en éthanol est le titre alcoométrique volumique ou TAV en %vol (ABV en %v/v en Anglais), défini comme le nombre de litres d'éthanol contenu dans 100 L de mélange à 20°C [JOCE, 2000].

Tableau 0-1. *Caractéristiques principales de l'étape de distillation des eaux-de-vie AOC.*

Eau-de-vie	Matière première	Caractéristiques de la distillation
Cognac AOC depuis 1935	Raisin blanc	- Double distillation discontinue à feu nu TAV distillat : ≤ 72,4 %vol - Production 2011 : 715 000 hL d'alcool pur
Armagnac AOC depuis 1936	Raisin blanc	- Distillation continue multiétagée à feu nu TAV distillat : 52,0 %vol - 72,4%vol - Double distillation discontinue à feu nu (<5 % production) TAV distillat : 65,0 %vol - 72,4 %vol - Production 2011 : 21 600 hL d'alcool pur
Calvados AOC depuis 1942	Pomme, poire	- Distillation continue multiétagée à feu nu TAV distillat : ≤ 72,0 % vol - Double distillation discontinue à feu nu (Calvados Pays d'Auge) - Production 2011 : 18 200 hL d'alcool pur
Rhum Martinique AOC depuis 1996	Jus de canne	- Distillation continue multiétagée à la vapeur TAV distillat : 65,0 % vol - 75,0 % vol - Production 2011 : 69 200 hL d'alcool pur

Concernant la méthode de distillation continue, il existe des multiples configurations qui varient selon le produit. En distillation d'Armagnac, les unités sont connues comme alambics armagnacais. Leur utilisation a démarré au milieu du XIX^{ème} siècle, en remplacement progressif des alambics à double chauffe, inspirés de l'industrie du Cognac. Un alambic armagnacais, schématisé dans la **figure 0-1**, est constitué d'un foyer, d'une chaudière surmontée d'une colonne et d'un ensemble de chauffe-vin/réfrigérant, enfermant un serpentin. La colonne de distillation est munie de plateaux comportant des éléments de barbotage. Le nombre total de plateaux est au maximum égal à 15, le nombre de plateaux de concentration (au-dessus de l'alimentation en vin)

étant limité à 2. La chaudière permet de produire la vapeur à partir du résidu dit vinasse par action du feu généré au sein du foyer. L'ensemble chauffe-vin/réfrigérant est un échangeur de chaleur permettant simultanément de chauffer le vin et de condenser puis refroidir la vapeur de distillat qui circule à l'intérieur du serpentin. Des extractions supplémentaires peuvent être placées sur les circuits du distillat vapeur (sur le passage de la colonne vers le chauffe-vin ou sur les spires du serpentin interne) ou du vin préchauffé (en tête du chauffe-vin). L'ensemble chauffe-vin/réfrigérant est normalement alimenté par du vin. Parfois, le fluide de refroidissement du réfrigérant est remplacé par de l'eau froide, afin d'avoir un meilleur contrôle de la température du distillat, eau-de-vie de coulage [JORF, 2014].

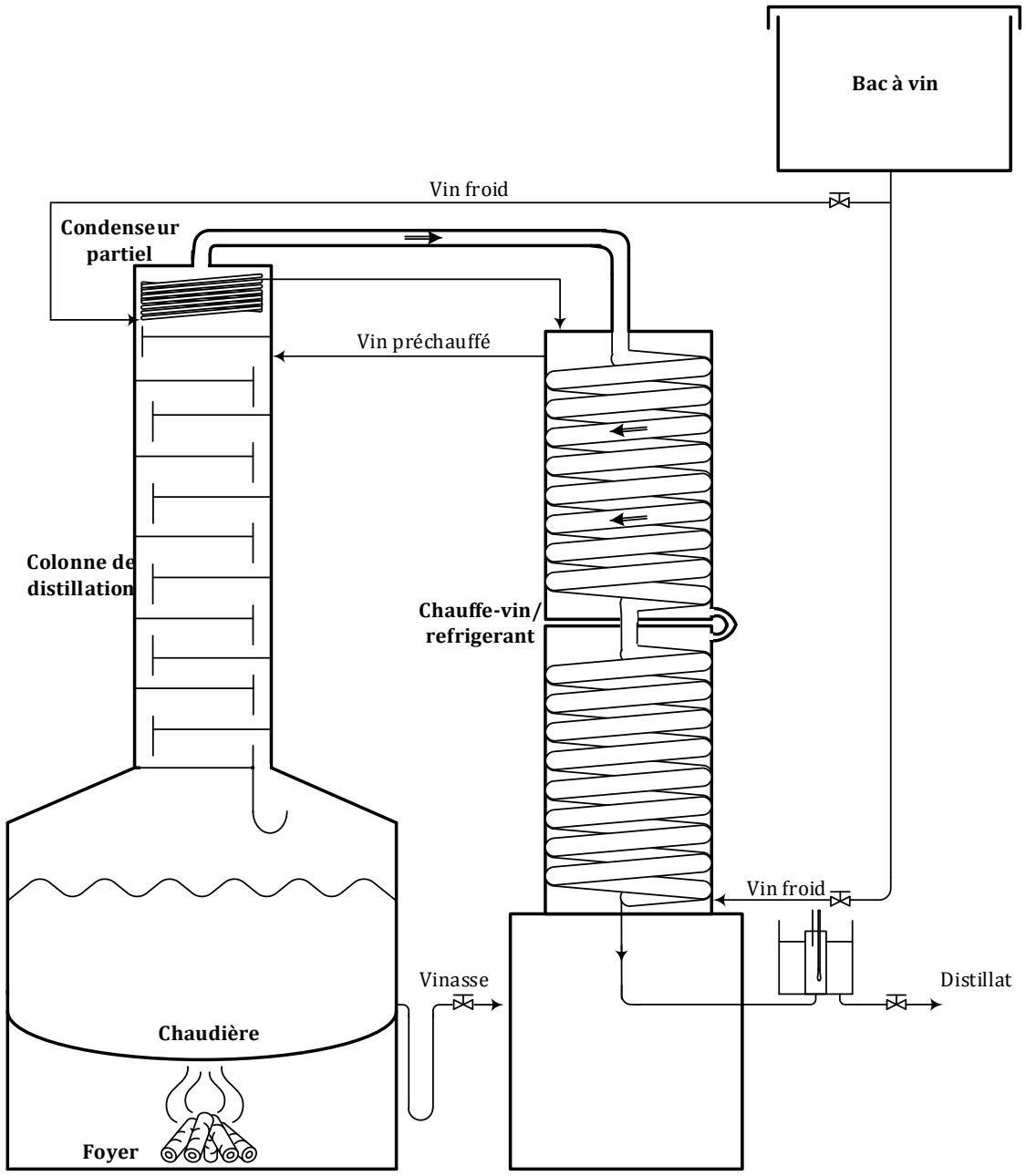

Figure 0-1. *Unité de distillation typique d'Armagnac. Adapté de [Decloux et Joulia, 2009].*

Pour ce qui est de la production du Calvados, toute installation à fonctionnement continu est composée des équipements déjà indiqués mais, contrairement à l'Armagnac, la colonne est le plus souvent séparée physiquement en deux tronçons. Un tronçon d'épuisement, alimenté par le cidre préchauffé et un tronçon de concentration, traversé par la vapeur produite dans la chaudière et provenant du tronçon d'épuisement. Le montage type est présenté dans la **figure 0-2**.

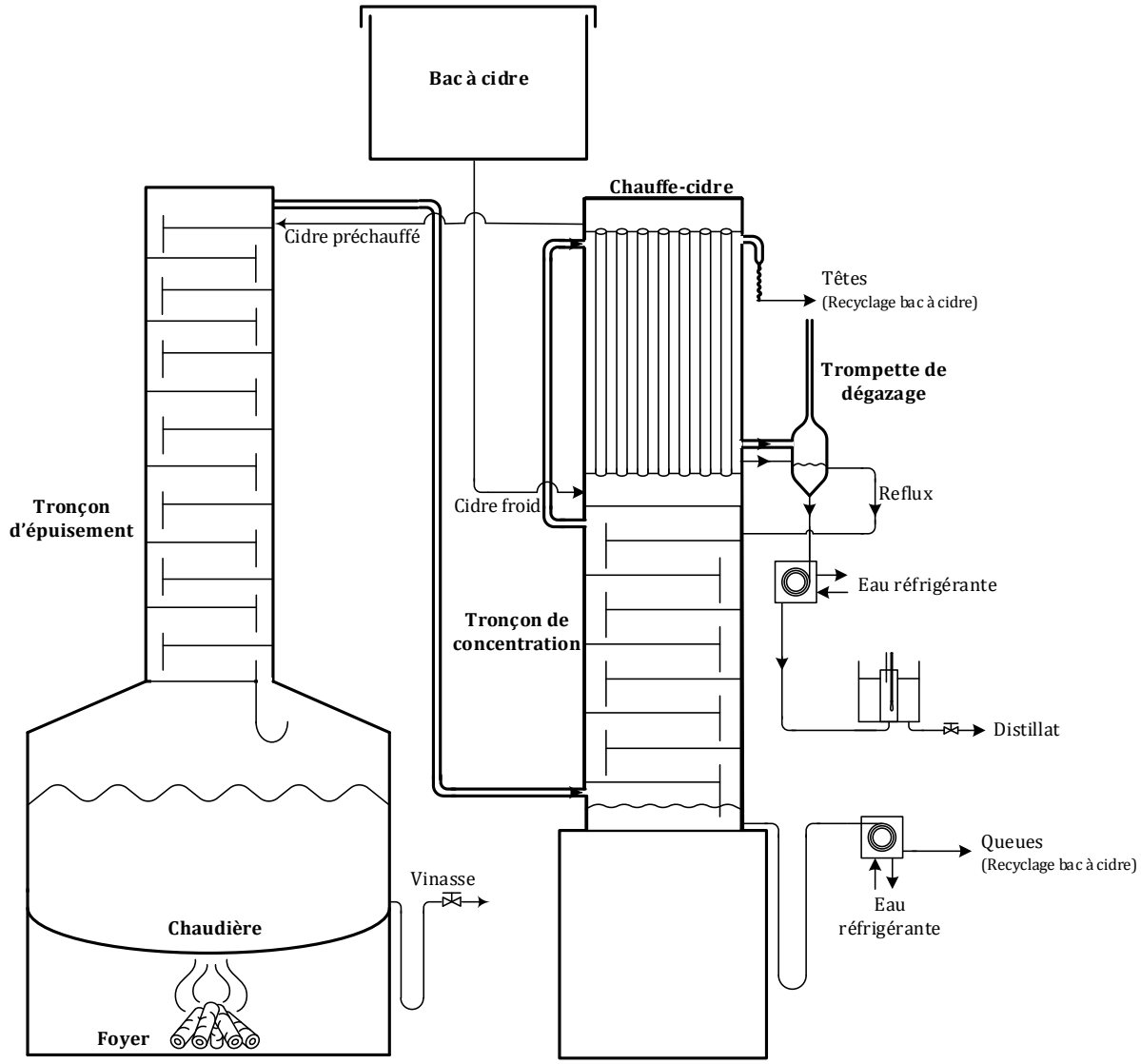

Figure 0-2. *Unité de distillation type de Calvados. Adaptation de [Decloux et Fabian, 2007].*

Dans le tronçon d'épuisement, le nombre de plateaux est limité à 19, tandis que dans le tronçon de concentration, le nombre maximum de plateaux est de 12. A la base de la colonne de concentration, un résidu, dénommé queues, est évacué puis renvoyé dans le bac à cidre. Des extractions supplémentaires peuvent être appliquées sur le circuit de distillat, avant ou après condensation, notamment au moyen de trompettes de dégazage ou au niveau du chauffe-cidre. Cette dernière est connue comme extraction de têtes et généralement est recyclée dans le bac à cidre. Quant à l'ensemble chauffe-cidre/réfrigérant, il s'agit d'un échangeur tubulaire vertical avec circulation du cidre à l'intérieur de tubes et de la vapeur issue du tronçon de concentration dans l'enceinte extérieure [Decloux et Fabian, 2007].

Une différence cruciale entre la distillation d'Armagnac et de Calvados est la génération du reflux liquide. Dans les unités d'Armagnac, le reflux est produit par condensation partielle de la vapeur de distillat en tête de colonne. La condensation a lieu sur les parois de la colonne et, s'il est présent, sur un serpentin dans lequel circule du vin. De ce fait, la composition du reflux est différente de celle du distillat, produit qui correspond à la fraction vapeur restante, envoyée vers l'ensemble chauffe-vin/réfrigérant. Dans les unités de Calvados, le reflux est une fraction du condensat issu du chauffe-cidre, renvoyé par rétrogradation en tête de colonne. Sa composition est donc la même que celle du distillat. Aucune des installations ne comporte de serpentin en tête du tronçon de concentration, le vapeur émise du dernier plateau étant envoyée directement au chauffe-cidre.

En ce qui concerne la méthode discontinue, elle est utilisée principalement pour la production de Cognac. La distillation s'effectue en deux chauffes, au moyen d'un alambic, dit *charentais*, composé d'une chaudière qui contient le liquide à distiller. Une installation classique est présentée dans la **figure 0-3**.

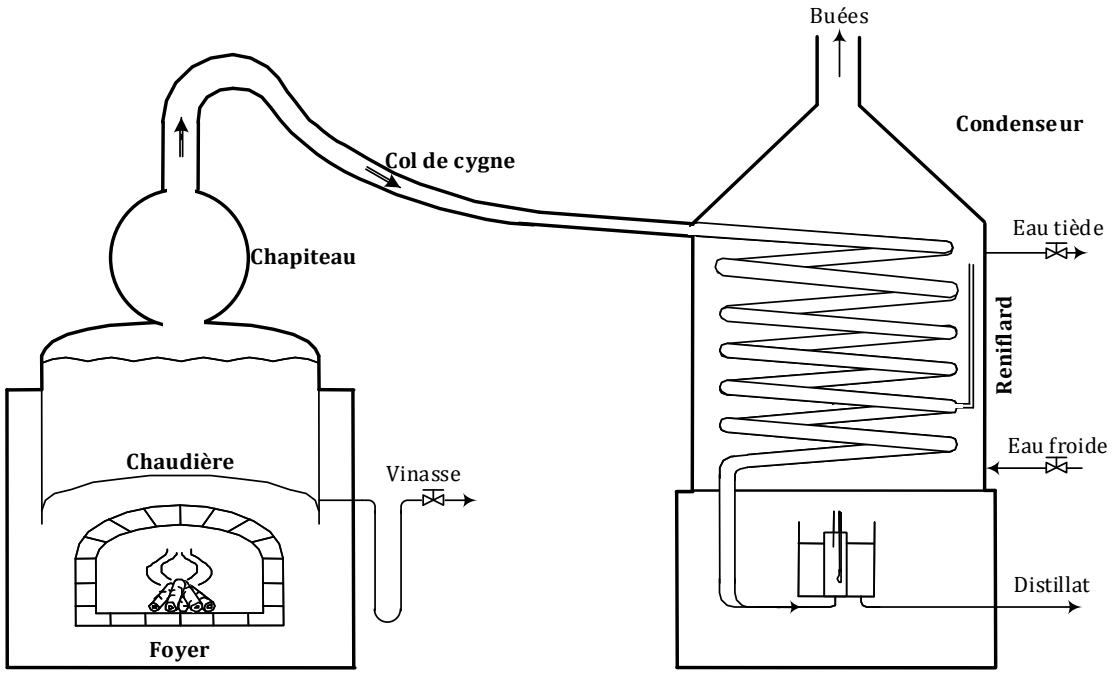

Figure 0-3. *Schéma d'un alambic charentais.*

La chaudière est chauffée à feu nu. Elle est surmontée d'un chapiteau qui canalise la vapeur émise et permet un recyclage dans la chaudière d'une partie sous forme de liquide (reflux). Le chapiteau est prolongé par un col de cygne qui assure l'écoulement de la vapeur sortant du chapiteau vers le serpentin. La vapeur peut traverser un équipement optionnel nommé chauffe-vin afin de préchauffer le vin destiné à être distillé lors d'un prochain cycle. Le col de cygne se prolonge en serpentin qui traverse un condenseur-réfrigérant appelé pipe où la vapeur se condense et se refroidie afin de former le distillat.

Lors de la première distillation dite chauffe de vin, le vin est introduit dans la chaudière et porté à ébullition. La distillation se poursuit jusqu'à ce que le TAV du distillat soit d'environ 2 %vol. L'ensemble du distillat constitue le brouillis. Le brouillis, titrant de 27 à 30 %vol, est redistillé lors de la deuxième chauffe, dite bonne chauffe. La première fraction de distillat qui coule, appelée têtes, très riche en éthanol et autres composés très volatils, est écartée. Vient ensuite le cœur qui

est coulé jusqu'à environ 60 %vol afin d'avoir un titre moyen au maximum de 72,4 %vol. Puis viennent les fractions de secondes puis queues et enfin les petites eaux qui rejoignent le résidu de distillation. Généralement les têtes et les queues sont recyclées dans le vin et les secondes sont recyclées dans le brouillis de la bonne chauffe qui suit. Ce mode de distillation, bien que millénaire, est encore mal maîtrisé du fait de l'état instationnaire permanent et des nombreux recyclages.

Dans la filière des eaux-de-vie, la plupart des installations sont en cuivre et ne sont pas isolées. L'utilisation du cuivre comme matériel de construction est justifiée non seulement par sa bonne résistance à la corrosion, mais également par sa conductivité thermique permettant une distribution homogène de la chaleur dans les installations à feu nu. De plus, le cuivre joue un rôle catalytique pour certaines réactions chimiques de conversion de composés indésirables, dont les acides gras, thiols et mercaptans [Cantagrel et al., 1990].

En matière de consommation énergétique, la méthode de distillation discontinue, composée d'au moins deux cycles de chauffe, est nettement plus énergivore que la distillation continue en colonne. Tandis que l'énergie consommée pour la production de Cognac à double chauffe est proche de 700 kWh par hectolitre d'alcool pur [Ferrari et al., 2011], la demande en distillation continue pour la production d'Armagnac et de Rhum agricole est de l'ordre de 250 kWh par hectolitre d'éthanol [Decloux et al., 2004 ; BNIA, 2010]. Des économies d'énergie de 30 % à 50 % sont possibles par recompression mécanique des vapeurs de distillat ou par préchauffage du moût fermenté sur l'extraction des vinasses, résidu de la distillation. Cependant, l'influence de ces modifications sur la qualité des distillats n'est pas connue [Cantagrel et al., 1990 ; Esteban-Decloux et al., 2013].

Pour une meilleure maîtrise de la distillation, les connaissances et techniques du génie des procédés apportent une méthodologie solide et prometteuse. Dans l'industrie chimique, la révolution informatique des années 1980 a conduit au développement d'une approche innovante d'ingénierie assistée par ordinateur. La simulation des procédés se positionne ainsi comme un outil très performant d'aide à la conception, l'analyse et l'optimisation des procédés. Néanmoins, dans l'industrie agroalimentaire et plus particulièrement dans le domaine des eaux-de-vie, l'utilisation de simulateurs s'avère encore limitée par le manque connaissance sur les équilibres liquide-vapeur des composés volatils d'arôme en milieu hydroalcoolique, élément fondamental pour l'étude scientifique de la distillation des eaux-de-vie.

Dans ce contexte, cette thèse de doctorat, réalisée dans le cadre d'une allocation de recherche octroyée par l'école doctorale ABIES de l'Université Paris-Saclay, a un double objectif de :

- *Contribuer à la compréhension du comportement des composés volatils d'arôme des eaux-de-vie au cours de différents modes de distillation.*
- *Donner des bases* scientifiques à la conduite des unités par le biais de modules de simulation.

L'étude s'est focalisée sur la distillation continue d'Armagnac et de Calvados en colonnes multiétagées. Les modules de simulation sont développés dans l'environnement du simulateur ProSimPlus® et intègrent des modèles thermodynamiques capables de représenter de manière satisfaisante les équilibres entre phases. Leur construction est basée sur la caractérisation expérimentale du fonctionnement des unités de distillation, constituant ainsi un outil d'aide à leur analyse et à leur conduite, pour une meilleure maîtrise de la composition des eaux-de-vie.

L'utilisation d'un logiciel générique de génie chimique est possible dans ce domaine pour deux raisons : en premier lieu parce que les modules de distillation disposent de modèles rigoureux et d'algorithmes performants permettant une représentation fiable de l'opération unitaire et deuxièmement, parce que, malgré la complexité du moût fermenté, sa description comme un mélange modèle multiconstituant à l'état liquide et/ou vapeur est tout à fait satisfaisante pour la problématique d'étude [Kadir, 2009 ; Lambert, 2015].

Pour atteindre les objectifs de cette recherche, le point de départ a été la sélection d'un groupe représentatif de composés volatils d'arôme présents dans l'ensemble des eaux-de-vie. Les données d'équilibre liquide–vapeur en milieu hydroalcoolique des composés sélectionnés ont été ensuite acquises, en suivant trois voies : information de la littérature, approche expérimentale et approche prédictive avec les modèles UNIFAC et COSMO. Ces données ont permis la détermination des paramètres d'interaction binaire du modèle NRTL, sélectionné pour la représentation thermodynamique du système. En parallèle, trois campagnes expérimentales dans plusieurs ateliers ont été menées en vue de caractériser précisément le fonctionnement des unités de distillation et de définir ainsi un point nominal d'opération pour chacune. Les bilans matière et énergie ont été établis après réconciliation des données brutes obtenues sur le terrain. Sur la base de cet ensemble d'informations, les modules de simulation ont été développés et validés. L'étude a été conclue avec une analyse de l'influence de certains paramètres opératoires sur la composition du distillat dans le but d'élucider la synergie existant entre le procédé et le comportement des composés volatils d'arôme.

L'ensemble du travail a été mené en étroite collaboration entre l'équipe CaliPro de l'UMR GENIAL (Unité Mixte de Recherche Ingénierie Procédés Aliments), les centres de recherche LGC (Laboratoire de Génie Chimique de Toulouse), UMR GMPA (Unité Mixte de Recherche Génie et Microbiologie des Procédés Alimentaires) et UCP (Unité de Chimie et Procédés de l'ENSTA ParisTech), la société ProSim, le laboratoire d'analyse UNGDA (Union Nationale des Groupements des Distillateurs d'Alcools) et enfin les syndicats de producteurs des eaux-de-vie, réunis dans le groupe distillation du réseau français de Produits Fermentés et Distillés, RMT FIDELE.

PLAN DU MANUSCRIT

Ce manuscrit est présenté sous forme d'une thèse sur publications. L'ouvrage est structuré en 6 chapitres. Le **chapitre 1** présente le cadre théorique nécessaire à la réalisation des travaux ainsi que la démarche de recherche mise en œuvre. Des notions fondamentales sur la distillation, les équilibres entre phases et la simulation des procédés sont présentées. Le cœur des travaux de recherche est présenté dans les chapitres 2 à 5. Les chapitres 2, 3 et 4 concernent l'acquisition de données d'équilibre liquide-vapeur des composés volatils d'arôme en milieu hydroalcoolique. Le **chapitre 2** est consacré à la synthèse bibliographique des données d'équilibre disponibles dans la littérature et à la détermination des paramètres d'interaction binaire du modèle NRTL des couples composé volatil d'arôme–éthanol et composé volatil d'arôme–eau. Le **chapitre 3** porte sur les mesures expérimentales pour un composé volatil d'arôme ciblé, le lactate d'éthyle, avec l'estimation des paramètres d'interaction binaire correspondants. Sur ce même composé ; le **chapitre 4** traite de la prédiction des données d'équilibre à l'aide des modèles UNIFAC et COSMO-SAC. Le **chapitre 5** aborde en détail la caractérisation expérimentale d'une unité de distillation et

développe une méthodologie de simulation en régime stationnaire pour l'analyse de son fonctionnement et pour l'étude du comportement des composés volatils d'arôme. Un état de l'art spécifique à la thématique abordée est développé dans chaque chapitre. Enfin, le **chapitre 6** présente une synthèse des travaux, accompagnée des principales contributions et perspectives pour la suite de ce doctorat.

Les **chapitres 2**, **3** et **5** sont des articles en anglais déjà soumis dans des journaux internationaux ou en cours de révision. La méthodologie de calcul et de comparaison développée pour le lactate d'éthyle dans le **chapitre 4** sera appliquée à un groupe de 34 composés volatils d'arôme afin d'évaluer les capacités prédictives des modèles UNIFAC et COSMO. Les résultats de ces travaux ne sont pas présentés dans ce manuscrit mais feront l'objet d'un article en cours de préparation. Finalement, les résultats de simulation des trois unités de distillation étudiées pendant cette thèse seront exposés dans un article à rédiger. Ils feront également l'objet de rapports de synthèse pour les partenaires industriels du projet.

CHAPITRE 1. CADRE THEORIQUE ET DEMARCHE MISE EN ŒUVRE

Ce chapitre présente de manière succincte les bases théoriques requises à la compréhension de ce doctorat. En première lieu, des notions générales sur la distillation sont abordées, suivies de la définition des équilibres liquide-vapeur et d'une description simplifiée des modèles thermodynamiques utilisés dans ces travaux. Enfin, les principes de la simulation des procédés et les bases fondamentales de la modélisation de la distillation en régime stationnaire sont explicitées. La deuxième partie du chapitre est consacrée à la démarche mise en œuvre pour l'étude systématique du comportement des composés volatils d'arôme par le biais des modules de simulation.

1.1. CADRE THEORIQUE

1.1.1. DISTILLATION

La distillation est une opération unitaire de séparation des constituants d'un mélange liquide par application d'énergie. La séparation est basée sur la différence de volatilité entre les constituants du mélange, mettant en jeu des transferts de matière et de chaleur entre une phase liquide et une phase vapeur en contact intime et à contre-courant.

L'art de la distillation est né dans l'antiquité. Les premières références apparaissent dans l'Epopée de Gilgamesh, laquelle décrit une forme primitive de distillation d'huiles pratiquée en Babylonie 3000 avant J.C. Des registres archéologiques prouvent que la production d'alcool par distillation était déjà une activité économique consolidée en Taxila, dans le nord-ouest du Pakistan, 500 avant J.C. 150 ans après, les pratiques traditionnelles se répandirent vers le moyen orient et l'Europe du sud, et furent décrites dans les textes d'Aristote et de Sinedrius. L'expansion en Europe de l'ouest eut lieu à partir du XI^{ème} siècle après l'invasion des Maures en Espagne. Plusieurs textes du moyen âge, ainsi que des gravures sur bois, décrivent la concentration de vapeurs d'alcool pour l'obtention d'*aqua vitae* ou eau-de-vie à partir de vin bouillant [Piggot, 2009 ; Owens et Dikty, 2011].

Aujourd'hui, la distillation constitue l'opération de séparation industrielle la plus répandue avec une technologie assez mature et des techniques de conception standardisées. Néanmoins, elle fait encore l'objet de nombreuses recherches concernant notamment la réduction de la consommation énergétique, la conception de systèmes plus compacts et le développement de stratégies de régulation plus robustes [Darton, 1992 ; Emtir et Etoumi, 2009 ; Truong et al, 2010 ; Harwardt et Marquardt, 2012 ; Wu et al. 2014].

La distillation est utilisée dans des domaines très variés des industries chimique, pharmaceutique et pétrolière. Les applications comprennent entre autres : le raffinage du pétrole, la production de bioéthanol, le traitement des eaux usées, la production d'extraits de parfum, la concentration d'additifs de polymères, le raffinage de solutions d'extraction, la séparation de produits secondaires de réaction, la récupération de solvants et élimination de composés organiques de déchets. Dans l'industrie agroalimentaire, la distillation occupe une place prépondérante dans la récupération des arômes ainsi que dans la production d'eaux-de-vie et d'alcool surfin, ce dernier étant la matière première pour la production de vodka et d'alcool pour la pharmacie et la parfumerie [Kadir, 2009].

1.1.1.1. Distillation continue multiétagée

Dans la plupart des applications industrielles, la distillation est effectuée dans une colonne verticale comportant plusieurs étages où ont lieu des cycles successifs de vaporisation–condensation agencés à contre-courant. Un schéma simplifié d'une colonne de distillation est présenté dans la **figure 1-1**. Une installation classique comporte un bouilleur en bas de colonne ainsi qu'un condenseur et un régulateur de reflux en tête.

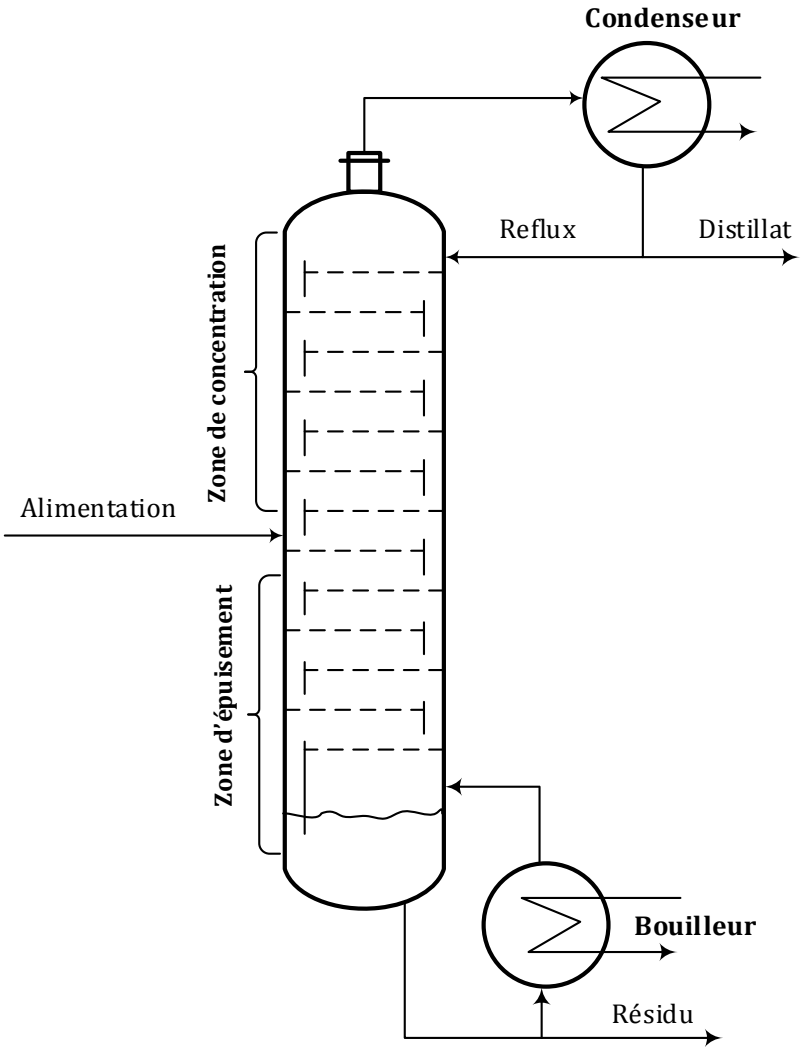

Figure 1-1. *Schéma d'une colonne de distillation.*

L'alimentation est introduite dans une position intermédiaire de la colonne, définissant ainsi deux tronçons de séparation : (i) un tronçon supérieur de concentration ou rectification et (ii) un tronçon inférieur d'épuisement. Dans le premier tronçon, la phase vapeur monte et s'enrichit en composés les plus volatils du mélange grâce au transfert de matière avec le liquide descendant. Ce liquide, connu comme reflux, est produit par condensation d'une fraction de la vapeur en tête de colonne. La fraction soutirée de la colonne (pouvant être à l'état vapeur, liquide ou liquide-vapeur selon le fonctionnement du condenseur) correspond pour sa part au distillat ou produit de tête. Le reflux permet l'enrichissement de la phase vapeur car sa composition en composés les plus volatils est toujours supérieure à celle du liquide en équilibre thermodynamique avec la vapeur avec laquelle le reflux entre en contact intime. Concernant le tronçon d'épuisement, la phase liquide s'écoule par gravité et s'appauvrit en composés les plus volatils, par transfert avec la phase vapeur produite dans le bouilleur. Cette phase est issue de la vaporisation partielle du courant de liquide descendant. Le liquide non vaporisé est évacué en bas de colonne et constitue ainsi le résidu de la distillation [Sinha and De, 2012].

Les unités de distillation peuvent être classées à partir de critères de type opérationnel et technologique. En fonction du régime d'opération, la distillation peut être continue ou discontinue. Dans le premier cas, le mélange à distiller et les produits générés circulent sans

interruption dans l'installation et leurs propriétés sont constantes au cours du temps. En distillation discontinue, le mélange est retenu dans l'unité et ses propriétés, ainsi que celles du distillat, évoluent dans le temps. En fonction de la technologie employée pour assurer le contact entre les phases liquide et vapeur, se distinguent les colonnes à plateaux et à garnissage. Un plateau est un dispositif utilisé pour faire barboter la vapeur à travers le liquide grâce à des cheminées coiffées de dispositifs rabattant la vapeur dans le liquide [Decloux et Fabian, 2007]. Le garnissage est pour sa part un ensemble d'éléments de remplissage destiné à maximiser la surface de contact liquide–vapeur, tout en minimisant la perte de charge. Dans ce cas, le transfert de matière a lieu à la surface du liquide, sans occlusion importante de bulles de vapeur [Copigneaux, 1993].

Dans le domaine des eaux-de-vie, les premières colonnes fonctionnelles ont été conçues par Aeneas Coffey vers 1830 et étaient destinées à la distillation de moûts fermentés de grains entiers [Piggott, 2009]. Ces unités opèrent en continu et sont équipées de plateaux. Les plateaux assurent le barbotage de la vapeur dans le liquide par des pièces en cuivre à bords crantés. Arrivée par le bas, la vapeur traverse la cheminée et change de direction avant de sortir par les fentes, fissures de la pièce de barbotage. Un déversoir trop plein garantit la présence de liquide sur le plateau et force la vapeur à barboter à travers lui, formant une émulsion. Les fentes permettent de diviser la vapeur en différents jets dans le but d'accroître la surface de contact liquide–vapeur.

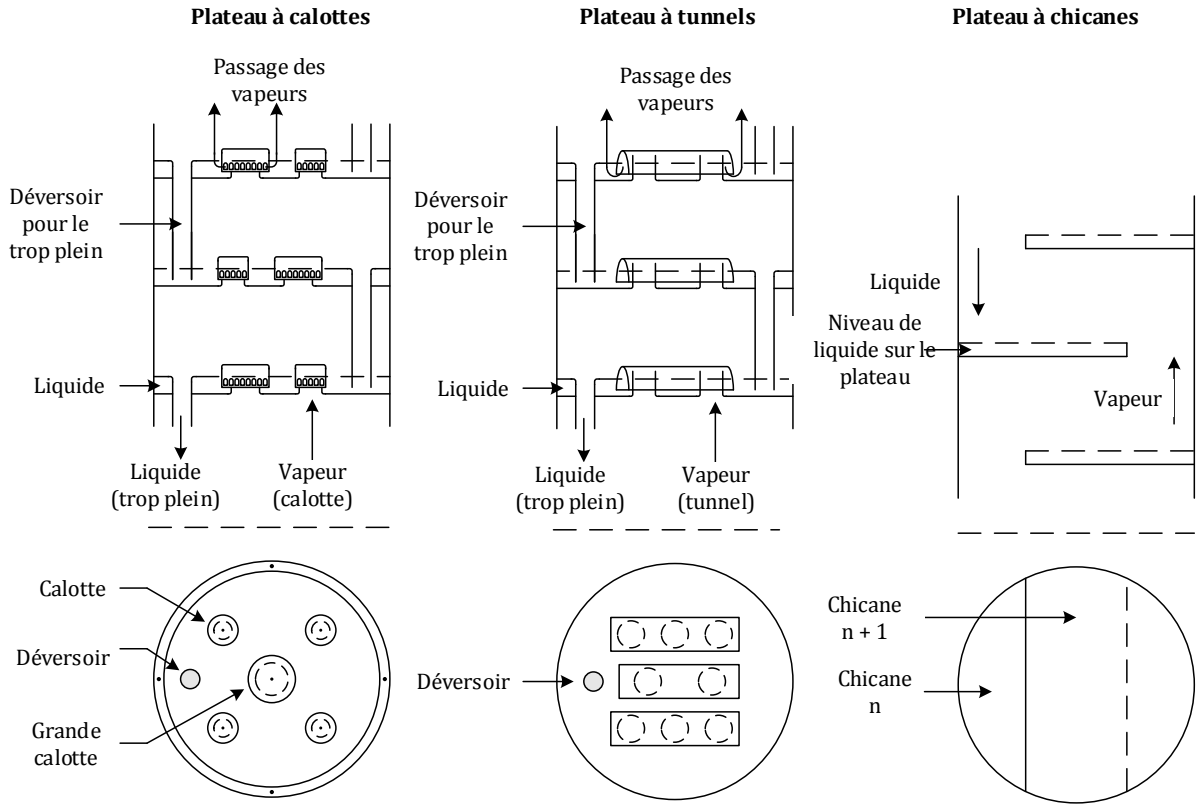

Figure 1-2. *Configuration des plateaux retrouvés dans la distillation des eaux-de-vie. Source [Decloux et Fabian, 2007].*

Les pièces de barbotages retrouvés dans les installations du domaine sont en général des calottes et des tunnels. Elles sont schématisées dans la **figure 1-2**. Leur quantité par plateau varie selon le constructeur, la capacité de la colonne et le tronçon considéré. Sur certaines colonnes, les plateaux sont démunis de ces pièces et leur rôle se limite à celui des chicanes, modifiant le cheminement naturel des phases liquide et vapeur [Decloux et Fabian, 2007].

1.1.1.2. Etage théorique et efficacité

La description classique de la distillation continue repose sur deux concepts fondamentaux : étage théorique et efficacité. Un étage théorique ou idéal désigne une section de l'unité de distillation dans laquelle se produit un cycle de vaporisation–condensation obéissant à trois conditions : (i) opération en régime stationnaire avec un produit liquide descendant et un produit vapeur ascendant, (ii) contact intime et parfait mélange entre le liquide et la vapeur (iii) équilibre thermodynamique entre le liquide et la vapeur quittant l'étage [Kister, 1992].

Le concept d'efficacité est introduit pour tenir compte de la non-idéalité d'un étage réel dans une colonne. En effet, les opérations de séparation atteignent rarement l'état d'équilibre et leur performance dépend donc des transferts de matière et de chaleur engendrés par des gradients de potentiel chimique et de température [Taylor et al., 2003 ; Gil et al., 2011]. L'efficacité vise à quantifier le degré d'écart entre le transfert de matière réel et la condition hypothétique d'équilibre dans les étages. Parmi les définitions disponibles dans la littérature, la plus connue et celle qui sera utilisée dans ces travaux, est l'efficacité de Murphree. L'équation de calcul pour un composé i dans l'étage n est la suivante [Murphree, 1925] :

$$E_{i,n}=\frac{y_{i,n}-y_{i,n+1}}{y^{*}_{i,n}-y_{i,n+1}} \qquad [1.1]$$

Ici, y_n^* correspond à la composition de la phase vapeur en équilibre avec le liquide sortant du plateau n, $y_{i,n+1}$ et $y_{i,n}$ sont les compositions moyennes des phases vapeurs entrant et sortant du plateau n. Nonobstant sa simplicité, l'utilisation de l'efficacité Murphree présente deux inconvénients principaux : (i) sa définition n'est pas homogène puisqu'elle compare une valeur locale (à l'interface) à une valeur globale de composition, (ii) elle varie non seulement entre étages mais également d'un constituant à l'autre [Wauquier, 1998 ; Taylor et al., 2003]. Au vu de ces limitations, ce paramètre sera utilisé dans ces travaux comme une variable d'ajustement représentant une moyenne des phénomènes de transfert dans un étage donné pour tous les constituants du mélange étudié.

1.1.1.3. Distillation des mélanges multiconstituants

Le traitement des mélanges multiconstituants est un problème courant dans les procédés industriels. En distillation, trois processus gouvernent la séparation de ces mélanges [Wauquier, 1998] :

- Récupération intégrale d'une partie des constituants très volatils, dans le distillat.
- Récupération intégrale d'une partie des constituants peu volatils, dans le résidu.
- Distribution d'une partie des constituants entre le distillat et le résidu.

Le comportement de la distillation est défini selon la répartition des composés distribués. Sa description est souvent basée sur deux corps de référence ou corps clefs, entre lesquels la séparation principale doit avoir lieu. Le corps clef plus volatil est connu comme clef légère et le moins volatil comme clef lourde.

La clef légère est un constituant qui doit être récupéré majoritairement dans le distillat. Si tous les constituants de l'alimentation sont présents dans le résidu, le constituant le plus volatil correspond donc à la clef légère. Dans la même logique, la clef lourde doit passer principalement dans le résidu. Si tous les constituants se trouvent dans le distillat à des concentrations non négligeables, la clef lourde doit être définie comme le constituant le moins volatil du mélange. Les autres constituants du mélange sont des composés non-clefs. Ceux-ci peuvent être distribués entre le distillat ou le résidu ou bien ils peuvent être récupérés en un seul produit de la distillation. Les composés distribués sont connus comme composés intermédiaires, leur volatilité étant intermédiaire entre celle de la clef légère et celle de la clef lourde. Pour leur part, les constituants plus volatils que la clef légère sont nommés composés légers et ceux moins volatils que la clef lourde, composés lourds [Kister, 1992 ; Thakore et Bhatt, 2007]. Ce principe de description sera utilisé dans cette étude pour le classement du comportement des composés volatils d'arôme, en sélectionnant l'éthanol et l'eau comme corps clefs légère et lourde du système, respectivement.

1.1.2. Equilibre entre phases

Un grand nombre d'opérations de séparation est fondé sur la formation de deux ou plusieurs phases à partir d'une autre. La maîtrise de cette transformation nécessite une connaissance approfondie de la distribution des constituants du mélange dans les phases générées. L'étude des équilibres entre phases est basée sur la théorie des solutions dans une seule phase combinée avec les principes régissant l'équilibre thermodynamique. Un système multiconstituant de multiples phases est en équilibre lorsque trois conditions sont satisfaites : équilibre mécanique (égalité des pressions dans toutes les phases), équilibre thermique (égalité des températures dans toutes les phases) et équilibre chimique, condition qui traduit l'égalité de potentiels chimiques de chaque constituant présent dans les différentes phases. Le potentiel chimique est une grandeur intensive gouvernant les transferts de matière entre phases. Pour le calcul des équilibres entre phases, l'égalité des potentiels chimiques est souvent substituée par l'égalité des fugacités. Cette propriété, en qualité de pression généralisée, exprime la tendance d'un constituant à s'échapper d'une phase. Elle est plus facile à utiliser et interpréter. Aussi, la solution de tout problème d'équilibre revient au calcul de la fugacité de chaque constituant dans chaque phase et à l'application de la condition d'égalité [Lewis and Randal, 1923 ; Renon et al., 1971 ; Prausnitz et al., 1999 ; Rios, 2009].

1.1.2.1. Données d'équilibre liquide – vapeur

Le principe physique gouvernant la distillation est l'équilibre liquide–vapeur. La distribution des constituants d'un mélange entre les phases liquide et vapeur est un phénomène complexe qui dépend des conditions physiques et des interactions moléculaires. Deux propriétés sont utilisées pour la caractérisation de l'équilibre : la volatilité absolue et la volatilité relative. La volatilité absolue, aussi nommée coefficient de partition ou constante d'équilibre, indique la tendance d'un

constituant à se vaporiser. Pour un constituant i, elle est définie comme le rapport des fractions molaires en phase vapeur (y_i) et en phase liquide (x_i) [Kister, 1992] :

$$K_i = \frac{y_i}{x_i} \quad [1.2]$$

Une valeur élevée de K_i indique que le constituant est très volatil et se concentre dans la phase vapeur, tandis qu'une valeur faible signifie qu'il reste majoritairement dans la phase liquide. Pour sa part, la volatilité relative compare la volatilité absolue de deux constituants i et j :

$$\alpha_{i/j} = \frac{K_i}{K_j} \quad [1.3]$$

D'une manière générale ce paramètre mesure la faisabilité d'une séparation. Une séparation par distillation est d'autant plus simple lorsque la valeur $\alpha_{i/j}$ est éloignée de 1 [Dahm and Visco, 2015]. Dans cette étude, la volatilité relative des composés volatils d'arôme, indicateur de leur comportement en distillation, est définie par rapport aux constituants de la matrice hydroalcoolique, l'éthanol et l'eau. Un composé volatil d'arôme est plus ou moins volatil que l'espèce de référence si sa volatilité relative est supérieure ou inférieure à 1, respectivement. La disponibilité de données de volatilité absolue et relative dans le domaine des eaux-de-vie est très limitée en raison de la variété des espèces chimiques et de leur faible concentration dans la matrice hydroalcoolique. Une partie importante de cette thèse a ainsi été consacrée à l'acquisition de ces données et à leur adaptation à des fins de simulation.

Il convient de souligner que dans certains systèmes fortement non idéaux, l'occurrence d'équilibres de type liquide–liquide–vapeur est possible, en raison des limites de solubilité de certaines espèces qui conduisent à la démixtion de la phase liquide. Dans cette étude, ce phénomène sera négligé, en considérant que les concentrations des composés volatils d'arôme sont très faibles et que les composés majoritaires, l'éthanol et l'eau, sont parfaitement miscibles.

1.1.2.2. Modélisation thermodynamique des équilibres liquide–vapeur

La description analytique des équilibres entre phases est l'élément de communication entre la thermodynamique et la simulation numérique. Des modèles capables de représenter les propriétés thermophysiques des phases liquide et vapeur, ainsi que la distribution des constituants entre les deux phases, sont indispensables à la construction des modules de simulation d'une colonne de distillation.

Comme indiqué précédemment, la solution du problème d'équilibre liquide–vapeur est basée sur le calcul des fugacités des constituants dans les deux phases, en fonction de la température, la pression et la composition. Actuellement, il existe trois approches de calcul [Gmehling, 2003 ; ProSim, 2014] :

- Approche dite homogène : car l'état de référence pour les phases liquide et vapeur est le même et correspond au gaz parfait. Un même modèle, généralement une équation d'état applicable à toute la zone fluide avec des règles de mélange classiques, permet de calculer les fugacités dans les deux phases. Cette approche est particulièrement bien adaptée aux systèmes peu ou non polaires à haute pression, car elle assure la continuité existant dans la zone critique entre

le liquide et la vapeur. Les secteurs d'application privilégiés sont les industries du raffinage, de la pétrochimie et du traitement de gaz.

- Approche dite hétérogène : car les états de référence pour les phases vapeur et liquide sont différents : gaz parfait et mélange idéal, respectivement. Des modèles distincts sont alors utilisés pour décrire chaque phase. Pour la phase vapeur, la fugacité est calculée au moyen d'une équation d'état, tandis que pour la phase liquide, le calcul est basé sur un modèle d'enthalpie libre d'excès, basé sur la définition du coefficient d'activité qui traduit l'écart à l'idéalité. L'approche peut être appliquée à des mélanges qui donnent lieu à des interactions complexes de type associations chimiques ou polaires, à basses et moyennes pressions (inférieures à 20 bar), et dans un intervalle de température entre 0 et 200 °C. Les secteurs d'application sont alors les industries chimiques et parachimiques (pharmacie, biotechnologie et agroalimentaire).
- Approche combinée : il s'agit d'une approche homogène alternative, dans laquelle le calcul des fugacités est fait au travers d'équations d'état applicables à toute la zone fluide et incluant des règles de mélanges complexes basées sur des modèles d'enthalpie libre d'excès. Grâce à ce type de traitement, il est possible d'étendre le domaine d'application des équations d'état à des systèmes polaires.

En considérant la nature du système étudié ainsi que les conditions opératoires des unités de distillation des eaux-de-vie, l'approche hétérogène constitue le meilleur compromis pour la représentation analytique des équilibres liquide–vapeur. Bien que la nature des modèles d'activité soit très variable, deux catégories de modèle se distinguent dans cette étude : les modèles semi-empiriques et les modèles prédictifs. Les équations des modèles sont présentées dans les **chapitres 2, 3** et **4**.

Dans les modèles semi–empiriques, les expressions pour le calcul des coefficients d'activité font intervenir des paramètres d'interaction binaire, dont les valeurs sont estimées à partir de données expérimentales d'équilibre. Dans cette catégorie, les modèles les plus souvent utilisés dans les simulateurs de procédés sont basés sur le concept de composition locale non aléatoire et incluent : Wilson [Wilson, 1964], NRTL (Non Random Two Liquids) [Renon et Prausnitz, 1968] et UNIQUAC (Universal Quasi Chemical) [Abrams et Prausnitz, 1975]. Dans cette étude, le modèle NRTL est utilisé pour la représentation du système composés volatils d'arôme–éthanol–eau. Ce choix est appuyé sur les recommandations de différents auteurs dans les domaines de la thermodynamique et de la simulation appliqués à la distillation de boissons alcoolisées [Faundez et Valderrama, 2004 ; Athès et al., 2008 ; Batista et. al, 2011 ; Valderrama et. al, 2012a ; Esteban-Decloux et al., 2014]. Dans les simulateurs de procédés, le modèle NRTL est apprécié comme un modèle performant, non seulement pour sa cohérence au regard des principes thermodynamiques, mais également pour une bonne efficacité d'utilisation traduite par un jeu de paramètres assez réduit et pour sa capacité à représenter de manière satisfaisante les équilibres liquide-vapeur, les chaleurs de mélange, les solubilités mutuelles (équilibres liquide-liquide) et les coefficients d'activité à dilution infinie d'un grand nombre de systèmes binaires et multiconstituants polaires ou non polaires [ProSim, 2014].

En ce qui concerne les modèles prédictifs, ils permettent la détermination des coefficients d'activité sans qu'il soit nécessaire d'avoir recours à une estimation de paramètres binaires à

partir de données expérimentales spécifiques. Deux types de modèles sont évalués dans ces travaux : UNIFAC et COSMO. Le modèle UNIFAC (UNIQUAC Functional-group Activity Coefficients) [Fredenslund et al., 1975] est fondé sur la notion de contribution de groupes et sa formulation découle directement du formalisme du modèle UNIQUAC. Les modèles prédictifs basés sur la théorie COSMO (Conductor-like Screening Model), prédisent le comportement d'une solution à partir des principes de la mécanique quantique. Les versions COSMO-SAC (COSMO Segment Activity Coefficient) et COSMO-RS (COSMO for Real Solvent) permettent d'évaluer les coefficients d'activité au moyen des profils de densité de charge surfacique. Ils combinent le traitement quantique de solutés et de solvants avec une méthodologie basée sur la thermodynamique statistique pour la description des interactions moléculaires [Klamt et Eckert, 2000 ; Lin and Sandler, 2002].

1.1.3. SIMULATION

La simulation de procédés consiste en la représentation du fonctionnement d'un procédé de transformation chimique et/ou physique sur la base d'un modèle mathématique qui intègre essentiellement les équations de bilans matière et énergie, d'équilibres entre phases, de transferts et de cinétiques chimiques. Elle permet de calculer les caractéristiques (température, pression, débit, composition et autre propriétés physiques) des courants dans toute l'installation, d'effectuer un pré-dimensionnement des principaux équipements et entre autres applications, d'optimiser les conditions de fonctionnement du procédé par rapport à des critères de type économique ou environnemental. La solution d'un problème de simulation en régime permanent exige la connaissance des constituants, des équilibres entre phases et des propriétés thermodynamiques des systèmes mis en jeu dans le procédé étudié, de l'agencement des différents équipements de l'installation (le *flowsheet*), des caractéristiques géométriques et des conditions opératoires des équipements à modéliser et, en présence de réactions chimiques, des schémas réactionnels et des paramètres cinétiques de ces réactions chimiques. Actuellement, la simulation constitue un outil de base en ingénierie des procédés assistée par ordinateur. Outre l'analyse et le suivi d'unités existantes, la simulation facilite la prévision du comportement d'un procédé, l'étude des modifications ou des améliorations, le développement de nouveaux procédés avec une importante réduction des expérimentations et également la formation d'opérateurs sur les sites industriels [Joulia, 2008 ; Gil et al., 2011].

1.1.3.1. Caractéristiques des simulateurs de procédés

Un simulateur de procédés est un logiciel utilisé pour modéliser le comportement d'un procédé en régimes stationnaire ou dynamique, composé de différentes opérations de transformation de la matière. Pour le traitement de tout problème de modélisation, un simulateur doit comporter les éléments suivants : une interface utilisateur pour l'acquisition des données spécifiques au problème, un serveur de calcul des propriétés physiques et d'équilibres entre phases, des modèles d'opérations unitaires, appelés modules, et enfin des techniques de résolution numérique. L'origine des simulateurs peut être située dans les années 1960 avec le développement du software PROCESS, destinée à la simulation de colonnes de distillation. Dans le marché actuel, l'offre commerciale est très diversifiée, avec des logiciels tels que ProSimPlus®, Aspen Plus®, Aspen Hysys®, ChemCAD®, Hysim®, SimSci PRO/II®, UniSim Design® et gPROMS® [Joulia,

2008 ; Gil et al, 2011 ; Foo et Elyas, 2017]. Le simulateur utilisé dans ces travaux est ProSimPlus®. Il a été développé sous Microsoft Windows et permet l'exportation des résultats principaux d'une simulation vers le tableur Microsoft Excel® [ProSimPlus, 2014]. L'architecture de ce simulateur est schématisée dans la **figure 1-3.**

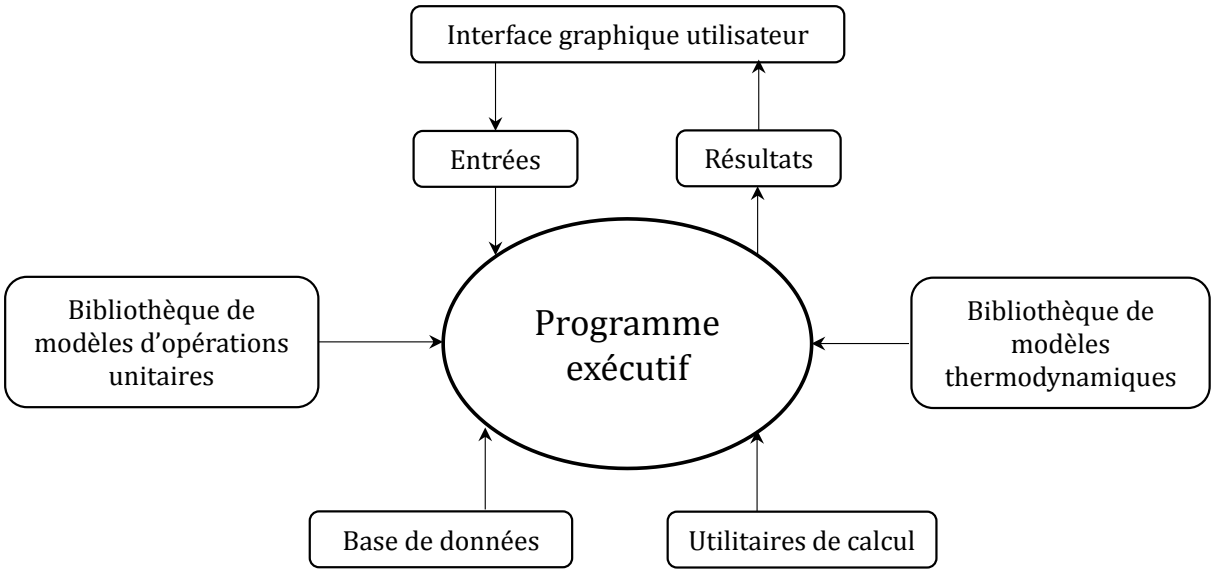

Figure 1-3. *Architecture d'un simulateur de procédé modulaire. Source [Kadir, 2009].*

1.1.3.2. Simulation en régime stationnaire de colonnes de distillation

L'étude scientifique de la distillation est l'une des activités phares du génie chimique du XX^{ème} siècle. La modélisation des colonnes de distillation a été intimement liée aux développements industriels et aux avancées en informatique du dernier siècle. De ce fait, trois approches peuvent être distinguées [Truong et al., 2010] :

- Modélisation fondamentale : basée sur les propriétés physiques du système et les principes de conservation. Cette approche est de validité globale et permet une meilleure compréhension de l'opération. Toutefois, son implémentation nécessite des outils informatiques performants.
- Modélisation empirique (boîte noire) : appuyée sur les informations d'entrée et de sortie du système sans considérer sa dynamique interne. Il s'agit d'une approche dominante dans l'industrie en vertu de sa simplicité. Cependant, sa construction est spécifique à une installation donnée, limitant sa capacité d'extrapolation.
- Modélisation hybride (boîte grise) : combine la modélisation fondamentale avec des outils empiriques. C'est une approche flexible mais exigeant tout de même une bonne connaissance du système et des informations expérimentales fiables.

Dans le cadre de cette thèse, une approche fondamentale classique sera utilisée pour la représentation des unités de distillation en régime stationnaire. Intégré dans les modules standards du logiciel ProSim®, il s'agit d'un modèle d'équilibre rigoureux qui repose sur un ensemble de relations fondamentales connues comme équations MESH. Cet ensemble comprend pour chaque plateau les bilans matière (*Material*) global et partiels, les relations d'équilibre (*Equilibrium*), les équations de sommation (*Summation*) et les bilans énergie (*Heat*) [Kister, 1992 ; Wauquier, 1998].

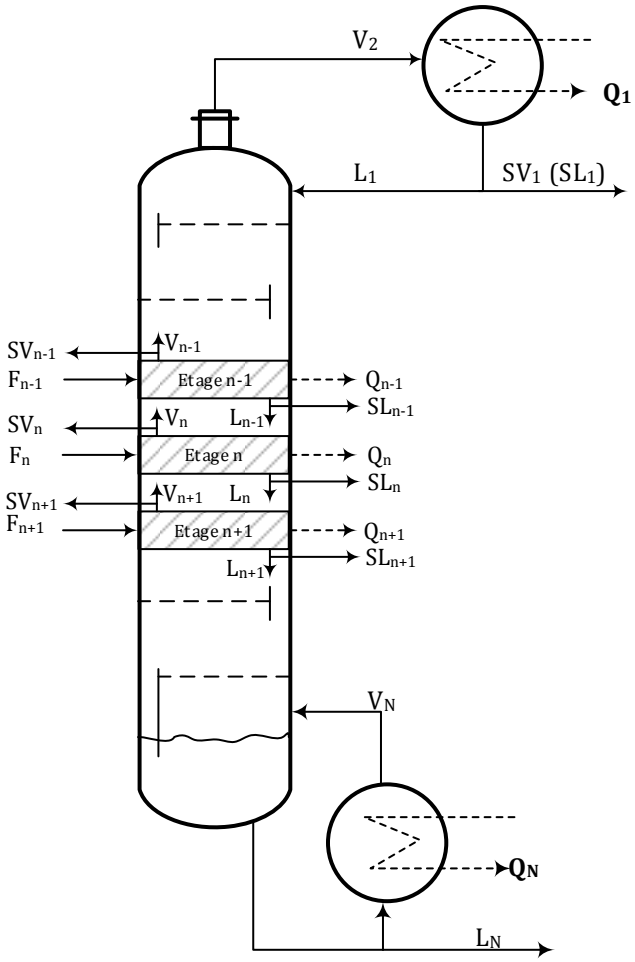

Figure 1-4. *Modèle généralisé d'une colonne de distillation.*

La **figure 1-4** présente un schéma généralisé d'une colonne à N étages, dans laquelle chaque étage peut présenter une alimentation spécifique, des soutirages de liquide ou vapeur ainsi que des échanges thermiques. Basée sur les concepts d'étage théorique et efficacité de Murphree, la modélisation de chaque étage de la colonne, destinée au traitement d'un mélange de C constituants, peut être formulée de la manière suivante :

- Bilan matière :

Bilan global dans l'étage n :

$$[F_n + L_{n-1} + V_{n+1}] - [L_n + SL_n + V_n + SV_n] = 0 \qquad [1.4]$$

Bilan partiel du composé i dans l'étage n :

$$\left[F_n z_{i,n} + L_{n-1} x_{i,n-1} + V_{n+1} y_{i,n+1}\right] - \left[(L_n + SL_n) x_{i,n} + (V_n + SV_n) y_{i,n}\right] = 0 \qquad [1.5]$$

- Equation d'équilibre du composé i avec correction par efficacité de Murphree à l'étage n :

$$y_{i,n} = E_n K_{i,n}(T_n, P_n, \boldsymbol{x_n}, \boldsymbol{y_n}) x_{i,n} + (1 - E_n) y_{i,n+1} \qquad [1.6]$$

- Equation de sommation à l'étage n :

$$\sum_{i=1}^{C} x_{i,n} - \sum_{i=1}^{C} y_{i,n} = 0 \qquad [1.7]$$

- Bilan enthalpique à l'étage n :

$$\left[F_n h_{F,n}(T_{F,n}, P_{F,n}, \boldsymbol{z_n}) + L_{n-1} h_{L,n-1}(T_{n-1}, P_{n-1}, \boldsymbol{x_{n-1}}) + V_{n+1} h_{V,n+1}(T_{n+1}, P_{n+1}, \boldsymbol{y_{n+1}})\right] - \left[(L_n + SL_n) h_{L,n}(T_n, P_n, \boldsymbol{x_n}) + (V_n + SV_n) h_{V,n}(T_n, P_n, \boldsymbol{y_n})\right] - Q_n = 0 \quad [1.8]$$

Dans ces équations, F_n est le débit molaire d'alimentation à l'étage n, L_{n-1} et L_n sont les débits molaires de liquide entrant et sortant, V_{n+1} et V_n sont les débits molaires de phase vapeur entrant et sortant, SL_n et SV_n sont les débits molaires de soutirage de liquide et vapeur; $z_{i,n}$ est la fraction molaire du constituant i dans l'alimentation de l'étage n, $x_{i,n-1}$ et $x_{i,n}$ sont les fractions molaires du constituant i dans le liquide entrant et sortant, $y_{i,n+1}$ et $y_{i,n}$ sont les fractions molaires du constituant i dans la vapeur entrant et sortant; E_n est l'efficacité de Murphree moyenne pour l'ensemble de constituants du mélange dans l'étage n ; $K_{i,n}$ est la volatilité absolue du constituant i dans l'étage n (fonction de la température T_n, de la pression P_n, de la composition globale de la phase liquide $\boldsymbol{x_n}$ et de la composition globale de la phase vapeur $\boldsymbol{y_n}$) ; $h_{F,n}$ est l'enthalpie de l'alimentation de l'étage n, $h_{L,n-1}$ et $h_{L,n}$ sont les enthalpies du liquide entrant et sortant, $h_{V,n+1}$ et $h_{V,n}$ sont les enthalpies de la vapeur entrant et sortant et Q_n est le flux thermique échangé entre l'étage n et l'environnement. Les enthalpies de l'alimentation, du liquide et de la vapeur dépendent de la température, de la pression et de la composition globale des phases respectives.

Pour une colonne comportant N étages pour séparer un mélange de C constituants, le nombre total d'équations à résoudre est de *N(2C+3)*, valeur qui correspond aux variables d'état de la colonne, à savoir les températures de chaque étage, les débits internes de liquide et de vapeur ainsi que les compositions de chaque phase. Le problème est donc solvable si la séparation est physiquement faisable et si l'ensemble standard de spécifications est connu et cohérent. Cet ensemble comprend : les caractéristiques des courants d'alimentation (température, pression, débits et composition), les paramètres de dimensionnement (nombre d'étages *N*, positions des alimentations et des soutirages, type de condenseur) et les paramètres de fonctionnement (pressions, débits de soutirage liquide et vapeur, apports ou pertes de chaleur).

Pour une colonne de distillation simple avec deux produits (distillat et résidu) le degré de liberté est égal à 2, après spécification des alimentations, des paramètres de dimensionnement et du profil de pression. Les deux paramètres standards qui peuvent être imposés pour résoudre le problème de modélisation incluent le débit (ou taux) de reflux, le débit de distillat ou les flux thermiques du condenseur et du bouilleur [Wauquier, 1998 ; Kadir, 2009].

Finalement, il convient de mentionner l'existence d'une approche alternative de modélisation fondamentale, développée depuis les années 2000. Cette voie, regroupant des modèles de transfert ou de non-équilibre, revient sur la description directe des phénomènes de transfert à l'aide de la théorie du double film. Les relations fondamentales sont connues comme équations MERSHQ et incluent : les bilans matière des deux phases à l'interface, les bilans d'énergie, les équations de transfert de matière et de chaleur, les équations de sommation, les équations hydrauliques et les équations d'équilibre à l'interface [Taylor et al., 2003 ; Gil et al., 2011]. Malgré la robustesse de cette approche, leur implémentation dans les simulateurs de procédés reste encore limitée par rapport aux modèles d'équilibre pour deux raisons : (i) des problèmes de convergence associés à des initialisations insuffisantes ou des modèles thermodynamiques

fortement non-linéaires, (ii) manque d'informations pour l'estimation de paramètres supplémentaires (dont les coefficients de transfert, les aires interfaciales, la perte de pression et les propriétés physiques de transport) ainsi que pour l'établissement des modèles d'écoulement, entraînement et pleurage [Wauquier, 1998 ; Gil et al., 2011].

Pour les objectifs de cette recherche, la simulation basée sur un modèle rigoureux d'équilibre s'est avérée tout à fait satisfaisante, d'une part car les connaissances sur l'hydrodynamique des unités de distillation des eaux-de-vie sont très limitées, mais d'autre part car l'utilisation de plateaux comme éléments de contact fait que les phénomènes de transfert ne soient pas limitants. L'application du concept d'étage théorique et sa correction par un paramètre d'efficacité s'adaptent bien à la nature du système étudié [Kister, 1992 ; Wauquier, 1998]. Dans ce contexte, la recherche a été focalisée sur l'étude des équilibres entre phases, la validation des principes de conservation en régime stationnaire et la caractérisation globale du comportement des composés volatils d'arôme.

1.2. DEMARCHE DE RECHERCHE MISE EN ŒUVRE

L'étude du comportement des composés volatils d'arôme par simulation nécessite d'allier des domaines de compétences complémentaires allant de la chimie analytique au génie des procédés. La démarche mise en œuvre dans cette thèse comprend ainsi quatre axes de travail : (i) sélection des composés volatils d'arôme, (ii) acquisition des données d'équilibre liquide-vapeur, (iii) caractérisation expérimentale des unités de distillation et (iv) simulation des procédés. Une description des activités menées dans chaque axe est proposée ci-dessous.

1.2.1. SELECTION DES COMPOSES VOLATILS D'AROME

Quatre-vingt-cinq (85) composés volatils d'arôme ont été sélectionnés en considérant les critères suivants :

- présence dans les trois eaux-de-vie : Armagnac, Calvados et Cognac,
- impact sur la qualité du produit,
- disponibilité des méthodes de dosage au laboratoire UNGDA,
- disponibilité des données d'équilibre liquide-vapeur,
- disponibilité dans la base de données du logiciel ProSim®,
- étude dans les publications scientifiques du domaine.

Les composés retenus appartiennent à huit familles chimiques : acétals, alcools, composés carbonylés, acides carboxyliques, esters, furanes, terpènes et norisoprénoïdes. La liste détaillée est présentée dans le **tableau 1-1** accompagnée du type d'information disponible pour chaque espèce. Les composés sont repérés avec la nomenclature de l'IUPAC et présentés dans chaque famille par ordre croissant de masse molaire.

Tableau 1-1. *Liste des composés volatils d'arôme répertoriés dans cette étude.*

Famille chimique	Composé volatil d'arôme	No. CAS	Disponibilité			Validation modèles prédictifs	Simulation
			Base de données ProSim®	Données d'équilibre	Dosage UNGDA		
Acetals	1,1-Diethoxyethane	105-57-7	×	×	×	×	
	1,1,3-Triethoxypropane	7789-92-6			×		
Alcools	Méthanol	67-56-1	×	×	×	×	×
	2-propen-1-ol	107-18-6	×	×	×	×	
	Propan-1-ol	71-23-8	×	×	×	×	×
	Propan-2-ol	67-63-0	×	×		×	
	Butan-1-ol	71-36-3	×	×	×	×	×
	Butan-2-ol	78-92-2	×		×		
	2-Methylpropan-1-ol	78-83-1	×	×	×	×	×
	2-Methylpropan-2-ol	75-65-0	×	×			
	Pentan-1-ol	71-41-0	×				
	2-Methylbutan-1-ol	137-32-6	×	×	×	×	×
	3-Methylbutan-1-ol	123-51-3	×	×	×	×	×
	(Z)-Hex-3-en-1-ol	928-96-1		×	×		×
	Hexan-1-ol	111-27-3	×	×	×	×	×
	Heptan-2-ol	543-49-7	×		×		
	2-Phenylethan-1-ol	60-12-8	×	×	×	×	×
	Octan-1-ol	111-87-5	×		×		×
	Decan-1-ol	112-30-1	×		×		×
	Dodecan-1-ol	112-53-8	×		×		×
	Tetradecan-1-ol	112-72-1	×		×		×
Composés carbonylés	Méthanal	50-00-0	×				
	Ethanal	75-07-0	×	×	×	×	×
	Propanal	123-38-6	×	×		×	
	Prop-2-enal	107-02-8	×	×			

Table 1-2. *Liste des composés volatils d'arôme répertoriés dans cette étude. Continuation.*

Famille chimique	Composé volatil d'arôme	No. CAS	Disponibilité			Validation modèles prédictifs	Simulation
			Base de données ProSim®	Données d'équilibre	Dosage UNGDA		
Composés carbonylés	Butanal	123-72-8	×	×		×	
	2-Methylpropanal	78-84-2	×	×		×	
	Pentanal	110-62-3	×	×		×	
	3-methylbutanal	590-86-3	×	×		×	
Acides carboxyliques	Acide méthanoïque	64-18-6	×	×	×	×	×
	Acide éthanoïque	64-19-7	×	×	×	×	×
	Acide propanoïque	79-09-4	×	×	×	×	×
	Acide butanoïque	107-92-6	×	×	×	×	×
	Acide 2-methylpropanoïque	79-31-2	×	×	×	×	×
	Acide 2-hydroxypropanoïque	50-21-5	×		×		
	Acide pentanoïque	109-52-4	×				
	Acide 2-methylbutanoïque	116-53-0	×	×	×		
	Acide 3-methylbutanoïque	503-74-2	×	×	×		×
	Acide hexanoïque	142-62-1	×	×	×	×	×
	Acide octanoïque	124-07-2	×	×	×	×	×
	Acide decanoïque	334-48-5	×		×		
	Acide dodecanoïque	143-07-7	×		×		
	Acide tetradecanoïque	544-63-8	×		×		
	Acide (9Z)-hexadec-9-enoïque	373-49-9			×		
	Acide hexadecanoïque	57-10-3	×		×		
	Acide (9Z,12Z,15Z)-9,12,15-octadecatrienoïque	463-40-1	×		×		
	Acide (9Z,12Z)-9,12-octadecadienoïque	60-33-3	×		×		
	Acide (9Z)-octadec-9-enoïque	112-80-1	×		×		
	Acide octadecanoïque	57-11-4	×		×		

Tableau 1-3. *Liste des composés volatils d'arôme répertoriés dans cette étude. Continuation.*

Famille chimique	Composé volatil d'arôme	No. CAS	Disponibilité			Validation modèles prédictifs	Simulation
			Base de données ProSim®	Données d'équilibre	Dosage UNGDA		
Esters	Methanoate d'éthyle	109-94-4	×				
	Ethanoate d'éthyle	141-78-6	×	×	×	×	×
	Ethanoate de propan-2-yle	108-21-4	×	×		×	
	Methanoate 2-methylpropyle	542-55-2	×	×			
	Butanoate d'éthyle	105-54-4	×		×		×
	2-methylpropanoate d'éthyle	97-62-1	×	×		×	
	2-hydroxypropanoate d'éthyle	97-64-3	×		×	×	
	3-methylbutanoate d'éthyle	108-64-5	×	×		×	
	Ethanoate de 3-methylbutyle	123-92-2	×	×	×	×	×
	Ethanoate de (Z)-hexen-3-yle	3681-71-8			×		
	Hexanoate d'éthyle	123-66-0		×	×		×
	Ethanoate de hexyle	142-92-7	×		×		×
	Ethanoate de 2-phenylethyle	103-45-7		×	×		×
	Octanoate d'éthyle	106-32-1		×	×		×
	Butane-1,4-dioate de diéthyle	123-25-1	×	×	×	×	×
	Decanoate d'éthyle	110-38-3		×	×		
	Octanoate de 3-methylbutyle	2035-99-6			×		×
	Dodecanoate d'éthyle	106-33-2			×		
	Octanoate de 2-phenylethyle	5457-70-5			×		
	Tetradecanoate d'éthyle	124-06-1			×		
	Dodecanoate de 3-methylbutyle	6309-51-9			×		
	Hexadecanoate d'éthyle	628-97-7			×		
	(9Z,12Z,15Z)-9,12,15-octadecatrienoate d'éthyle	1191-41-9			×		
	(9Z,12Z)-9,12-octadecadienoate d'éthyle	544-35-4			×		
	(9Z)-octadec-9-enoate d'éthyle	111-62-6			×		
	Octadecanoate d'éthyle	111-61-5			×		

Tableau 1-4. *Liste des composés volatils d'arôme répertoriés dans cette étude. Continuation.*

Famille chimique	Composé volatil d'arôme	No. CAS	Disponibilité			Validation modèles prédictifs	Simulation
			Base de données ProSim®	Données d'équilibre	Dosage UNGDA		
Furanes	Furan-2-carbaldehyde	98-01-1	×	×	×	×	
	Furan-2-carboxylate d'éthyle	614-99-3			×		
Terpènes	3,7-Dimethylocta-1,6-dien-3-ol	78-70-6	×	×	×	×	×
	2-(4-methyl-1-cyclohex-3-enyl)propan-2-ol	98-55-5	×		×		
	2-[(2R,5S)-5-ethenyl-5-methyloxolan-2-yl]propan-2-ol	5989-33-3	×	×	×	×	
	2-[(2S,5S)-5-ethenyl-5-methyloxolan-2-yl]propan-2-ol	34995-77-2	×	×	×	×	
	(Z)-3,7,11-Trimethyl-1,6,10-dodecatrien-3-ol	3790-78-1			×		
	(E)-3,7,11-Trimethyl-1,6,10-dodecatrien-3-ol	40716-66-3			×		
Norisoprénoïdes	1,1,6-trimethyl-1,2-dihydronaphthalene	30364-38-6			×		
	(E)-1-(2,6,6-trimethyl-1-cyclohexa-1,3-dienyl)but-2-en-1-one	23696-85-7			×		

1.2.2. GENERATION DES DONNEES D'EQUILIBRE DES COMPOSES VOLATILS D'AROME EN MILIEU HYDROALCOOLIQUE

La connaissance des équilibres liquide-vapeur est d'importance capitale pour la simulation des unités de distillation. Trois voies complémentaires ont été mises en place afin de créer une base de données d'équilibre pour les espèces sélectionnées en milieu hydroalcoolique à pression atmosphérique. L'objectif final fut d'estimer les paramètres d'interaction binaire du modèle thermodynamique NRTL, utilisé pour la représentation du système multiconstituant non idéal.

1.2.2.1. Approche 1 – Information de la littérature

Une base de données contenant toutes les données d'équilibre disponibles dans la littérature a été créée sur Microsoft Excel®. D'après le **Tableau 1-1**, cette base comprend 43 des 85 composés volatils d'arôme sélectionnés. Les informations incluent : des données de composition et de température à l'équilibre, des données de volatilité absolue ou relative et des modèles empiriques de calcul de la volatilité relative en fonction de la teneur en éthanol. Cinq de ces composés (cis-hex-3-en-1-ol, hexanoate d'éthyle, éthanoate 2-phenylethyle, octanoate d'éthyle, decanoate d'éthyle) ont dû être ajoutés à la base de données de ProSimPlus®. Les informations à renseigner dans ce cas incluent les propriétés des composés purs et une loi de pression de vapeur, déterminée à partir de données de la littérature et nécessaire dans les calculs d'équilibre liquide-vapeur.

Cette synthèse bibliographique, accompagnée du calcul des paramètres d'interaction binaire du modèle NRTL, fait l'objet du **chapitre 2**, article soumis à *Industrial and Engineering Chemistry Research* : *Review and thermodynamic modeling with NRTL model of vapor-liquid equilibria (VLE) of aroma compounds highly diluted in ethanol-water mixtures at 101.3 kPa*.

1.2.2.2. Approche 2 – Détermination expérimentale

Pour les 42 espèces sans données d'équilibre, la première alternative envisagée a été la détermination expérimentale. Une méthodologie a été développée pour l'étude du 2-hydroxypropanoate d'éthyle (lactate d'éthyle) en milieu hydroalcoolique à l'aide de l'appareil Labodest VLE 602™. Cette approche permet la génération de données de composition et de température. L'intérêt porté sur le lactate d'éthyle provient du fait qu'il s'agit d'un des esters majoritaires avec un impact sur la qualité des eaux-de-vie. Des données expérimentales de distillation sont disponibles dans la littérature [Cantagrel et al., 1990 ; Ségur et Bertrand, 1992], mais aucune information fiable des équilibres liquide-vapeur en milieu hydroalcoolique n'a été trouvée.

Les résultats de ces travaux sont présentés dans le **chapitre 3** et sont valorisés sous la forme d'un article soumis à *Journal of Chemical and Engineering Data* : *Vapor-liquid equilibrium (VLE) of ethyl lactate highly diluted in ethanol-water mixtures at 101.3 kPa. Experimental measurements and thermodynamic modeling using semiempirical models*.

1.2.2.3. Approche 3 – Prédiction théorique

Bien que l'approche expérimentale constitue la voie la plus fiable et la plus rigoureuse pour se doter des données d'équilibre, le travail requis peut être très contraignant de par l'importante

consommation de temps et de ressources matérielles et humaines. L'approche prédictive a été proposée comme une alternative pour pouvoir étudier l'ensemble des composés volatils d'arôme sélectionnés. Deux types de modèles ont été comparés : UNIFAC et COSMO, ce dernier dans les versions COSMO-SAC et COSMO-RS. Les travaux sur cette approche ont été menés en collaboration avec l'UCP de l'ENSTA ParisTech. Du fait de son caractère théorique, une étape préalable de validation par comparaison à des données connues a été nécessaire afin d'évaluer la capacité prédictive des modèles et ses limitations. Des recommandations peuvent être ensuite établies pour orienter le choix du modèle, en vue de la prédiction de données d'équilibre pour des composés volatils d'arôme dont aucune information n'est disponible. Dans le cadre de cette thèse, seule l'étape de validation a été menée pour un groupe de 35 composés volatils d'arôme.

La méthodologie de validation est appliquée à l'étude du lactate d'éthyle en milieu hydroalcoolique et fait l'objet du **Chapitre 4**. L'extension au groupe de 35 composés, dont le lactate d'éthyle, fera l'objet d'un article en cours de préparation qui sera soumis à *Fluid Phase Equilibria : Predictive modeling of vapor–liquid equilibria (VLE) for aroma compounds highly diluted in ethanol – water mixtures at 101.3 kPa using UNIFAC and COSMO models.*

1.2.3. CARACTERISATION EXPERIMENTALE DES UNITES DE DISTILLATION

Pour une véritable compréhension du comportement des composés volatils d'arôme, il s'avère essentiel de caractériser précisément le fonctionnement des unités de distillation. La caractérisation expérimentale s'est focalisée sur la description des unités et la validation des bilans matière et énergie, permettant de définir un régime nominal d'opération. Dans le cadre de cette thèse, l'attention a été portée sur la production d'Armagnac et de Calvados par distillation continue multiétagée.

1.2.3.1. Description des unités

Ce volet comprend le repérage des circuits, la mesure des dimensions caractéristiques des équipements et l'établissement des diagrammes de procédé avec les plans de circulation de fluides.

1.2.3.2. Validation des bilans matière et énergie

Ce volet est composé de deux étapes d'acquisition et réconciliation de données pour l'établissement des bilans matière et énergie. L'étape d'acquisition comprend les mesures expérimentales de débit, température et composition des différents courants de procédé.

En association avec des distilleries partenaires, trois campagnes expérimentales ont été conduites : deux campagnes en Armagnac (atelier CPR, du 30 novembre au 4 décembre 2015 ; atelier Janneau, du 15 au 17 novembre 2016) et une en Calvados (atelier Préaux, du 18 au 19 avril 2016). Dans les deux premières campagnes, les ateliers comportaient plusieurs unités de distillation dont l'approvisionnement en moût fermenté et gaz de combustion était fait en série. L'unité sélectionnée pour l'étude a donc dû être isolée pour minimiser les perturbations du point nominal d'opération et pour pouvoir établir correctement les bilans matière. Les mesures expérimentales ont été effectuées sur une période d'au moins cinq heures, après établissement du régime stationnaire.

L'acquisition des données a représenté un vrai challenge dans ces travaux. Un diagnostic précédant les campagnes a mis en évidence une importante limitation en instrumentation. Les quelques capteurs installés ne sont pas étalonnés périodiquement. Les distillateurs s'en servent exclusivement pour vérifier que les conditions globales d'opération ne sont pas altérées. Dans ce contexte, des capteurs non intrusifs ont été acquis pour les mesures de température et débit. Un débitmètre à ultrason a été testé lors de la première campagne. Cependant la comparaison avec d'autres mesures a montré que le débit d'alimentation était surestimé avec des écarts très importants, de l'ordre de 50%. Ce dysfonctionnement peut être associé à deux facteurs limitant la précision : faible vitesse dans la canalisation (de l'ordre de 0,2 m/s, 5 fois inférieure à la vitesse standard conseillée de 1 m/s) et présence intense de bulles et/ou de particules solides dans le fluide. Au vu de ces inconvénients, les débits ont été déterminés soit en chronométrant le temps d'écoulement d'une certaine masse de fluide dans un récipient gradué et pesé soit par suivi de la variation du niveau des cuves de stockage épalées sur une période de temps précis.

Concernant l'étude des compositions, des échantillons globaux des courants de procédé ont été constitués à partir de prélèvements ponctuels. Les courants échantillonnés incluent : le moût fermenté (vin ou cidre), le distillat ou eau-de-vie nouvelle (Armagnac ou Calvados) et le résidu (vinasse ou cidrasse). La teneur en éthanol a été déterminée par densimétrie électronique, selon les recommandations de l'OIV [OIV, 1994]. Pour les échantillons de moût fermenté et résidu, une étape préliminaire de distillation par entrainement à la vapeur a été appliquée pour éliminer les matières sèches qui modifient la masse volumique du liquide. Cette opération a lieu à volume constant afin d'éviter l'altération de la teneur en éthanol. Pour ce qui est des composés volatils d'arôme, les concentrations ont été estimées par chromatographie en phase gazeuse. 66 des 85 composés répertoriés ont pu être quantifiés. Les analyses ont été effectuées au laboratoire UNGDA, en suivant leurs protocoles de dosage. Aucune modification de ces protocoles n'a été proposée, mais un travail conséquent de compréhension et d'appropriation a été nécessaire pour leur application dans cette thèse.

La deuxième étape consiste en la réconciliation des données brutes, basée sur les contraintes de bilan matière. L'objectif fut de générer un ensemble d'informations fiables et statistiquement cohérent pour une spécification correcte des modules de simulation. Des estimations supplémentaires du bilan énergie, y compris les puissances de chauffe et de condensation ainsi que les pertes thermiques, ont été calculées à partir de données réconciliées du bilan matière et des dimensions des équipements.

1.2.4. SIMULATION DES PROCEDES

Le dernier axe de la démarche de recherche comprend la construction et la validation des modules de simulation dans ProSimPlus® en utilisant l'ensemble des informations issues de la génération des données d'équilibre liquide–vapeur et de la caractérisation des unités de distillation.

1.2.4.1. Création et validation des modules de simulation

La construction des modules de simulation s'est appuyée sur la connaissance de la configuration des unités de distillation, schématisée dans le diagramme de procédé avec le plan de circulation de fluides. Pour l'étude du comportement des composés volatils d'arôme, deux éléments

supplémentaires sont indispensables : les propriétés physicochimiques des composés purs, disponibles dans la base de données du simulateur, ainsi que les équilibres entre phases, représentés au moyen d'un modèle thermodynamique. L'adéquation du problème de modélisation est complétée avec les spécifications de fonctionnement, déterminées lors des campagnes expérimentales. Pour les unités étudiées, ces informations incluent : caractéristiques de la colonne (nombre de plateaux, position du ou des plateaux d'alimentation et perte de charge globale), alimentations (débit, température, pression et composition), pertes thermiques par plateau, puissance de condensation et débit de distillat. L'efficacité de Murphree des plateaux a été ajustée afin de vérifier les compositions en éthanol des courants de sortie (distillat et résidu), mesurées expérimentalement.

Suivant un schéma progressif, deux niveaux de simulation ont été proposés :

- Niveau binaire éthanol – eau : permet de valider le bilan matière en éthanol ainsi que la cohérence des profils simulés (température, débits et compositions des liquides et vapeurs).
- Niveau multiconstituant composés volatils d'arôme – éthanol – eau : permet de valider les bilans matière en composés volatils d'arôme, de comparer les données expérimentales de récupération dans le distillat, puis de classer les composés suivant leurs comportements caractérisés par les profils de composition dans la colonne de distillation. Pour les trois campagnes expérimentales, 32 composés volatils d'arôme (13 alcools, 1 composé carbonylé, 8 acides, 9 esters et 1 terpène), quantifiés par chromatographie et dont les données d'équilibre liquide-vapeur étaient disponibles, ont pu être simulés.

Il est important de souligner que l'occurrence de réactions chimiques n'a pas été prise en compte dans les modules de simulation. La connaissance de ces phénomènes est très limitée dans le domaine des eaux-de-vie et leur étude est en dehors du domaine de compétences et des objectifs de ce doctorat.

1.2.4.2. Influence des paramètres opératoires sur le comportement des composés volatils d'arôme

Afin de disposer d'un outil d'étude du comportement des composés volatils d'arôme en fonction des conditions de distillation, une analyse de l'influence de divers paramètres opératoires a été effectuée pour conclure cette recherche. Les paramètres ont été choisis en fonction des besoins des industriels et comprennent : composition en éthanol et température de refroidissement du distillat, pertes thermiques, regroupement des alimentations (cas des installations avec plusieurs entrées), et enfin influence des courants d'extraction de produits de têtes ou de queues.

La méthodologie de simulation et l'ensemble des résultats pour une unité d'Armagnac sont traités en détail dans le **Chapitre 5**, article à soumettre à *Food and Bioproducts Processing : Simulation of continuous distillation of spirits for a better understanding of aroma compounds behavior: Application to Armagnac production.* La totalité des travaux sur les trois unités de distillation étudiées dans ce doctorat n'est pas présentée dans ce manuscrit. Néanmoins ces résultats seront valorisés par le biais d'un article complémentaire, à préparer ultérieurement.

CHAPITRE 2. SYNTHESE DES DONNEES D'EQUILIBRE DES COMPOSES VOLATILS D'AROME

Ce chapitre présente une synthèse des données publiées dans la littérature sur les équilibre liquide-vapeur des composés volatils d'arôme à faible concentration en milieu hydroalcoolique. La synthèse comprend 44 composés d'arôme présents dans les eaux-de-vie et appartenant à 7 familles chimiques : acétals, alcools, composés carbonylés, acides carboxyliques, esters, furanes et terpènes. Les données d'équilibres sont modélisées en suivant une approche hétérognène, dans laquelle la phase vapeur est considérée comme un gaz parfait (avec une correction pour tenir compte des phénomènes de dimérisation dans le cas des acides carboxyliques) et la non idéalité de la phase liquide est répresentée au moyen du modèle NRTL. Un jeu de paramètres d'interactions binaires adapté aux fins de la simulation est proposé. La connaissance acquise sur les volatilités relatives par rapport à l'éthanol et l'eau permet d'établir une classification des composés volatils d'arôme sur toute la gamme de concentration en éthanol dans la phase liquide. La synthèse conclut avec une comparaison de la qualité de la répresentation des données expérimentales, obtenue avec le jeu paramètres ici calculé et avec deux jeux supplémentaires, estimés à partir de données d'équilibre de systèmes binaires (composé volatil d'arôme–éthanol, composé volatil d'arôme–eau) et ternaires (composé volatil d'arôme–éthanol–eau). Le but de cette comparaison est d'évaluer la capacité d'extrapolation du modèle NRTL.

Review and thermodynamic modeling with NRTL model of vapor-liquid equilibria (VLE) of aroma compounds highly diluted in ethanol-water mixtures at 101.3 kPa.

Cristian Puentes, Xavier Joulia, Violaine Athès et Martine Esteban-Decloux.

Soumis au journal *Industrial & Engineering Chemistry Research.*

2.1. INTRODUCTION

The knowledge of vapor-liquid equilibria is the starting point for the simulation and optimization of distillation processes, including the production of alcoholic beverages [Ashour et al., 1996; Cadoret et al., 2009; Esteban-Decloux et al., 2014]. In this last field, an accurate description of the compounds is relatively complex, because the wine and the final products are highly non-ideal mixtures containing many chemical species. These solutions can be considered as a mixed solvent system, composed of ethanol and water (main components, representing over 96% of the total mass), with hundreds of volatile organic compounds, also called congeners. They belong to a wide variety of chemical families (acetals, alcohols, carbonyl compounds, carboxylic acids, esters, furans and terpenes) and come either from the raw material or are produced during the fermentation and distillation steps [Baler, 2001 ; Apostolopoulou et al., 2005 ; Valderrama et al., 2012].

The congeners are present at low concentrations, ranging from a few $ng.L^{-1}$ to several $mg.L^{-1}$ (molar fraction lower than or equal to 10^{-4}), and their influence on the thermal properties (such as enthalpy and specific heat) of the system is negligible. However, from a sensory point of view, these compounds determine the quality of wine and distillate, whence their designation as aroma compounds and the use of their concentration levels as enological parameters [Heitz, 1960 ; Williams, 1962 ; Ortega et al., 2001 ; Câmara et al., 2006 ; Athès et al., 2008 ; Mati et al., 2013].

The relationship between the concentration of the aroma compounds and the organoleptic quality of a distilled beverage is so intricate that trace compounds can have a greater impact than the compounds at higher concentrations. Furthermore, while some compounds have a positive effect at low levels, their behaviour may become radically opposite when their concentrations exceed certain levels, adding unpleasant aromatic notes [MacNamara et al., 2010].

These phenomena evince that vapor-liquid equilibria information is fundamental to understand the behaviour of aroma compounds during distillation, and therefore to master their concentration to the desired levels, through thermodynamic modeling and simulation.

The equilibrium behaviour of an aroma compound (AC) in hydro-alcoholic medium (solvent), which depends on the physical conditions (T, P) and on the solvent composition, can be characterized by means of three parameters:

- The partition coefficient, equilibrium constant or absolute volatility (K_{AC}), which quantifies the distribution between the vapor (y_{AC}) and liquid phases (x_{AC}).
- The relative volatilities with respect to ethanol (Et) ($\alpha_{AC/Et}$) and water (W) ($\alpha_{AC/W}$), indicator of the repartition of the aroma compounds between the top and bottoms product in distillation [Dahm and Visco, 2015].
- The activity coefficient at infinite dilution (γ_{AC}^{∞}), a thermodynamic parameter that characterizes the aroma compound (solute) – mixed solvent interactions in the absence of solute – solute interactions, providing accurate information about the deviation from ideality [Coquelet et al., 2008 ; Barrera et al., 2009].

As regards the thermodynamic modeling, a classical heterogeneous approach can be applied for the Aroma Compounds – Ethanol – Water systems, since all the chemical species involved are

polar and the distillation units operate at atmospheric pressure. In this case, the vapor phase is often represented as an ideal gas, whereas the main deviations from ideal behaviour are associated to the liquid phase and are described with an excess Gibbs energy (G^E) model [Faundez et al., 2006].

Two categories of models can be identified in this method: semi-empirical and predictive. The semi-empirical models are based on the concept of local composition and need experimental data to determine the binary parameters that describe the interactions between the molecules of the system. Among these models, the NRTL model is used in this work because of its ease of implementation and availability in most process simulators. This model has been used to correlate with satisfactory results the equilibrium data for Ethanol – Water system [Voutsas et al., 2011 ; Lai et al., 2014] as well as some binary (aroma compound – ethanol and aroma compound – water) [Faundez and Valderrama, 2004 ; Pena-Tejedor et al., 2005 ; Faundez et al., 2006 ; Vu et al., 2006] and multicomponent aroma systems [Athès et al., 2008 ; Faundez et al., 2009 ; Deterre et al., 2012].

Equilibrium data for systems containing aroma compounds in hydroalcoholic medium are scarce in the literature and the nature of this information is variable. Several synthesis studies have been carried out by Valderrama and Faundez's research group [Valderrama and Faundez, 2003 ; Faundez et al., 2006 ; Faundez and Valderrama, 2009 ; Valderrama et al., 2012]. They have worked on the modeling of binary and ternary equilibrium data from specialized monographs and databases, using different thermodynamics approaches such as semi-empirical activity coefficient models (including NRTL) and predictive equations of state.

Although the results of their research could be useful for general understanding and simulation purposes, they suffer from some drawbacks: (i) they deal with a limited number of aroma compounds (between 8 and 12) and (ii) the experimental data used for modeling correspond to binary or ternary mixtures in which the ranges of concentration of the aroma compounds are generally much higher than those found in wine distillation. For ternary mixtures aroma compound – ethanol – water, the molar fractions in the liquid phase vary between 8×10^{-4} and 8×10^{-1}, while for binary mixtures aroma compound – ethanol and aroma compound – water the whole concentration interval in the liquid phase is included ($0<x_{AC}<1$). In both cases, the concentration interval is very different from the case of alcoholic beverages, in which the aroma compounds are present at high or infinite dilution.

In this context, the objectives of the current study are to generate a database containing all the information available in the open literature on the vapor-liquid equilibria of aroma compounds highly diluted in ethanol – water mixtures at atmospheric pressure and to generate new binary interaction parameters of NRTL model for simulation purposes. 44 representative aroma compounds present in distilled beverages such as Armagnac, Calvados and Cognac, are considered. With the purpose of evaluating the extrapolation capability of NRTL model, the study is concluded by a comparison of the equilibrium representation obtained when using the new set of parameters and the one derived from parameters estimated from binary or ternary mixture data at high concentrations.

The paper is organized as follows: a general description of the equilibrium information available in the literature is presented, followed by some elements on the thermodynamic modeling approach. Using the literature data, a set of binary interaction parameters is estimated, followed by a classification of the aroma compounds and finally by a comparison of the representation obtained with different sets of interaction parameters.

2.2. Compilation and thermodynamic modeling of vapor-liquid equilibrium data

2.2.1. Compilation of vapor-liquid equilibrium data of aroma compounds

The experimental research work on vapor-liquid equilibria of aroma compounds highly diluted in hydro-alcoholic mixtures is a relatively unexplored field. This is probably due to the high variety of chemical species and their presence at low concentrations, which implies a high complexity in the chemical analysis of the vapor and liquid phases, sometimes disturbed by the presence of variable amounts of ethanol [Athès et al., 2007].

Despite this limitation, some relevant studies have been reported in the literature. The earliest one dates back to the 1960s, with the compilation made by Williams (1962), including 29 compounds from 6 chemical families, followed by a series of publications by Ikari et al [Ikari and Kubo, 1975 ; Ikari et al., 1984 ; Ikari et al., 1990 ; Ikari et al., 1998a ; Ikari et al., 1998b], which concern 11 aroma compounds from 4 families. Other studies that consider several aroma compounds have been published by Athès et al. (2008) (13 brandy aroma compounds, including 5 alcohols, 2 carbonyl compounds and 6 esters), Martin et al. (2009) (10 compounds, including 1 acetal, 5 alcohols and 4 esters) and Deterre et al. (2012), who studied 5 bitter orange aroma compounds, including 2 monoterpene hydrocarbons and 3 oxygenated terpenes.

Specific measurements for ternary systems have also been reported. The aroma compounds considered are ethanal [Heitz, 1960] and ethyl lactate [Puentes et al., 2017b], this latter study carried out by the same authors of this paper.

In general, the data are of very variable nature, but in all cases (ternary and multicomponent systems), they are related, directly or indirectly, to the absolute and relative volatilities at 101.3 kPa. No studies presenting experimental data of activity coefficients at infinite dilution and equilibrium conditions were found in the open literature.

One important point in common between the different studies is that the measurements were performed via a dynamic method with recirculating stills. In this method, known for providing rapid and accurate vapor-liquid equilibria data, the vapor, evolved from a liquid phase, is continuously separated under steady-state conditions and directed to the condenser, configured to prevent, or at least minimize, any risk of reflux [Heitz, 1960; Soni, 2003]. The recirculation is maintained until the composition variation of the vapor or liquid phases is no longer appreciable [Othmer, 1943].

The recirculating devices can be classified in two categories:

- In the first one, only the vapor phase circulates within the apparatus, while the liquid remains in the boiling chamber. For measurements involving aroma compounds, all the devices are based on the design of Altsheler and Othmer stills [Othmer, 1943; Othmer, 1948].
- In the second category, the vapor and liquid phased are recirculated and maintained in intimate contact before they are disengaged. This case covers the Gillespie-type stills [Gillespie, 1946] and more particularly the Labodest still, developed by i-Fischer Engineering GmbH. A detailed description of this latter has been already presented in several experimental works [Athès et al., 2008 ; Dias et al., 2013 ; Nala et al., 2013; Puentes et al., 2017b].

The second category of recirculating stills has been recommended for equilibrium measurements of diluted mixtures at temperatures higher than 298.15 K, when coupled to an accurate analysis technique of the liquid and condensed vapor composition [Christensen, 1998; Rall and Muhlbauer, 1998]. However, given the highlighted scarcity of vapor-liquid data of aroma compounds – ethanol – water systems, all the information found in the open literature, concerning both the categories of recirculating devices, will be retained in the current work.

In **table 2-1**, the different studies are summarized, classified according to the recirculating method. This synthesis includes information about the experimental measurements (composition analysis, type of equilibrium data and aroma compounds studied) as well as main features of the thermodynamic modeling, when performed.

As a result of this compilation, vapor-liquid equilibrium data at 101.3 kPa for 44 aroma compounds were extracted. The references and some specifications for each chemical species are presented in **table 2-2**, including the number of data points and, if available, the composition ranges of ethanol and the aroma in the vapor and liquid phases.

For most of the chemical species studied in this work, including ethanol and water, the physical properties were available in the Simulis® Thermodynamics database, software developed by ProSim and used for the equilibrium calculations presented in the current work. Regarding 5 missing species, the properties were extracted from literature and subsequently added to the database. These compounds are: (Z)-hex-3-en-1-ol, ethyl hexanoate, 2-phenylethyl ethanoate, ethyl octanoate and ethyl decanoate. For equilibrium calculations, the whole set of information provided to characterize each chemical species was: CAS Number, Molecular formula, molecular mass (MM), boiling temperature at 101.3 kPa (T_b) and vapor pressure (P^0). Most of these values were taken from NIST Chemistry Webbook [US, 2016]. Further information about the calculation of vapor pressures for these compounds are presented in section 2.3.

Table 2-1. *Research works published in the open literature on vapor-liquid equilibrium data of aroma compounds highly diluted in ethanol-mixtures at 101.3 kPa.*

Experimental measurements								Thermodynamic modeling	
Equilibrium method	**Reference**	**Device**	**Composition analysis**	**Type of equilibrium data**	**Type of system**	**Aroma compounds**		**Approach**	**Model**
						Chemical family	**Number**		
Recirculation of vapor phase only	Williams, 1962	Altsheler-type still Othmer-type still : For esters	*Ethanol in liquid phase:* Pycnometry. Calibration curve of volume concentration with mass density. *Ethanol in vapor phase*: Empirical correlation with liquid molar fraction. *Aroma compounds:* Klett colorimetric comparisons and gas chromatography (alcohols and carbonyl compounds), hot saponification (esters), neutralization titration (carboxylic acids). Calibration curves of volume composition.	Absolute and relative volatilities as a function of ethanol molar fraction in the liquid phase	Ternary - Model solution Multicomponent - Model solution: For esters	Carboxylic acids Carbonyl compounds Furans Acetals Alcohols Esters	7 6 1 1 9 5	-	-
	Ikari et al., 1984	Othmer-type still	*Ethanol:* Densimetry. Calibration curve of molar composition with liquid density at 20°C. *Aroma compounds:* Spectrophotometry. Calibration curve of molar composition with absorbance at 277 nm.	Absolute volatility as a function of ethanol molar fraction in the liquid phase	Ternary - Model solution	Furans	1	-	-
	Ikari et al., 1990	Othmer-type still	*Ethanol:* Densimetry. Calibration curve of molar composition with liquid density at 20 °C. *Aroma compounds:* Gas chromatography coupled to detection by flame ionization. Calibration curves of mass composition with peak area.	Absolute volatility as a function of ethanol molar fraction in the liquid phase	Multicomponent - Model solution	Alcohols	3	-	-
	Ikari et al., 1998a	Othmer-type still	*Ethanol:* Densimetry. Calibration curve of molar composition with liquid density at 20 °C. *Aroma compounds:* Gas chromatography coupled to detection by flame ionization. Calibration curves of mass composition with peak area.	Liquid phase composition and absolute volatility	Multicomponent - Model solution	Carbonyl compounds Esters	1 2	-	-
	Ikari et al., 1998b	Othmer-type still	*Ethanol:* Densimetry. Calibration curve of molar composition with liquid density at 20 °C. *Aroma compounds:* Gas chromatography coupled to detection by flame ionization. Calibration curves of mass composition with peak area.	Phases composition and absolute volatility	Multicomponent - Model solution	Alcohols Carbonyl compounds	1 2	-	-
	Martin et al., 2009	Modified Othmer-type still	*Ethanol:* Densimetry. Calibration curve of molar composition with liquid density. *Aroma compounds:* Gas chromatography coupled to detection by flame ionization. Calibration curves of mass composition with peak area ratio (aroma compound - internal standard).	Empirical correlation of relative volatility of the aroma compound with respect to ethanol as a function of ethanol molar fraction in the liquid phase	Multicomponent - Real wine	Acetals Alcohols Esters	1 5 4	-	-

Continuation Table 2-1. *Research works published in the open literature on vapor-liquid equilibrium data of aroma compounds highly diluted in ethanol-mixtures at 101.3 kPa.*

		Experimental measurements						Thermodynamic modeling	
Equilibrium method	**Reference**	**Device**	**Composition analysis**	**Type of equilibrium data**	**Type of system**	**Aroma compounds**		**Approach**	**Model**
						Chemical family	**Compounds**		
Recirculation of vapor and liquid phases	Heitz, 1960	Modified Gillespie-type still with a vapor-condensate cooler	*Ethanol:* Oxidation to acetic acid by potassium dichromate in acid solution. *Aroma compound:* Addition reaction of sodium bisulphite in aqueous solution.	Temperature and phase composition	Ternary - Model solution	Carbonyl compounds	1	-	-
	Athès et al., 2008	Gillespie-type still : Labodest VLE 602™	*Ethanol:* High-performance liquid chromatography coupled to detection by refractometry. Calibration curve of volume concentration with change in refractive index of the chromatographic effluent *Aroma compounds:* Gas chromatography coupled to detection by flame ionization. Calibration curves of mass composition with peak area ratio (aroma compound - internal standard).	Temperature and phase composition	Multicomponent - Model solution	Alcohols Carbonyl compounds Esters Furans Terpenes	4 1 6 1 1	Semi-empirical Predictive	NRTL COSMO-SAC
	Deterre et al., 2012	Gillespie-type still : Labodest VLE 602™	*Ethanol and Aroma compounds:* Gas chromatography coupled to detection by flame ionization. Calibration curves of mass composition with peak area ratio (aroma compound - internal standard).	Temperature and phase composition	Multicomponent - Model solution	Terpenes	2	Semi-empirical	NRTL, Henry's Law
	Puentes et al., 2017	Gillespie-type still : Labodest VLE 602™	*Ethanol:* From temperature measurements. Correlation with molar composition through thermodynamic modeling of vapor-liquid equilibrium for Ethanol - Water system *Aroma compounds:* Gas chromatography coupled to detection by flame ionization. Calibration curves of mass composition with peak area ratio (aroma compound - internal standard).	Temperature and phase composition	Ternary - Model solution	Esters	1	Semi-empirical Predictive	NRTL, UNIQUAC UNIFAC, COSMO-SAC

Table 2-2. *Synthesis of the vapor-liquid equilibrium data available in the open literature for aroma compounds highly diluted in ethanol-mixtures at 101.3 kPa.*

Chemical family	Aroma compound			Reference	Independent data	T range /K		x_{AC} range		x_{Et} range		y_{AC} range		y_{Et} range	
	Common name	IUPAC name	No. CAS			Min	Max	Min	Max	Min	Max	Min	Max	Min	Max
Acetals	Acetal	1,1-Diethoxyethane	105-57-7	Williams, 1962	9	-	-	-	-	0.01	0.85	-	-	-	-
Alcohols	Methanol	Methanol	67-56-1	Ikari et al, 1998b	18	-	-	1.64×10^{-4}	4.19×10^{-3}	0.00	0.99	1.03×10^{-3}	6.35×10^{-3}	0.00	0.99
	2-Propenol	Prop-2-en-1-ol	107-18-6	Williams, 1962	12	-	-	-	-	0.00	0.85	-	-	-	-
	1-Propanol	Propan-1-ol	71-23-8	Williams, 1962	11	-	-	-	-	0.00	0.86	-	-	-	-
	1-Propanol	Propan-1-ol		Ikari et al, 1990	11	-	-	-	-	0.00	1.00	-	-	-	-
	1-Propanol	Propan-1-ol		Martin et al, 2009	-	-	-	-	-	0.00	0.60	-	-	-	-
	Isopropanol	Propan-2-ol	67-63-0	Williams, 1962	11	-	-	-	-	0.00	0.86	-	-	-	-
	1-Butanol	Butan-1-ol	71-36-3	Williams, 1962	11	-	-	-	-	0.00	0.86	-	-	-	-
	Isobutanol	2-Methylpropan-1-ol	78-83-1	Williams, 1962	12	-	-	-	-	0.00	0.87	-	-	-	-
	Isobutanol	2-Methylpropan-1-ol		Ikari et al, 1990	11	-	-	-	-	0.00	1.00	-	-	-	-
	Isobutanol	2-Methylpropan-1-ol		Athès et al, 2008	9	351.9	366.4	1.76×10^{-5}	7.73×10^{-5}	0.02	0.63	2.80×10^{-5}	4.58×10^{-4}	0.28	0.71
	Isobutanol	2-Methylpropan-1-ol		Martin et al, 2009	-	-	-	-	-	0.00	0.60	-	-	-	-
	Tert-butanol	2-Methylpropan-2-ol	75-65-0	Williams, 1962	11	-	-	-	-	0.00	0.88	-	-	-	-
	2-Methylbutanol	2-Methylbutan-1-ol	137-32-6	Williams, 1962	12	-	-	-	-	0.00	0.86	-	-	-	-
	Isopentanol	3-Methylbutan-1-ol	123-51-3	Williams, 1962	15	-	-	-	-	0.00	0.87	-	-	-	-
	Isopentanol	3-Methylbutan-1-ol		Ikari et al, 1990	11	-	-	-	-	0.00	1.00	-	-	-	-
	Isopentanol	3-Methylbutan-1-ol		Athès et al, 2008	9	351.9	366.4	2.68×10^{-5}	1.23×10^{-4}	0.02	0.63	1.88×10^{-5}	7.16×10^{-4}	0.28	0.71
	Isopentanol	3-Methylbutan-1-ol		Martin et al, 2009	-	-	-	-	-	0.00	0.60	-	-	-	-
	Cis-3-hexenol	(Z)-Hex-3-en-1-ol	928-96-1	Athès et al, 2008	9	351.9	366.4	8.30×10^{-8}	2.85×10^{-7}	0.02	0.63	1.09×10^{-8}	1.18×10^{-6}	0.28	0.71
	1-Hexanol	Hexan-1-ol	111-27-3	Williams, 1962	8	-	-	-	-	0.03	0.28	-	-	-	-
	2-Phenylethanol	2-Phenylethan-1-ol	60-12-8	Athès et al, 2008	9	351.9	366.4	6.15×10^{-6}	1.03×10^{-4}	0.02	0.63	1.39×10^{-7}	6.40×10^{-6}	0.28	0.71
Carbonyl compounds	Acetaldehyde	Ethanal	75-07-0	Heitz, 1960	28	336.7	367.2	1.70×10^{-4}	8.52×10^{-2}	0.02	1.00	1.06×10^{-2}	4.82×10^{-1}	0.18	0.98
	Acetaldehyde	Ethanal		Williams, 1962	14	-	-	-	-	0.01	0.37	-	-	-	-
	Acraldehyde	Prop-2-enal	107-02-8	Williams, 1962	11	-	-	-	-	0.01	0.80	-	-	-	-
	Propionaldehyde	Propanal	123-38-6	Williams, 1962	8	-	-	-	-	0.02	0.86	-	-	-	-
	Butyraldehyde	Butanal	123-72-8	Williams, 1962	4	-	-	-	-	0.15	0.86	-	-	-	-
	Isobutyraldehyde	2-Methylpropanal	78-84-2	Williams, 1962	18	-	-	-	-	0.01	0.84	-	-	-	-
	Isobutyraldehyde	2-Methylpropanal		Ikari et al, 1998a	14	-	-	5.70×10^{-5}	1.45×10^{-3}	0.11	1.00	-	-	-	-
	Isobutyraldehyde	2-Methylpropanal		Athès et al, 2008	9	351.9	366.4	6.45×10^{-7}	6.72×10^{-6}	0.02	0.63	2.15×10^{-5}	6.25×10^{-5}	0.28	0.71
	Valeraldehyde	Pentanal	110-62-3	Williams, 1962	7	-	-	-	-	0.01	0.86	-	-	-	-
	Isovaleraldehyde	3-Methylbutanal	590-86-3	Ikari et al, 1998b	18	-	-	0.00	1.50×10^{-3}	0.00	0.99	0.00	1.86×10^{-3}	0.00	0.99

Continuation table 2-2. *Synthesis of the vapor-liquid equilibrium data available in the open literature for aroma compounds highly diluted in ethanol-mixtures at 101.3 kPa. NP: unpublished data in the original paper but provided by the authors for the current work.*

Chemical family	Aroma compound			Reference	Independent data	T range /K		x_{AC} range		x_{Et} range		y_{AC} range		y_{Et} range	
	Common name	IUPAC name	No. CAS			Min	Max	Min	Max	Min	Max	Min	Max	Min	Max
Carboxylic acids	Formic acid	Methanoic acid	64-18-6	Williams, 1962	9	-	-	-	-	0.00	0.84	-	-	-	-
	Acetic acid	Ethanoic acid	64-19-7	Williams, 1962	11	-	-	-	-	0.00	0.96	-	-	-	-
	Propionic acid	Propanoic acid	79-09-4	Williams, 1962	10	-	-	-	-	0.00	0.85	-	-	-	-
	Butyric acid	Butanoic acid	107-92-6	Williams, 1962	10	-	-	-	-	0.00	0.86	-	-	-	-
	Isobutyric acid	2-Methylpropanoic acid	79-31-2	Williams, 1962	10	-	-	-	-	0.00	0.85	-	-	-	-
	2-Methylbutyric acid	2-Methylbutanoic acid	116-53-0	Williams, 1962	4	-	-	-	-	0.08	0.42	-	-	-	-
	Isovaleric acid	3-Methylbutanoic acid	503-74-2	Williams, 1962	10	-	-	-	-	0.00	0.87	-	-	-	-
	Caproic acid	Hexanoic acid	142-62-1	Athès et al, 2008[NP]	8	351.8	365.2	9.40×10^{-7}	1.05×10^{-5}	0.04	0.68	3.82×10^{-8}	4.65×10^{-6}	0.27	0.74
	Caprylic acid	Octanoic acid	124-07-2	Athès et al, 2008[NP]	8	351.8	365.2	1.92×10^{-7}	8.84×10^{-6}	0.04	0.68	2.78×10^{-8}	6.54×10^{-6}	0.27	0.74
Esters	Ethyl acetate	Ethyl ethanoate	141-78-6	Ikari et al, 1998a	14	-	-	8.90×10^{-5}	1.59×10^{-3}	0.11	1.00	-	-	-	-
	Ethyl acetate	Ethyl ethanoate		Athès et al, 2008	9	351.9	366.4	2.01×10^{-6}	2.90×10^{-5}	0.02	0.63	7.47×10^{-5}	3.05×10^{-4}	0.28	0.71
	Isopropyl acetate	Propan-2-yl ethanoate	108-21-4	Williams, 1962	5	-	-	-	-	0.06	0.82	-	-	-	-
	Isobutyl formate	2-Methylpropyl methanoate	542-55-2	Williams, 1962	5	-	-	-	-	0.06	0.82	-	-	-	-
	Ethyl isobutyrte	Ethyl 2-methylpropanoate	97-62-1	Williams, 1962	5	-	-	-	-	0.06	0.82	-	-	-	-
	Ethyl lactate	Ethyl 2-hydroxypropanoate	97-64-3	Puentes et al, 2017	17	352.3	370.0	1.38×10^{-4}	3.45×10^{-4}	0.01	0.63	2.38×10^{-5}	3.81×10^{-4}	0.12	0.72
	Ethyl isovalerate	Ethyl 3-methylbutanoate	108-64-5	Williams, 1962	5	-	-	-	-	0.06	0.82	-	-	-	-
	Isopentyl acetate	3-Methylbutyl ethanoate	123-92-2	Ikari et al, 1998a	14	-	-	5.49×10^{-5}	1.27×10^{-3}	0.11	1.00	-	-	-	-
	Isopenyl acetate	3-Methylbutyl ethanoate		Athès et al, 2008	9	351.9	366.4	2.03×10^{-7}	6.44×10^{-6}	0.02	0.63	3.52×10^{-6}	7.12×10^{-5}	0.28	0.71
	Ethyl caproate	Ethyl hexanoate	123-66-0	Athès et al, 2008	9	351.9	366.4	5.69×10^{-8}	4.32×10^{-6}	0.02	0.63	1.38×10^{-6}	1.41×10^{-4}	0.28	0.71
	Ethyl caproate	Ethyl hexanoate		Martin et al, 2009	-	-	-	-	-	0.00	0.60	-	-	-	-
	2-Phenylethyl acetate	2-Phenylethyl ethanoate	103-45-7	Athès et al, 2008	9	351.9	366.4	7.62×10^{-7}	3.90×10^{-6}	0.02	0.63	6.29×10^{-8}	1.14×10^{-5}	0.28	0.71
	Ethyl caprylate	Ethyl octanoate	106-32-1	Athès et al, 2008	9	351.9	366.4	5.28×10^{-9}	5.93×10^{-7}	0.02	0.63	6.84×10^{-8}	9.64×10^{-6}	0.28	0.71
	Diethyl succinate	Diethyl butane-1,4-dioate	123-25-1	Martin et al, 2009	-	-	-	-	-	0.00	0.60	-	-	-	-
	Ethyl caprate	Ethyl decanoate	110-38-3	Athès et al, 2008	9	351.9	366.4	1.00×10^{-9}	5.33×10^{-7}	0.02	0.63	2.75×10^{-8}	1.19×10^{-5}	0.28	0.71
Furans	Furfural	Furan-2-carbaldehyde	98-01-1	Williams, 1962	9	-	-	-	-	0.01	0.85	-	-	-	-
	Furfural	Furan-2-carbaldehyde		Ikari et al, 1984	13	-	-	-	-	0.00	1.00	-	-	-	-
	Furfural	Furan-2-carbaldehyde		Athès et al, 2008	9	351.9	366.4	1.88×10^{-6}	5.06×10^{-6}	0.02	0.63	7.18×10^{-7}	9.84×10^{-6}	0.28	0.71
Terpens	Linalool	3,7-dimethylocta-1,6-dien-3-ol	78-70-6	Athès et al, 2008	9	351.9	366.4	3.27×10^{-7}	4.51×10^{-6}	0.02	0.63	1.22×10^{-7}	2.66×10^{-5}	0.28	0.71
	Linalool	3,7-dimethylocta-1,6-dien-3-ol		Deterre et al, 2012	27	351.5	370.0	1.54×10^{-6}	6.80×10^{-5}	0.01	0.88	1.40×10^{-6}	2.93×10^{-4}	0.09	0.89
	Linalool oxide	2-(Tetrahydro-5-methyl-5-vinyl-2-furyl) propan-2-ol	60047-17-8	Deterre et al, 2012	27	351.5	370.0	6.73×10^{-6}	7.33×10^{-5}	0.01	0.88	1.24×10^{-6}	2.08×10^{-4}	0.09	0.89

2.2.2. THERMODYNAMIC MODELING

The principle for vapor-liquid equilibrium modeling is the equality of chemical potentials of every species in both phases, in conditions of thermal and mechanical equilibrium. For engineering applications, the equilibrium condition is written in terms of fugacity, variable that corresponds to a generalized partial pressure and that depends on the temperature (T), pressure (P) and composition [Prausnitz et al., 1999 ; Rios, 2009].

By following a classical heterogeneous approach, also known as gamma-phi (γ-ϕ) method, the vapor phase fugacity of the component i, $f_i^V(T,P,y)$, can be expressed as a function of the fugacity coefficient, $\phi_i^V(T,P,y)$, and the liquid phase fugacity, $f_i^L(T,P,x)$, as a function of the activity coefficient, $\gamma_i(T,x)$, and the standard state liquid fugacity, $f_i^{OL}(T,P)$. The resulting expressions are:

$$f_i^V(T,P,y) = f_i^L(T,P,x) \quad [2\text{-}1]$$

$$\phi_i^V(T,P,y) y_i P = \gamma_i(T,x) x_i f_i^{OL}(T,P) \quad [2\text{-}2]$$

At atmospheric pressure, the standard state liquid fugacity can be approximated to the vapor pressure of the pure component at the temperature of the system, $P_i^O(T)$, and the vapor phase can be considered as an ideal gas mixture, which means that fugacity coefficient is equal to 1. In this way, equation 2-2 becomes:

$$y_i P = \gamma_i(T,x) x_i P_i^O(T) \quad [2\text{-}3]$$

Which can in turn be rewritten to obtain an expression for the absolute volatility, as follows:

$$K_i(T,P,x) = \frac{y_i}{x_i} = \frac{\gamma_i(T,x) P_i^O(T)}{P} \quad [2\text{-}4]$$

The relative volatility with respect to ethanol and water are defined as the ratio of absolute volatilities, that is:

$$\alpha_{i/Et}(T,x) = \frac{K_i}{K_{Et}} = \frac{y_i/x_i}{y_{Et}/x_{Et}} = \frac{\gamma_i(T,x) P_i^O(T)}{\gamma_{Et}(T,x) P_{Et}^O(T)} \quad [2\text{-}5]$$

$$\alpha_{i/W}(T,x) = \frac{K_i}{K_W} = \frac{y_i/x_i}{y_W/x_W} = \frac{\gamma_i(T,x) P_i^O(T)}{\gamma_W(T,x) P_W^O(T)} \quad [2\text{-}6]$$

In the case of carboxylic acids, it is necessary to use a supplementary term that account for the chemical equilibrium [Detcheberry et al., 2016]. Indeed, theoretical and experimental studies [Allen and Galdin, 1953 ; Vawdrey et al., 2004] have demonstrated that this kind of compounds can exist either as monomer (single molecules) or dimers, due to strong hydrogen bonds. This phenomenon is referred to as association or dimerization interactions and essentially takes place in the vapor phase. Higher polymerization and heterodimerization (formation of dimers from monomers of different chemical species) have also been discussed in the literature [Miyamoto et al., 2001 ; Zhu et al., 2013], but they will not be taken into account in this work for the sake of simplicity.

For a carboxylic acid Ac_i the reactions and corresponding chemical equilibrium constant (KD_{Aci}) can be expressed as follows:

$$2Ac_i \rightleftharpoons Ac_{i2} \qquad KD_{Aci}(T)=\upsilon\left(10^{\,L_{Aci}+M_{Aci}/T}\right) \qquad [2\text{-}7]$$

T is given in K and the parameter υ is a correction factor to express KD_{Aci} in kPa^{-1}, equal to 7.5.

Based on this representation, Detcheberry et al. (2016) have proposed the following correction for the Equation 2-3:

$$\frac{y_i P}{\phi_i^{OV}(T,P_i^O(T))}=\gamma_i(T,x)x_i P_i^O(T) \qquad For\ i=Ac_i \qquad [2\text{-}8]$$

Where the term $\phi_i^{OV}(T,P_i^O(T))$ can be calculated with the following relation:

$$\phi_i^{OV}(T,P_i^O(T))=\frac{-1+\left[4KD_i(T)P_i^O(T)\right]^{1/2}}{2KD_i(T)P_i^O(T)} \qquad For\ i=Ac_i \qquad [2\text{-}9]$$

Therefore, the alternative equations for calculating K_i and $\alpha_{i/Et}$ are:

$$K_i(T,P,x)=\frac{y_i}{x_i}=\frac{\gamma_i(T,x)P_i^O(T)\phi_i^{OV}(T,P_i^O(T))}{P} \qquad For\ i=Ac_i \qquad [2\text{-}10]$$

And

$$\alpha_{i/Et}(T,x)=\frac{K_i}{K_{Et}}=\frac{y_i/x_i}{y_{Et}/x_{Et}}=\frac{\gamma_i(T,x)P_i^O(T)\phi_i^{OV}(T,P_i^O(T))}{\gamma_{Et}(T,x)P_{Et}^O(T)} \qquad For\ i=Ac_i \qquad [2\text{-}11]$$

$$\alpha_{i/W}(T,x)=\frac{K_i}{K_W}=\frac{y_i/x_i}{y_W/x_W}=\frac{\gamma_i(T,x)P_i^O(T)\phi_i^{OV}(T,P_i^O(T))}{\gamma_W(T,x)P_W^O(T)} \qquad For\ i=Ac_i \qquad [2\text{-}12]$$

The parameters L_{ACi} and M_{ACi} for the calculation of the chemical equilibrium constants were taken from the DECHEMA literature, available through the Simulis® Thermodynamics software [Gmehling et al., 2001]. The values for 2-methylbutanoic acid and subsequent acids were estimated by interpolation or extrapolation, by only taking account of the number of carbon atoms.

In the region of very low concentration, it is customary to define the activity of the component i with respect to its fugacity at infinite dilution, at the temperature and pressure of the mixture. The liquid fugacity is then expressed in an alternative way, the so called Henry law [Vidal, 2003]:

$$f_i^L(T,P,x)=x_i\mathcal{H}_i(T,P,x_s) \qquad [2\text{-}13]$$

$\mathcal{H}_i$, or Henry constant, corresponds to the reference liquid fugacity, and is defined by the following relation:

$$\mathcal{H}_i(T,P,x_s)=\lim_{x_i\to 0}\frac{f_i^L(T,P,x)}{x_i} \qquad [2\text{-}14]$$

$\mathcal{H}_i$ depends not only on temperature and pressure, but also on the solvent nature (here ethanol – water) and its composition, x_s. By comparison with equation 2-3, $\mathcal{H}_i$ can also be expressed as the product $P_i^O(T)$ and $\gamma_i(T,\boldsymbol{x})$ at infinite dilution or $\gamma_i^\infty(T,x_s)$:

$$\mathcal{H}_i(T,x_s)=\gamma_i^{\infty}(T,x_s)P_i^0(T) \quad [2\text{-}15]$$

Or, by comparison with equation 2-4, as a function of the absolute volatility and total pressure:

$$\mathcal{H}_i(T,x_s)=K_iP \quad [2\text{-}16]$$

In the current study, the vapor pressure of ethanol, water and the aroma compounds have been calculated with the Riedel equation [Vetere, 1991], an extended version of the Antoine equation:

$$P_i^0(T) = \frac{1}{1000} exp\left(A_i + \frac{B}{T} + C_i ln(T) + D_i T^{E_i}\right) \quad [2\text{-}17]$$

With $P_i^0(T)$ given in kPa and T in K. A_i, B_i, C_i, D_i, E_i are coefficients specific for each chemical species. Two sources were used to obtain them:

- For the compounds already included in the Simulis Thermodynamics database, the coefficients were taken from the DIPPR Database [Rowley et al].
- For the five compounds added to the Simulis Thermodynamics database, the coefficients were estimated by regression of experimental data available in the literature. [Dreisbach and Shrader, 1949; Verevkin et Heintz, 1999; Covarrubias-Cervantes et al., 2004 ; Zaitsau et al., 2009; Benziane et al., 2011; Kozlovskiy et al., 2015; Stejfa et al., 2015; GESTIS, 2016; INIST, 2016]. The minimized objective function (OF) is as follows:

$$\mathrm{OF}(P^0)=\sum_{k=1}^{N}\left(\frac{P^0_{k\text{-}exp}-P^0_{k\text{-}calc}}{P^0_{k\text{-}exp}}\right)^2 \quad [2\text{-}18]$$

And the absolute average relative error (*AAD%*) between experimental and calculated pressure was obtained with **equation 2-19**:

$$\mathrm{AAD\%}(\mathrm{P^0})=\sum_{k=1}^{N}\left|\frac{P^0_{k\text{-}exp}-P^0_{k\text{-}calc}}{P^0_{k\text{-}exp}}\right| 100\% \quad [2\text{-}19]$$

Due to the relatively limited number of experimental values, the coefficients D_i and E_i were fixed to 0. The data used for this estimation are compiled in **Appendix A1**. The values of AAD% vary between 1% for 2-phenylethyl ethanoate and 6% for ethyl decanoate.

For the set of 44 aroma compounds, the coefficients are valid in the temperature range of vapor-liquid equilibrium for hydro-alcoholic mixtures at 101.3 kPa, from 351.4 K to 373.15 K.

With regard to the activity coefficient, the NRTL (Non-Random Two Liquid) model was used in this work [Renon and Prautnitz, 1968]. It is a pressure-independent model of liquid solution based on the concept of local composition introduced by Wilson (1964), valid at low pressures (less than 1000 kPa) and widely recommended for the description of hydro-alcoholic solutions [Valderrama et al., 2012].

According to the NRTL model, the activity coefficient of a component i in a mixture of n components as a function of composition and temperature is given by:

$$ln\,\gamma_i\,(T,\boldsymbol{x}) = \frac{\sum_{j=1}^{n}\tau_{ji}G_{ji}x_j}{\sum_{k=1}^{n}G_{ki}x_k} + \sum_{j=1}^{n}\frac{G_{ij}x_j}{\sum_{k=1}^{n}G_{kj}x_k}\left(\tau_{ij} - \frac{\sum_{k=1}^{n}\tau_{kj}G_{kj}x_k}{\sum_{k=1}^{n}G_{kj}x_k}\right) \quad [2\text{-}20]$$

With

$$G_{ij} = exp\,(-c_{ij}\tau_{ij}) \quad [2\text{-}21]$$

Here, G_{ij}, c_{ij} and τ_{ij} are binary interaction parameters. Their temperature dependence is evaluated according to the following formalism, included in the Simulis® Thermodynamics package:

$$c_{ij} = c_{ij}^{0} + c_{ij}^{T}(T\text{-}273.15) \quad [2\text{-}22]$$

$$\tau_{ij} = \frac{g_{ij} - g_{jj}}{RT} = \frac{A_{ij}^{0} + A_{ij}^{T}(T\text{-}273.15)}{RT} \quad [2\text{-}23]$$

In **equation 2-23**, R is the ideal gas constant. The interaction variables A_{ij}^{0}, A_{ij}^{T} (non-symmetric, $A_{ij}^{0} \neq A_{ji}^{0}$ and $A_{ij}^{T} \neq A_{ji}^{T}$), c_{ij}^{0} and c_{ij}^{T} (symmetric, $c_{ij}^{0} = c_{ji}^{0}$ and $c_{ij}^{T} = c_{ji}^{T}$) are specific to each pair of chemical species. They must be obtained by the least-square method, from experimental equilibrium data and/or other thermophysical properties of the liquid phase. The estimation of these parameters for the different aroma compounds, object of this paper, is presented in the next section.

2.3. Results and discussion

A database including all the experimental vapor-liquid equilibria data previously presented was created and used for the generation of a set of binary interaction parameters of the NRTL model. This set, named NRTL-0, will be used to simulate distillation units involved in the production of alcoholic beverages. In this section, the estimation methodology and the parameters obtained are presented (section 2.3.1.), followed by a classification of the aroma compounds according to their relative volatilities (section 2.3.2.) using the model representation over the whole ethanol concentration range in the liquid phase ($0<x_{Et}<1$). The discussion is concluded with a comparison of the equilibrium representation for some aroma compounds using several sets of parameters (section 2.3.3.): (i) The main set (NRTL-0), (ii) a set estimated from binary data for mixtures aroma compound – ethanol and aroma compound – water (named NRTL-B) and (iii) a set from ternary data for mixtures aroma compound at finite concentration – ethanol – water (named NRTL-T). Given that data at high dilution are scarce and more difficult to measure, the objective of this comparison is to evaluate if the representation from equilibrium data at finite concentration would be accurate enough for simulation purposes of other aroma compounds, similar in nature to those studied in this work, in the alcoholic beverages field.

2.3.1. GENERATION OF A SET OF BINARY INTERACTION PARAMETERS

The objective of modeling with the NRTL model is to determine a set of interaction parameters for the group of 44 aroma compounds in ethanol-water mixtures, using directly the source of experimental information found in the literature. In consideration of the big number of chemical species, the following assumptions are considered to simplify the model identification problem:

- The main one is that the interactions between aroma compounds are neglected, as their molar fractions in the liquid phase are equal or lower than $x_{AC}<10^{-4}$, the limit of infinite dilution defined by Alessi et al. (1991). This means that $\tau_{ij}=0$, when i and j are both aroma compounds. In this way, the only interaction parameters considered are those associated to the solvent binary ethanol (2) – water (3) and to the pairs aroma compound (1) – ethanol (2) and aroma compound (1) – water (3).
- The non-randomness parameters, c_{ij}^{0} and c_{ij}^{T}, are respectively set to 0.3 and 0 for all binaries. This assumption is valid for systems in vapor-liquid equilibrium [Renon et Prausnitz, 1968].
- For the binaries aroma compound (1) - ethanol (2) and aroma compound (1) - water (3), A_{ij}^{T}, the temperature-dependent parameter of τ_{ij}, is neglected. Two factors justify this approximation: (1) the number of experimental data is limited and (2) the equilibrium temperature interval is reduced (from 351.44 K to 373.15 K).
- The interaction parameters of the binary ethanol (2) - water (3) are obtained from the literature [Kadir, 2009]. The values are presented in **table 2-3**. The reliability of these parameters was verified by fitting the experimental data (79 independent points) measured by different authors [Lai et al., 2014; Arce et al., 1996; Yang and Wang, 2002; Kamihama et al., 2012]. The average relative deviation between the experimental and the calculated temperatures was 0.2 % and that of the absolute volatilities of ethanol and water, 3.1 % and 2.2 %, respectively. The equilibrium diagram including the experimental data and the NRTL representation is presented in **figure 2-1**.

In this way, the problem was reduced to the estimation of a set of 4 parameters for each aroma compound, that is, 176 parameters:

- 88 associated with each binary aroma compound (1) - ethanol (2): A_{12}^{0}, A_{21}^{0}.
- 88 associated with each binary aroma compound (1) - water (3): A_{13}^{0}, A_{31}^{0}.

The parameters were estimated by minimizing an objective function through the Excel Solver for non-linear problems [Solver, 2017]. The equilibrium property considered was the relative volatility of the aroma compound with respect to ethanol, $\alpha_{AC/Et}$. This selection is due to the fact that the interaction parameters will be used for the simulation of distillation units, whose separation performance is directly based upon the difference of volatilities between the chemical species. The relative volatility condenses all the information about the equilibrium distribution of an aroma compound and its behaviour with respect to ethanol, main component of the distillate, the product of interest.

Table 2-3. *Interaction parameters of the of the NRTL model for the binary ethanol (2) – water (3) and fitting quality statistics with respect to four experimental data sets obtained from literature.*

A_{23}^0 / cal·mol^{-1}	A_{32}^0 / cal·mol^{-1}	A_{23}^T / cal·mol^{-1}·K^{-1}	A_{32}^T / cal·mol^{-1}·K^{-1}	K_{Et}				K_W				T			
				Range		RMSE	AAE%	Range		RMSE	AAE%	Range		RMSE	AAE%
				Min	Max			Min	Max			Min	Max		
34.02	850.12	-1.80	5.65	1.0	38.8	2.9	3.1%	0.6	1.1	0.0	2.2%	351.3	373.2	0.3	0.2%

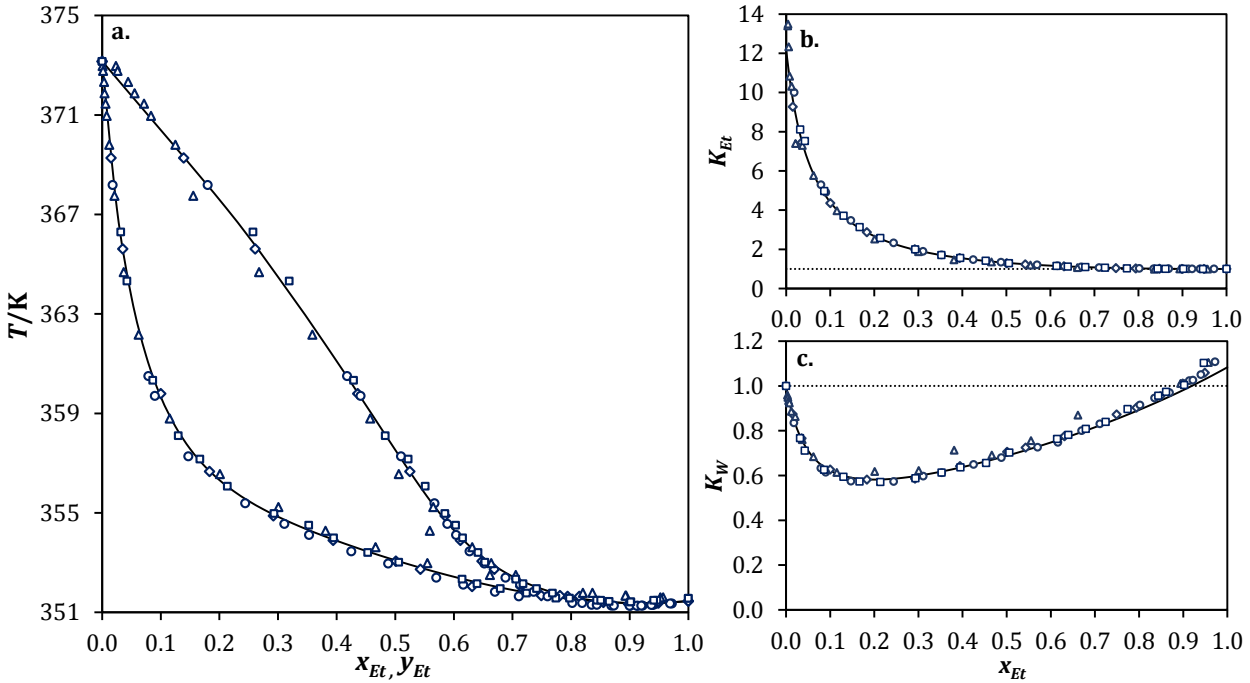

Figure 2-1. *a. Vapor-liquid equilibrium diagram of the binary system ethanol – water at 101.3 kPa (T is the temperature, y_{Et} the ethanol mole fraction in the vapor phase and x_{Et} the ethanol mole fraction in the liquid phase). b. Evolution of the absolute volatility of ethanol (K_{Et}) with liquid composition (x_{Et}). c. Evolution of the absolute volatility of water (K_W) with liquid composition (x_{Et}). Experimental data from:* ◇ *Lai et al., 2014).*[20] *(□ Arce et al., 1996). (△ Yang and Wang, 2002). (○ Kamihama et al., 2012). (——) NRTL model using the interaction parameters calculated by Kadir (2009).*

The objective function is written in terms of an absolute deviation, formulation that gives more weight to high values of $\alpha_{AC/Et}$:

$$OF(\alpha)=\sum_{k=1}^{N}\left(\alpha_{AC/Et\ Exp_k}-\alpha_{AC/Et\ Calc_k}\right)^2 \quad [2\text{-}24]$$

Where N is the number of independent data, $\alpha_{AC/Et\ Exp_k}$ is the experimental value of $\alpha_{AC/Et}$ and $\alpha_{AC/Et\ Calc_k}$ the valued calculated with the NRTL model. For the majority of aroma compounds, the relative volatility is higher when the ethanol concentration in the liquid phase is low and this corresponds to the region in which distillation of alcoholic beverages takes place.

The calculation of $\alpha_{AC/Et}$ was carried out using the Bubble Temperature algorithm of the Simulis® Thermodynamics package. The values of two variables were fixed to the experimental values, namely, pressure (P) and composition in the liquid phase ($\boldsymbol{x}$). The algorithms allows to compute the temperature (T) and the compositions of the vapor phase ($\boldsymbol{y}$) in equilibrium. $\alpha_{AC/Et}$ is obtained with equation 2-5 or equation 2-11, for carboxylic acids.

The fitting quality is evaluated with respect to three variables (U): K_{AC}, $\alpha_{AC/Et}$ and $\alpha_{AC/W}$. Two statistics were calculated:

Absolute average relative error (*AAE%*):

$$AAD\ \%=\frac{1}{N}\sum_{k=1}^{N}\left|\frac{U_{k\ Exp}-U_{k\ Calc}}{U_{k\ Exp}}\right|100\% \quad [2\text{-}25]$$

Root-mean-squared error (*RMSE*):

$$RMSE=\left[\frac{1}{N}\sum_{k=1}^{N}\left(U_{Exp\ i}-U_{i\ Calc}\right)^2\right]^{1/2} \quad [2\text{-}26]$$

With reference to the interaction parameters already published in the literature, only those proposed for ethyl lactate by the same authors [Puentes et al., 2017] are directly used in this work. For uniformity reasons, those presented by Athès et al. (2008) and Deterre et al. (2012) were recalculated from the corresponding equilibrium data, as in both cases $A_{ij}^{T} \neq 0$. In relation to the parameters from Athès et al. (2008), it is important to indicate that an alternative formalism was used by the authors to evaluate the temperature dependence of the interaction parameter τ_{ij}. The expression is:

$$\tau_{ij}=a_{ij}+\frac{b_{ij}}{T} \quad [2\text{-}27]$$

By comparison with equation 2-23, the following equivalence with the formalism of the current work is deduced:

$$\frac{A_{ij}^{0}}{RT}+\frac{A_{ij}^{T}(T\text{-}273.15)}{RT}=a_{ij}+\frac{b_{ij}}{T}$$

$$\frac{A_{ij}^{T}}{R}+\frac{A_{ij}^{0}\text{-}273.15A_{ij}^{T}}{RT}=a_{ij}+\frac{b_{ij}}{T}$$

Whence,

$$A_{ij}^{T}=a_{ij}R \quad [2\text{-}28]$$

$$A_{ij}^{0}=b_{ij}R+273.15A_{ij}^{T}=R(b_{ij}+273.15a_{ij}) \quad [2\text{-}29]$$

And consequently, since $a_{ij}\neq 0$, necessarily $A_{ij}^{T}\neq 0$, as stated above.

The new set of interaction parameters for the 44 aroma compounds as well as the statistics of fitting are summarized in **table 2-4**. According to these information, the RMSE of K_{AC} varies between 0.0 and 6.9 with an overall average of 1.3, error that remains small regarding the order of magnitude of this property, between 10^0 and 10^2. For $\alpha_{AC/Et}$ (order of magnitude between 10^0 and 10^1), the RMSE is in the range from 0.0 to 1.1 with an overall average of 0.2, and for $\alpha_{AC/Et}$ (order of magnitude between 10^0 and 10^2) the overall average is 2.1. Regarding AAE%, the overall average is about 12% for the three equilibrium variables with a variation range between 1% and 33%. The analysis by chemical family indicates that the lowest deviations are associated to acetals, overall AAE% around 7%, while the highest deviation concern the terpenes, with an overall AAE% of the order of 25%.

The evolution of absolute and relative volatilities with the ethanol composition in the liquid phase is presented in **figures 2-2 to 2-4** for 6 representative aroma compounds: ethyl ethanoate, ethanal, propan-1-ol, furan-2-carbaldehyde, ethanoic acid and methanoic acid. These compounds were classified according to the criterion presented in section 3.2: ethyl ethanoate and ethanal as light compounds, propan-1-ol and furan-2-carbaldehyde as intermediary compounds, and ethanoic and methanoic acid as heavy compounds. In some of these figures, the representation with different sets of interaction parameters is also depicted. A comparative interpretation of theses curves is developed later, in section 3.3.

Regarding the experimental data, one can observe that they are globally well represented by the NRTL model, using the interaction parameters calculated in this work (NRTL-0 set). For all compounds, both K_{AC} and $\alpha_{AC/W}$ decrease when the liquid phase is enriched in ethanol, behaviour that have already been identified for other aroma compounds [*Athès et al., 2008; Puentes et al., 2017b*]. Concerning $\alpha_{AC/Et}$, the evolution with composition are more variable, independently of its order of magnitude. Three trends can be identified: (i) decreasing (for ethyl ethanoate, propan-1-ol, furfural and most of the aroma compounds studied in this work), (ii) slightly linear increasing (for ethanoic acid) and (iii) nearly constant, in the case of ethanal, after a slight increase of $\alpha_{AC/Et}$ in the region of low ethanol concentration ($x_{Et}<1$).

As for the Henry constant of aroma compounds, this parameter can be calculated at boiling conditions by using directly the absolute volatility data, according to equation 2-16. The values of $\ln \mathcal{H}_{AC}$ as a function of T^{-1} are depicted in **figure 2-5** for the same aroma compounds. As in the previous figures, model curves obtained with different parameters sets are plotted.

Table 2-4. *Binary interactions parameters of the NRTL model for aroma compounds (1) highly diluted in ethanol (2) –water (3) mixtures at 101.3 kPa. Intervals and statistics of fitting quality for absolute and relative volatilities.*

Aroma compound	i	j	A_{ij}^0 / cal·mol^{-1}	A_{ji}^0 / cal·mol^{-1}	K_{AC}				$\alpha_{AC/Et}$				$\alpha_{AC/W}$			
					Range		RMSE	AAE%	Range		RMSE	AAE%	Range		RMSE	AAE%
					Min	Max			Min	Max			Min	Max		
1,2-Diethoxyethane	1	2	3606.7	1070.8	6.1	39.9	1.0	7%	3.3	6.8	0.4	7%	5.6	40.0	1.5	7%
	1	3	14141.7	2768.4												
Methanol	1	2	501.4	-479.1	1.5	6.8	0.2	5%	0.6	1.5	0.1	4%	1.4	6.8	0.2	9%
	1	3	44211.4	502.1												
Prop-2-en-1-ol	1	2	-779.8	1121.2	0.5	10.8	0.1	5%	0.5	0.9	0.0	5%	0.5	10.8	0.2	5%
	1	3	4799.4	992.2												
Propan-1-ol	1	2	-452.9	685.7	0.6	16.8	1.6	16%	0.6	1.4	0.2	12%	0.5	16.9	2.2	21%
	1	3	-434.4	2536.2												
Propan-2-ol	1	2	65.5	-33.5	0.9	22.0	0.3	2%	0.9	1.8	0.0	2%	0.8	22.0	0.3	2%
	1	3	-245.4	2067.3												
Butan-1-ol	1	2	-1059.5	1792.1	0.2	23.1	0.4	4%	0.2	1.9	0.0	4%	0.2	23.1	0.5	4%
	1	3	-490.7	3423.3												
2-Methylpropan-1-ol	1	2	-935.2	1560.0	0.4	29.9	0.3	3%	0.4	2.5	0.0	3%	0.3	30.0	0.4	3%
	1	3	-505.1	3358.8												
2-Methylpropan-2-ol	1	2	-679.6	805.4	0.7	33.1	0.5	2%	0.7	2.7	0.1	2%	0.7	33.2	0.6	2%
	1	3	-60.2	2182.1												
2-Methylbutan-1-ol	1	2	25.2	-25.9	0.1	30.1	1.5	27%	0.1	2.5	0.2	27%	0.1	30.2	1.9	27%
	1	3	412.9	2994.5												
3-Methylbutan-1-ol	1	2	-1914.3	4567.3	0.1	32.0	0.6	10%	0.1	2.7	0.1	10%	0.1	32.1	0.6	10%
	1	3	-506.6	4070.5												
(Z)-Hex-3-en-1-ol	1	2	-1429.0	1893.1	0.0	23.4	0.2	12%	0.0	1.9	0.2	23%	0.0	23.4	1.0	10%
	1	3	1901.2	3040.5												
Hexan-1-ol	1	2	2396.1	-431.6	0.1	35.2	1.9	33%	0.1	2.9	0.1	24%	0.1	35.3	2.4	33%
	1	3	2429.5	3342.0												
2-Phenylethanol	1	2	-1747.3	3693.2	0.0	1.3	0.1	26%	0.0	0.1	0.0	23%	0.0	1.3	0.2	26%
	1	3	-1363.3	5732.5												

Continuation Table 2-4. *Binary interactions parameters of the NRTL model for aroma compounds (1) highly diluted in ethanol (2) –water (3) mixtures at 101.3 kPa.*

Aroma compound	i	j	A_{ij}^0 / cal·mol^{-1}	A_{ji}^0 / cal·mol^{-1}	K_{AC}				$\alpha_{AC/Et}$				$\alpha_{AC/W}$			
					Range		RMSE	AAE%	Range		RMSE	AAE%	Range		RMSE	AAE%
					Min	Max			Min	Max			Min	Max		
Ethanal	1	2	1125.5	-670.2	5.7	61.3	6.9	18%	5.1	6.3	0.8	12%	5.3	61.6	8.3	18%
	1	3	70.5	1343.1												
Prop-2-enal	1	2	43743.2	134.3	2.7	29.6	0.8	14%	2.4	4.5	0.6	14%	2.4	30.1	2.0	14%
	1	3	47491.6	1505.7												
1-Propanal	1	2	23119.1	-235.3	1.8	51.0	0.8	11%	1.8	6.5	0.5	11%	1.7	51.3	2.2	11%
	1	3	1250.8	1040.5												
Butanal	1	2	-539.5	963.0	1.7	124.4	1.2	10%	1.7	10.5	0.4	10%	1.5	125.9	1.6	10%
	1	3	1399.3	2243.2												
2-Methylpropanal	1	2	5260.8	-791.7	1.1	154.5	5.6	22%	1.1	12.8	1.1	18%	1.0	154.6	12.5	26%
	1	3	1276.8	2169.7												
Pentanal	1	2	-812.4	1629.9	0.9	121.4	6.6	12%	0.9	10.1	1.0	11%	0.8	122.9	9.3	12%
	1	3	1096.0	2928.6												
3-Methylbutanal	1	2	676.5	-19.9	1.3	235.0	0.1	3%	1.3	19.8	0.1	4%	1.2	239.6	0.1	3%
	1	3	1183.4	3145.6												
Methanoic acid	1	2	3499.5	-1064.2	0.1	0.5	0.0	4%	0.0	0.1	0.0	1%	0.1	0.5	0.0	4%
	1	3	926.0	-562.5												
Ethanoic acid	1	2	1018.8	-397.0	0.1	0.8	0.0	1%	0.1	0.1	0.0	1%	0.1	0.8	0.0	1%
	1	3	-492.8	1590.0												
Propanoic acid	1	2	3535.6	-589.3	0.1	1.0	0.0	5%	0.1	0.1	0.0	5%	0.0	1.0	0.0	5%
	1	3	-211.6	1848.5												
Butanoic acid	1	2	-1114.2	2026.4	0.0	2.0	0.0	2%	0.0	0.2	0.0	2%	0.0	2.0	0.0	2%
	1	3	-838.0	3724.0												
2-Methylpropanoic acid	1	2	1770.5	-702.0	0.0	2.1	0.1	9%	0.0	0.2	0.0	9%	0.0	2.1	0.1	9%
	1	3	761.6	1841.7												
2-Methylbutanoic acid	1	2	-1395.3	1472.7	0.0	2.0	0.0	6%	0.0	0.2	0.0	6%	0.0	2.0	0.0	6%
	1	3	477.4	2222.9												
3-Methylbutanoic acid	1	2	-1223.8	2147.9	0.0	4.0	0.4	14%	0.0	0.3	0.0	4%	0.0	4.0	0.4	14%
	1	3	-566.0	3887.2												
Hexanoic acid	1	2	1139.6	960.7	0.0	8.1	0.7	25%	0.0	0.7	0.1	25%	0.0	8.1	0.9	26%
	1	3	-846.2	5941.1												

Aroma compound	i	j	A_{ij}^0 / cal·mol^{-1}	A_{ji}^0 / cal·mol^{-1}	K_{AC}				$\alpha_{AC/Et}$				$\alpha_{AC/W}$			
					Range		RMSE	AAE%	Range		RMSE	AAE%	Range		RMSE	AAE%
					Min	Max			Min	Max			Min	Max		
Octanoic acid	1	2	1991.7	1810.6	0.0	17.2	0.0	24%	0.0	1.4	0.0	23%	0.0	17.2	0.1	24%
	1	3	10939.2	6231.9												
Ethyl ethanoate	1	2	1601.5	-433.2	1.8	129.5	3.6	12%	1.8	10.8	0.6	13%	1.6	131.2	8.1	17%
	1	3	715.2	2560.2												
1-methylethyl ethanoate	1	2	-1405.6	3226.0	1.7	169.1	0.8	2%	1.7	14.2	0.1	2%	1.7	172.0	1.1	2%
	1	3	-1028.5	5115.6												
2-methylpropyl methanoate	1	2	3952.5	104.9	1.7	72.3	0.4	4%	1.7	6.0	0.1	4%	1.6	72.8	0.5	4%
	1	3	290.7	2872.8												
Ethyl 2-methylpropanoate	1	2	1282.8	-18.7	1.0	384.0	2.7	5%	1.0	33.0	0.1	5%	0.9	399.3	3.0	5%
	1	3	1990.7	3770.8												
Ethyl 2-hydroxypropanoate	1	2	455.5	-343.5	0.1	3.9	0.1	10%	0.1	0.3	0.0	10%	0.1	3.9	0.1	10%
	1	3	-349.3	2758.1												
Ethyl 3-methylbutanoate	1	2	-362.5	1232.4	0.5	214.8	2.6	7%	0.5	18.1	0.4	8%	0.4	219.5	3.5	7%
	1	3	3205.5	3937.3												
3-Methylbutyl ethanoate	1	2	-1574.4	2894.8	0.1	223.8	1.5	20%	0.1	18.5	0.3	18%	0.1	224.0	4.4	23%
	1	3	2324.7	4048.3												
Ethyl hexanoate	1	2	7760.3	1590.9	0.6	81.6	1.8	11%	0.6	6.7	0.5	11%	0.5	81.6	3.7	11%
	1	3	6440.1	4451.2												
2-Phenylethyl ethanoate	1	2	-1662.4	2717.4	0.0	18.8	1.8	22%	0.0	1.5	0.0	17%	0.0	18.8	3.0	23%
	1	3	603.8	5060.5												
Ethyl octanoate	1	2	-2025.0	4702.3	0.0	339.3	1.0	22%	0.0	28.0	0.2	20%	0.0	339.4	2.9	25%
	1	3	1091.0	6332.6												
Diethyl butane-1,4-dioate	1	2	4366.2	1227.9	0.1	1.9	0.0	6%	0.1	0.2	0.0	6%	0.1	1.9	0.0	6%
	1	3	-629.7	4389.9												
Ethyl decanoate	1	2	-2077.9	4754.5	0.0	1005.0	0.5	27%	0.0	82.9	0.1	27%	0.0	1005.3	1.5	29%
	1	3	1600.1	8104.5												
Furan-2-carbaldehyde	1	2	136.1	411.2	0.1	5.3	0.5	17%	0.1	0.4	0.0	14%	0.1	5.3	0.7	19%
	1	3	350.5	2429.3												
Linalool	1	2	-2256.0	3773.8	0.0	99.4	5.7	24%	0.0	8.2	1.0	23%	0.0	99.5	8.6	26%
	1	3	2698.1	4988.9												
Linalool oxide	1	2	-602.6	3207.8	0.1	63.3	2.6	27%	0.0	5.2	0.3	27%	0.1	63.4	3.1	29%
	1	3	-1151.9	8266.7												

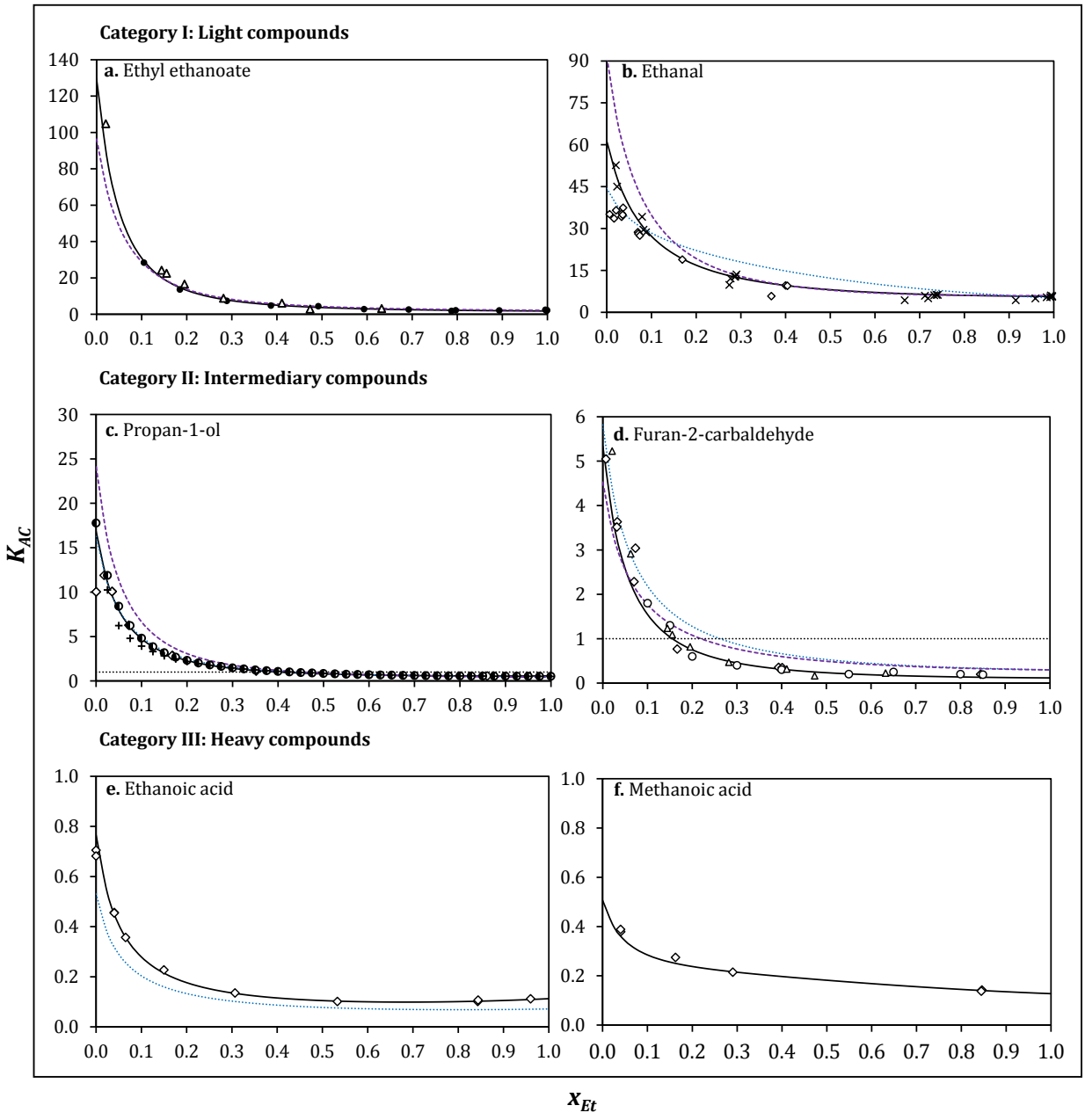

Figure 2-2. *Evolution of the absolute volatility of aroma compounds (K_{AC}) with the ethanol composition in the liquid phase (x_{Et}) at 101.3 kPa for: Category I. Light compounds: a. Ethyl ethanoate; b. Ethanal. Category II. Intermediary compounds: c. Propan-1-ol; d. Furan-2-carbaldehyde. Category III. Heavy compounds: e. Ethanoic acid; f. Methanoic acid. Experimental data at high dilution from: (✕ Heitz 1960) (◇ Williams, 1962) (△ Athès et al., 2008) (○ Ikari et al., 1984) (◐ Ikari et al., 1990) (● Ikari et al., 1998) (✚ Martin et al., 2009). Calculation with NRTL model using: (——) NRTL-0 parameters set (estimated from data at high dilution, Table 2-4). (·····) NRTL-B parameters set (estimated from binary data, Table 2-8). NRTL-T parameters set (·– – –) (estimated from ternary data, Table 2-9).*

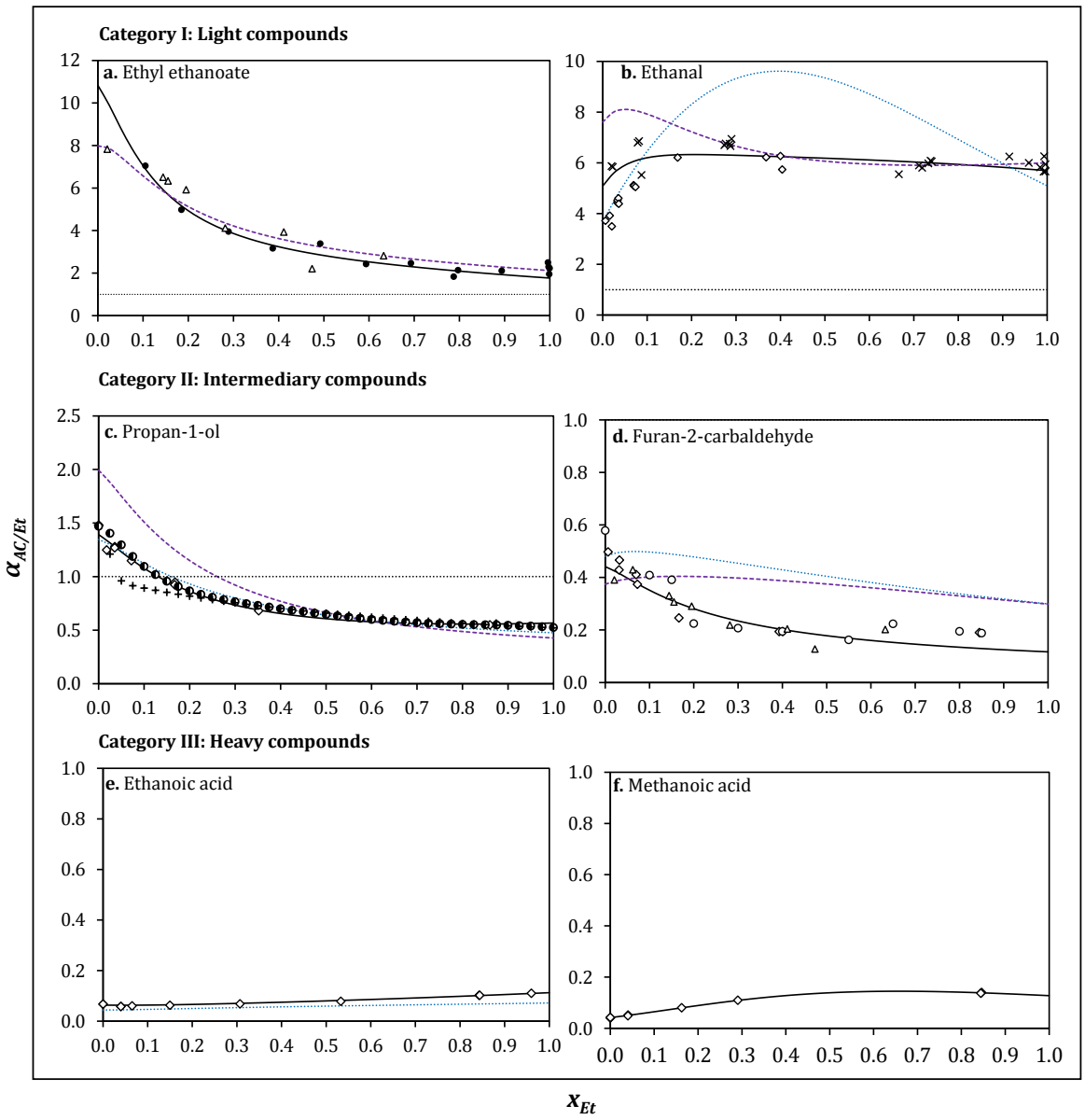

Figure 2-3. *Evolution of the relative volatility of aroma compounds with respect to ethanol ($\alpha_{AC/Et}$) with the ethanol composition in the liquid phase (x_{Et}) at 101.3 kPa for: Category I. Light compounds: a. Ethyl ethanoate; b. Ethanal. Category II. Intermediary compounds: c. Propan-1-ol; d. Furan-2-carbaldehyde. Category III. Heavy compounds: e. Ethanoic acid; f. Methanoic acid. Experimental data at high dilution from: (✕ Heitz 1960) (◇ Williams, 1962) (△ Athès et al., 2008) (○ Ikari et al., 1984) (◐ Ikari et al., 1990) (● Ikari et al., 1998) (✚ Martin et al., 2009). Calculation with NRTL model using: (——) NRTL-0 parameters set (estimated from data at high dilution, Table 2-4). (·····) NRTL-B parameters set (estimated from binary data, Table 2-8). NRTL-T parameters set (- - - -) (estimated from ternary data, Table 2-9).*

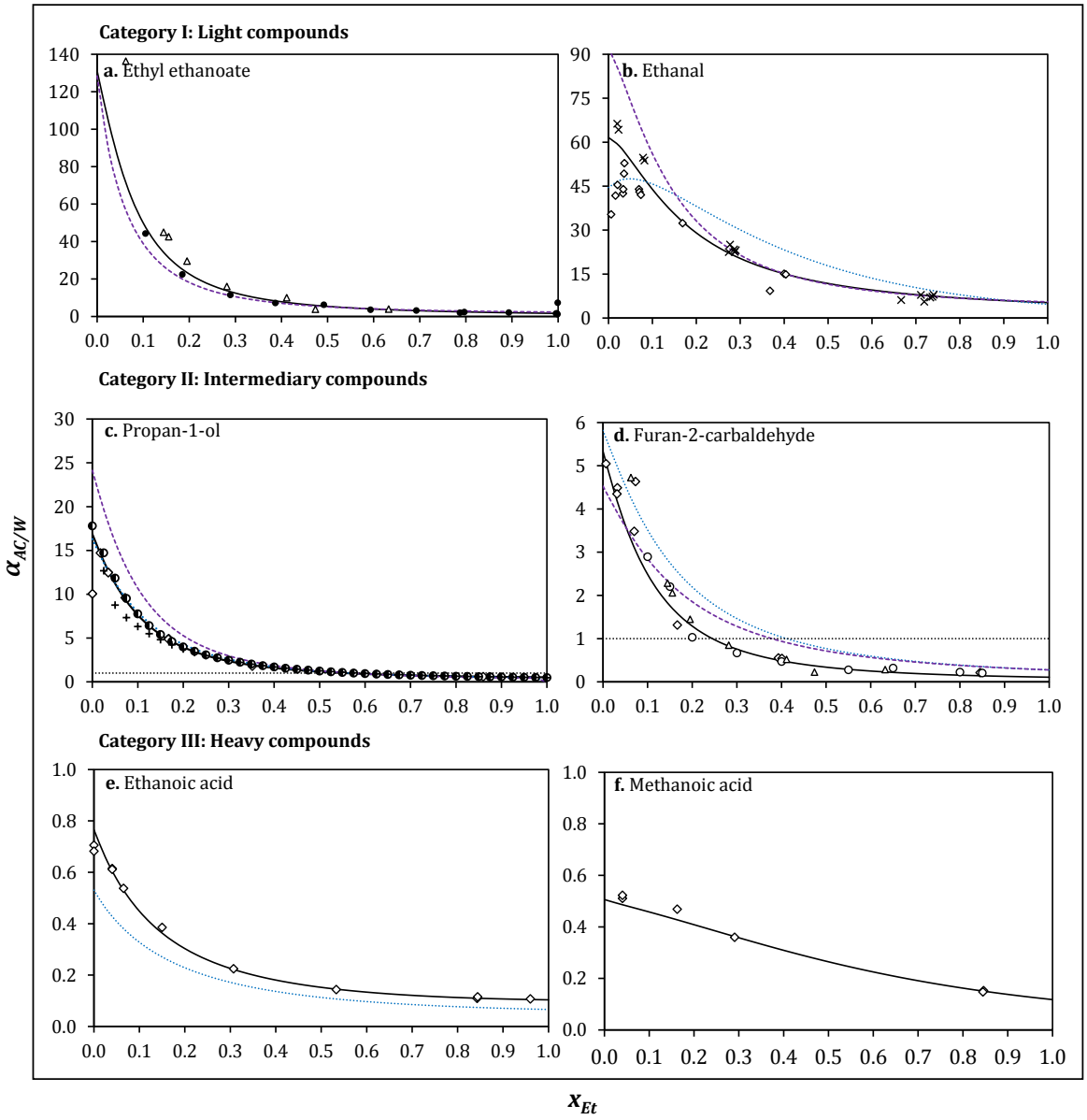

Figure 2-4. *Evolution of the relative volatility of aroma compounds with respect to ethanol ($\alpha_{AC/W}$) with the ethanol composition in the liquid phase (x_{Et}) at 101.3 kPa for: Category I. Light compounds: a. Ethyl ethanoate; b. Ethanal. Category II. Intermediary compounds: c. Propan-1-ol; d. Furan-2-carbaldehyde. Category III. Heavy compounds: e. Ethanoic acid; f. Methanoic acid. Experimental data at high dilution from: (✕ Heitz 1960) (◇ Williams, 1962) (△ Athès et al., 2008) (○ Ikari et al., 1984) (◐ Ikari et al., 1990) (● Ikari et al., 1998) (✚ Martin et al., 2009). Calculation with NRTL model using: (——) NRTL-0 parameters set (estimated from data at high dilution, Table 2-4). (·····) NRTL-B parameters set (estimated from binary data, Table 2-8). NRTL-T parameters set (- - -) (estimated from ternary data, Table 2-9).*

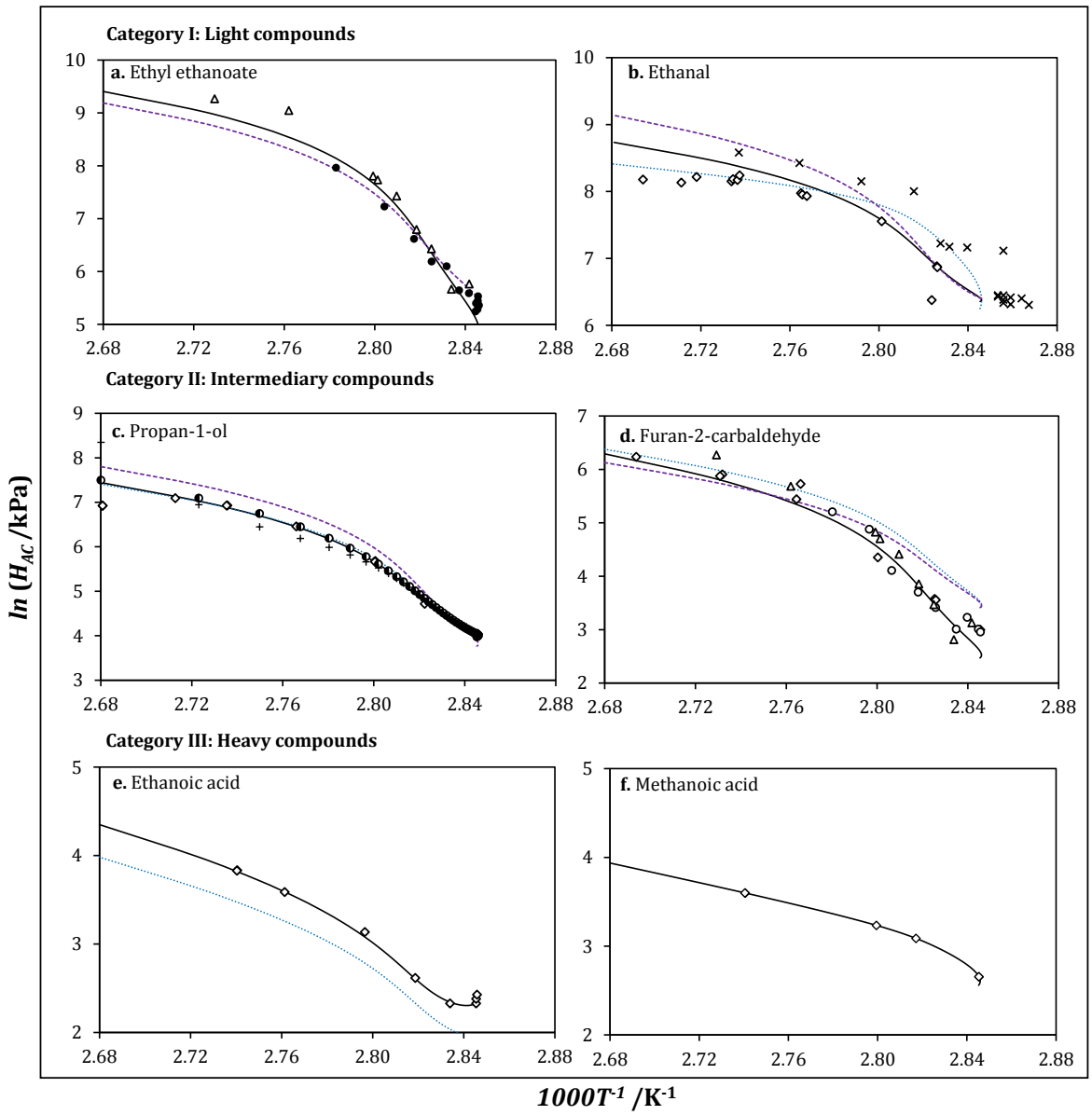

Figure 2-5. *Evolution of ln H with T^{-1} at 101.3 kPa for: Category I. Light compounds: a. Ethyl ethanoate; b. Ethanal. Category II. Intermediary compounds: c. Propan-1-ol; d. Furan-2-carbaldehyde. Category III. Heavy compounds: e. Ethanoic acid; f. Methanoic acid. Experimental data at high dilution from: (✕ Heitz 1960) (◇ Williams, 1962) (△ Athès et al., 2008) (○ Ikari et al., 1984) (◐ Ikari et al., 1990) (● Ikari et al., 1998) (✚ Martin et al., 2009). Calculation with NRTL model using: (——) NRTL-0 parameters set (estimated from data at high dilution, Table 2-4). (·····) NRTL-B parameters set (estimated from binary data, Table 2-8). NRTL-T parameters set (- - - -) (estimated from ternary data, Table 2-9).*

In general terms, the activity model represents correctly the experimental data. Regarding ethanal (figure 2-5 b), even if an important dispersion of the experimental data is observed, the model follows the global trend in most of the temperature interval. In all cases, the continuous representation with the NRTL model shows that the evolution of ln $\mathcal{H}_{AC}$ is decreasing and concave for all compounds, and not linear, as observed in a pure solvent. This is due to the fact that the temperature and the composition of the liquid phase are not independent at boiling conditions: each bubble temperature T corresponds to a different mole fraction of ethanol.

In this way, considering the great diversity of chemical species and data resources, the whole of results are acceptable and confirm that the NRTL model can correctly represent the vapor-liquid equilibria of aroma compounds in hydroalcoholic mixtures, a conclusion already established in other synthesis works.

2.3.2. CLASSIFICATION OF AROMA COMPOUNDS

The set of interaction parameters estimated will be used for simulation purposes at a later stage, with the aim of understanding the behaviour of aroma compounds in alcoholic beverages distillation. Given the considerable number of studied species, a systematic classification turns out be useful for identifying general trends.

By following a classic approach of multicomponent distillation, two key components governing the separation are firstly selected: ethanol as light key and water as heavy key. The first will be recovered to a significant extent in the top product, whereas the second, less volatile, will mainly be recovered in the bottom product. Then, by taking as criterion the relative volatility with respect to both key components over the entire ethanol composition range, three categories of aroma compounds can be defined:

- Category I. Light compounds: The minimal value of $\alpha_{AC/Et}$ is higher than the unity ($\alpha_{AC/Et\text{-}MIN}>1$). They are lighter than light key and will be therefore mainly present in the top product or distillate.
- Category II. Intermediary or distributed compounds: The minimal value of $\alpha_{AC/Et}$ is lower than the unity ($\alpha_{AC/Et\text{-}MIN}<1$) and the maximal value of $\alpha_{AC/W}$ is higher than the unity ($\alpha_{AC/W\text{-}MAX}>1$). Their volatility are intermediate between that of light and heavy key. They will be distributed in top and bottoms products.
- Category III. Heavy compounds: the maximal value of $\alpha_{AC/W}$ is lower than the unity ($\alpha_{AC/W\text{-}MAX}<1$). They are heavier than heavy key and will be therefore mainly recovered in the bottom product.

For simulation purposes, an accurate representation of phase equilibrium for intermediary compounds is fundamental to correctly estimate the ratio of distribution between the top and bottom product.

The classification of the aroma compounds studied in this work is presented in **table 2-5.** The compounds are arranged in a decreasing order of relative volatilities. According to this approach, most of the compounds, 32, are intermediary compounds. 10 compounds, mainly carbonyl compounds, are light compounds and only 2 carboxylic acids, methanoic and ethanoic are heavier than water. In table 2-5 the compounds of each group are arranged in a decreasing order of relative volatilities. The aroma compounds presented in figures 2-2 to 2-4 are classified on the basis of this criterion, from the more (ethyl ethanoate) to the less volatile (methanoic acid).

Table 2-5. *Classification of aroma compounds according to their relative volatilities with respect to ethanol and water, over the whole ethanol composition range in the liquid phase.*

Category	Aroma compound	$\alpha_{AC/Et}$			$\alpha_{AC/W}$		
		Min	Max	Average	Min	Max	Average
I. Light	3-Methylbutanal	1.3	19.8	10.5	1.2	239.6	120.4
	Propan-2-yl ethanoate	1.7	14.2	7.9	1.7	172.0	86.8
	2-Methylpropanal	1.1	12.8	6.9	1.0	154.6	77.8
	Ethyl ethanoate	1.8	10.8	6.3	1.6	131.2	66.4
	Butanal	1.7	10.5	6.1	1.5	125.9	63.7
	Ethanal	5.1	6.3	5.7	5.3	61.6	33.4
	1,1-Diethoxyethane	3.3	6.8	5.0	5.6	40.0	22.8
	Propanal	1.8	6.5	4.2	1.7	51.3	26.5
	2-Methylpropyl methanoate	1.7	6.0	3.9	1.6	72.8	37.2
	Prop-2-enal	2.4	4.5	3.5	2.4	30.1	16.3
II. Intermediary	Ethyl decanoate	0.0	82.9	41.5	0.0	1005.3	502.6
	Ethyl 2-methylpropanoate	1.0	33.0	17.0	0.9	399.3	200.1
	Ethyl octanoate	0.0	28.0	14.0	0.0	339.4	169.7
	3-Methylbutyl ethanoate	0.1	18.5	9.3	0.1	224.0	112.1
	Ethyl 3-methylbutanoate	0.5	18.1	9.3	0.4	219.5	110.0
	Pentanal	0.9	10.1	5.5	0.8	122.9	61.8
	Linalool	0.0	8.2	4.1	0.0	99.5	49.7
	Ethyl hexanoate	0.6	6.7	3.7	0.5	81.6	41.1
	Linalool oxide	0.0	5.2	2.6	0.1	63.4	31.8
	2-Methylpropan-2-ol	0.7	2.7	1.7	0.7	33.2	16.9
	Hexan-1-ol	0.1	2.9	1.5	0.1	35.3	17.7
	Propan-2-ol	0.9	1.8	1.4	0.8	22.0	11.4
	3-Methylbutan-1-ol	0.1	2.7	1.4	0.1	32.1	16.1
	2-Methylpropan-1-ol	0.4	2.5	1.4	0.3	30.0	15.2
	2-Methylbutan-1-ol	0.1	2.5	1.3	0.1	30.2	15.1
	Butan-1-ol	0.2	1.9	1.1	0.2	23.1	11.7
	(Z)-Hex-3-en-1-ol	0.0	1.9	1.0	0.0	23.4	11.7
	Propan-1-ol	0.6	1.4	1.0	0.5	16.9	8.7
	Methanol	0.6	1.5	1.0	1.4	6.8	4.1
	2-Phenylethyl ethanoate	0.0	1.5	0.8	0.0	18.8	9.4
	Octanoic acid	0.0	1.4	0.7	0.0	17.2	8.6
	Prop-2-en-1-ol	0.5	0.9	0.7	0.5	10.8	5.6
	Hexanoic acid	0.0	0.7	0.3	0.0	8.1	4.1
	Furan-2-carbaldehyde	0.1	0.4	0.3	0.1	5.3	2.7
	Ethyl 2-hydroxypropanoate	0.1	0.3	0.2	0.1	3.9	2.0
	3-Methylbutanoic acid	0.0	0.3	0.2	0.0	4.0	2.0
	2-Methylpropanoic acid	0.0	0.2	0.1	0.0	2.1	1.1
	Butanoic acid	0.0	0.2	0.1	0.0	2.0	1.0
	Diethyl butane-1,4-dioate	0.1	0.2	0.1	0.1	1.9	1.0
	2-Methylbutanoic acid	0.0	0.2	0.1	0.0	2.0	1.0
	2-Phenylethan-1-ol	0.0	0.1	0.1	0.0	1.3	0.6
	Propanoic acid	0.1	0.1	0.1	0.0	1.0	0.5

III. Heavy	Ethanoic acid	0.1	0.1	0.1	0.1	0.8	0.4
	Methanoic acid	0.0	0.1	0.1	0.1	0.5	0.3

It should be noted that the classification is proposed over the whole ethanol composition range in the liquid phase ($0<x_{Et}<1$). Given that the relative volatilities vary with composition, the classification could be different when considering a more restricted composition interval.

2.3.3. Comparison of the representation obtained from data at high dilution and that obtained from binary and ternary data at higher concentrations of aroma compounds

The discussion concludes with a comparison between: (1) the representation of the equilibrium data using the set of parameters calculated in this work, from data at high dilution regarding the aroma compounds (table 2 and table 4) and (2) the one obtained with parameters fitted to data for binary and ternary systems, in which the aroma compounds are present at high concentrations. These parameters are available in the literature for some aroma compounds [Faundez and Valderrama, 2003 and 2004 and 2009 ; Tan et al., 2004 ; Tan et al., 2005 ; Faundez et al., 2006 ;Valderrama et al., 2012]. However, according to the writing of equations 2-20 and 2-21, they cannot be used directly for two reasons: (i) the formalisms to evaluate the temperature dependence of the interaction parameters c_{ij} and τ_{ij} are not the same of this work and (ii) the non-randomness parameters c_{ij}^{0} is different the value set in this work (0.3), which does not make possible the conversion of the parameters G_{ij} and τ_{ij} in the different formalisms.

Consequently, new interaction parameters are estimated from experimental data, by following an analogous procedure to that described in section 2.3.1. Information on the aroma compounds considered, the data references as well as the temperature and composition intervals are summarized in **table 2-6** for binary systems (aroma compound – ethanol and aroma compound – water) and in **table 2-7** for ternary systems (aroma compound – ethanol – water). 9 aroma compounds from 5 chemical families are considered [Heitz, 1960; Tan et al., 2004; Tan et al., 2005; Amer et al., 1989; Delzenne, 1958; Slobodyanik and Babuskhina, 1966; Dunlop, 1977; Ocon et al., 1958; Kohoutova et al., 1970; Gay, 1927; Ochi and Kojima, 1969; Chu et al., 1950; Smirnova, 1959; Dobroserdov and Llina, 1961; Andiappan and Mc Clean, 1972; Suska, 1979; Perry, 1950; Rius et al., 1959; Brown et al., 1950; Conti et al., 1977; Sebastiani and Lacquaniti, 1967; Kharin et al., 1977; Mains, 1922; Griswold and Dinwiddie, 1942; Hughes and Maloney, 1952; Kojima et al., 1969; Kharin et al., 1971a,b,c; Suska et al., 1970; Kharin et al., 1972; Griswold et al., 1949; Van Zandijcke and Verhoeye, 1974].

Table 2-6. *Synthesis of vapor-liquid data for binary systems aroma compound (1) – ethanol (2) and aroma compound (1) – water (3) at 101.3 kPa.*

Aroma compound	Solvent	Data reference	Independent data	*T* range /K		x_{AC} range		y_{AC} range	
				Min	Max	Min	Max	Min	Max
Methanol	Ethanol	Amer et al, 1956; Delzenne, 1958; Slobodyanyk et al, 1966	58	337.9	351.6	0.00	1.00	0.00	1.00
	Water	Dunlop, 1948; Ocon & Rebolleda, 1958; Kohoutova et al, 1970	66	337.7	373.2	0.00	1.00	0.00	1.00
Propan-1-ol	Ethanol	Gay, 1927; Ochi & Kojima, 1979	32	351.5	370.8	0.00	1.00	0.00	1.00
	Water	Chu et al, 1950; Smirnova, 1959; Droboserdov & Ilina, 1961	51	360.7	373.2	0.00	1.00	0.00	1.00
3-Methylbutan-1-ol	Ethanol	Gay, 1927	17	351.5	404.2	0.00	1.00	0.00	1.00
	Water	Andiappan & McLean, 1972	11	368.3	381.2	0.00	0.88	0.11	0.43
Ethanal	Ethanol	Suska, 1979	21	293.6	351.5	0.00	1.00	0.00	1.00
	Water	Perry, 1950; Suska, 1979	27	293.3	373.2	0.00	1.00	0.00	1.00

Table 2-7. *Synthesis of vapor-liquid data for ternary systems aroma compound (1) – ethanol (2) – water (3) at 101.3 kPa.*

Aroma compound	Data reference	Independent data	*T* range /K		x_{AC} range		x_{Et} range		x_W range		y_{AC} range		y_{Et} range		y_W range	
			Min	Max	Min	Max	Min	Max	Min	Max	Min	Max	Min	Max	Min	Max
Methanol	Griswold & Dimviddie, 1942; Huges & Maloney, 1952; Delzenne, 1958	80	340.0	360.7	0.0	0.9	0.0	0.8	0.0	0.9	0.1	0.9	0.0	0.8	0.0	0.5
Propan-1-ol	Ochi & Kojima, 1969; Kharin et al, 1970b; Tan et al, 2005	70	351.2	368.8	0.0	1.0	0.0	0.9	0.0	1.0	0.0	0.9	0.0	0.9	0.0	0.9
Propan-2-ol	Kojima et al, 1969; Kharin et al, 1971a; Tan et al, 2004	80	351.2	361.9	0.0	0.9	0.0	0.9	0.0	0.9	0.0	0.9	0.0	0.9	0.0	0.7
2-Methylpropan-1-ol	Suska et al, 1970; Kharin et al, 1971b	37	351.9	362.2	0.0	0.5	0.1	1.0	0.0	0.9	0.0	0.3	0.1	1.0	0.0	0.6
3-Methylbutan-1-ol	Kharin et al, 1972	31	351.7	366.1	0.0	0.5	0.1	0.8	0.1	0.9	0.0	0.1	0.4	0.8	0.2	0.6
Ethanal	Heitz, 1960	40	316.9	372.2	0.0	0.4	0.0	1.0	0.0	1.0	0.0	0.8	0.0	1.0	0.0	1.0
Ethyl ethanoate	Griswold et al, 1949; Vans Zandijcke & Verhoeye, 1974	147	343.8	358.6	0.0	0.9	0.1	1.0	0.0	0.9	0.0	0.9	0.1	1.0	0.0	0.6
Furan-2-carbaldehyde	Kharin et al, 1971c	25	353.2		0.0	0.5	0.1	0.9	0.1	0.9	0.0	0.1	0.4	0.9	0.1	0.6

The objective function is expressed in terms of the relative deviation of temperature and absolute volatility data:

$$OF(T,K)=\sum_{k=1}^{N}\left(\frac{T_{Exp_k}-T_{Calc_k}}{T_{Exp_k}}\right)^2+\sum_{k=1}^{N}\sum_{i=1}^{n}\left(\frac{K_{i\,Exp_k}-K_{i\,Calc_k}}{K_{i\,Exp_k}}\right)^2 \qquad [2\text{-}30]$$

T_{Calc_k} and $K_{i\,Calc_k}$ are computed with the Bubble Temperature algorithm of the Simulis® Thermodynamics package, by fixing the pressure (P) and composition in the liquid phase ($\boldsymbol{x}$) to the experimental data. In all cases, the interaction parameters of the binary ethanol – water used for the equilibrium calculations were those used previously in this work [Kadir, 2009]. The fitting quality is evaluated with respect to T and K_i, by considering the parameters *AAE%* (equation 2-25) and *RMSE* (equation 2-26).

In comparison to equation 2-24, used for the parameter estimation from data at high dilution (NRTL-0 set), the formulation of equation 2-30 was chosen for three reasons: (i) relative deviations were preferred to absolute ones since the function includes two variables with different magnitude orders; (ii) temperature was added because in binary and ternary systems the corresponding intervals are variable, whereas that of high dilution systems is always the same at 101.3 kPa (from 351.4 K to 373.2 K), as it is fixed by the ethanol – water binary; (iii) absolute volatilities were used because they do not give more weight to a component with respect to another, which is more appropriate for this estimation since all the species concerned are present at wide concentration intervals (from 0 to 1). The formulation of equation 2-24 is more adapted to systems with aroma compounds highly diluted, as it privileges this species in relation to ethanol and water.

Thereby, the set interaction parameters derived from binary data (identified as NRTL-B) is given in **table 2-8** and that from ternary data (identified as NRTL-T) in **table 2-9**. In both tables the fitting statistics, with the temperature and absolute volatilities ranges are presented. According to these values, all the concerned systems are globally well represented with the NRTL model, with an overall relative error of 1% for temperature (variation between 0% and 3%) and of 7% for absolute volatilities (variation between 1% and 24%).

The comparison with data at high dilution is performed in relation to the fitting quality of the equilibrium data. The values of RMSE and AAE% for the 9 aroma compounds are presented in **table 2-10**, using the 3 sets of interaction parameters: NRTL-0 (from ternary or multicomponent data at low concentration of the aroma compound), NRTL-B and NRTL-T.

The evolution of K_{AC}, $\alpha_{AC/Et}$ and $\alpha_{AC/W}$ is also represented with the different sets of interaction parameters in figures 2-2 to 2-4**.** The number of curves for each compound varies according to the binary and ternary data available, reported in tables 2-6 and 2-7 (three curves for ethanal, propan-1-ol and furan-2-carbaldehyde; 2 curves for ethyl ethanoate and ethanoic acid; 1 curve for methanoic acid, for which no binary or ternary data were found in the open literature). These figures make evident that the experimental data of K_{AC} and $\alpha_{AC/W}$ at high dilution can be represented with reasonable precision using any of the sets. The decreasing tendency obtained is correct. However, as for $\alpha_{AC/Et}$, the representation is only relatively good for ethyl acetate and propanol-1-ol. For ethanoic acid the curve is systematically shifted from the experimental data,

while for ethanal and furan-2-carbaldehyde, the representation with the NRTL-B and NRTL-T sets is not coherent.

The statistics indicate that the fitting quality is clearly better when using the main parameters estimated in this work (NRTL-0). Only for two aroma compounds, methanol and 1-propanol, the deviations with respect to experimental data from the NRTL-B set are acceptable and comparable. When comparing the NRTL-B and NRTL-T sets, the deviations associated to the first one are always lower (*AAE%* between 4% and 56% for NRTL-B, against *AAE%* between 22% and 72% for NRTL-T). The representation from ternary data are probably less accurate since the composition intervals of the solvent components (ethanol and water) are restricted and do not cover all the composition range (from 0 to 1) in the liquid phase.

In general terms, these results suggest that an accurate representation of the vapor-liquid behaviour of aroma compounds in alcoholic distillation requires data at low concentration. The NRTL model could be used to extrapolate the equilibrium data at high concentration to the high dilution region, but only with rough precision. However, if no data at high dilution are available, binary data in which the solvent components are present over the entire composition range, are recommended for the estimation of interaction parameters used for engineering purposes in the alcoholic beverages field.

Table 2-8. *NRTL-B set: Interaction parameters calculated from binary mixture data of aroma compounds (1) at high concentrations in ethanol (2) and water (3). Fitting statistics for temperature and absolute volatilities.*

Aroma compound	i	j	A_{ij}^0 / cal·mol^{-1}	A_{ji}^0 / cal·mol^{-1}	K_{AC}				K_{Et} / K_W				T			
					Range		RMSE	AAE%	Range		RMSE	AAE%	Range		RMSE	AAE%
					Min	Max			Min	Max			Min	Max		
Methanol	1	2	-104.8	87.1	1.0	2.2	0.1	3%	0.6	1.0	0.1	3%	337.9	351.6	0.4	0%
	1	3	-97.4	674.4	1.0	7.4	0.1	1%	0.4	1.0	0.0	2%	337.7	373.2	0.5	0%
Propan-1-ol	1	2	-208.0	240.8	0.5	1.0	0.0	1%	1.0	1.9	0.0	1%	351.5	370.8	0.2	0%
	1	3	20.3	1971.9	0.8	18.1	0.6	4%	0.7	3.1	0.1	4%	360.7	373.2	0.7	0%
3-Methylbutan-1-ol	1	2	-19.4	31.0	0.1	1.0	0.0	2%	1.0	5.6	0.0	1%	351.5	404.2	0.2	0%
	1	3	-461.2	2808.0	0.3	54.0	16.7	24%	0.8	4.8	0.1	5%	368.3	381.2	1.6	0%
Ethanal	1	2	12922.7	-103.5	1.0	4.4	0.0	0%	0.1	1.0	0.0	1%	293.6	351.5	0.2	0%
	1	3	1347.5	390.0	1.0	50.0	3.8	3%	0.0	1.0	0.0	16%	293.3	373.2	2.0	0%
Ethanoic acid	1	2	64.4	-116.3	0.1	1.0	0.0	7%	1.0	2.1	0.1	5%	350.0	389.0	0.8	0%
	1	3	-256.8	1000.8	0.7	1.0	0.1	5%	1.0	2.1	0.2	7%	373.2	391.3	0.3	0%
Furan-2-carbaldehyde	1	2	179.5	1032.0	0.1	0.4	0.1	15%	1.0	30.3	2.9	5%	351.6	407.2	3.8	1%
	1	3	430.5	2435.4	0.1	5.5	0.3	11%	0.9	8.5	0.3	2%	371.1	434.9	2.3	0%

Table 2-9. *NRTL-T set: Interaction parameters calculated from ternary mixture data of aroma compounds at high concentrations (1) in ethanol (2) –water (3) mixtures. Fitting statistics for temperature and absolute volatilities.*

Aroma compound	i	j	A_{ij}^0 / cal·mol^{-1}	A_{ji}^0 / cal·mol^{-1}	K_{AC}				K_{Et}				K_W				T			
					Range		RMSE	AAE%	Range		RMSE	AAE%	Range		RMSE	AAE%	Range		RMSE	AAE%
					Min	Max			Min	Max			Min	Max			Min	Max		
Methanol	1	2	1100.3	-610.3	1.1	6.4	0.3	6%	0.5	6.7	0.5	8%	0.29	0.87	0.1	12%	340.0	360.7	0.6	0%
	1	3	-113.3	741.2																
Propan-1-ol	1	2	-430.8	455.9	0.4	50.0	2.3	12%	1.0	17.8	1.5	12%	0.5	3.9	0.3	8%	351.2	368.8	1.0	0%
	1	3	73.1	2212.6																
Propan-2-ol	1	2	-337.0	413.6	0.8	8.4	0.4	5%	1.0	5.8	0.1	4%	0.6	1.4	0.0	3%	351.2	361.9	0.3	0%
	1	3	-61.7	1712.7																
2-Methylpropan-1-ol	1	2	866.7	-434.5	0.4	14.5	0.5	11%	1.0	5.9	0.2	3%	0.5	1.6	0.1	5%	351.9	362.2	0.7	0%
	1	3	197.5	2888.0																
3-Methylbutan-1-ol	1	2	-759.8	1093.0	0.1	4.9	0.1	7%	1.0	3.6	0.1	1%	0.6	1.8	0.0	2%	351.7	366.1	0.3	0%
	1	3	-69.4	3907.1																
Ethanal	1	2	-1010.5	1620.2	1.9	120.7	15.8	12%	0.2	9.0	0.6	15%	0.2	1.0	0.2	13%	316.9	372.2	3.5	1%
	1	3	-239.4	1972.7																
Ethyl ethanoate	1	2	682.7	-10.1	0.9	42.4	1.7	9%	0.9	4.1	0.1	4%	0.2	2.2	0.2	16%	343.8	358.6	0.4	0%
	1	3	500.2	2465.3																
Furan-2-carbaldehyde	1	2	-146.5	1351.8	0.1	1.5	0.2	8%	1.0	4.4	0.1	3%	0.6	1.9	0.2	6%	353.2		2.9	3%
	1	3	507.0	2198.2																

Table 2-10. *Statistics of fitting quality for absolute and relative volatilities of aroma compounds at 101.3 kPa using different three NRTL parameters sets: NRTL-0 (Table 2-4), NRTL-B (Table 2-8), and NRTL-T (Table 2-9).*

Aroma compound	Parameters set	K_{AC}		$\alpha_{AC/Et}$		$\alpha_{AC/W}$	
		RMSE	AAE%	RMSE	AAE%	RMSE	AAE%
Methanol	NRTL-0	0.2	5%	0.1	4%	0.2	9%
	NRTL-B	0.4	6%	0.3	4%	0.2	12%
	NRTL-T	0.7	22%	0.3	22%	0.7	32%
Propan-1-ol	NRTL-0	1.6	16%	0.2	12%	2.2	21%
	NRTL-B	1.6	16%	0.2	13%	2.3	21%
	NRTL-T	4.0	30%	0.4	26%	3.9	36%
Propan-2-ol	NRTL-0	0.3	2%	0.0	2%	0.3	2%
	NRTL-T	0.7	7%	0.1	7%	0.8	7%
2-Methylpropan-1-ol	NRTL-0	0.3	3%	0.0	3%	0.4	3%
	NRTL-T	1.0	15%	0.4	16%	1.8	21%
3-Methylbutan-1-ol	NRTL-0	0.6	10%	0.1	10%	0.6	10%
	NRTL-B	3.4	19%	0.3	19%	3.7	19%
	NRTL-T	5.6	55%	0.6	55%	6.3	55%
Ethanal	NRTL-0	6.9	18%	0.8	12%	8.3	18%
	NRTL-B	7.4	34%	1.8	26%	8.9	32%
	NRTL-T	15.7	35%	2.0	31%	21.4	37%
Ethanoic acid	NRTL-0	0.0	1%	0.0	1%	0.0	1%
	NRTL-B	0.1	28%	0.0	28%	0.1	28%
Ethyl ethanoate	NRTL-0	3.6	12%	0.6	13%	8.1	17%
	NRTL-T	12.4	19%	0.6	14%	21.1	26%
Furan-2-carbaldehyde	NRTL-0	0.5	17%	0.0	14%	0.7	19%
	NRTL-B	0.5	55%	0.1	56%	0.8	55%
	NRTL-T	0.7	68%	0.2	72%	0.9	68%

2.4. CONCLUSIONS

A new set of binary interaction parameters for the NRTL model has been generated for 44 aroma compounds highly diluted in ethanol-water mixtures at 101.3 kPa. The experimental data were obtained from 10 research works published in the open literature between 1960 and 2017. They were measured through a dynamic method using two modes of recirculation: with vapor phase only and with vapor and liquid phases.

The fitting quality of the regressions is good, with respective overall RMSE and AEE% values of 1.3 and 12% for the absolute volatility K_{AC}, 0.2 and 12% for the relative volatility with respect to ethanol, $\alpha_{AC/Et}$, and 2.1 and 13% for the relative volatility with respect to water, $\alpha_{AC/W}$, of the aroma compounds. Thus, the NRTL model, coupled to the ideal gas equation or to an association model taking into account the chemical equilibrium when dealing with carboxylic acids, is recommended for the simulation of continuous and batch distillation processes involved in the production of alcoholic beverages.

Using the proposed set of parameters, the aroma compounds can be classified in three categories according to their volatility with respect to ethanol (light key) and water (heavy key), over the whole ethanol composition range in the liquid phase ($0<x_{Et}<1$): (I) light (10 compounds, including acetals, carbonyl compounds, and esters), (II) intermediary (32 compounds, including alcohols, carbonyl compounds, carboxylic acids, esters, furans, and terpenes) and (III) heavy (2 carboxylic acids).

Finally, the comparison with the parameters estimated from binary or ternary mixture data including an aroma compound at high concentration indicates that the equilibrium representation is roughly acceptable, as the orders of magnitude of the absolute and relative volatilities are correct, yet the values of *RMSE* and *AAEE%* are higher than those obtained with parameter derived from data at high dilution. Accurate data at low concentration ranges are therefore necessary to correctly represent the equilibrium properties of aroma compounds and consequently, to generate reliable simulations of distillation units. Only when this information is not available, and cannot be measured or predicted, binary data should be used for the estimation of interaction parameters for engineering applications.

CHAPITRE 3. MESURES EXPERIMENTALES DES DONNEES D'EQUILIBRE LIQUIDE-VAPEUR

L'objet de ce chapitre est le développement de l'approche expérimentale pour la génération de données d'équilibre liquide-vapeur. Cette voie est appliquée à l'étude du système ternaire lactate d'éthyle–éthanol–eau, dans lequel le composé volatil d'arôme est présent à faible concentration. Les mesures sont effectuées à pression atmosphérique dans un intervalle de températures d'ébullition entre 352,3 K et 370,0 K. L'appareillage opère selon une méthode dynamique avec recirculation des phases liquide et vapeur. La concentration en lactate d'éthyle est déterminée par chromatographie en phase gazeuse. La modélisation thermodynamique des données suit les mêmes principes que ceux exposés dans le chapitre précédent. Deux modèles d'activité semi-empiriques, NRTL et UNIQUAC, sont évalués. Finalement, en analogie au chapitre 2, la qualité de la représentation des données, obtenue avec le jeu de paramètres d'interaction issu de ce travail, est comparée avec celle basée sur un jeu de paramètres rapporté dans la littérature, lequel a été déterminé à partir des données pour les binaires lactate d'éthyle–éthanol et lactate d'éthyle–eau.

Vapor-liquid equilibrium (VLE) of ethyl lactate highly diluted in ethanol -water mixtures at 101.3 kPa. Experimental measurements and thermodynamic modeling using semi-empirical models.

Cristian Puentes, Xavier Joulia, Patrice Paricaud, Pierre Giampaoli, Violaine Athès et Martine Esteban-Decloux

Soumis au *Journal of Chemical and Engineering Data*.

3.1. INTRODUCTION

Process simulation is a powerful tool to design, analyze and optimize chemical and biochemical processes. For the correct simulation of separation units, there are two factors of crucial importance: (1) a reliable and accurate knowledge of the phase equilibria, and (2) a suitable choice of thermodynamic models to correctly describe the volumetric behaviour of the involved phases [Rhodes, 1966; Baburao and Visco, 2011; Hsieh et al., 2010; Kang et al., 2010; Valderrama et al., 2012; Esteban-Decloux et al., 2014; Valderrama et al., 2014].

In alcoholic distillation, some simulation studies have been performed over the last 50 years with the aim of identifying and predicting the influence of operating parameters on process variables such as product quality and efficiency [Esteban-Decloux et al., 2014; Valderrama et al., 2014]. These researches have been focused on continuous processes for the production of Whisky [Gaiser et al., 2002], neutral alcohol [Esteban-Decloux et al., 2014; Valderrama et al., 2014; Decloux and Coustel, 2005], bioethanol [Batista et al., 2009; Batista et al., 2011; Tgarguifa et al., 2017], Cachaça [Batista and Meirelles, 2011] and anhydrous fuel ethanol [Bastidas et al., 2012]. In batch distillation, simulation has been applied for the analysis of the recovery process of ethanol produced from banana culture waste [Coelho et al., 2012], as well as the production of Pisco [Osorio et al., 2004; Carvallo et al., 2011], cachaça in a lab-scale pot still [Scanavini et al., 2010; Scanavini et al., 2012], Whisky [Valderrama et al., 2012], pear distillates [Sacher et al., 2013], and bitter orange distillates [Esteban-Decloux et al., 2014]. The simulations were performed by either implementing in-house made mathematical models of mass and energy balances or using commercial software as AspenPlus, Aspen Dynamics, BatchColumn, ChemCAD, Pro/II and ProSimPlus.

The common point among these studies is that the feedstock was modelled as a simplified mixture of ethanol and water with several minor volatile species, known as congeners or aroma compounds. The number of aroma compounds considered varies between 0 and 16 and the chemical families included are acetals (acetal), alcohols (methanol, propan-1-ol, propan-2-ol, 1-propen-2-ol, 2-methylpropan-1-ol, butan-1-ol, butan-2-ol, 2-methylbutan-1-ol, 3-methylbutan-1-ol, pentan-1-ol, pentan-2-ol, hexan-1-ol, 2-phenylethanol), carbonyl compounds (acetaldehyde, acetone), carboxylic acids (acetic acid, propionic acid, octanoic acid), esters (methyl acetate, ethyl acetate, ethyl hexanoate, ethyl decanoate), furanes (furfural) and terpenes (pinene, limonene, linalool, linalool oxide). Carbon dioxide has also been considered in some researches, in order to analyze its influence on the product composition [Valderrama et al., 2012; Batista et al., 2009; Batista et al., 2012; Bastidas et al., 2012].

In alcoholic beverages production, the understanding of aroma compounds behaviour in distillation is fundamental since they are responsible for the product quality. Several hundred of aroma compounds are mainly generated at low concentrations during the fermentation step and a lower proportion during distillation and maturation [Maarse and Van Der Berg, 1994; Suomalainen and Lehtonen, 1979; Ebeler, 2001; Ortega et al., 2001; Marti et al., 2003; Jiang and Zang, 2010]. The simulation studies from the literature have included some of the most representative species. However, other important aroma compounds, such as ethyl lactate, have never been analyzed.

Ethyl 2-hydroxypropanoate, commonly known as ethyl lactate, is produced by the reaction of lactic acid, from malolactic fermentation, with ethanol. This compound has been quantified in wine and distilled beverages at very different concentration levels. In wine from traces to 500 $mg \cdot L^{-1}$ and in distillates up to 400 $mg \cdot L^{-1}$ [Nykanen and Suomalainen, 1983; Apostolopoulou et al., 2005; Ledauphin et al., 2010]. Together with ethyl acetate, they constitute the main esters found in distillates [Bankfort and Ward, 2014]. From a sensory point of view, ethyl lactate may act as a stabilizer of the distillate flavor as well as a softener of the harsh flavor characteristics if it is present at low concentrations. However, at higher concentration levels, caused by lactic acid bacteria spoilage, this compound deteriorates the organoleptic quality of distillates [Apostolopoulou et al., 2005; Bankfort and Ward, 2014]. In this case, process simulation may represent a useful tool to predict and control the concentration of this aroma compound to the desired levels.

As part of a confidential study carried out in our research group about cognac distillation [Decloux, 2009], the composition profiles of ethanol and 23 aroma compounds, including ethyl lactate, were simulated using the commercial software BatchColumn provided by ProSim. The thermodynamic models chosen for the representation of the vapor and liquid phases were respectively the ideal gas equation and the predictive model UNIFAC 1993 [Weidlich and Gmehling, 1987; Gmehling and Schiller, 1993].

According to **figure 3-1**, in which simulation is compared to validated experimental data from a distillation campaign at atmospheric pressure [Cantagrel et al., 1990], the temporal evolution of ethyl lactate concentration in the distillate is not at all well represented during the two series batch distillations of the traditional process, known as Charentaise distillation. In the first distillation, figure 3-1a, the concentration is highly underestimated and follows a strongly decreasing trend, against a rather constant path of the experimental data. In the second one, figure 3-1b, the composition profile has a maximum in the middle of the distillation period, whereas the experimental data follow an increasing trend before the depletion of ethyl lactate in the boiler, towards the end of the operation. From these experimental data, one can conclude that ethyl lactate is mainly found in the tails fraction (last cut of the second distillation), even if it is also present in the core distillate fractions, and that its volatility is therefore presumably low.

In this context, the knowledge of vapor-liquid equilibrium data of this aroma compound and a better thermodynamic model choice are indispensable to correctly describe and predict its behaviour in distillation. To our knowledge vapor- liquid equilibrium data for ethyl lactate highly diluted in ethanol – water mixtures at 101.3 kPa have not been reported in the literature. Only binary equilibrium data have been generated: (1) at isobaric conditions for the ethyl lactate (EL) – ethanol (Et) system at 101.3 kPa [Pena-Tejedor at al., 2005] and (2) isothermal conditions for the ethyl lactate (EL) – ethanol (Et) system (at 313.15 K, 333.25 K and 353.35 K) and for the ethyl lactate (Et) – water (W) system (at 313.15 K, 333.15 K) [Vu et al., 2006]. Isobaric equilibrium data for the ethyl lactate (EL) – lactic acid (LA) – ethanol (Et) – water (W) quaternary system at 101.3 kPa has also been reported [Delgado et al., 2007].

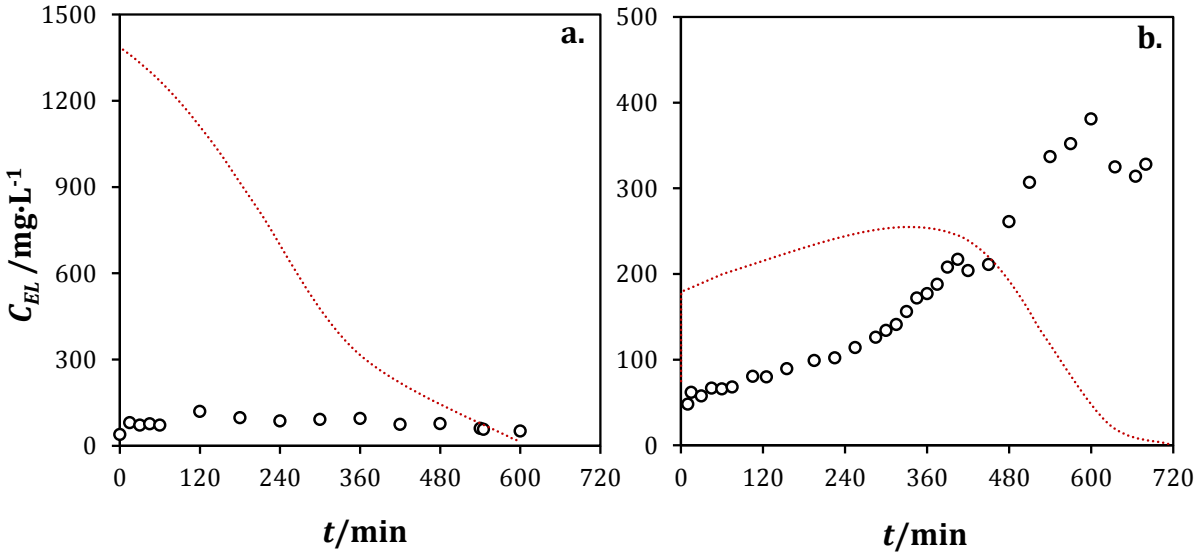

Figure 3-1. *Evolution of the ethyl lactate concentration (C_{EL}) in the distillate at 20 °C over time (t) during the (a) first batch distillation and (b) second batch distillation. (○) Experimental data from Cantagrel et al. (1990) (·····) Simulation using UNIFAC 1993 and the ideal gas equation.*

For the binary measurements, the whole liquid composition range of ethyl lactate was considered, x_{EL} = (0 to 1) mole fraction, whereas for the quaternary system, the interval is more reduced, x_{EL} = (0.02 to 0.20) mole fraction. In both cases the number of experimental data in the vicinity of x_{EL} = 0 is very reduced. Concerning the ternary mixture ethyl lactate – ethanol – water, only experimental distillation data are available, including those presented in figure 3-1 for Cognac distillation [Cantagrel et al., 1990] and some composition profiles of ethyl lactate concentration in the distillate as a function of the ethanol volume fraction in Armagnac distillation [Bertrand, 2003].

The objective of this work is thus to generate experimental vapor – liquid equilibrium data of ethyl lactate highly diluted over a composition range of the ethanol – water solution corresponding to a temperature interval from (352.3 to 370.0) K at 101.3 kPa. The equilibrium measurements are performed with a recirculation Gillespie-like still [Gillespie, 1946], a device based on a dynamic method recommended in the literature for measurements at temperatures higher than 298.15 K. This procedure provides a direct and simple way to determine the equilibrium behaviour of dilute mixtures, when coupled to an accurate quantitative analysis of the liquid and condensed vapor composition [Christensen, 1998; Rall and Muhlbauer, 1998] and has been used to estimate activity coefficients of methanol and ethanol highly diluted in water [Christensen, 1998] as well as partition coefficients of aroma compounds in hydro-alcoholic mixtures [Athès et al., 2008; Deterre et al., 2012].In both cases, the results proved to be consistent with respect to distillation data and model correlation.

The equilibrium data are then correlated with the NRTL and UNIQUAC models in order to determine the interaction parameters required in process simulators for the simulation of the ethyl lactate composition profiles in both continuous and discontinuous distillation of alcoholic beverages. These models have been used to correlate with satisfactory results the equilibrium data for ethanol – water system [Lai et al., 2014] as well as some binary (aroma compound – ethanol and aroma compound – water) [Pena-Tejedor at al., 2005; Vu et al., 2006; Faundez and

Valderrama, 2004; Faundez et al., 2006] and multicomponent aroma systems [Athès et al., 2008; Deterre et al., 2012; Faundez and Valderrama, 2009].

3.2. EXPERIMENTAL STUDY

3.2.1. MATERIALS

The chemical compounds studied in this work are listed in **table 3-1**, which includes the suppliers and some of their physicochemical properties. De-ionized water was obtained using a Milli-Q system (Millipore waters. Molsheim, France). Concerning the total volatile compounds content, a supplementary purity test for ethyl lactate and ethanol was performed by gas chromatography with flame ionization detection (GC-FID). No further purification of both compounds was needed since their experimental purities were estimated to be higher than 99.8 %.

Table 3-1. *Some properties of the compounds studied in this work.*

Compound	CAS	Molecular formula	MM /g.mol^{-1}	T_b /K[c]	Supplier purity %mass	Experimental purity [d]
(R,S)-ethyl 2-hydroxypropanoate[a]	97-64-3	$C_5H_{10}O_3$	118.31	427.65	≥98.00%	99.81%
Ethanol[b]	64-17-5	C_2H_6O	46.07	351.44	≥99.90%	99.98%
Water	7732-18-5	H_2O	18.01	373.15		

[a] A racemic mixture of L- and D- enantiomers, thereafter designed as ethyl lactate. Supplier: Sigma-Aldrich (Saint-Quentin Fallavier, France). [b] Supplier : Carlo Erba (Val de Reuil, France) [c] From Riddick et al [1986].[c] This experimental volatile purity was calculated as the ratio between the surface area of the gas chromatographic peak associated to the chemical compound and the total area of all peaks detected. MM is the molecular weight and T_b the Boiling point at 101.3 kPa.

The initial ternary mixtures for equilibrium measurements were prepared by precisely weighing known quantities of the three compounds. Due to the important quantity required for each equilibrium measurement (85 mL per ternary mixture, without considering the mixing flask mass), two weighing scales were necessary: one for ethyl lactate with an accuracy of ±0.0001 g and a maximum capacity of 100 g (Mettler AE240S weighing scale. L.P. Pesage. Angervilliers, France), and another for ethanol and water with an accuracy of ±0.01 g and a maximum capacity of 1000 g (Sartorious A2612. L.P. Pesage. Angervilliers, France).

Seventeen solutions with ethanol mass fractions ranging from x_{mEt} = (6.2×10^{-2} to 9.1×10^{-1}) (or in mole fractions x_{Et} = (2.5×10^{-2} to 8.0×10^{-1})) were independently brought into equilibrium. The concentration of ethyl lactate was fixed in ever initial solution to x_{mEL}=1.0×10^{-3}, which corresponds to a mole composition interval x_{EL} = (1.4×10^{-4} to 3.5×10^{-4}).

3.2.2. MEASUREMENTS OF VAPOR-LIQUID EQUILIBRIUM

Vapor-liquid equilibrium measurements were carried out by using the apparatus Labodest VLE 602™ (i-Fischer Engineering GmbH. Waldbüttelbrunn, Germany**)**, an all-glass still of the Gillespie type based on a dynamic method at adiabatic and isobaric conditions, with recirculation of both liquid and vapor phases.

This equipment, **figure 3-2,** has been previously used in our laboratory to measure vapor-liquid equilibria data for other aroma compounds. A detailed description has been already reported [Athès et al., 2008; Nala et al., 2013; Dias et al., 2014]. Some elements are recalled below.

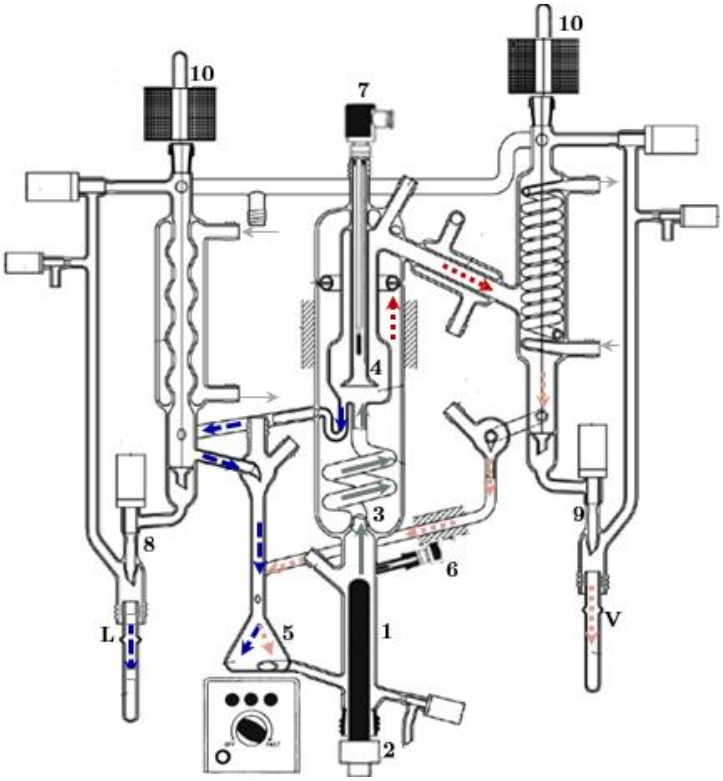

Figure 3-2. *Schema of the Labodest VLE 602™. Adapted from Dias et al. (2014). (1) Boiler, (2) Electrical resistance, (3) Contact path, (4) Separation chamber, (5) Mixing chamber, (6) Pt100 liquid probe, (7) Pt100 vapor probe, (8) Liquid sample port, (9) Vapor sample port, (10), Solenoid valves. (⟶) Vapor-Liquid, (⇢) Liquid (L), (⇢) Vapor (V), (⇢) Condensed vapor, (⟶) Refrigerant.*

Each ternary mixture (a charge of 85 mL) is heated and partially evaporated in the boiler. The rising vapor, carrying fine boiling droplets, goes through a contact path and arrives to a chamber where phase separation takes place, owing to a reduction of the flow velocity. Both phases, liquid and vapor (after condensation), circulate separately back to a mixing chamber connected to the boiler until thermodynamic equilibrium is reached. They are finally sampled for chromatographic analysis.

Two parameters were considered to ensure the equilibrium state: temperature, governed by the binary system ethanol – water (components in largest proportion), and composition. The time needed to reach a stable temperature (with a maximal standard uncertainty of ±0.3 K) was 30 min, whereas the time to reach composition equilibrium for this ternary system was determined by gas chromatography analysis to be about 2 h, once the temperature was constant.

The equilibrium temperature was measured by means of two Pt100 platinum probes (accuracy of ±0.05 K. i-Fischer Engineering GmbH. Waldbüttelbrunn, Germany), periodically calibrated against a reference platinum resistance thermometer (Pt100 Testo 735, accuracy of ±0.05 K; GFF. Chilly-Mazarin, France).

In order to promote a continuous and smooth evaporation of the mixtures, the heating power was adjusted in such a way that the condensed vapor rate was 2 drops.s^{-1}.

Concerning the total pressure, it was monitored using a digital manometer (P-10 WIKA, accuracy of ±0.1 kPa. i-Fischer Engineering GmbH. Waldbüttelbrunn, Germany) and controlled to the

desired value with an electronic pressure controller (i-Fischer Engineering GmbH. Waldbüttelbrunn, Germany), which regulates the flow of dry nitrogen into or from the still. In this study, the set point was maintained at 101.3 kPa with a maximal standard uncertainty of ±0.5 kPa.

3.2.3. DETERMINATION OF EQUILIBRIUM COMPOSITIONS

3.2.3.1. Ethyl lactate mass fractions

The analysis of ethyl lactate in the coexistent liquid and condensed vapor phases was performed by gas chromatography at the UNGDA laboratory. The equipment, a chromatograph 5890 series II, Hewlett Packard (Agilent Technologies. Ulis, France) was coupled to a flame ionization detector (T = 220 °C, H_2: 40 mL.min^{-1}, Air: 450 mL.min^{-1}, make up gas He: 45 mL.min^{-1}. Agilent Technologies. Ulis, France). A polar, polyethylene glycol capillary column (DB-WAX. 60 m linear length, 0.50 mm internal diameter, 0.25 μm film thickness. Agilent Technologies. Ulis, France) was used as stationary phase for the analysis. Hydrogen was used as the carrier gas at constant flow rate of 2.1 mL.min^{-1}. 2 μL of sample were directly injected with a split ratio of 1/30.

The initial oven temperature was set at 45 °C, followed by a linear increase rate of 5 °C.min^{-1} to 130 °C and a final linear increase rate of 15 °C.min^{-1} to 210 °C. The total running time per analysis was 22 min. The chromatographic data were acquired with the Hewlett-Packard Chemstation software B 0204 from Agilent Technologies.

The mass compositions of ethyl lactate were determined through calibration curves including butan-1-ol (CAS 71-36-3, mass purity: 99.50 %. Carlo Erba. Val de Reuil, France) as internal standard to minimize variability.

The calibration curves were established by diluting ethyl lactate in two different solvents: absolute ethanol and an ethanol - water mixture (ethanol mass fraction z_{mEt} = 0.5), in order to take account of the variations of injections and column performances due to matrix effects. In both calibration curves, the ethyl lactate mass fraction range varies from x_{mEL} = (0.2×10^{-4} to 50.0×10^{-4}), suitable for the analysis of the equilibrium samples. Seven calibration points were considered in both solvents.

The calculated detection and quantification limits derived from the analytical treatment of the calibration results were, respectively, DL = 6.5×10^{-6} g.g^{-1} and QL = 50.0×10^{-6} g.g^{-1} in absolute ethanol, and DL = 2.0×10^{-5} g.g^{-1} and QL = 14.0×10^{-5} g.g^{-1} in the ethanol-water mixture.

For mixtures with ethanol mass fractions lower than 0.50, a quantitative dilution in ethanol was done to reach z_{mEt} = 0.50 and the ethyl lactate compositions were calculated by using the calibration curve in the mixed solvent. For mixtures with higher ethanol fractions, the ethyl lactate compositions were calculated without any dilution. The calibration curve in absolute ethanol was used for mixtures with ethanol mass fractions between 0.75 and 1.00, and that in the mixed solvent, for mixtures with ethanol mass fractions between 0.50 and 0.75.

Each equilibrium sample as well as each calibration point was injected in triplicate. The relative standard uncertainty of the ratio between the ethyl lactate peak area and that of butan-1-ol, $u_r(R_{AEL\text{-}IS})$, varies from 0.05 % to 5.03 % with an average value of 0.44 %. This result enables to

validate the repeatability of the chromatographic analysis, and therefore the precision of the composition calculated with the calibration curves.

The initial ternary mixtures, before equilibrium and of known composition, were also analyzed in order to validate the accuracy of the analysis. The average relative deviation (AAD %) between the experimental (determined by weighing) and the analytical (from chromatographic analysis) mass fractions of ethyl lactate varies between 0.69 % and 10.46 %. This error interval remains quite acceptable in relation to the analysis technique.

3.2.3.2. Ethanol mass fractions

The ethanol mass compositions in the liquid and vapor phases were computed from the following experimental data: temperature, pressure and global composition, by considering that the bubble temperature and compositions of ethanol and water depend exclusively on the ethanol - water binary equilibrium. This assumption is valid because the concentration of ethyl lactate in both phases is significantly low (maximum liquid mole fraction on the order of 10^{-4}), which means that its influence on the equilibrium of the system is negligible [Deterre et al., 2012].

The calculation was carried out using the Flash TP algorithm of the Simulis® Thermodynamics Package by ProSim, which enables to calculate equilibrium compositions at fixed temperature, pressure and global composition. The thermodynamic model used to represent the vapor-liquid equilibrium of the binary system ethanol-water at 101.3 kPa was NRTL, with the interaction parameters reported by Kadir (2009).

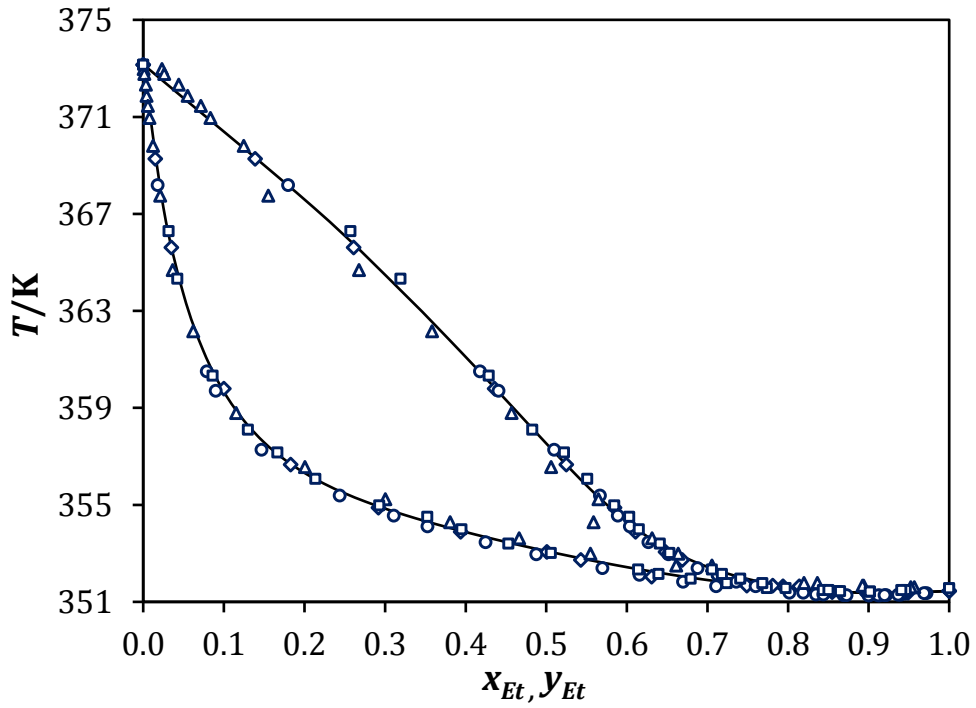

Figure 3-3. *Equilibrium diagram of the binary system Ethanol – Water at 101.3 kPa. (◇ Lai et al., 2014). (□ Arce et al., 1996) (△ Yang and Wang, 2002). (○ Kamihama et al, 2012). (——) NRTL model using the interaction parameters calculated by Kadir (2009). T is the equilibrium temperature, x_{Et} the ethanol mole fraction in the liquid phase and y_{Et} the ethanol mole fraction in the vapor phase.*

The reliability of these parameters was verified by fitting the experimental data measured by different authors [Lai et al., 2014; Arce et al., 1996 ; Yang and Wang, 2002 ; Kamihama et al., 2012]. The average relative deviation between the experimental and the calculated temperatures was 0.2 % and that of mole fractions in the vapor phase 3.0 %. The equilibrium diagram including the experimental data and the NRTL representation is presented in **figure 3-3**.

3.2.3.3. Mole fractions

The mass fractions of water were calculated by difference. The mole fractions of the liquid and vapor phases were then computed from the mass fractions and the mole weights of the three compounds.

3.2.4. COMPUTATION OF UNCERTAINTIES

The uncertainties of the equilibrium variables were calculated by using the law of propagation of uncertainties, as they were not measured directly but determined from other quantities through a functional relation [Taylor and Kuyatt, 1994]. The propagation of standard uncertainties is associated with four main factors: (1) the mass measurements with the weighing scales ($u(m_1)$ = 0.00006 g for the first one and $u(m_2)$ = 0.006 g for the second one), (2) the repeatability of the injections in chromatographic analysis, expressed in terms of the area ratio between the ethyl lactate and internal standard peaks ($0.001 \leq u(R_{AEL\text{-}IS}) \leq 0.081$), (3) the temperature measurements ($0.1\ K \leq u(T) \leq 0.3\ K$), and (4) the pressure measurements ($0.2\ kPa \leq u(P) \leq 0.5\ kPa$), both during the equilibrium experiments. The calculation was simplified by assuming that the estimates of the input quantities to calculate each equilibrium variable were uncorrelated. The resulting values are presented in the results sections.

3.3. THERMODYNAMIC MODELING

In this section, some elements about the thermodynamic models used in this work are presented. A suitable choice of these models is fundamental in process simulation for a correct representation of the aroma compound behaviour during distillation and other separation processes. For aroma compounds – ethanol – water systems at low pressures, the deviations from ideal behaviour are usually associated to the liquid phase and can therefore be described with the excess Gibbs energy approach, widely used and recommended in the literature. Among the models of this approach, the semi-empirical methods are considered in this work since they are easy for implementation and are available in most process simulators.

3.3.1. FUNDAMENTAL EQUATION OF PHASE EQUILIBRIUM

Vapor – liquid phase equilibria are computed by satisfying the equality of fugacities of all components i present in the two phases [Prausnitz et al., 1999 ; Rios, 2009]:

$$f_i^V(T,P,\boldsymbol{y}) = f_i^L(T,P,\boldsymbol{x}) \qquad [3\text{-}1]$$

Here f_i^V and f_i^L are the vapor and liquid fugacity of the species i, respectively. This property is a function of the temperature (T), the pressure (P) and the corresponding vector of mole composition ($\boldsymbol{y}$ or $\boldsymbol{x}$).

Since the pressure is low (<1000 kPa) and always below the critical pressure of the pure components, the vapor phase can be assumed as an ideal gas mixture and the properties of the liquid phase pressure – independent. As a result, equation 3-1 can be approximated as:

$$y_i P = \gamma_i(T,\boldsymbol{x}) x_i P_i^O(T) \quad [3\text{-}2]$$

In equation 3-2, γ_i is the activity coefficient of the species i in the liquid phase, $P_i^O(T)$ the vapor pressure of pure compound, and y_i and x_i the respective equilibrium mole fractions in the vapor and liquid phases.

Moreover, the equilibrium behaviour of an aroma compound (AC) in hydro-alcoholic mixtures depends not only on the physical conditions (T, P) but also on the solvent composition (ethanol and water), and can be described by means of two properties: the partition coefficient and the relative volatility.

The partition coefficient (K_{AC}), also known as physical equilibrium constant or absolute volatility, represents the aroma compound distribution between the vapor and liquid phases and is defined as:

$$K_{AC} = \frac{y_{AC}}{x_{AC}} \quad [3\text{-}3]$$

The relative volatility with respect to ethanol ($\alpha_{AC/Et}$), is an indicator of the species behaviour during the distillation of aroma compounds - ethanol – water mixtures [Dahm and Visco, 2015]:

$$\alpha_{AC/Et} = \frac{K_{AC}}{K_{Et}} = \frac{y_{AC}/x_{AC}}{y_{Et}/x_{Et}} = \frac{y_{mAC}/x_{mAC}}{y_{mEt}/x_{mEt}} \quad [3\text{-}4]$$

By combining equations 3-2 and 3-3, the partition coefficient can also be computed as:

$$K_i = \frac{y_i}{x_i} = \frac{\gamma_i(T,\boldsymbol{x}) P_i^O(T)}{P} \quad [3\text{-}5]$$

In the current study, it is useful to consider the infinite dilution as the reference state for ethyl lactate, as this compound is present at very low concentrations (maximum liquid mole fraction on the order of 10^{-4}).

In this case, the Henry constant, $\mathcal{H}_i$ is defined by the following relation [Letcher, 2007]:

$$\mathcal{H}_i(T,P,\boldsymbol{x}) = \lim_{x_i \to 0} \frac{f_i^L(T,P,\boldsymbol{x})}{x_i} \quad [3\text{-}6]$$

At low pressures, this variable can also be written as a function of $P_i^O(T)$ and $\gamma_i(T,\boldsymbol{x})$ at infinite dilution or $\gamma_i^\infty(T,\boldsymbol{x_s})$, which depends on the temperature and solvent composition, $\boldsymbol{x_s}$:

$$\mathcal{H}_i(T,\boldsymbol{x_s}) = \gamma_i^\infty(T,\boldsymbol{x_s}) P_i^O(T) \quad [3\text{-}7]$$

The activity coefficient at infinite dilution, γ_i^∞, provides accurate information about the aroma compound – mixed solvent interactions and therefore about the deviation from the ideal solution [Coquelet et al., 2008].

In this work, the vapor pressure of the three compounds have been calculated with the Riedel equation [Veterre, 1991], an extended version of the Antoine equation:

$$P_i^0(T) = \frac{1}{1000} exp\left(A_i + \frac{B_i}{T} + C_i ln(T) + D_i T^{E_i}\right) \quad [3\text{-}8]$$

With $P_i^0(T)$ given in kPa and T in K. A_i, B_i, C_i, D_i, E_i are coefficients specific for each compound. They were taken from the DIPPR Database available through the Simulis® Thermodynamics Package and are summarized in **table 3-2**. According to the values of T_{min} and T_{max}, the coefficients are valid for the three compounds in the temperature range of the equilibrium measurements (from 352.3 to 370.0) K.

Table 3-2. *Coefficients of the Riedel equation for calculating vapor pressures in kPa at a given temperature in K. Tmin and T_{max} are temperatures that define the interval of validity of the empirical equation. Information available in Simulis® thermodynamics package.*

Component	A_i	B_i	C_i	D_i	E_i	T_{min} /K	T_{max} /K
Ethyl lactate	7.8774×10^{1}	-6.7153×10^{3}	-9.5666	1.4993×10^{-2}	1	247.15	588.00
Ethanol	7.3304×10^{1}	-7.1223×10^{3}	-7.1424	2.8853×10^{-6}	2	159.05	514.00
Water	7.3649×10^{1}	-7.2582×10^{3}	-7.3037	4.1653×10^{-6}	2	273.16	647.10

3.3.2. CALCULATION OF ACTIVITY COEFFICIENTS

With regard to the activity coefficient, two semi-empirical models of the excess Gibbs energy (G^E) approach were used in this work: NRTL and UNIQUAC. Both models provide pressure-independent activity coefficients as a function of temperature and composition [Li and Parricaud, 2012]. The main working equations are presented in this section. The reader is directed to the principal references indicated for each model for further details about their theoretical basis.

NRTL (Non-Random Two Liquid) and UNIQUAC (Universal Quasi Chemical) are models of liquid solution based on the concept of local composition introduced by Wilson [Wilson, 1964]. They are valid at low pressures (less than 1000 kPa) and are widely recommended for the description of hydro-alcoholic solutions. The activity coefficient of a component i as a function of composition and temperature is given by the equations summarized in **table 3-3**. The UNIQUAC pure compound parameters for the three species studied in this work are presented in **table 3-4**.

Table 3-3. *Activity coefficient (γ_i) equations of NRTL and UNIQUAC models.*

Model	Reference	Equations	Parameters
NRTL	Renon and Prausnitz (1968)	$\ln \gamma_i (T,\boldsymbol{x}) = \frac{\sum_{j=1}^{n} \tau_{ji} G_{ji} x_j}{\sum_{k=1}^{n} G_{ki} x_k} + \sum_{j=1}^{n} \frac{G_{ij} x_j}{\sum_{k=1}^{n} G_{kj} x_k} \left(\tau_{ij} - \frac{\sum_{k=1}^{n} \tau_{kj} G_{kj} x_k}{\sum_{j=1}^{n} G_{kj} x_k} \right)$ $G_{ij} = exp(-c_{ij}\tau_{ij})$ $c_{ij} = c_{ij}^0 + c_{ij}^T (T-273.15)$ $\tau_{ij} = \frac{g_{ij}-g_{jj}}{RT} = \frac{A_{ij}^0 + A_{ij}^T (T-273.15)}{RT}$	- Binary interaction parameters A_{ij}^0, A_{ij}^T, c_{ij}^0, c_{ij}^T
UNIQUAC	Abrams and Prausnitz (1975) Anderson and Prausnitz (1978)	$\ln \gamma_i (T,\boldsymbol{x}) = \ln \gamma_i^C + \ln \gamma_i^R$ Combinatorial contribution, $\ln \gamma_i^C$ Staverman-Guggenheim term $\ln \gamma_i^C = \ln \frac{\varphi_i}{x_i} + \frac{Z}{2} q_i \ln \frac{\theta_i}{\varphi_i} + l_i - \frac{\varphi_i}{x_i} \sum_{j=1}^{n} x_j l_j$ $l_i = \frac{Z}{2}(r_i - q_i) - (r_i - 1)$ $\varphi_i = \frac{r_i x_i}{\sum_{j=1}^{n} r_j x_j}$ Residual contribution, $\ln \gamma_i^R$ $\ln \gamma_i^R = q'_i - q'_i \ln \left(\sum_{j=1}^{n} \theta_i \tau_{ji} \right) - q'_i \sum_{j=1}^{n} \frac{\theta'_i \tau_{ji}}{\sum_{k=1}^{n} \theta'_k \tau_{kj}}$ $\theta_i = \frac{q_i x_i}{\sum_{j=1}^{n} q_j x_j}$ $\theta'_i = \frac{q'_i x_i}{\sum_{j=1}^{n} q'_j x_j}$ $\tau_{ij} = exp\left(-\frac{g_{ij}-g_{jj}}{RT}\right) = exp\left(-\frac{A_{ij}^0 + A_{ij}^T T}{RT}\right)$	- Coordination number, Z=10 - Van der Waals volume, r_i - Van der Waals surface, q_i and q_i' - Binary interaction parameters A_{ij}^0, A_{ij}^T

τ_{ij} , g_{ij}, G_{ij} are binary interaction variables between species *i* and *j* in both activities models. φ_i is a volume fraction, θ_i, θ_i' are surface fractions and l_i is a supplementary parameter of the combinatorial contribution in UNIQUAC model. *R* is *the* ideal gas constant (1.9872 cal.mol^{-1}.K^{-1}) and *n* the number of chemical species in the systems, three in this work.

Table 3-4. *UNIQUAC parameters for the studied system.*

Component	r_i [a]	q_i [a]	q_i' [b]
Ethyl lactate	4.4555	3.9280	3.9280
Ethanol	2.1055	1.9720	0.9600
Water	0.9200	1.4000	1.0000

[a]Delgado et al, 2007 [b]Anderson and Prausnitz, 1978. r_i is the Van der Waals volume, and q_i and q_i' are Van der Waals surfaces.

In both semi-empirical models, the temperature dependence of c_{ij} and τ_{ij} are evaluated according to the original formalisms, included in the Simulis® Thermodynamics package. The variables A_{ij}^{0}, A_{ij}^{T} (non-symmetric), c_{ij}^{0} and c_{ij}^{T} (symmetric) are binary interaction parameters specific to each system. They must be obtained by regression of experimental equilibrium data and/or other thermophysical properties of the liquid phase. The estimation of these parameters for the studied system is presented in the results section.

3.4. Results and discussions

3.4.1. Experimental data

The vapor –liquid equilibrium data of the ternary system at 101.3 kPa are given in **table 3-5**. In order to characterize the behaviour of ethyl lactate in the hydro-alcoholic medium, the values of γ_{EL}^{∞}, $\mathcal{H}_{EL}$, K_{EL} and $\alpha_{EL/Et}$ are reported in **table 3-6.** Activity coefficients and Henry constants derive from the equilibrium relations, equations 3-2 and 3-7, and volatilities were directly calculated from composition data, according to equations 3-3 and 3-4. For the measurements of temperature and pressure, the values are reported with their respective standard uncertainties. For the other equilibrium variables, the reported uncertainties are the combined expanded ones, using a confidence level of 95 % that corresponds to a coverage factor of k=2.

The evolution of absolute and relative volatilities as a function of ethanol composition in the liquid phase is presented in **figure 3-4**. According to this figure, the volatility of ethyl lactate decreases when increasing ethanol concentration. This behaviour, already identified for other aroma compounds highly diluted [Athès et al., 2008; Deterre et al., 2012], can be explained by two reasons: (1) the equilibrium temperature of the system decreases as the ethanol liquid concentration is increased (according to the *Txy* diagram, figure 3-3) which leads to a reduction of the vapor pressure of the aroma compound and (2) the chemical nature of the aroma compound is closer to ethanol (presence of a carbon chain and of a C-OH (carbon – hydroxyl) bond) than to water. Thus, when the system is enriched with the organic solvent (ethanol), the difference between the cohesive forces (like molecules) and adhesive forces (unlike molecules) in the liquid phase is reduced and the transition of ethyl lactate to the vapor phase becomes less favorable.

Table 3-5. *Vapor-liquid equilibrium data of the system ethyl lactate highly diluted (EL) – ethanol (Et) – water (W) at P = 101.3 kPa.*

T /K	$u(T)$ /K	$u(P)$ /kPa	Mole composition of liquid phase (x)						Mole composition of vapor phase (y)					
			x_{EL}	$U_c(x_{EL})$	x_{Et}	$U_c(x_{Et})$	x_W	$U_c(x_W)$	y_{EL}	$U_c(y_{EL})$	y_{Et}	$U_c(y_{Et})$	y_W	$U_c(y_W)$
370.0	0.3	0.2	1.38×10^{-4}	1.08×10^{-6}	0.012	3.35×10^{-4}	0.988	3.35×10^{-4}	3.81×10^{-4}	7.85×10^{-6}	0.117	3.40×10^{-3}	0.882	3.40×10^{-3}
365.6	0.1	0.2	1.62×10^{-4}	8.29×10^{-7}	0.035	6.40×10^{-4}	0.965	6.40×10^{-4}	3.02×10^{-4}	2.10×10^{-6}	0.264	4.84×10^{-3}	0.735	4.84×10^{-3}
363.8	0.1	0.2	1.64×10^{-4}	1.26×10^{-6}	0.049	9.03×10^{-4}	0.951	9.03×10^{-4}	2.44×10^{-4}	5.89×10^{-6}	0.321	5.91×10^{-3}	0.678	5.91×10^{-3}
363.7	0.1	0.2	1.55×10^{-4}	1.36×10^{-6}	0.050	9.59×10^{-4}	0.950	9.59×10^{-4}	2.31×10^{-4}	5.48×10^{-6}	0.323	6.26×10^{-3}	0.677	6.26×10^{-3}
362.0	0.1	0.2	1.82×10^{-4}	1.24×10^{-6}	0.066	1.23×10^{-3}	0.934	1.23×10^{-3}	2.37×10^{-4}	2.07×10^{-6}	0.375	6.92×10^{-3}	0.624	6.92×10^{-3}
362.0	0.2	0.3	1.77×10^{-4}	6.38×10^{-6}	0.066	1.69×10^{-3}	0.934	1.69×10^{-3}	2.34×10^{-4}	3.31×10^{-6}	0.376	9.50×10^{-3}	0.623	9.50×10^{-3}
360.0	0.1	0.2	1.78×10^{-4}	8.96×10^{-7}	0.095	1.76×10^{-3}	0.905	1.76×10^{-3}	1.30×10^{-4}	1.14×10^{-6}	0.432	8.00×10^{-3}	0.567	8.00×10^{-3}
359.1	0.1	0.5	1.83×10^{-4}	9.44×10^{-7}	0.111	2.06×10^{-3}	0.889	2.06×10^{-3}	1.16×10^{-4}	1.70×10^{-6}	0.457	8.47×10^{-3}	0.543	8.47×10^{-3}
358.9	0.1	0.4	1.76×10^{-4}	3.03×10^{-6}	0.114	2.12×10^{-3}	0.886	2.12×10^{-3}	1.21×10^{-4}	1.20×10^{-6}	0.461	8.55×10^{-3}	0.539	8.55×10^{-3}
358.3	0.1	0.3	1.92×10^{-4}	1.07×10^{-6}	0.129	2.40×10^{-3}	0.871	2.40×10^{-3}	7.23×10^{-5}	7.33×10^{-7}	0.479	8.89×10^{-3}	0.521	8.89×10^{-3}
358.2	0.1	0.5	1.80×10^{-4}	9.48×10^{-7}	0.130	2.44×10^{-3}	0.869	2.44×10^{-3}	7.72×10^{-5}	1.04×10^{-6}	0.481	8.93×10^{-3}	0.519	8.93×10^{-3}
357.8	0.1	0.4	2.17×10^{-4}	2.84×10^{-6}	0.143	2.66×10^{-3}	0.857	2.66×10^{-3}	8.56×10^{-5}	1.01×10^{-6}	0.494	9.17×10^{-3}	0.506	9.17×10^{-3}
357.7	0.1	0.4	2.02×10^{-4}	2.18×10^{-6}	0.146	2.72×10^{-3}	0.854	2.72×10^{-3}	8.28×10^{-5}	1.65×10^{-6}	0.496	9.22×10^{-3}	0.503	9.22×10^{-3}
353.9	0.1	0.5	2.68×10^{-4}	2.70×10^{-5}	0.392	7.35×10^{-3}	0.608	7.35×10^{-3}	2.89×10^{-5}	1.32×10^{-6}	0.615	1.15×10^{-2}	0.385	1.15×10^{-2}
353.9	0.1	0.3	2.71×10^{-4}	6.06×10^{-6}	0.401	7.52×10^{-3}	0.599	7.52×10^{-3}	3.21×10^{-5}	1.11×10^{-6}	0.618	1.16×10^{-2}	0.382	1.16×10^{-2}
352.3	0.1	0.5	3.45×10^{-4}	3.76×10^{-6}	0.624	1.18×10^{-2}	0.375	1.18×10^{-2}	2.75×10^{-5}	3.81×10^{-7}	0.714	1.35×10^{-2}	0.286	1.35×10^{-2}
352.3	0.1	0.4	2.82×10^{-4}	3.10×10^{-6}	0.626	1.18×10^{-2}	0.374	1.18×10^{-2}	2.38×10^{-5}	6.96×10^{-7}	0.715	1.35×10^{-2}	0.285	1.35×10^{-2}

T and the equilibrium temperature of the vapor and liquid phases. u is the standard uncertainty and U_c the expanded combined uncertainty (95% level of confidence, $k = 2$).

Table 3-6. *Equilibrium variables describing the behaviour of ethyl lactate highly diluted in hydro-alcoholic mixtures at P=101.3 kPa.*

T /K	x_{Et}	Activity coefficients		Henry constants		Absolute volatility		Relative volatility	
		γ_{EL}^{∞}	$U_c(\gamma_{EL}^{\infty})$	$\mathcal{H}_{EL}$ /kPa	$U_c(\mathcal{H}_{EL})$ /kPa	K_{EL}	$U_c(K_{EL})$	$\alpha_{EL/Et}$	$U_c(\alpha_{EL/Et})$
370.0	0.012	18.89	0.66	278.97	12.31	2.75	6.07×10^{-2}	0.27	1.18×10^{-2}
365.6	0.035	15.19	0.22	189.50	3.54	1.87	1.61×10^{-2}	0.25	5.61×10^{-3}
363.8	0.049	12.98	0.37	150.18	4.59	1.49	3.78×10^{-2}	0.23	7.37×10^{-3}
363.7	0.050	13.03	0.37	151.05	4.77	1.48	3.75×10^{-2}	0.23	7.49×10^{-3}
362.0	0.066	12.41	0.20	133.88	2.68	1.30	1.44×10^{-2}	0.23	5.08×10^{-3}
362.0	0.066	12.21	0.55	131.88	6.66	1.32	5.12×10^{-2}	0.23	1.09×10^{-2}
360.0	0.095	7.42	0.12	73.91	1.47	0.73	7.35×10^{-3}	0.16	3.29×10^{-3}
359.1	0.111	7.31	0.13	69.89	1.53	0.63	9.85×10^{-3}	0.15	3.58×10^{-3}
358.9	0.114	6.68	0.17	64.14	1.81	0.69	1.37×10^{-2}	0.17	4.48×10^{-3}
358.3	0.129	4.10	0.07	38.19	0.79	0.38	4.36×10^{-3}	0.10	2.06×10^{-3}
358.2	0.130	4.67	0.09	43.33	0.98	0.43	6.17×10^{-3}	0.12	2.56×10^{-3}
357.8	0.143	4.58	0.09	41.59	1.00	0.39	6.94×10^{-3}	0.11	2.73×10^{-3}
357.7	0.146	4.38	0.12	39.91	1.18	0.41	9.32×10^{-3}	0.12	3.36×10^{-3}
353.9	0.392	1.55	0.15	12.01	1.16	0.11	1.14×10^{-2}	0.07	7.24×10^{-3}
353.9	0.401	1.40	0.07	10.93	0.53	0.12	4.88×10^{-3}	0.08	3.24×10^{-3}
352.3	0.624	1.11	0.02	8.08	0.20	0.08	1.41×10^{-3}	0.07	1.20×10^{-3}
352.3	0.626	1.18	0.04	8.54	0.31	0.08	2.64×10^{-3}	0.07	2.29×10^{-3}

[a] T is the equilibrium temperature of the vapor and liquid phases. x_{Et} is the mole fraction of ethanol in the liquid phase at equilibrium. U_c is the combined expanded uncertainty (95% level of confidence, $k = 2$).

According to figure 3-4a, the vapor phase is richer in ethyl lactate (K_{EL}> 1) when the liquid ethanol mole fraction is lower than x_{Et} = 0.1. For higher fractions, the phenomenon is reversed and the aroma compound becomes 2 to 10 times more abundant in the liquid phase. Concerning relative volatility, ethanol is more volatile than ethyl lactate over the entire concentration range of the solvent, as evidenced in figure 3-4b. This volatility ratio varies by a factor of 4, from 0.27, when x_{Et} tends to 0, to 0.07, when x_{Et} tends to 1.

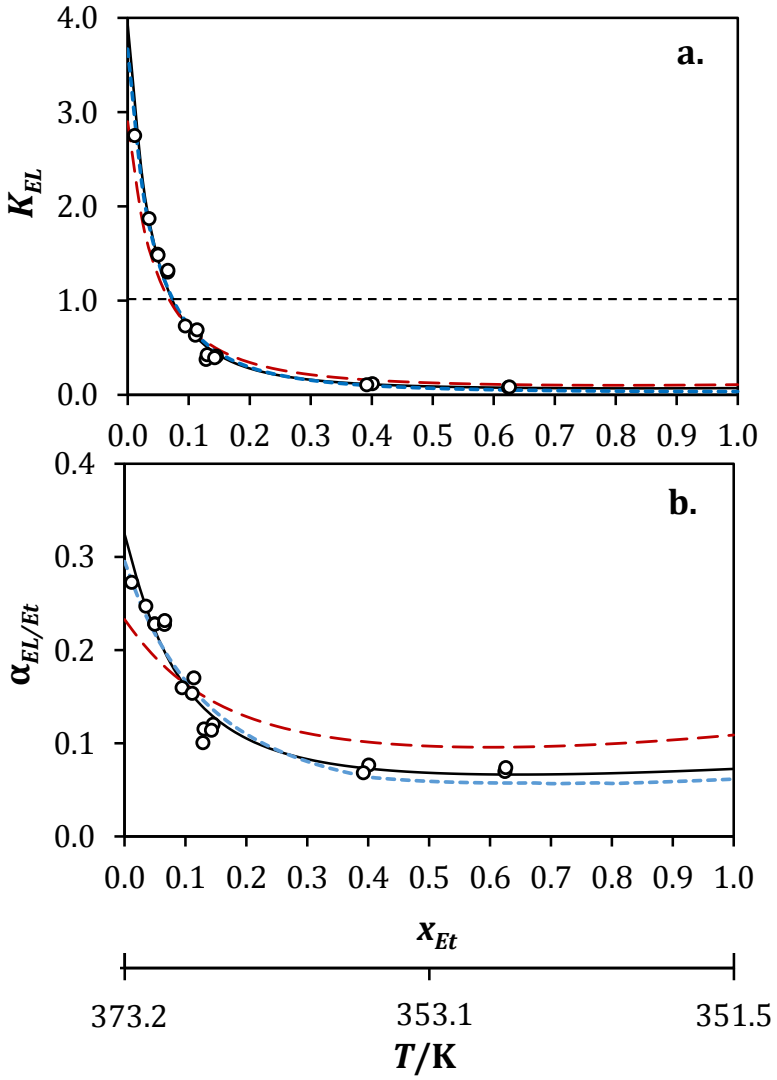

Figure 3-4. *Evolution of (a) absolute (K_{EL}) and (b) relative volatilities ($\alpha_{EL/Et}$) of ethyl lactate at 101.3 kPa as a function of ethanol composition (mole fraction) in the liquid phase. T is the corresponding equilibrium temperature. (○) Experimental data, (——) NRTL model, (- - -) UNIQUAC model, (— —) UNIQUAC model with interaction parameters fitted to binary data [Pena-Tejedor et al., 2005 ; Delgado et al., 2007].*

3.4.2. Modeling using semi-empirical models

Experimental equilibrium data were correlated by using the NRTL and UNIQUAC models. The objective was to determine the interaction parameters for the binary subsystems: ethyl lactate (1) – ethanol (2), ethyl lactate (1) – water (3) and ethanol (2) – water (3), which corresponds to 18 parameters for the NRTL model and 12 for the UNIQUAC model.

In order to reduce the number of parameters, the following assumptions were considered:

- For the NRTL model, the non-randomness parameter, c_{ij}^0, is set to 0.3 for all binaries. This assumption is valid for systems in vapor-liquid equilibrium [Renon and Prausnitz, 1968].
- For the ethyl lactate - ethanol and ethyl lactate - water binaries, A_{ij}^T, the temperature-dependent parameter of τ_{ij}, was neglected. Two factors justify this approximation: (1) the number of experimental data is limited and (2) the equilibrium temperature interval is reduced (from 352.3 to 370.0) K.

The interaction parameters of the binary ethanol (2) - water (3) are fixed to the values presented in the literature and reported in **table 3-7.** As previously stated, the reliability of these parameters was verified by fitting different experimental data sets [Lai et al., 2014; Arce et al., 1996 ; Yang and Wang, 2002; Kamihama et al., 2012]. The deviations of the temperature and vapor mole fractions calculated with NRTL and UNIQUAC models are also reported in table 3-7.

In this way, the problem was reduced to the regression of 4 parameters:

- 2 associated with the binary ethyl lactate (1) - ethanol (2): A_{12}^0, A_{21}^0.
- 2 associated with the binary ethyl lactate (1) - water (3): A_{13}^0, A_{31}^0.

The parameters were fitted by minimizing an objective function with the generalized reduced gradient method [Lasdon et al., 1974]. The regressed properties were K_{EL} and $\alpha_{EL/Et}$. These parameters will be later considered for the simulation of distillation units, in which the separation performance is directly based upon the difference of volatilities between the chemical species.

Two objective functions were evaluated:

$$\mathrm{OF}(\alpha)=\sum_{i=1}^{N} w_i\left(\alpha_{EL/Et\ i\ Exp}-\alpha_{EL/Et\ i\ Model}\right)^2 \quad [3\text{-}9]$$

$$\mathrm{OF}(K)=\sum_{i=1}^{N} w_i\left(K_{EL\ i\ Exp}-K_{EL\ i\ Model}\right)^2 \quad [3\text{-}10]$$

Where N is the number of data and w_i, a weighting factor depending on the uncertainty of the experimental data ($\alpha_{i\ Exp}$, $K_{i\ Exp}$). An experimental value having a high standard uncertainty is supposed to be less reliable and has therefore a lower weighting factor than an experimental value with a low uncertainty.

The weighting factors were normalized ($\sum w_i = 1$) and calculated as:

$$w_i=\frac{1/U_c(i)}{\sum_{i=1}^{N} 1/U_c(i)} \quad [3\text{-}11]$$

where U_c is the estimated expanded combined uncertainty for each experimental value.

The calculation of equilibrium properties ($\alpha_{EL/Et\ i\ Model}$, $K_{EL\ i\ Model}$) was carried out using the Bubble Temperature algorithm of the Simulis® Thermodynamics package, at the experimental pressure (P) and composition in the liquid phase (x). The algorithms allows to compute the saturated temperature (T) and the composition of the vapor phase (y) in equilibrium.

Table 3-7. *Interaction parameters for the binary ethanol (2) – water (3) and fitting quality statistics with respect to five experimental data sets obtained from literature.*

Model	A_{23}^{0}/cal.mol^{-1}	A_{32}^{0}/cal.mol^{-1}	A_{23}^{T}/cal.mol^{-1}.K^{-1}	A_{32}^{T} / cal.mol^{-1}.K^{-1}	*T* /K		y_{Et}	
					AAD%	*RMSE*	*AAD%*	*RMSE*
NRTL[a]	34.02	850.12	-1.8	5.65	0.2%	0.3	2.99%	0.01
UNIQUAC[b]	1448.61	-1504.21	-3.68	4.96	0.2%	0.3	3.10%	0.01

These parameters are fixed for the correlation of equilibrium data of the ternary system ethyl lactate highly diluted – ethanol – water. [a]Kadir, 2009 [b]Delgado et al., 2007
T the equilibrium temperature, y_{Et} the ethanol mole fraction in the vapor phase, *AAD%* the average absolute deviation, and *RMSE* the root-mean-squared deviation.

Table 3-8. *Binary interaction parameters for the ternary system ethyl lactate highly diluted (1) – ethanol (2) – water (3) and fitting quality statistics.*

Model	OF	Binary	A_{ij}^{0} /cal.mol^{-1}	A_{ji}^{0} /cal.mol^{-1}	*T* /K		y_{Et}		y_{EL}		K_{EL}		$\alpha_{EL/Et}$	
					AAD%	*RMSE*	*AAD%*	*RMSE*	*AAD%*	*RMSE*	*AAD%*	*RMSE*	*AAD%*	*RMSE*
NRTL	α	(1) i – (2) j	455.52	-343.55	0.1%	0.1	0.34%	1.74×10^{-3}	9.63%	1.57×10^{-5}	10.63%	1.00×10^{-1}	9.59%	1.79×10^{-2}
		(1) i – (3) j	-349.32	2758.14										
	K	(1) i – (2) j	54.97	-639.44	0.1%	0.1	0.34%	1.74×10^{-3}	12.51%	1.70×10^{-5}	9.51%	8.43×10^{-2}	12.49%	2.10×10^{-2}
		(1) i – (3) j	386.75	1969.48										
UNIQUAC	α	(1) i – (2) j	96.98	-148.76	0.1%	0.1	0.44%	1.73×10^{-3}	10.16%	1.64×10^{-5}	11.20%	1.04×10^{-1}	10.18%	2.14×10^{-2}
		(1) i – (3) j	289.50	107.21										
	K	(1) i – (2) j	95.89	-156.38	0.1%	0.1	0.43%	1.70×10^{-3}	13.35%	1.85×10^{-5}	10.11%	8.89×10^{-2}	13.38%	2.57×10^{-2}
		(1) i – (3) j	356.06	66.13										

OF is the objective function used to determine the interaction parameters, *T* is the equilibrium temperature, y_{Et} the ethanol mole fraction in the vapor phase, y_{EL} the ethyl lactate mole fraction in the vapor phase, K_{EL} the ethyl lactate absolute volatility, $\alpha_{EL/Et}$ the ethyl lactate relative volatility with respect to ethanol, *AAD%* the average absolute deviation, and *RMSE* the root-mean-squared deviation.

Table 3-9: *Interaction parameters of UNIQUAC models for the binaries ethyl lactate (1) – ethanol (2) and ethyl lactate (1) – water (3) from the literature.*

Binary	A_{ij}^{0} /cal.mol^{-1}	A_{ji}^{0} /cal.mol^{-1}	*T* /K		y_{Et}		y_{EL}		K_{EL}		$\alpha_{EL/Et}$	
			AAD%	*RMSE*	*AAD%*	*RMSE*	*AAD%*	*RMSE*	*AAD%*	*RMSE*	*AAD%*	*RMSE*
(1) i – (2) j[a]	679.2	-295.4	0.1%	0.1	0.44%	$1.77E\times10^{-3}$	23.11%	3.15×10^{-5}	23.11%	1.92×10^{-1}	23.34%	3.41×10^{-2}
(1) i – (3) j[b]	198.3	128.2										

[a]Peña-Tejedor et al. (2005) [b]Delgado et al. (2007)

T is the equilibrium temperature, y_{Et} the ethanol mole fraction in the vapor phase, y_{EL} the ethyl lactate mole fraction in the vapor phase, K_{EL} the ethyl lactate absolute volatility, $\alpha_{EL/Et}$ the ethyl lactate relative volatility with respect to ethanol, *AAD%* the average absolute deviation, and *RMSE* the root-mean-squared deviation.

The fitting quality was judged with respect to four variables (E): T, y_{Et} and y_{EL}, K_{EL} and $\alpha_{EL/Et}$. Two deviations were calculated:

- Average absolute relative deviation (*AAD%*):

$$\text{AAD }\% = \frac{1}{N}\sum_{i=1}^{N}\left|\frac{E_{i\,Exp}-E_{i\,Model}}{E_{i\,Exp}}\right| 100\% \qquad [3\text{-}12]$$

- Root-mean-squared deviation (*RMSE*):

$$\text{RMSE} = \left[\frac{1}{N}\sum_{i=1}^{N}\left(E_{Exp\,i}-E_{i\,Model}\right)^2\right]^{1/2} \qquad [3\text{-}13]$$

The results obtained are summarized **in table 3-8**. Comparing the statistics, one can conclude that for both models, the fitting quality is globally better with the regression based on *OF(α)*. Indeed, while the fitting quality is the same with both formulations for T and y_{Et}, for the variables related to ethyl lactate, the overall *AAD%* values obtained with *OF(α)* are more favorable. In this way, using the binary interaction parameters derived from *OF(α)*, the obtained evolution of K_{EL} and $\alpha_{EL/Et}$ as a function of ethanol composition is shown in **figure 3-4**. Both models correlate correctly the experimental data. A slight difference is noted only in the high ethanol concentration, from x_{Et} = 0.5.

3.4.2.1. Comparison with literature data

Concerning the information from the literature, the interaction parameters for ethyl lactate - ethanol and ethyl lactate – water pairs have been reported for the UNIQUAC model by Peña-Tejedor et al (2005) and Delgado et al. (2007). The values are presented in **table 3-9**. They were estimated from isobaric experimental data of the corresponding binary systems, in which ethyl lactate is present over the entire composition range, from x_{EL}= (0 to 1).

The volatility curves of ethyl lactate as a function of ethanol composition, calculated with these latter parameters, are shown in figure 3-4. The values of RMSE and AAD% for the different equilibrium values are summarized in table 3-9. One can observe that the representation of the experimental data for the ternary system is globally acceptable, but the evolution of $\alpha_{EL/Et}$ with respect to ethanol composition exhibits some non-negligible differences: in the low ethanol concentration region ($x_{Et} \leq 0.1$), the volatility is underestimated (with an average error of 16%) and overestimated from x_{Et} = 0.1 with a mean error of about 29 %. As a result, for simulation purposes in alcoholic beverages distillation, where relative volatility is the key parameter of separation, the interaction parameters calculated in this work are recommended.

3.4.2.2. Evolution of γ_{EL}^{∞} and $\mathcal{H}_{EL}$ with temperature and ethanol composition

The evolution of the activity coefficient of ethyl lactate, γ_{EL}^{∞}, as a function of temperature and ethanol composition is shown in **figure 3-5**. The activity coefficient is always higher than unity. In this case, the positive deviation from ideality ($\gamma_{EL}^{\infty}>1$) means that the interactions forces between the solvent molecules and the ethyl lactate molecules are unfavorable, especially with water. It is observed that γ_{EL}^{∞} increases as the equilibrium temperature is increased and decreases when the liquid phase is enriched in ethanol. Both trends are linked since the activity coefficient is

determined along the ethanol – water vapor – liquid equilibrium curve. The increase of γ_{EL}^{∞} indicates that the interaction forces between the ethyl lactate molecules are reduced, which leads to an increase of its partial pressure and therefore of its volatility. This behaviour is logical since the volatility of ethyl lactate is higher in the low ethanol concentration region, where equilibrium temperatures are higher.

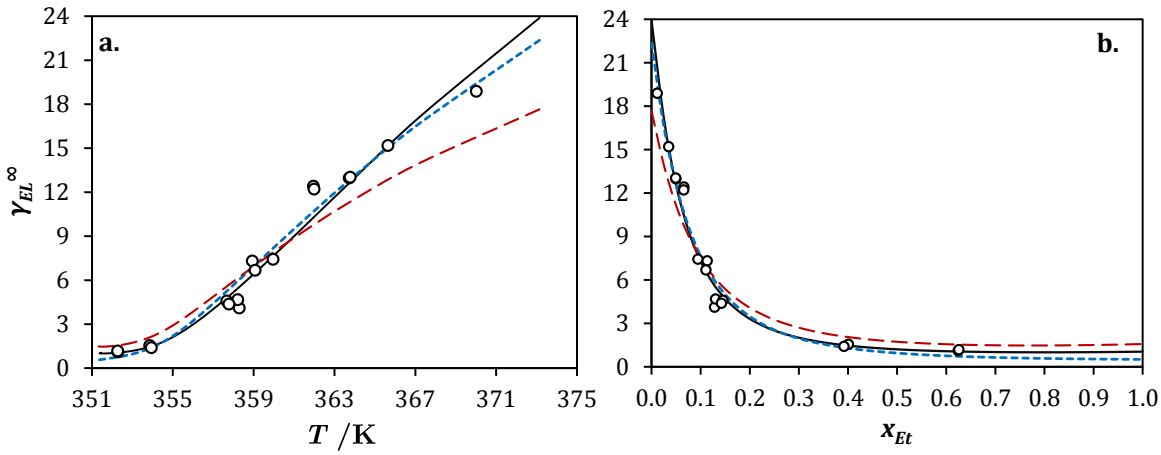

Figure 3- 5. *Evolution of the activity coefficient of ethyl lactate (γ_{EL}^{∞}) with respect to (a) equilibrium temperature (T) at 101.3 kPa and (b) ethanol composition in the liquid phase (xEt). (○) Experimental data, (——) NRTL model, (- - -) UNIQUAC model, (— —) UNIQUAC with interaction parameters fitted to binary data [Pena-Tejedor et al., 2005 ; Delgado et al., 2007].*

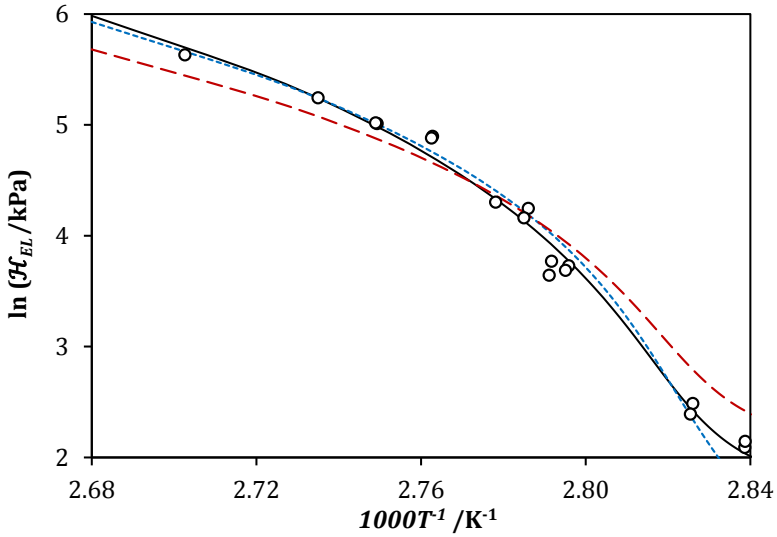

Figure 3-6. *Representation of Ln $\mathcal{H}_{EL}$ with respect to 1/T at 101.3 kPa. (○) Experimental data, (——) NRTL model, (- - -) UNIQUAC model, (— —) UNIQUAC model with interaction parameters fitted to binary data [Pena-Tejedor et al., 2005 ; Delgado et al., 2007]. $\mathcal{H}_{EL}$ is the Henry constant of ethyl lactate and T the equilibrium temperature.*

Concerning the Henry constant, the evolution of $ln\,\mathcal{H}_{EL}$ as a function of $1/T$ (**figure 3-6)**, calculated with the NRTL and UNIQUAC models, exhibits not a linear trend but a concave decreasing behaviour. This can be explained by the fact that the temperature and the composition of the liquid phase are not independent at boiling conditions: a change in boiling temperature corresponds to a variation in the liquid composition and vice versa. As noted in equation 3-7, $\mathcal{H}_{EL}$ is a function of both temperature and composition, as the solvent is not a pure compound but a mixture of ethanol and water.

3.5. CONCLUSIONS

The vapor-liquid equilibrium of ethyl lactate highly diluted in ethanol – water mixtures at 101.3 kPa for boiling temperatures from (352.3 to 370.0) K were measured with a recirculation still. The ethanol compositions were determined from temperature measurements and the ethyl lactate compositions by gas chromatography. It is observed experimentally that the volatility of ethyl lactate decreases when the ethanol content in the liquid phase is increased. Ethyl lactate is always less volatile than ethanol and its relative volatility is reduced by a factor of 4 over the entire solvent composition range in the liquid phase. The ternary system exhibits positive deviation from ideality (γ_i>1).

The experimental data were correlated with two semi – empirical models (NRTL and UNIQUAC), and a good description is obtained with overall average relative deviations between 0.1 % and 10.2 %. A correct order of magnitude of the absolute and relative volatilities of ethyl lactate at high dilution can also be obtained with the binary parameters available in the literature for the UNIQUAC model. However, for simulation purposes in alcoholic beverages distillation, a more accurate representation of the ethyl lactate behaviour is fundamental since this aroma compound contributes to the product quality. This accurate representation is only obtained by using the interaction parameters presented in this work, fitted to equilibrium data at very low concentrations.

CHAPITRE 4. PREDICTION THEORIQUE DES DONNEES D'EQUILIBRE LIQUIDE-VAPEUR

La troisième approche d'acquisition de données d'équilibre développée dans ces travaux repose sur les prédictions théoriques des modèles d'estimation de coefficients d'activité. Ce chapitre est dédié à l'application de cette voie de calcul à l'étude des équilibres liquide-vapeur du lactate d'éthyle à faible concentration en milieu hydroalcoolique. Deux modèles sont évalués : le modèle UNIFAC dans ses versions 1975 et 1993, et le modèle COSMO-SAC dans ses versions 2002, 2006, 2010 et 2014. La modélisation thermodynamique est effectuée en fixant le comportement du binaire éthanol–eau à sa représentation par modèle le NRTL, ceci dans la but de focaliser la prédiction exclusivement sur le comportement du composé volatil d'arôme. Les données expérimentales présentées dans le chapitre 2 sont prises comme référence pour juger la capacité prédictive des modèles.

La méthodologie développée dans ce chapitre fera également l'objet d'un article en cours de préparation sur la prédiction des données d'équilibre pour un groupe de 35 composés d'arôme, dont le lactate d'éthyle.

Predictive thermodynamic modelling of vapor–liquid equilibria (VLE) for aroma compounds highly diluted in ethanol – water mixtures at 101.3 kPa using UNIFAC and COSMO-SAC models.

Cristian Puentes, Patrice Paricaud, Xavier Joulia, Martine Esteban-Decloux.

A soumettre au journal *Fluid Phase Equilibria*.

4.1 INTRODUCTION

The design and simulation of industrial separation processes require a reliable and accurate knowledge of the involved phase equilibria [Ashour and Aly, 1996; Cadoret et al., 2009; Hsieh et al., 2010; Voutsas et al., 2011; Valderrama et al., 2012; Esteban-Decloux et al., 2014]. In alcoholic beverages distillation, the description of vapor-liquid equilibria is a challenging task due to the complexity and the non-ideal behaviour of the raw material, a solution mainly composed of ethanol, water and several hundred of volatile aroma compounds at low concentrations [Soumalainen and Lehtonen, 1979; Ebeler, 2001; Ortega et al., 2001; Marti et al., 2003; Jiang et. al, 2010].

The equilibrium behaviour of an aroma compound (AC) in hydroalcoholic mixtures can be described by means of two properties: the partition coefficient and the relative volatility. The partition coefficient (K_{AC}), also known as absolute volatility, represents the aroma compound distribution between the vapor and liquid phases and is defined as:

$$K_{AC}=\frac{y_{AC}}{x_{AC}} \quad [4\text{-}1]$$

where y_{AC} and x_{AC} are the molar fractions in vapor and liquid phase, respectively.

The relative volatility with respect to ethanol ($\alpha_{AC/Et}$) and water ($\alpha_{AC/W}$), is an indicator of the species behaviour during distillation of aroma compounds - ethanol – water mixtures [Dahm and Visco, 2015]:

$$\alpha_{AC/Et}=\frac{K_{AC}}{K_{Et}}=\frac{y_{AC}/x_{AC}}{y_{Et}/x_{Et}} \quad [4\text{-}2]$$

$$\alpha_{AC/W}=\frac{K_{AC}}{K_{W}}=\frac{y_{AC}/x_{AC}}{y_{W}/x_{W}} \quad [4\text{-}3]$$

Since the concentrations of aroma compounds in the solution are very low (liquid molar fraction lower than 10^{-4}), the phase equilibrium can also be characterized by the activity coefficient at infinite dilution, a parameter that provides accurate information about the aroma compound – mixed solvent interactions and therefore about the deviation from the ideal solution [Coquelet et al., 2008].

Equilibrium data for systems containing aroma compounds highly diluted are relatively scarce in the literature. Some studies were done by Williams, (1962) (29 aroma compounds including 1 acetal, 9 alcohols, 7 carboxylic acids, 6 carbonyl compounds, 5 esters, and 1 furan), [Ikari et al., 1984 ; Ikari et al., 1990 ; Ikari et al., 1998a ; Ikari et al., 1998b] (11 aroma compounds, including 4 alcohols, 4 carbonyl compounds, 2 esters, and 1 furan), Athès et al. (2008) (13 brandy aroma compounds, including 5 alcohols, 2 carbonyl compounds and 6 esters) and Deterre et al. (2012) (5 bitter orange aroma compounds, 2 monoterpene hydrocarbons and 3 oxygenated terpenes). Notwithstanding, the number of species studied is still limited and other aroma compounds with an important impact on the organoleptic properties of alcoholic beverages have never been studied to date.

The classic way to obtain equilibrium data is through experimental measurements with static [Malanowski, 1982] or dynamic methods [Rall and Mühlbauer, 1998], coupled to accurate

quantitative tools for the analysis of the coexisting phases. However, despite its relative simplicity, this approach is time and resources consuming. Thus, given the important number of aroma compounds in the hydroalcoholic matrix, alternative strategies based on predictive modelling could be very useful for faster and less expensive data generation.

For aroma compounds–ethanol–water systems at low pressures (< 1000 kPa), the deviations from ideal behaviour are usually associated to the liquid phase and can be described with the excess Gibbs energy approach, based on the calculation of activity coefficients. Two main types of predictive models from this approach have been used in the literature for the modelling of hydroalcoholic mixtures: UNIFAC [Fredenslund et al, 1975] and COSMO-SAC models [Lin and Sandler, 2002]. UNIFAC models has been tested by Faundez et al. (2006) for the prediction of vapor-liquid equilibria of ternary systems containing 8 aroma compounds at high concentrations (liquid molar fraction between 8.0×10^{-4} and 7.8×10^{-1}). Acceptable averages deviations were obtained for temperature measurements (between 0.10 and 2.10%) and rather high values for aroma compound molar fractions in the vapor phase (between 4.30% and 39.30%). The COSMO-SAC model was used by Athès et al. (2008) for the prediction of vapor-liquid data of a multicomponent mixture containing 13 aroma compounds highly diluted in ethanol – water mixtures. They showed that it was possible to estimate the partition coefficients for all of the considered alcohols and aldehydes with reasonable precision, but that the values are rather underestimated for ethyl esters with long carbon chain.

In this context, the objective of this work is to assess the capability of both UNIFAC and COSMO-SAC models to predict vapor–liquid data of aroma compounds highly diluted in ethanol – water mixtures. As part of our ongoing research on alcoholic distillation, own experimental data for the ternary system ethyl lactate (Ethyl 2-hydroxypropanoate)–ethanol–water were used as reference for validation purposes [Puentes et al., 2017b]. These data, reported for the first time in the literature, were measured with a recirculation Gillespie-like still [Gillespie, 1946] over a composition range of the ethanol–water solution corresponding to a temperature interval from 352.3 K to 370.0 K at 101.3 kPa. The ethyl lactate composition in the coexisting phases was quantified by gas chromatography coupled to flame ionization detection, whereas the ethanol concentration was estimated from temperature measurements. Further details on the experimental procedure and data correlation are presented in a companion paper [Puentes et al., 2017].

The accuracy of both predictive models are discussed in order to define the suitable thermodynamic approach for the correct design and simulation of distillation units involving the studied system and others of similar nature. A more complete study, including several aroma compounds from different chemical families and different validation data, will be developed in a future work.

The paper is organized as follows: some elements on modeling principles of vapor –liquid equilibria are presented, followed by a description of the proposed methodology for the prediction of such data in aroma compounds – ethanol – water systems. A detailed comparison between experimental and predicted values is then developed, and finally an estimation of the infinite dilution limit for ethyl lactate is presented based on activity coefficient predictions.

4.2 THERMODYNAMIC MODELLING

4.2.1. FUNDAMENTAL EQUATIONS OF PHASE EQUILIBRIA

The thermodynamic modelling of vapor – liquid equilibria is based on the equality of three intensive variables: (1) temperature, (2) pressure and (3) chemical potentials of the species present in every phase. The third condition can also be expressed by the equality of fugacities, variable that corresponds to a generalised partial pressure [Prausnitz et al., 1999; Rios, 2009].

$$f_i^V(T,P,\boldsymbol{y}) = f_i^L(T,P,\boldsymbol{x}) \quad [4\text{-}4]$$

By following a classical heterogeneous approach to describe hydro-alcoholic mixtures, the vapor phase fugacity of the component i, $f_i^V(T,P,\boldsymbol{y})$, can be expressed as a function of the fugacity coefficient, $\phi_i^V(T,P,\boldsymbol{y})$, and the liquid phase fugacity, $f_i^L(T,P,\boldsymbol{x})$, as a function of the activity coefficient, $\gamma_i(T,\boldsymbol{x})$, and the fugacity of the pure compound under the same conditions of temperature and pressure, $f_i^{OL}(T,P)$. Thus, the vapor-liquid equilibrium of each component in the mixture can be described with the following expression:

$$\phi_i^V(T,P,\boldsymbol{y})y_iP=\gamma_i(T,\boldsymbol{x})x_if_i^{OL}(T,P) \quad [4\text{-}5]$$

Since the total pressure is low (<1000 kPa) and the temperature always below the critical temperatures of the pure components, the vapor phase can at P and $P_i^O(T)$ can be assumed as an ideal gas mixture and the properties of the liquid phase pressure – independent. As a result, equation 4-5 can be approximated as:

$$y_iP=\gamma_i(T,\boldsymbol{x})x_iP_i^O(T) \quad [4\text{-}6]$$

Where $P_i^O(T)$ is the vapor pressure of pure compound at the equilibrium temperature. The partition coefficient can be computed from equation 4-1 as:

$$K_i=\frac{y_i}{x_i}=\frac{\gamma_i(T,\boldsymbol{x})P_i^O(T)}{P} \quad [4\text{-}7]$$

In the current study, the volatile aroma compound will be considered at infinite dilution, as this species is present at very low concentrations in the ethanol-water matrix. Hence, the corresponding activity coefficient is symbolized as $\gamma_i^\infty(T,x_s)$ and only depends on temperature and solvent composition, x_s. The approximation of infinite dilution for the reference experimental data is validated in section 4.3.1. On the other hand, $P_i^O(T)$ is calculated with the Riedel equation, an extended version of the Antoine equation [Vetere, 1991]:

$$P_i^O(T)=\frac{1}{1000}exp\left(A_i+\frac{B_i}{T}+C_iln(T)+D_iT^{E_i}\right) \quad [4\text{-}8]$$

With $P_i^O(T)$ given in kPa and T in K. A_i, B_i, C_i, D_i, E_i are coefficients specific for each compound, available in the DIPPR Database and accessible through the Simulis® Thermodynamics Package, software for calculations of phase equilibria and other thermophysical properties developed by ProSim.

4.2.2. CALCULATION OF ACTIVITY COEFFICIENTS

Two kinds of predictive models were used in this work to compute the activity coefficients: UNIFAC and COSMO-SAC models. All models provide pressure-independent activity coefficients as a function of temperature and composition [Li and Paricaud, 2012]. The main working equations are presented in **Appendix A.3**. The reader is directed to the principal references indicated for each model for further details about their theoretical basis.

4.2.2.1. UNIFAC models

Based on the group-contribution concept, the molecule properties are described as a sum of contributions from several blocks corresponding to different chemical functional groups [Nieto-Draghi et al, 2015]. UNIFAC (UNIQUAC Functional-group activity coefficients) combines the solution of functional groups with an activity coefficient model derived from an extension of UNIQUAC and contains at least two adjustable parameters per pair of functional groups. Two version were considered for comparison, UNIFAC 1975 [Fredenslund et al, 1975] and UNIFAC 1993 [Weidlich et al., 1987; Gmehling et al., 1993]. The matrix of binary interaction parameters is available for both model versions via the Simulis® Thermodynamics package.

4.2.2.2. COSMO-based models

In the COSMO approach, a liquid phase is described as a mixture of solvent and solutes molecules: each solute molecule is delimited by a cavity surrounded by a dielectric continuum that represents the solvent [Nieto-Draghi et al, 2015]. The combination of this theory with a chemical potential model led to the development of the COSMO-RS (Conductor-like Screening for real solvent) model by Klamt and Eckert (2000) which represents molecules as interacting segments [Nala et al., 2013]. The COSMO-SAC (Conductor-like Screening Model – Segment Activity Coefficient) model, proposed by Lin and Sandler (2002), is a variation of COSMO-RS model that enables a direct calculation of activity coefficients.

In COSMO-type models, the only required inputs to characterise a chemical compound are ab initio data, obtained from quantum mechanical calculations and stored in COSMO-files. The objective of these calculations is to determine three variables: (1) the molecular surface, (2) the molecular volume and (3) the screening (polarisation) charges (σ) induced by solute molecule on its discretised surface or cavity. The surfaces charges are subsequently averaged on effective surface segments and represented in the form of a probability distribution function (or histogram), called sigma profile [Nala et al., 2013; Nieto-Draghi et al, 2015]. The weighted contributions of each chemical compound are averaged to obtain a final description of the liquid mixture [Nala et al., 2013].

For equilibrium predictions, COSMO models require some universal parameters that have been fitted over a large set of experimental vapor-liquid and liquid-liquid equilibrium data [Fan et al., 2011]. The COSMO-SAC model was chosen in this work because of the availability of a free web-based database of COSMO-files, known as VT-2005 and created by Mullins et al. [2006]. In comparison to COSMO-RS model, the accuracy of the equilibrium predictions are expected to be of the same order of magnitude [Nieto-Draghi et al, 2015].

All data from VT-2005 were calculated by means of DMol3 software by Accelrys' Material Studio, using the Density-Functional theory (DFT) and the COSMO-based models. The procedure for a molecule includes [Mullins et al., 2006]:

- A rough geometry optimization by adjusting bond lengths and bond angles.
- A geometry optimization in the ideal-gas phase using the DNP (Double Numerical basis with Polarization Functions) v4.0.0 basis set, recommended for COSMO-SAC models. The functional used is GGA/VWN-BP (Generalized Gradient Approximation with the Becke-Perdew version of the Volsko-Wilk-Nusair Functional) [Vosko et. al, 1980; Becke, 1986; Perdew, 1986; Koch, 2001], with a real space cutoff of 0.55 nm.
- Calculation of the surface screening charges in the condensed phases, assuming that the optimised gas-phase conformation is identical to that of the condensed-phase.
- Generation of sigma profile by averaging the segments of the molecular cavity.

The three compounds studied in the current work are registered in the VT-2005 database, thus the COSMO-files can be directly used for our equilibrium calculations. The corresponding sigma profiles as well as a graphical representation of the surface polarization charge density (referred to as sigma surfaces) are presented in **figure 4-1**. According to the sigma surfaces, three kinds of regions are identified: (i) weakly polar, represented by green to yellow and associated with alkyl groups in ethyl lactate and ethanol, (ii) strongly positive polar, identified with blue and corresponding to the polar hydrogen atoms in the three species and (iii) strongly negative polar, coded by red and related to oxygen atoms [Durand et al., 2011]. Concerning the sigma profiles, they provide useful information on the electronic distribution of polar and non-polar groups in a given polarity scale. The sigma profile of water is very symmetric because of the presence of two groups with similar inverse polarity, in this case two hydrogen atoms and one oxygen atom with two electron lone-pairs. In contrast, the sigma profiles of ethyl lactate and ethanol are rather asymmetric due to the coexistence of non-polar together with strongly polar fragments, associated with the carbonyl and hydroxyl groups [Palomar et al., 2008].

Four versions of the model were used and compared in this study: COSMO-SAC 2002 [Lin and Sandler, 2002], COSMO-SAC 2006 [Mullins et al., 2006], COSMO-SAC 2010 [Wang and Sandler, 2007; Hsieh et. al, 2010] and COSMO-SAC-dsp (2014) [Hsieh et. al, 2014a; Hsieh et. al, 2014b]. These models are available in a code developed by the UCP laboratory at ENSTA ParisTech (ENSTA code), and are fully automatized: .cosmo files as well as the chemical structure of molecules are automatically recognized by the code. The ENSTA code for the COSMO-SAC-dsp model has been recently implemented as a native model into Simulis® Thermodynamics Package. The ENSTA code is also fully compatible with the Simulis expert mode.

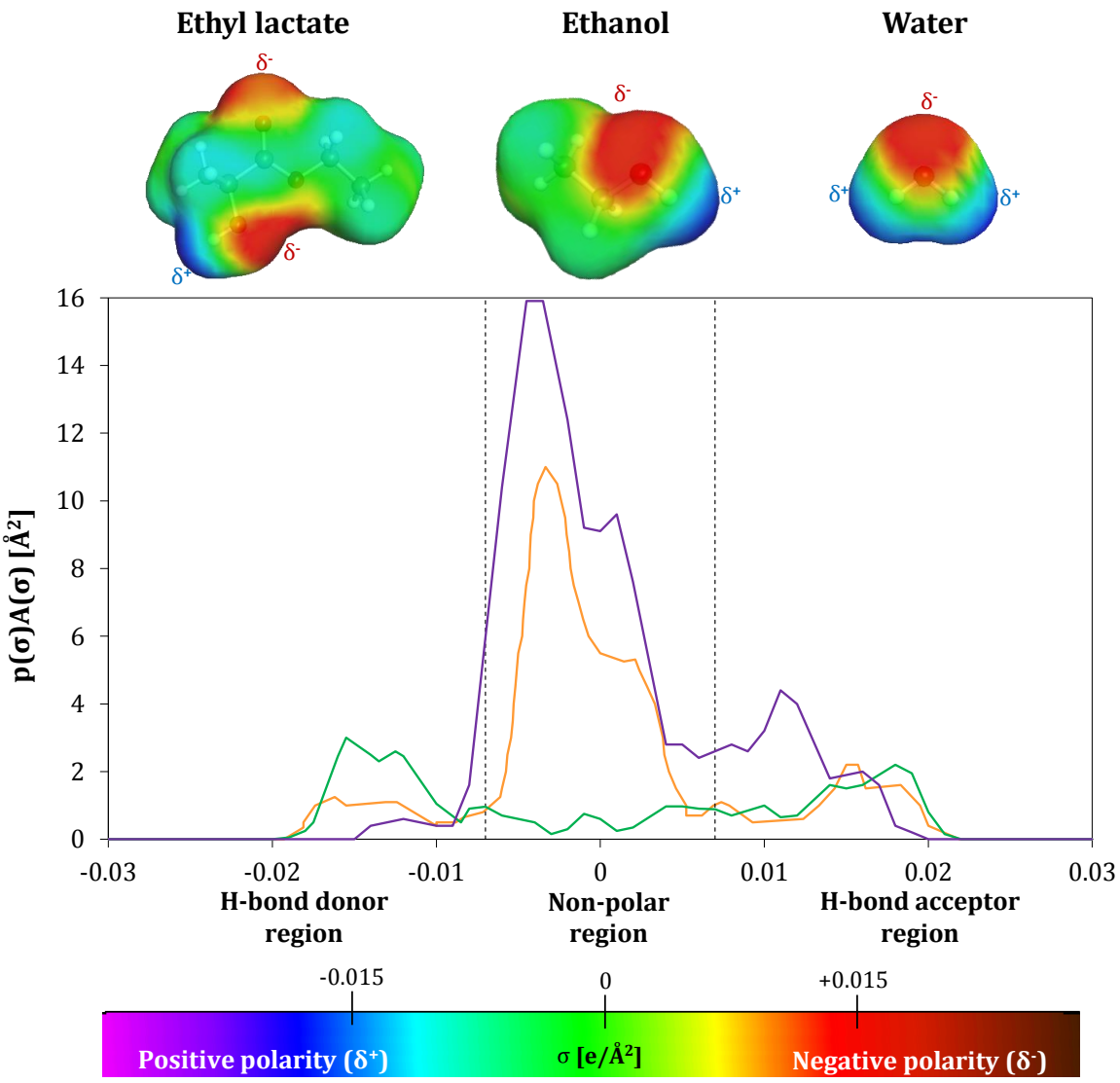

Figure 4-1. *Surface polarization charge density and sigma profiles for (——) Ethyl lactate, (——) Ethanol and (——) Water. Visualization with the software Accelrys' Material Studio. The local positions of strongly positive polar sites are represented with (δ+) and those strongly negative with (δ-).*

4.2.3. METHODOLOGY FOR THE PREDICTION OF VAPOR –LIQUID EQUILIBRIA OF AROMA COMPOUNDS

A simplified methodology is proposed to predict the equilibrium behaviour of aroma compounds infinitely diluted in ethanol – water solutions. The binary ethanol–water is modelled with an accurate semi-empirical model in order to assess the predictive capability of the models only with respect to the aroma compounds. The NRTL model [Renon and Prausnitz, 1968] was selected for this purpose since it has been widely recommended in the literature to represent the phase behaviour of hydroalcoholic liquid mixtures at low pressures [Faundez and Valderrama, 2004; Athès et al., 2008; Valderrama et al., 2012a]. This model includes binary interaction parameters calculated from experimental data. In this work, the interaction parameters for the binary ethanol – water were those proposed by Kadir [Kadir, 2009], and validated against different literature data sets at 101.3 kPa [Arce et al., 1996; Yang and Wang, 2002; Kamihama et al., 2012; Lai et al., 2014].

Considering this assumption, the methodology is comprised of the following steps:

- The ethanol–water liquid phase composition is fixed at the experimental data ($x_{s\text{-}EXP}$).
- The temperature of the ternary system is the bubble temperature calculated with the NRTL model ($T=T_{b\text{-}NRTL}$) at the experimental ethanol – water liquid phase composition. The temperature is assumed to be independent of aroma compounds presence due to their very low concentration.
- The activity coefficient for the aroma compound, γ_{AC}^{∞}, at $T=T_{b\text{-}NRTL}$ and $x_{s\text{-}EXP}$ is predicted with the UNIFAC and COSMO-SAC models.
- The partition coefficient, K_{EL}, at P=101.3 kPa is given by:

$$K_{AC\text{-}Pred}=\frac{\gamma_{AC}^{\infty}(T_{b\text{-}NRTL},x_{s\text{-}Exp})P_{AC}^{0}(T_{b\text{-}NRTL})}{P} \quad [4\text{-}9]$$

- Finally, the relative volatility, $\alpha_{AC/Et}$, is predicted with respect to the ethanol partition coefficient estimated with the NRTL model, as follows:

$$\alpha_{AC/Et\text{-}Pred}=\frac{K_{AC\text{-}Pred}}{K_{Et\text{-}NRTL}} \quad [4\text{-}10]$$

Specific application of this methodology for the system ethyl lactate–ethanol–water is presented in the following section.

4.3. Results and discussion

4.3.1. Comparison with experimental data

The results of the vapor – liquid equilibrium prediction for ethyl lactate infinitely diluted in ethanol – water mixtures at 101.3 kPa are summarized in **table 4-1**. The evolution of absolute (K_{EL}) and relative ($\alpha_{AC/Et}$) volatilities for the aroma compound over the entire liquid composition range is presented in **figure 4-2** together with the experimental data used as reference for validation purposes. All models predict a decreasing trend of the aroma compound volatility when the ethanol liquid composition is increased, yet the accuracy with respect to experimental data is variable.

The values of the activity coefficient (γ_{EL}^{∞}) in three reference solvents at their boiling point at 101.3 kPa are displayed in **figure 4-3**. In pure ethanol, γ_{EL}^{∞} is well predicted by UNIFAC models and slightly under-predicted by COSMO-SAC models. In pure water and the equimolar mixture, the best prediction of γ_{EL}^{∞} is obtained with COSMO-SAC 2002, while UNIFAC 1975 and the other COSMO-SAC versions give globally good predictions. UNIFAC 1993, in contrast, clearly overestimates γ_{EL}^{∞} for both solvents, predicting values two to four times larger than the real data.

Table 4-1. *Vapor-liquid Equilibrium prediction using UNIFAC and COSMO-SAC models for ethyl lactate infinitely diluted in ethanol-water mixtures at 101.3 kPa.*

x_{Et}	T /K	Activity coefficient, γ_{EL}^{∞}							Absolute volatility, K_{EL}							Relative volatility, $\alpha_{EL/Et}$						
		Experimental	UNIFAC			COSMO-SAC			Experimental	UNIFAC			COSMO-SAC			Experimental	UNIFAC			COSMO-SAC		
			1975	1993	2002	2006	2010	2014		1975	1993	2002	2006	2010	2014		1975	1993	2002	2006	2010	2014
0.0116	370.0	18.89	13.02	91.69	17.78	10.11	23.09	25.69	2.75	1.90	13.37	2.59	1.47	3.37	3.75	0.27	0.19	1.32	0.26	0.15	0.33	0.37
0.0349	365.6	15.19	9.39	69.87	12.61	8.02	15.47	17.12	1.87	1.16	8.60	1.55	0.99	1.90	2.11	0.25	0.15	1.14	0.21	0.13	0.25	0.28
0.0492	363.8	13.03	7.83	59.41	10.48	7.04	12.52	13.81	1.49	0.90	6.80	1.20	0.81	1.43	1.58	0.23	0.14	1.04	0.18	0.12	0.22	0.24
0.0496	363.7	12.98	7.79	59.13	10.43	7.01	12.45	13.73	1.48	0.89	6.75	1.19	0.80	1.42	1.57	0.23	0.14	1.04	0.18	0.12	0.22	0.24
0.0656	362.0	12.21	6.45	49.55	8.65	6.13	10.07	11.07	1.30	0.69	5.28	0.92	0.65	1.07	1.18	0.23	0.12	0.92	0.16	0.11	0.19	0.21
0.0660	362.0	12.41	6.43	49.37	8.62	6.11	10.03	11.02	1.32	0.68	5.26	0.92	0.65	1.07	1.17	0.23	0.12	0.92	0.16	0.11	0.19	0.21
0.0946	360.0	7.42	4.78	36.67	6.47	4.92	7.29	7.96	0.73	0.47	3.61	0.64	0.48	0.72	0.78	0.16	0.10	0.79	0.14	0.11	0.16	0.17
0.1108	359.1	6.68	4.11	31.25	5.61	4.41	6.24	6.79	0.63	0.39	2.96	0.53	0.42	0.59	0.64	0.15	0.09	0.72	0.13	0.10	0.14	0.16
0.1136	358.9	7.31	4.01	30.44	5.48	4.33	6.08	6.62	0.69	0.38	2.87	0.52	0.41	0.57	0.62	0.17	0.09	0.71	0.13	0.10	0.14	0.15
0.1286	358.3	4.10	3.54	26.47	4.87	3.94	5.36	5.81	0.38	0.33	2.43	0.45	0.36	0.49	0.53	0.10	0.09	0.65	0.12	0.10	0.13	0.14
0.1304	358.2	4.67	3.49	26.04	4.81	3.9	5.28	5.73	0.43	0.32	2.39	0.44	0.36	0.48	0.52	0.12	0.09	0.65	0.12	0.10	0.13	0.14
0.1425	357.8	4.38	3.18	23.36	4.41	3.63	4.81	5.21	0.39	0.29	2.10	0.40	0.33	0.43	0.47	0.11	0.08	0.61	0.11	0.09	0.12	0.14
0.1456	357.7	4.58	3.11	22.75	4.32	3.57	4.71	5.09	0.41	0.28	2.04	0.39	0.32	0.42	0.46	0.12	0.08	0.60	0.11	0.09	0.12	0.13
0.3920	353.9	1.40	1.12	4.80	1.58	1.44	1.77	1.85	0.11	0.09	0.37	0.12	0.11	0.14	0.14	0.07	0.05	0.23	0.08	0.07	0.09	0.09
0.4009	353.9	1.55	1.10	4.61	1.55	1.41	1.74	1.81	0.12	0.08	0.35	0.12	0.11	0.13	0.14	0.08	0.05	0.23	0.08	0.07	0.09	0.09
0.6244	352.3	1.11	0.89	2.17	1.04	0.95	1.26	1.28	0.08	0.06	0.16	0.07	0.07	0.09	0.09	0.07	0.06	0.14	0.07	0.06	0.08	0.08
0.6257	352.3	1.18	0.89	2.16	1.03	0.95	1.26	1.28	0.08	0.06	0.15	0.07	0.07	0.09	0.09	0.07	0.06	0.14	0.06	0.06	0.08	0.08

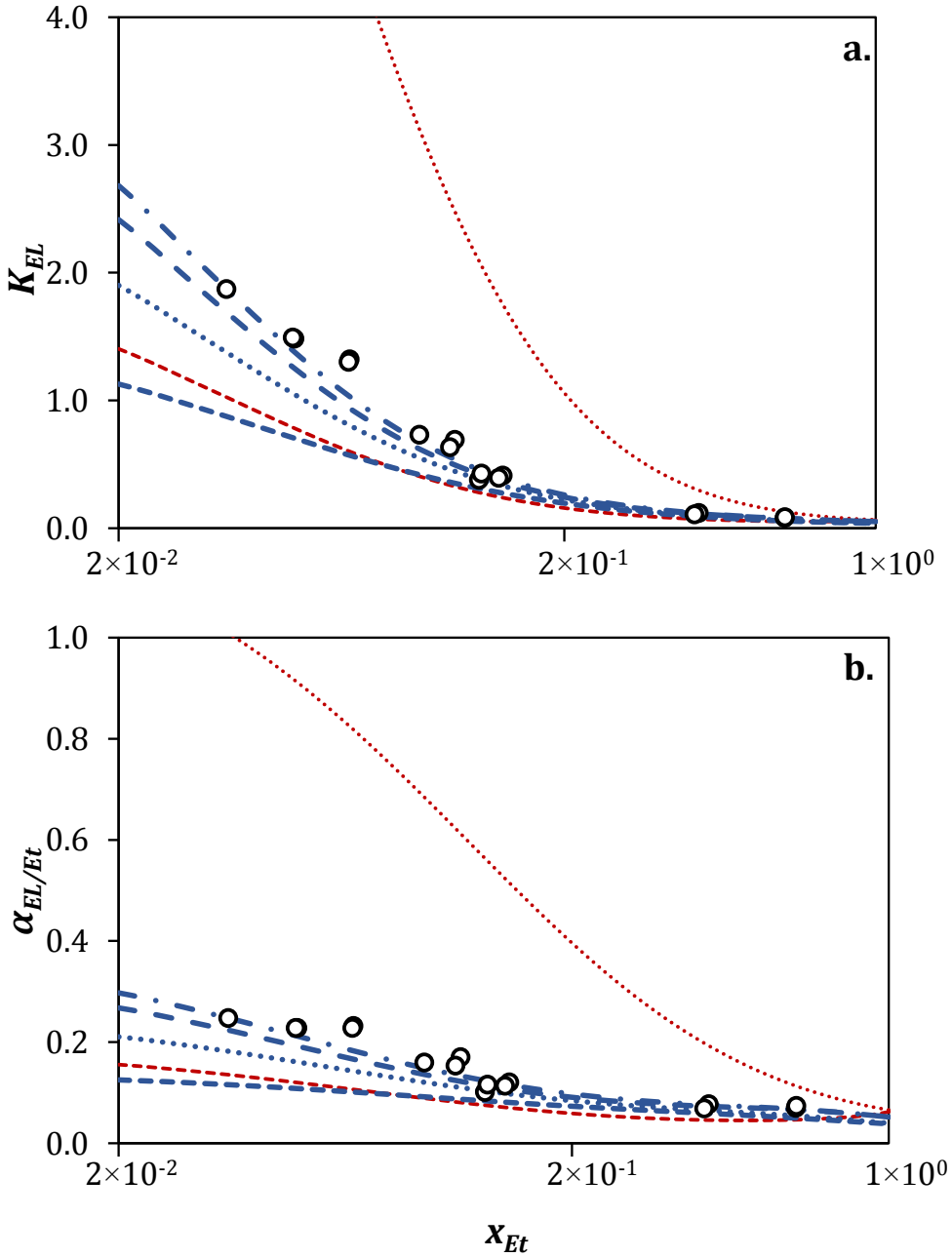

Figure 4-2. *Prediction of a. Absolute volatility and b. Relative volatility of ethyl lactate at 101.3 kPa with UNIFAC and COSMO-SAC models. (○) Experimental data [Puentes et al., 2017b], (– – –) UNIFAC 1975, (·····) UNIFAC 1993, (·····) COSMO-SAC 2002, (– – –) COSMO-SAC 2006, (— —) COSMO-SAC 2010, (— · —) COSMO-SAC 2014.*

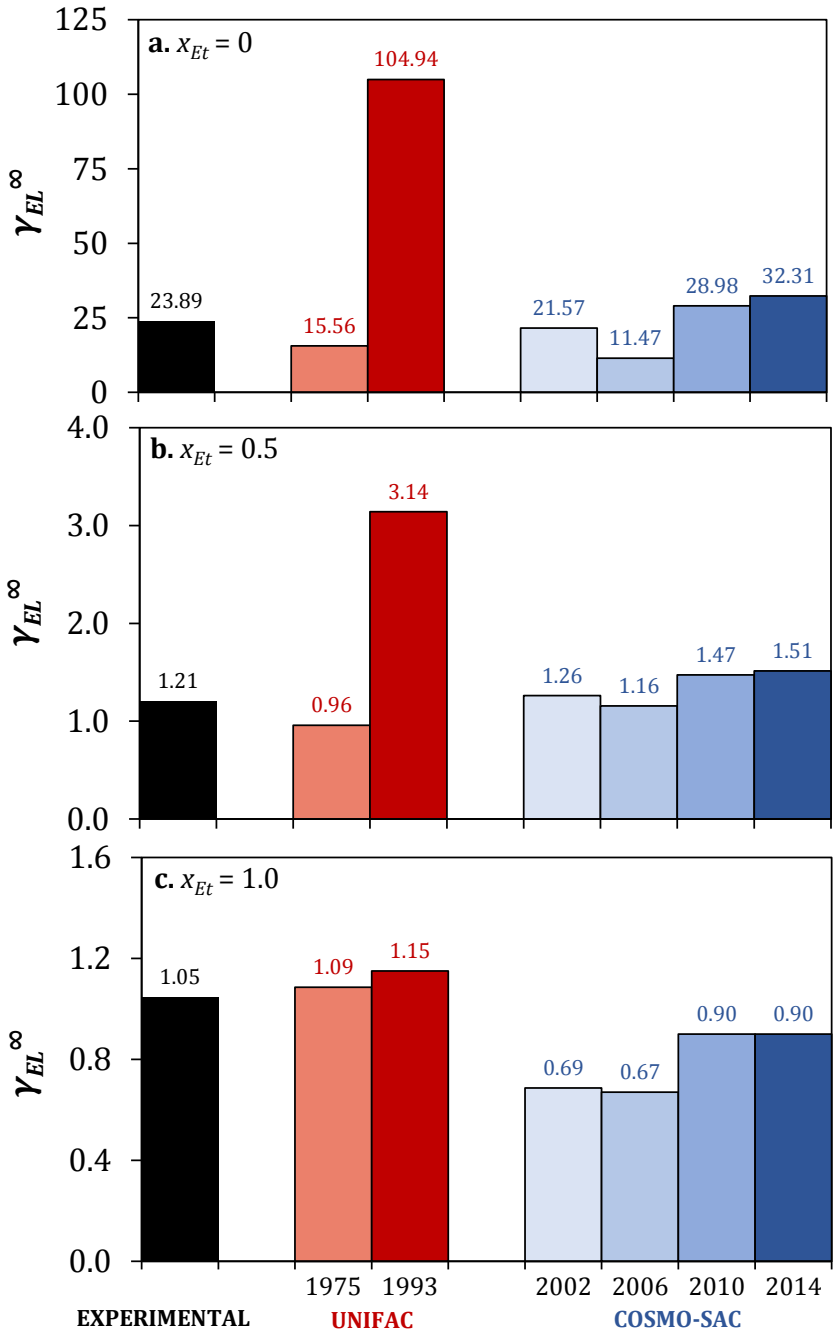

Figure 4-3. *Prediction of activity coefficients ethyl lactate at infinite dilution in three solvents at their boiling points at 101.3 kPa. a. Water, b. equimolar mixture of water–ethanol, c. ethanol.*

The predictive capability was quantified with two statistics, according to the following equations:

Average absolute relative deviation (*AAD%*):

$$\text{AAD }\% = \frac{1}{N}\sum_{i=1}^{N}\left|\frac{U_{i\,Exp}-U_{i\,Pred}}{U_{i\,Exp}}\right| 100\% \,. \qquad [4\text{-}11]$$

Root-mean-squared error (*RMSE*):

$$\text{RMSE} = \left[\frac{1}{N}\sum_{i=1}^{N}\left(U_{Exp\,i}-U_{i\,Pred}\right)^2\right]^{1/2} . \qquad [4\text{-}12]$$

U_i is an equilibrium variable (including in this case K_{EL}, $\alpha_{AC/Et}$ and γ_{EL}^{∞}) and N is the number of independent experimental data available. The deviations obtained are presented in **table 4-2.** It can be clearly seen that the equilibrium predictions with COSMO-SAC models are globally more accurate than those from the UNIFAC models.

Table 4-2. *Predictive capability of the UNIFAC and COSMO-SAC models. AAD% is equivalent for all the equilibrium variables.*

Statistics		UNIFAC		COSMO-SAC			
		1975	**1993**	**2002**	**2006**	**2010**	**2014**
AAD%	Average	33%	329%	16%	29%	14%	12%
	Maximum	48%	545%	42%	51%	31%	31%
	Minimum	14%	84%	2%	3%	0%	2%
RMSE	γ_{EL}^{∞}	3.61	33.43	1.89	4.20	1.78	1.38
	K_{EL}	0.42	4.04	0.26	0.51	0.20	0.18
	$\alpha_{EL/Et}$	0.07	0.61	0.03	0.07	0.03	0.02

The predictions with both thermodynamic models are shown as a parity plot in **figure 4-4.** Four of the six compared models under-estimate the partition coefficient, while the UNIFAC 1993 model gives high over-predictions. This important discrepancy had been already be detected when comparing experimental and simulation data of composition profiles for ethyl lactate in batch distillation, as stated by the authors in a companion paper [Decloux, 2009; Puentes et al., 2017b]. For this model, the deviations decreases when increasing the ethanol liquid concentration is increased, contrary to the other models, whose deviations are rather independent of the liquid composition. The same behaviour was identified for γ_{EL}^{∞} and $\alpha_{EL/Et}$.

According to the proximity of the predicted values to the bisector in figure 4-4 and to the deviations from table 4-2, one can conclude that the COSMO-SAC-dsp (2014 version) is the most accurate model to predict the equilibrium behaviour of ethyl lactate at infinite dilution.

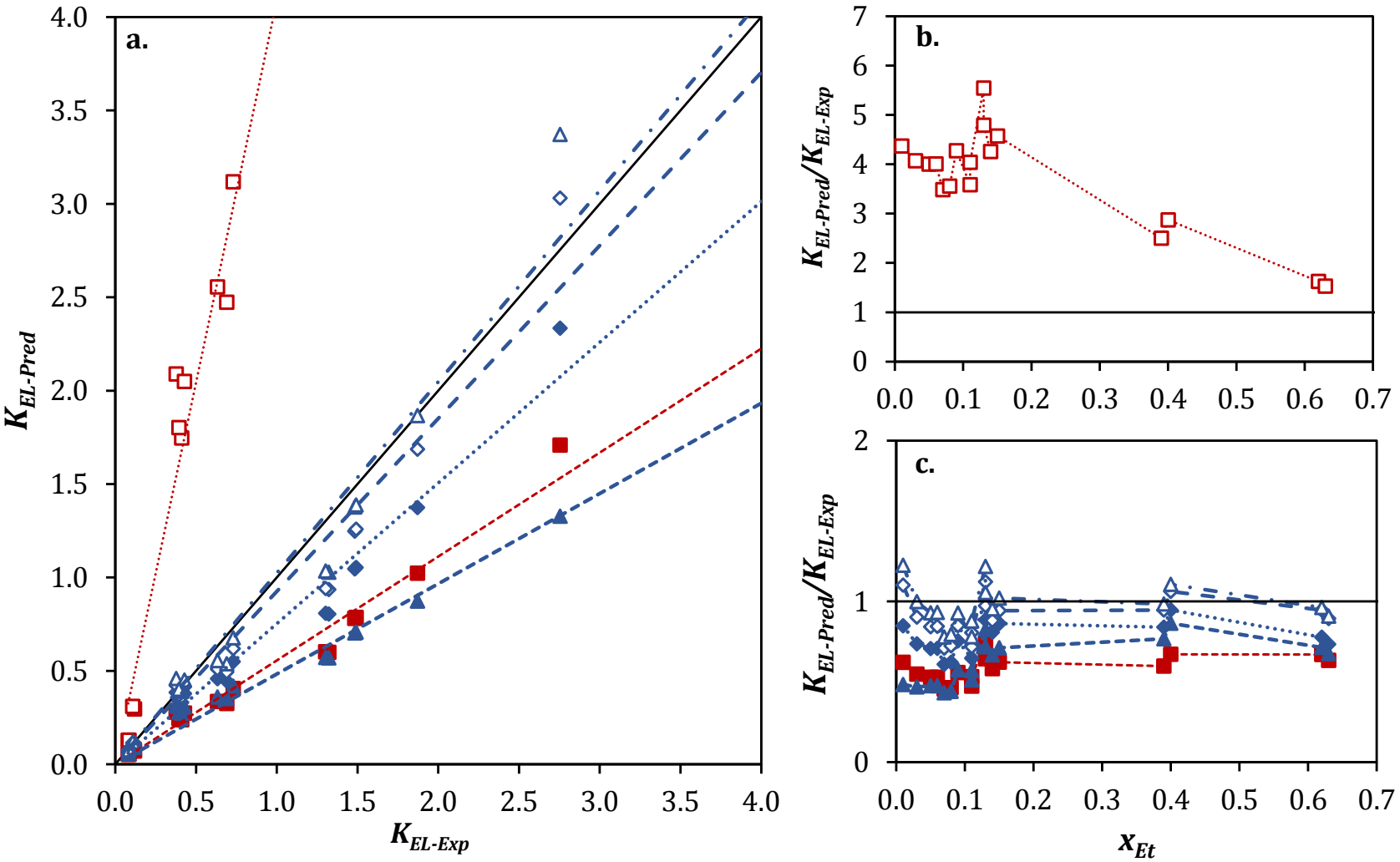

Figure 4-4. *a. Comparison of predictions and experimental data of absolute volatility at 101.3 kPa on a parity plot. b.-c. Evolution of the ratio $K_{EL\text{-}Pred}/K_{EL\text{-}Exp}$ with respect to ethanol composition in the liquid phase. (-■-) UNIFAC 1975, (···□···) UNIFAC 1993, (···◆···) COSMO-SAC 2002, (-▲-) COSMO-SAC 2006, (—◇—) COSMO-SAC 2010, (-·-△-·-) COSMO-SAC 2014.*

Concerning the UNIFAC models, the predictive capability of the 1975 version is much better than that of the 1993 version, for which the values of AAD % (average value 329 %) and RMSE (0.61 for $\alpha_{AC/EL}$, 4.04 for K_{EL} and 33.43 for γ_{EL}^{∞}) are the highest among all predictions. This remarkable difference could be explained by two reasons: the modification of the combinatorial term and the difference of interaction parameters between the two versions. The interaction parameters of the 1975 version, together with the Staverman-Guggenheim term (used in this version) seem to be more adapted to the description of this ternary system. Another hypothesis is that the temperature parametrisation for the pair of groups involved in the system is not accurate, leading to the over-prediction of activity coefficients.

Good agreement between experimental data and theoretical predictions is obtained with the four COSMO-SAC models. However, the highest deviations, obtained with the 2006 version, are not negligible (average AAD% of 29%). This results evidences that the local averaging of charge densities in the cavity segments has an important influence on equilibrium predictions. For the investigated system, the averaging procedure together with the original value for the misfit energy proposed by Lin and Sandler (2002) (used in the 2002, 2010 and 2014 versions) lead to a better prediction.

Moreover, according to the deviations for the other COSMO-SAC versions, the predictions given by the 2002 version are rigorously less accurate than those by the 2010 and 2014 (dsp) versions. This indicates that the separation of sigma profiles to better describe hydrogen-bonding interactions does entail a more reliable description of the studied ternary system. This result is consistent with the nature of the system, because the molecules contain non-hydrogen-bonding molecular fragments but also several donators and acceptor groups, as schematised in figure 4-1 and **figure 4-5**.

The predictive capability of the 2010 and 2014 (dsp) versions is very similar, even if the deviations from the experimental data are in general lower for the 2014 version. Hence, the consideration of the dispersive contribution in the calculation of activity coefficients can provide just a slight improvement of the vapor-liquid description for the studied system. Here, the electrostatic interactions largely dominates the dispersive interactions, since, as showed previously, all the chemical species are polar and can form hydrogen bonds with either like or unlike molecules. The dispersive interactions are always present in the liquid phase but they are weakened by competing interaction of the solute with the bulk solvent [Schneider, 2015].

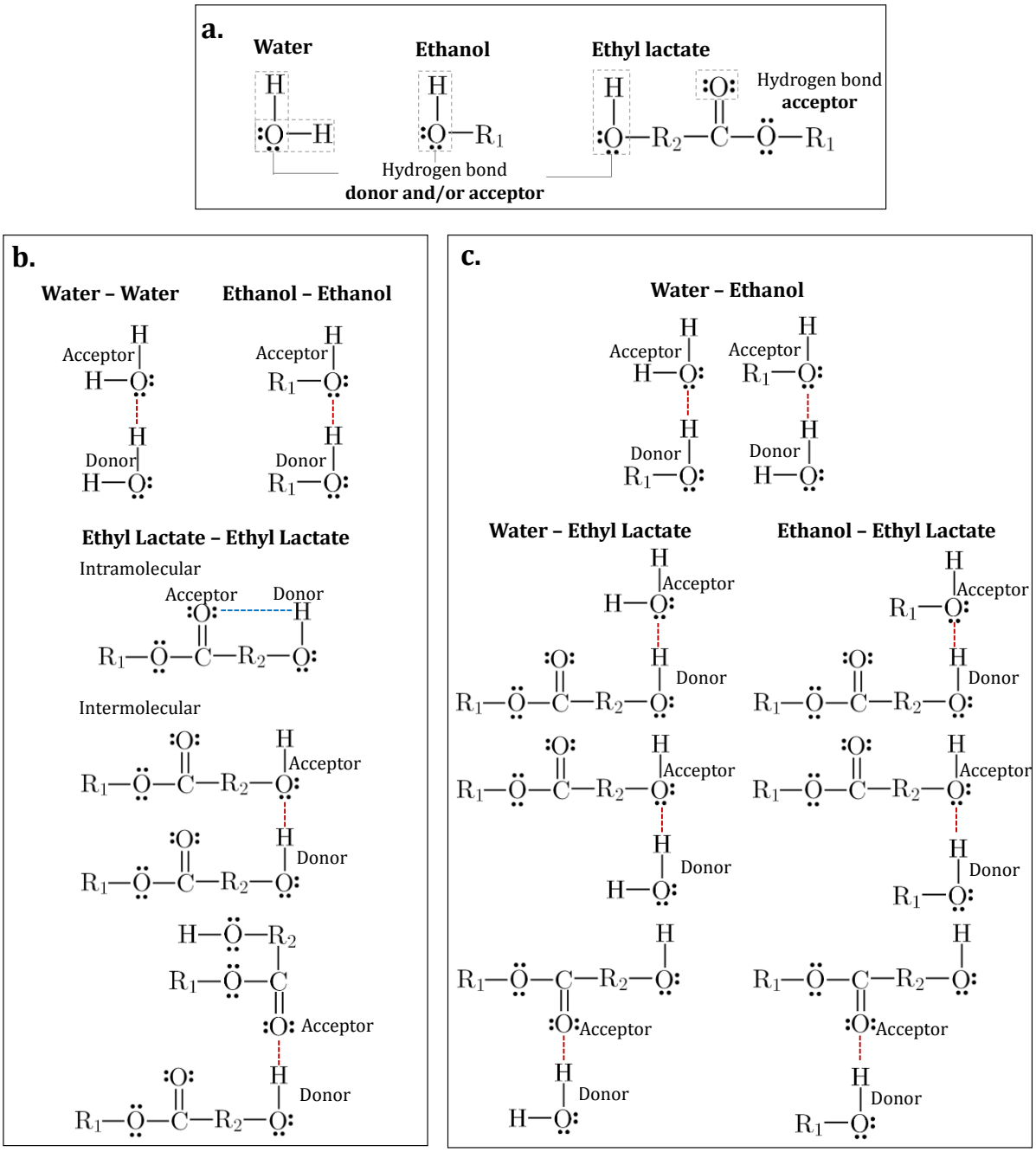

Figure 4-5. *Hydrogen-bonding interactions in the system ethyl lactate – ethanol – eau. Only binary interactions and strong hydrogen bonds are considered. a. Hydrogen bond accepting and donating groups. In ethyl lactate, the alkoxy group (O-R₁) is sterically hindered to form this kind of bonds [Aparicio and Alcalde, 2009a], b. Interactions between molecules of the same nature, c. Interaction between molecules of different nature. R₁: -CH₂-CH₃, R₂: -CH-CH₃*

Two reasons may explain the differences between the UNIFAC and COSMO-SAC predictions, according to Klamt and Eckert (2002):

1. UNIFAC models employ a mean field assumption to calculate the residual contribution of the activity coefficient. This approximation can lead to important errors in equilibrium predictions for systems containing strongly interacting species at very high or infinite dilution (ethyl lactate in this case), whose activities are much higher than one. A special parametrisation, such as the one proposed by Bastos et al. (1988), would be necessary to achieve more satisfying results. In this study, a standard parametrisation available in the Simulis® Thermodynamics Package was used, and probably the corresponding interaction parameters were fitted only to experimental data representing finite concentration activities.
2. As opposed to COSMO-based models, UNIFAC models can not recognize intramolecular interactions of functional groups, as the interaction parameters are independent of the environment. This makes it impossible to handle the reduction of external interactions caused by internal hydrogen bonds and reduces therefore the predictive capability of these models. The theoretical and experimental studies of liquid structures carried out by Aparicio et al. [Aparicio et al., 2008 ; Aparicio and Alcalde, 2009a ; Aparicio and Alcalde, 2009b] have demonstrated that ethyl lactate has the ability to develop both intra and intermolecular association through hydrogen bonding, owing to the presence and vicinity of hydroxyl and carbonyl groups. Mixed with water the behaviour is also very complex: in small quantities, the ethyl lactate tends to self-associate [Aparicio and Alcalde, 2009b], but it reinforces in turn the water networks and reduces the polarity of the liquid phase [Aparicio et al., 2008]. Nonetheless, it is important to mention that in solution, the intramolecular hydrogen bonding of ethyl lactate is weakened by the intermolecular associations, due to a movement out of the molecular plane of the hydroxyl group [Borho et al., 2006; Aparicio et al., 2008; Aparicio and Alcalde, 2009a].

4.3.2. Validation of the infinite dilution approximation

The predictive models are finally used to calculate the activity coefficients of ethyl lactate over the entire composition range. The evolution of γ_{EL} for the binary systems ethyl lactate – ethanol and ethyl lactate – water at 101.3 kPa is depicted in **figure 4-6**.

In water (binary ethyl lactate – water), all models predict the same trend: when ethyl lactate concentration is decreased, γ_{EL} becomes constant from x_{EL} lower than 1.0×10^{-3}, whereas in ethanol (binary ethyl lactate – ethanol), γ_{EL} does not vary from x_{EL} lower than 1.0×10^{-2}. The experimental ethyl lactate liquid composition for the reference data used in this work ($x_{EL\text{-}min} = 1.38\times10^{-4}$ – $x_{EL\text{-}max} = 3.45\times10^{-4}$) are lower than the dilution limits here defined, which confirms that the aroma compound is effectively at infinite dilution.

According to this result, predictive models can also be useful to improve the experimental design of vapor-liquid equilibria measurements. When dealing with molecules highly diluted, a previous prediction step could be used to define the upper limit of infinite dilution, which would enable experimentalists to work at the highest possible concentrations, thus ensuring better accuracy in the quantification of phase compositions.

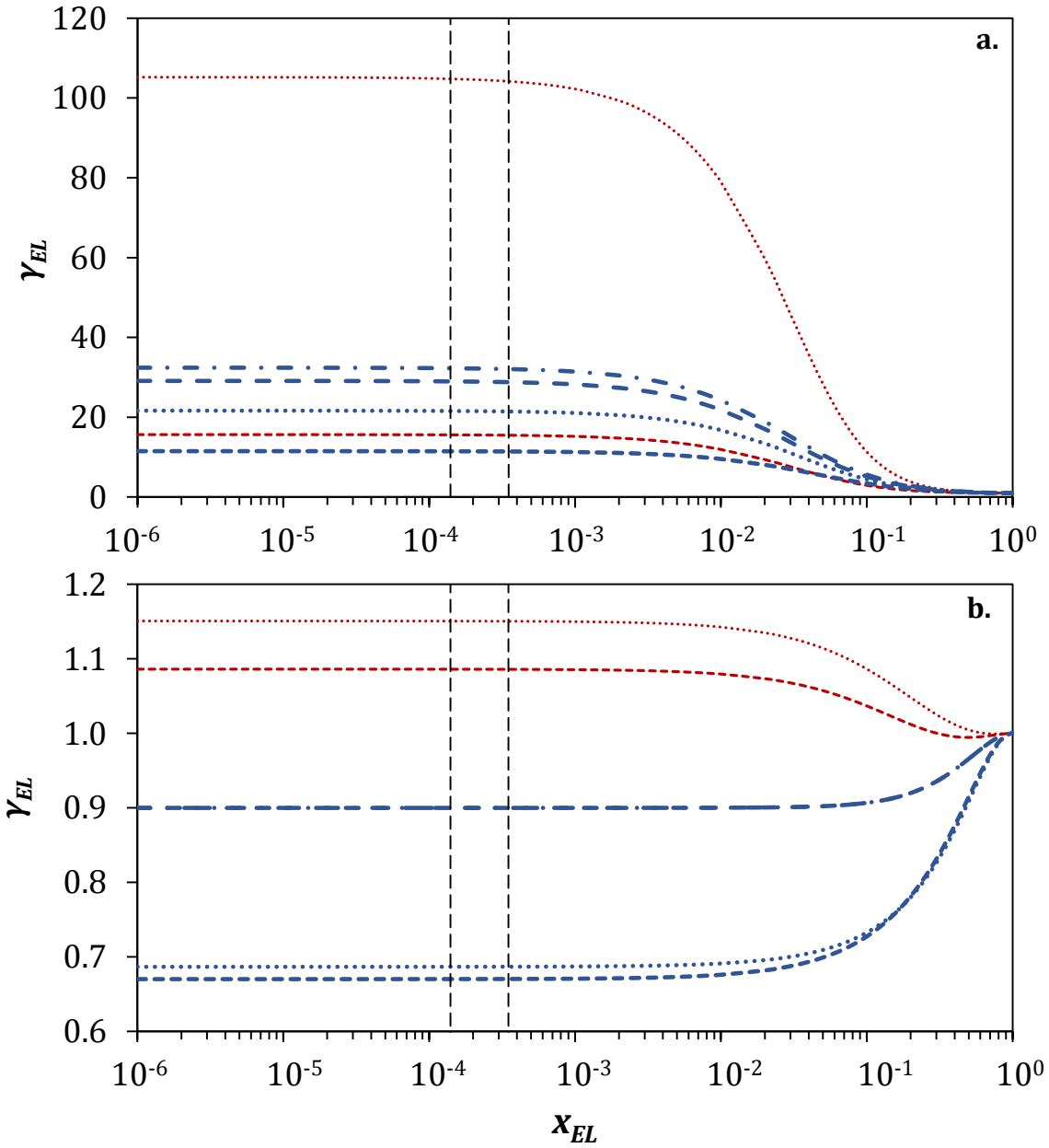

Figure 4-6. *Prediction of the activity coefficient of ethyl lactate at the mixture boiling point at 101.3 kPa in the binary systems a. ethyl lactate–water and b. ethyl lactate–ethanol. (– – –) UNIFAC 1975, (·····) UNIFAC 1993, (·····) COSMO-SAC 2002, (– – –) COSMO-SAC 2006, (— —) COSMO-SAC 2010, (— · —) COSMO-SAC 2014. The discontinuous vertical lines represent the interval of ethyl lactate liquid composition in which the experimental measurements were carried out.*

4.4. Conclusions

The predictive UNIFAC and COSMO-SAC models were used to study the equilibrium behaviour of ethyl lactate infinitely diluted in ethanol – water mixtures at 101.3 kPa. Reference data of the ternary system were measured by a dynamic method coupled to gas chromatography. Good agreement between the experimental data and theoretical predictions of volatilities and activity coefficients is obtained with all COSMO-SAC versions, whereas the deviations with UNIFAC models are larger. These models also made it possible to verify that the experimental interval of ethyl lactate liquid composition is correctly placed in the infinite dilution region.

Among the six predictive models, the most reliable predictions were obtained with COSMO-SAC-dsp (2014 version), with an overall average relative deviations of 12 % and a root mean squared error between 0.03 and 1.89 for ethyl lactate volatilities and activity coefficients. These results are coherent, keeping in mind three factors: (1) the COSMO-SAC model was deduced without any mean field approximation, (2) the system contains strongly interacting species that develop associations through hydrogen-bonding, and (3) the consideration of a dispersive contribution, always occurring in the condensed phases, can improve slightly the equilibrium predictions even if the electrostatic interaction dominates in the investigated system. As a result, the COSMO-SAC-dsp model (2014 version) is recommended to predict the vapor-liquid equilibria for ternary systems of the same nature, i.e. hydroxyl esters in hydroalcoholic medium.

The application of predictive models stands out as a competitive approach not only to reduce costs in the generation of equilibria data but also to improve experimental design. When experimental data are strictly required for validation purposes in highly diluted systems, this approach can be used to fix the upper limit of the infinite dilution region, aiming to facilitate the analysis of phase compositions.

ACKNOWLEDGEMENTS

The authors gratefully acknowledge the ABIES Doctoral School (AgroParisTech, Université Paris-Saclay) as well as the French network RMT FIDELE (Réseau Mixte Technologique Produits fermentés et distillés) for supporting this research.

CHAPITRE 5. SIMULATION DE LA DISTILLATION CONTINUE

Après l'identification du modèle thermodynamique sélectionné pour la description analytique des équilibres liquide-vapeur, la deuxième partie de cette recherche est consacrée à la simulation numérique des unités de distillation. Dans ce chapitre, une démarche pour la simulation de la distillation en régime stationnaire est développée et appliquée à l'analyse d'une unité de distillation d'Armagnac. La simulation est réalisée avec le logiciel ProSimPlus®. Des données expérimentales de distillation pour l'éthanol, l'eau et 66 composés volatils d'arôme ont été acquises lors d'une campagne de caractérisation de l'unité. Trente-deux (32) des 66 composés ont été simulés avec le modèle NRTL, en utilisant les paramètres d'interaction binaire déterminés dans le chapitre 2. En intégrant la connaissance sur les volatilités relatives, présentée dans le chapitre 2, avec les tendances de séparation obtenues par simulation, une classification des 32 composés volatils d'arôme simulés, spécifique de la distillation de l'Armagnac, est proposée. Après la validation du point nominal d'opération, les circuits d'extraction de têtes et de queues sont simulés, puis une analyse de l'influence de quelques paramètres opératoires est menée. L'ensemble des résultats confirme que la simulation est un outil fiable pour mieux comprendre la synergie existant entre l'opération des unités, leur rendement et la composition du distillat.

Simulation of continuous distillation of spirits for a better understanding of volatil aroma compounds behavior: Application to Armagnac production.

Cristian Puentes, Xavier Joulia, Jean-Paul Vidal et Martine Esteban-Decloux

A soumettre au journal *Food and Bioproducts Processing*.

5.1 INTRODUCTION

Spirits are alcoholic beverages produced from different agricultural raw materials, such as apple and pear (Calvados), barley (Whisky), grape (Cognac, Armagnac, Pisco) and sugar cane juice (Rum, Cachaça). For most commercial spirits, the production process is comprised of five main stages: raw material extraction, yeast fermentation, distillation of the fermented wash, ageing of the distillate in wooden barrels and final dilution to adjust the ethanol content to the desired level [Nykänien and Suomalainen, 1983; Carrau et al., 2008; Franitza et al., 2016].

In France, four main spirits are produced: Armagnac, Calvados, Cognac and Martinique agricultural rum. They are protected by the French label AOC (*Appellation d'Origine Contrôlée*), which delimits the production areas as well as the rules for their fabrication. Besides the raw material, the major differences among these distilled beverages are the geographic regions of production and distillation methods [Decloux and Joulia, 2009; Ledauphin et al., 2010].

From a chemical point of view, spirits are complex mixtures composed by an ethanol – water liquid matrix and a great variety of volatile compounds present at low concentrations. Many commercial spirits also contain substantial amounts of non-volatile material from ageing and finition [MacNamara and Hoffmann, 1998; MacNamara et al., 2010]. The volatile compounds, also known as congeners, are organic species from chemical families including acetals, alcohols, carbonyl compounds, carboxylic acids, esters, furans, norisoprenoids, sulphur compounds and terpenes. Some of them are derived from the original raw material or the extraction phase, but the majority are generated during fermentation and distillation, phases in which complex reactions take place. The alcoholic fermentation, main reaction of the process, leads together with ethanol, to the synthesis of the most abundant congeners (alcohols, fatty acids and their esters). Other involved reactions are malolactic fermentation, acetalization, ester hydrolysis, esterification, Maillard reaction, Stecker degradation and thermal degradation of pentoses [Cantagrel et al., 1990; Sourisseau, 2002]. Finally, the ageing phase also contributes to the complexity of spirits, with the formation of new volatile compounds from wood constituents, including phenolic compounds and lactones [Guymon, 1974; Maarse and Van Den Berg, 1994; Rodriguez et al., 2003; Ferrari et al., 2004].

The volatile species are also referred to as volatile aroma compounds since their presence and composition play an essential role on spirits quality [Guymon, 1974; Nykänen et al., 1968; Ferrari et al., 2004; Guichard et al., 2003; Apostolopoulou, 2005; Ledauphin et al., 2006; Ledauphin et. al, 2010; Morakul et al., 2011]. This quality is associated to the organoleptic properties of the product, such as flavor and aroma. Its evaluation and control are therefore essential for production purposes, as it influences the consumer preferences [Maarse and Van Den Berg, 1994]. The relationship between aroma and spirits composition is very complex because of the variety of volatile compounds, their variable natural occurring concentrations and their combined effects. Indeed, the sensory influence of each species depends on a triple factor: its concentration, its sensory threshold value and the concentration of other species in the solution. As a result, the contribution of trace level compounds with low sensory threshold to aroma and flavor may be more important than the impact of the most abundant volatile compounds. Nevertheless, analysis of these latter species remains fundamental, not only to describe the main character of the

product, but also to evaluate the production continuity and product authenticity [MacNamara and Hoffmann, 1998; MacNamara et al., 2010].

In the light of these facts, the control of volatile aroma compounds content in distillates is a fundamental aspect for the production of good quality spirits. The composition control is also important in matters of food safety, as the presence of specific volatile aroma compounds at high concentrations, for instance methanol and ethanal, is related to some health issues [Nykänen, 1986; Paine and Dayan, 2001]. Considering its origin, the control of volatile aroma compounds composition can be performed by manipulating two factors: the raw material or the production process. Some recent experimental works have demonstrated the high dependency between this latter factor and product composition [Rodriguez et al., 2003; Cacho et al., 2013; Franitza et al., 2016], which opens up prospects for the improvement of spirits production.

Focusing on the distillation stage, spirits can be produced by continuous multistage distillation or batch distillation [Decloux and Joulia, 2009; Piggot, 2009]. Currently, the adaptation and evolution of this process remains very limited, since the operation of the distillation units is mainly based on traditional methods derived from empirical knowledge. Thus, the implementation of chemical engineering methods, in particular process simulation, turns out be an efficient approach to represent, understand and optimize this separation process for a better quality control [Batista and Meirelles, 2011; Valderrama et. al, 2012b; Esteban-Decloux et.al, 2014].

Although the implementation of process simulators in food processing is relatively scarce, due to the complexity of the involved phenomena and the lack of property data [Joulia , 2008; Bon et. al, 2009], several works dealing with simulation of alcoholic continuous and batch distillation have been reported in the open literature. A synthesis of the main reports published since 2000 is presented in **Table 5-1**. This synthesis includes studies on diverse spirits: Cachaça [Scanavini, 2010; Batista and Meirelles, 2011; Scanavini, 2012], Fruits spirits [Claus and Berglund, 2009], Pisco [Osorio et al., 2004; Carvallo et al., 2011], Whisky [Gaiser et al., 2012; Valderrama et al., 2012b], pear distillate [Sacher et al., 2013] and bitter orange distillate [Esteban-Decloux et al., 2014]. Works on bioethanol [Batista and Meirelles, 2009; Batista et al., 2012; Batista et. al, 2013], neutral alcohol [Decloux and Coustel, 2005; Valderrama et al., 2012b; Batista et al., 2013; Esteban-Decloux et al., 2014] and anhydrous ethanol [Bastidas et al., 2012] are also summarized, as these products are also derived from agricultural raw material, sugar cane juice and molasses, in this specific case.

Two kinds of simulation tools were used in these works: commercial simulators (including AspenPlus®, Aspen Dynamics®, BatchColumn®, ChemCAD® and ProSimPlus®) or in-house made simulators developed by the authors. In both cases, the simulator is a software that allows the representation of the distillation process through a model that involves the mass and energy balances, coupled to phase equilibria and, in some cases, transport equations and chemical reactions [Gil et al., 2011].

In most of these researches two common points can be outlined:

- The objective of the simulation is to represent accurately the distillation units and to gain better insight into the ethanol and congeners distillation as well as process performance.

- The fermented wash and subsequent process streams are represented as a simplified ethanol – water mixture containing some of the major volatile aroma compounds common to most Spirits, namely: 1,1-diethoxyethane, methanol, prop-2-en-1-ol, propan-1-ol, propan-2-ol, 2-methylpropan-1-ol, butan-1-ol, butan-2-ol, 2-methylbutan-1-ol, 3-methylbutan-1-ol, pentan-1-ol, pentan-2-ol, hexan-1-ol, 2-phenylethanol, ethanal, propan-2-one, ethanoic acid, propanoic acid, octanoic acid, methyl ethanoate, ethyl ethanoate, ethyl hexanoate, ethyl decanoate and furan-2-carbaldehyde, α-pinene, limonene, linalool and linalool oxide. The number of volatile aroma compounds included in the simulations varies from 0 (only binary ethanol – water, Claus and Berglund, 2009) to 16 [Batista et al., 2012; Batista et al., 2013]. Some works also considered non-volatile species, such as glycerol [Bastidas et al., 2012, Tgarguifa et al., 2017], and carbon dioxide, which constitutes the major component of the non-condensable streams and may modify the phase equilibria [Batista and Meirelles, 2011; Batista et al., 2012; Bastidas et al., 2012; Batista et al., 2013].

Table 5-1. *Research works published in the open literature since 2000 on simulation of alcohol distillation.*

	Authors	Aim of the study	Simulation tool	Thermodynamic approach	Solution model
Continuous distillation	Gaiser et al., 2002 *Whisky*	- Representation of a patent unit (two columns). Comparison with literature data.	AspenPlus	*Vapor phase:* Ideal gas *Liquid phase:* NRTL	*Solvent:* ethanol, water *Aroma compounds:* propan-1-ol, 2-methylpropan-1-ol, 3-methylbutan-1-ol; ethanal
	Decloux and Coustel, 2005 *Neutral alcohol*	- Representation of an industrial plant (seven columns) and understanding of the role of the distillation units, regarding ethanol and aroma compounds behaviour. No comparison with experimental data.	ProSimPlus	*Vapor phase:* Ideal gas *Liquid phase:* UNIFAC	*Solvent:* ethanol, water Aroma compounds: methanol, propan-1-ol, 2-methylpropan-1-ol, 3-methylbutan-1-ol; ethanal; ethyl ethanoate
	Batista and Meirelles, 2009 *Bioethanol*	- Representation of an industrial plant (three columns) and analysis of the influence of operational conditions upon the concentration profiles in the distillation units. No comparison with experimental data. - Design of strategies for controlling the ethanal content in bioethanol using a PID controller, a degassing system as well as a new system configuration with two supplementary columns producing a second alcohol stream.	Aspen Plus and Aspen Dynamics	*Vapor phase:* Virial equation coupled to the Hayden-O'Connell model *Liquid phase:* NRTL	*Solvent:* ethanol, water *Aroma compounds*: methanol, propan-1-ol, propan-2-ol, 2-methylpropan-1-ol, 3-methylbutan-1-ol; ethanal; ethanoic acid; ethyl ethanoate *Other compounds:* Carbon dioxide
	Batista and Meirelles, 2011 *Cachaça*	- Representation of two industrial plants (1. Classic installation with 1 column, and a degassing system; 2. Pasteurized installation with 1 main column, 1 side column, and a degassing system) and analysis of the influence of operational parameters upon the product quality. Comparison with own experimental data. - Design of strategies for controlling the volatile content in the spirit using a PID controller linked to the degassing system.	Aspen Plus and Aspen Dynamics	*Vapor phase:* Virial equation coupled to the Hayden-O'Connell model *Liquid phase:* NRTL	*Solvent:* ethanol, water *Aroma compounds:* methanol, propan-1-ol, propan-2-ol, 2-methylpropan-1-ol, 3-methylbutan-1-ol; ethanal, propan-2-one; ethanoic acid; ethyl ethanoate *Other compounds:* Carbon dioxide
	Batista et al., 2012 *Bioethanol*	- Representation of an industrial plant (two columns with degassing systems, and a decanter), understanding of aroma compounds behaviour and analysis of the influence of operational and constructive variables on its performance, for the optimization of the equipments configuration. Comparison with own experimental data. - Development of control loops to compensate changes in wine concentration and prevent off-specification products	Aspen Plus and Aspen Dynamics	*Vapor phase:* Virial equation coupled to the Hayden-O'Connell model *Liquid phase:* NRTL	*Solvent:* ethanol, water *Aroma compounds:* methanol, propan-1-ol, propan-2-ol, 2-methylpropan-1-ol, butan-1-ol, butan-2-ol, 2-methylbutan-1-ol, 3-methylbutan-1-ol, pentan-1-ol, hexan-1-ol; ethanal, propan-2-one; ethanoic acid, propanoic acid; methyl ethanoate, ethyl ethanoate *Other compounds:* carbon dioxide

Table 5-1. *Research works published in the open literature since 2000 on simulation of alcohol distillation. Continuation.*

	Authors	Aim of the study	Simulation tool	Thermodynamic approach	Solution model
Continuous distillation	Bastidas et al., 2012 *Anhydrous fuel ethanol*	- Representation of an industrial plant (four distillation columns) and analysis of the influence of operating parameters upon its performance. Comparison with own experimental data. - Performance of thermal and hydraulic studies of the distillation columns to evaluate the possibility of expanding the net production rate.	AspenPlus	*Vapor phase:* Predictive Soave-Redlich-Kwong equation of state *Liquid phase:* NRTL	*Solvent:* ethanol, water *Aroma compounds:* methanol, propan-1-ol, propan-2-ol, 2-methylpropan-1-ol, butan-1-ol, 3-methylbutan-1-ol, pentan-1-ol; ethanal; ethanoic acid *Other compounds:* carbon dioxide
	Valderrama et al., 2012b *Neutral alcohol*	- Representation of an industrial plant (two columns and a light component separator) and analysis of the influence of feed beer composition on the composition profiles and product quality. Comparison with literature data.	ChemCAD	*Vapor phase:* Ideal gas *Liquid phase:* NRTL	*Solvent:* ethanol, water *Aroma compounds:* methanol, propan-1-ol, butan-1-ol, 3-methylbutan-1-ol, pentan-2-ol, acetic acid *Other compounds:* carbon dioxide, propane-1,2,3-triol
	Batista et al., 2013 *Bioethanol, Neutral alcohol*	- Representation of an industrial plant and analysis of the influence of operational and constructive conditions upon the purification of fuel bioethanol. Comparison with own experimental data. - Development of a new plant for neutral alcohol production considering the required quality standards and operational performance. Comparison with literature data.	Aspen Plus	*Vapor phase:* Virial equation coupled to the Hayden-O'Connell model *Liquid phase:* NRTL	*Solvent:* ethanol, water *Aroma compounds:* methanol, propan-1-ol, propan-2-ol, 2-methylpropan-1-ol, butan-1-ol, butan-2-ol, 2-methylbutan-1-ol, 3-methylbutan-1-ol, pentan-1-ol, hexan-1-ol; ethanal, propan-2-one; ethanoic acid, propanoic acid; methyl ethanoate, ethyl ethanoate *Other compounds:* carbon dioxide
	Esteban-Decloux et al., 2014 *Neutral alcohol*	- Representation of an industrial plant (four distillation columns, and a decanter) and understanding of the aroma compounds behaviour. Comparison with own experimental data. - Determination of new operation points to maximize productivity and improve product quality.	ProSimPlus	*Vapor phase:* Ideal gas *Liquid phase:* NRTL	*Solvent:* ethanol, water *Aroma compounds:* 1,1-diethoxyethane; methanol, prop-2-en-1-ol, propan-1-ol, 2-methylpropan-1-ol, butan-1-ol, butan-2-ol, 3-methylbutan-1-ol; ethanal; ethyl ethanoate
	Tgarguifa et al., 2017 *Bioethanol*	- Representation of an industrial plant (three vacuum columns) and analysis of operational conditions for the optimization of the energy consumption and operating costs. Comparison with own experimental data.	In-house made model (including equations of: mass balance, heat balance, thermodynamic equilibrium and summation)	*Vapor phase:* Virial equation coupled to the Hayden-O'Connell model *Liquid phase:* NRTL	*Solvent:* ethanol, water *Aroma compounds:* ethanal; ethanoic acid *Other compounds:* propane-1,2,3-triol

Table 5-1. *Research works published in the open literature since 2000 on simulation of alcohol distillation. Continuation.*

	Authors	Aim of the study	Simulation tool	Thermodynamic approach	Solution model
Discontinuous distillation	Osorio et al., 2004 *Pisco*	- Evaluation of a simulation strategy using artificial neural networks, with respect to the computing efficiency and accuracy in the representation of composition profiles. No comparison with experimental data.	In-house made differential model (including equations of: mass balance, heat balance, thermodynamic equilibrium, liquid hydraulics, liquid density, and reaction kinetics for some components)	*Vapor phase:* Ideal gas *Liquid phase:* Van Laar (Solvent), UNIFAC (aroma compounds)	*Solvent:* ethanol, water *Aroma compounds:* methanol; octanoic acid; ethyl hexanoate; linalool
	Claus and Berglund, 2009 *Fruits spirits*	- Setting of the operational parameters (reflux ratio, average distillate flow rate and time cutoff frames) required in the different operation steps for the simulation of two distillation units (one lab-scale and one pilot-scale). Adjustment and comparison with own experimental data.	ChemCAD	*Vapor phase:* Ideal gas *Liquid phase:* Comparison of NRTL and UNIFAC	*Solvent:* ethanol, water
	Scanavini et al., 2010 *Cachaça*	- Estimation of the temperature and ethanol composition profiles in the distillate as well as aroma compounds concentrations in different cuts of a lab-scale distillation unit (charentais alembic). Comparison with own experimental data.	In-house made differential model (including equations of: mass balance, heat balance, thermodynamic equilibrium and heat losses)	*Vapor phase:* Virial equation coupled to the Hayden-O'Connell model *Liquid phase:* NRTL	*Solvent:* ethanol, water *Aroma compounds:* methanol, propan-1-ol, 2-methylpropan-1-ol, 3-methylbutan-1-ol; ethanal; ethanoic acid; ethyl ethanoate
	Carvallo et al., 2011 *Pisco*	- Evaluation of a simulation strategy, with respect to ethanol composition profile, methanol concentration in different cuts and some operational variables in a pilot-scale distillation unit (composed of a boiler, a packed column and a partial condenser). Comparison with literature data as well as own experimental data.	In-house made differential model (including equations of: mass balance, heat balance, thermodynamic equilibrium, mass transfer and liquid properties)	*Vapor phase:* Ideal gas *Liquid phase:* NRTL	*Solvent:* ethanol, water *Aroma compounds:* methanol
	Scanavini et al., 2012 *Cachaça*	- Determination and understanding of ethanol and aroma compounds compositions profiles in the distillate as well as some operation parameters of a lab-scale distillation unit (charentais alembic). Comparison with own experimental data. - Experimental determination of heat transfer coefficients in the boiler from measured vaporization rates	In-house made differential model (including equations of: mass balance, heat balance, thermodynamic equilibrium and heat transfer)	*Vapor phase:* Virial equation coupled to the Hayden-O'Connell model *Liquid phase:* NRTL	*Solvent:* ethanol, water *Aroma compounds:* methanol, propan-1-ol, 2-methylpropan-1-ol, 3-methylbutan-1-ol; ethanal; ethanoic acid; ethyl ethanoate

Table 5-1. *Research works published in the open literature since 2000 on simulation of alcohol distillation. Continuation.*

	Authors	Aim of the study	Simulation tool	Thermodynamic approach	Solution model
Discontinuous distillation	Valderrama et al., 2012b *Whisky*	- Determination of the temporal evolution of aroma compounds concentrations in the distilled product, during the first distillation of a bi-distillation system in a classical industrial still. No comparison with experimental data.	ChemCAD	*Vapor phase:* Ideal gas *Liquid phase:* NRTL	*Solvent:* ethanol, water *Aroma compounds:* propan-1-ol, 2-methylpropan-1-ol, 3-methylbutan-1-ol; ethanal
	Sacher et al., 2013 *Pear distillate*	- Estimation of the ethanol composition profile in the distillate as well as aroma compounds concentrations in different cuts of a lab-scale distillation unit (charentais alembic). Comparison with own experimental data.	In-house made differential model (including equations of: mass balance, heat balance, thermodynamic equilibrium and heat transfer)	*Vapor phase:* Ideal gas Liquid phase: UNIFAC	*Solvent:* ethanol, water *Aroma compounds:* 1,1-diethoxyethane; methanol, propan-1-ol, 2-methylpropan-1-ol, butan-1-ol, butan-2-ol, 2-methylbutan-1-ol, 3-methylbutan-1-ol, 2-phenylethan-1-ol; ethanal; methyl ethanoate, ethyl ethanoate, ethyl hexanoate, ethyl decanoate; furan-2-carbaldehyde
	Esteban-Decloux et al., 2014 *Bitter orange distillate*	- Estimation and understanding of the temporal evolution of ethanol and aroma compounds concentrations in the distillate of an industrial still (composed of a boiler, a multistage column, and a total condenser). Comparison with own experimental data. - Improvement in the selection of the distillate cuts (considering the product quality, the recovery of ethanol in the heart fraction and the energy consumption) and understanding of the role of peels during distillation	BatchColumn	*Vapor phase:* Ideal gas *Liquid phase:* Henry's law	*Solvent:* ethanol, water *Aroma compounds:* α-Pinene, limonene, linalool, linalool oxide

Concerning French spirits, to the best of our knowledge, no reports on simulation of the specific distillation units have been reported to date. In this context, the objective of the present work is to develop a methodology for the simulation of spirits distillation at steady state using ProSimPlus®, in order to improve the understanding of volatile aroma compounds behavior and provide scientific basis for the operation of the distillation units. The simulations were performed with the NRTL model, highly recommended for the thermodynamic modeling of hydroalcoholic mixtures at low pressures [Renon and Prausnitz, 1968; Valderrama et al., 2012a]. Experimental distillation data for 66 volatile aroma compounds, having an impact on product quality, were acquired for this study. However, due to the lack of NTRL interaction parameters, only 32 species (including alcohols, carbonyl compounds, carboxylic acids and esters) were simulated.

The developed methodology was applied to the simulation of Armagnac distillation. This AOC spirit is produced by continuous distillation, in a column still known as *alambic armagnacais.* Double batch distillation is also performed in some plants, yet this method represents less than 5% of the production. By law, the distillation period has to be comprised between the end of the grapes harvest and the 31st march of the following year. The production region is located in southwestern France and covers more than 1000 ha divided in three areas: Bas-Armagnac, Tenareze and Haut Armagnac. The wash, wine in this case, is produced by fermentation of white grapes and its ethanol volume concentration at 20°C (named ABV, alcohol by volume) must be between 7.5 %v/v and 12.0% v/v [Bertrand, 2003; Decloux and Joulia, 2009; Ledauphin et al., 2010]. As for fresh distillates, before ageing, their minimum ABV is fixed to 52.0% v/v and the maximum allowed, according to the last regulation is 72.4% v/v [JORF, 2014]. The commercial product is obtained by dilution of aged distillates to a minimal ABV of 40% v/v. A classical composition analysis of commercial Armagnac after ageing is summarized in **Table 5-2** [Bertrand, 2003].

In relation to the literature reports on alcoholic distillation, some novel contributions of this research can be highlighted:

- Development of a methodology for the systematic classification and understanding of volatile aroma compounds behavior in distillation. 16 'new' species are included, namely: (Z)-Hex-3-en-1-ol, octan-1-ol, decan-1-ol, dodecan-1-ol, tetradecan-1-ol, methanoic acid, butanoic acid, 2-methylpropanoic acid, 3-methylbutanoic acid, hexanoic acid, ethyl butanoate, 3-methylbutyl ethanoate, hexyl ethanoate, 2-phenylethyl ethanoate, ethyl octanoate and diethyl butane-1,4-dioate.
- Thermodynamic modeling using binary interaction parameters estimated from experimental data at high dilution, closer to the real conditions of spirits distillation. The methodology is developed in a review published by the authors [Puentes et al., 2017].
- Focus on the influence of operating parameters such as extractions, thermal losses and reflux on distillate composition and energy consumption.

Table 5-2.*Typical Armagnac composition after aging and dilution. Analysis of 15 representative samples. Adapted from (Bertrand, 2003).*

Characteristic		Value	
		Average	**Uncertainty**
Ethanol volume concentration (ABV) at 20 °C	% v/v		
- Real		41.4	1.6
- Raw		40.1	2.3
Dry extract	$g.L^{-1}$	4.5	3.5
Total acidity as ethanoic acid	$g.L^{-1}$	153.9	57.6
Volatile acidity as ethanoic acid	$mg.L^{-1}$	440.9	155.3
Total volatile compounds	$mg.L^{-1}$	2823.9	346.1
Total alcohols	$mg.L^{-1}$	2022.0	180.8
- methanol		194.6	45.1
- propan-1-ol		204.5	55.9
- 2-methylpropan-1-ol		432.6	78.7
- butan-1-ol		0.8	2.1
- butan-2-ol		2.1	3.5
- 2-methyl + 3-methylbutan-1-ol		1186.5	137.4
Total aldehydes as ethanal	$mg.L^{-1}$	96.5	26.5
Total esters as ethyl ethanoate	$mg.L^{-1}$	453.7	143.7
- ethyl ethanoate		315.9	99.4
- Furan-2-carbaldehyde	$mg.L^{-1}$	5.0	1.2

The paper is organized as follows: the development of the simulation methodology is described in **section 5.2**. This includes the description of the process (5.2.1), experimental data acquisition (5.2.2) and reconciliation (5.2.3), as well as configuration of the simulation module in ProSimPlus® (5.2.4). In **section 5.3**, the simulation results of an industrial Armagnac unit are then presented and validated against experimental data. This validation is carried out on two levels (5.3.1): a first level, concerning exclusively the binary ethanol–water, and a second level that incorporates volatile aroma compounds. The behavior of volatile aroma compounds is classified in several categories by using a double criterion based on (i) their relative volatilities with respect to ethanol and water and (ii) the composition profiles in the distillation column. The work is concluded with the simulation of heads and tails extractions (5.3.2) and a detailed analysis of the influence of some operating parameters on the distillate composition and energy consumption (5.3.2). The impact on volatile aroma compounds is evaluated by category, according to the classification established in the previous section.

5.2 Construction of the simulation module

The construction of a simulation module for spirits distillation at steady state is developed in this section. The simulation is focused on the understanding of volatile aroma compounds behavior.

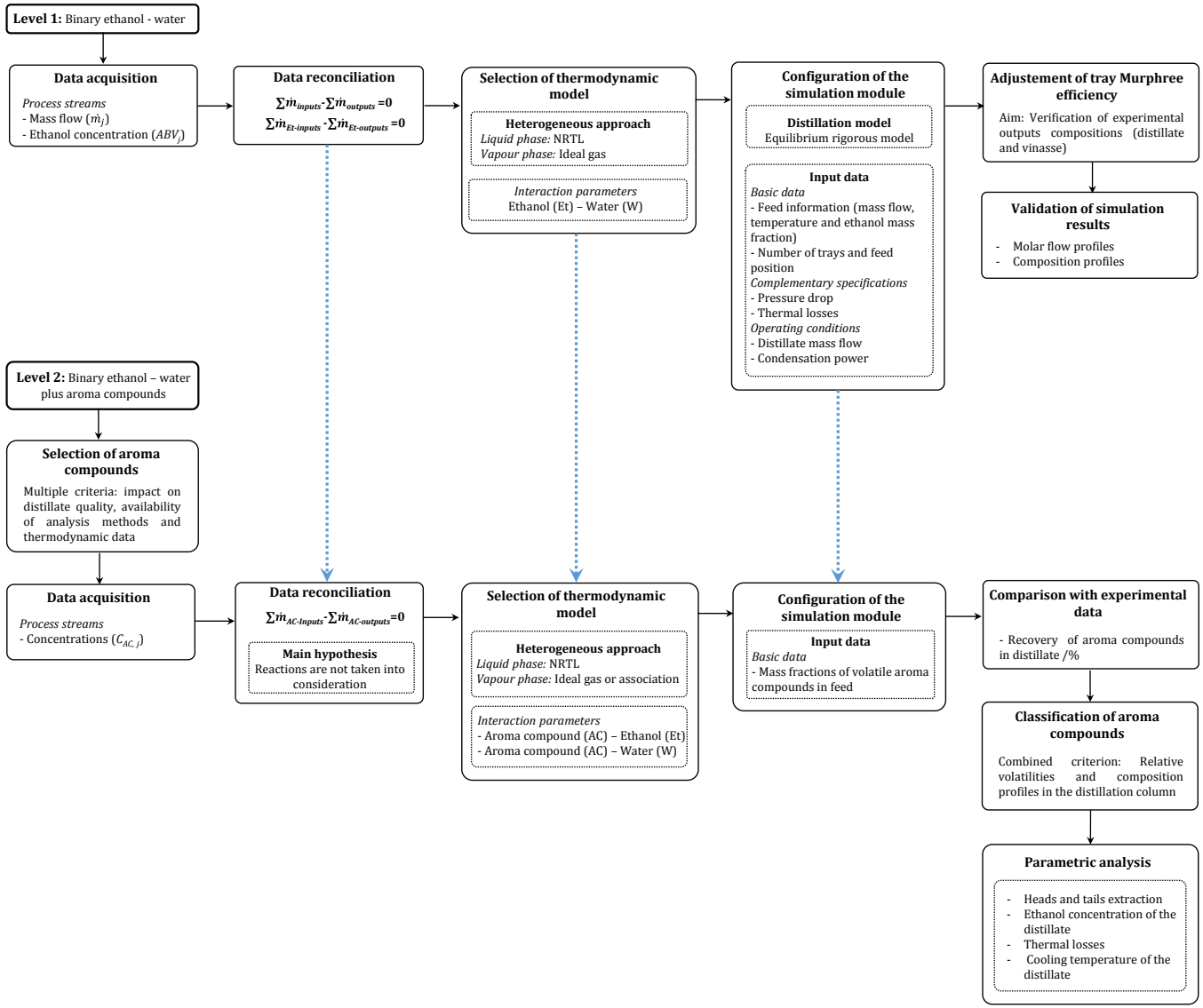

Figure 5-1. *General methodology for the construction of the simulation module.*

In **Figure 5-1**, a general schema of the framework is depicted. The module construction is comprised of the following phases:

- Selection and description of the distillation unit, aiming to identify the different circuits and their configuration.
- Data acquisition and reconciliation, for gathering of input data, and validation of mass and energy balances.
- Selection of a thermodynamic model, fundamental to correctly describe the phase equilibria and other volumetric properties.
- Configuration of the simulation module, which includes the selection of a distillation model, the introduction of input data and other specifications required to solve the modeling problem.

Two levels of simulation were considered: (i) a first level that only includes the two major components of the system, ethanol and water and (ii) a second level for the simulation of volatile aroma compounds distillation in the hydroalcoholic matrix. The aim of the fist level is to tune the global mass and energy balances using experimental reconciled data. Here, validation is based on coherence of the composition and flow profiles simulated in the column. Independent treatment from volatile aroma compounds is justified by the fact that the influence of these components on the mixture enthalpy, and therefore energy balance, can be neglected, since they are present at very low concentrations [Sacher et al., 2013]. Concerning the second level, the aim is to validate the mass balance of volatile aroma compounds with experimental data and then to classify them according to the composition profiles simulated in the column.

In this work, the methodology is applied to the simulation of a distillation unit for Armagnac production. However, it may be extended to other spirits. Further research on Calvados and comparison with Armagnac distillation will be reported in a companion paper.

It is important to mention that the simulation modules do not take into account the chemical reactions that may occur during the distillation. These phenomena are outside the scope of this work. Despite their influence on the generation of volatile compounds with an impact on product quality, information acquired in the spirits field is still very limited. To our knowledge, no analytical information about reactions kinetics in the conditions of spirits distillation have been published in the literature. Ongoing studies in our research team will provide some useful information for the simulation of the coupled distillation-reaction process.

5.2.1. Process Description

The installation selected for this study is an industrial unit for Armagnac distillation, located in the area of Armagnac Tenarèze. Its diary production capacity is about 20 hL of ethanol. The schema of the unit as well as the corresponding process flow diagram are presented in **Figure 5-2**. It is a classical *alambic armagnacais* divided in two parts: (i) a tray column on top of a direct-fired boiler and (ii) a wine heater. All the elements are made of annealed electrical grade copper. The boiler is comprised of two compartments and operates with a natural gas burner. The column has 12 large bubble-cap trays, 1 for concentration, above the feed entry, and 11 for stripping. Inside, at top of the column, a coil heat exchanger works as partial condenser. The wine heater is an

external coil heat exchanger used to preheat the wine while condensing and cooling the vapor distillate.

Wine (F_1) flows uninterruptedly by gravity from the load tank with a level regulation and is distributed between the wine heater (F_2) and the partial condenser (F_3) with a gate valve. In the wine heater, wine flows upwards in the external compartment and is heated by thermal transfer with the distillate (Va_2) flowing in the coil. Then, it enters the column, above the first tray of the stripping section and flows through the trays towards the boiler. The vapor produced in the boiler bubbles through the stripping trays and then reaches the concentration tray, where it is mixed with a reflux stream (R_1) generated in the internal partial condenser. Thus, the mass and energy transfer between both phases lead to the concentration of ethanol and the extraction of volatile aroma compounds in the vapor phase. The liquid phase is in turn enriched with the less volatile species, including water.

The vapor distillate (Va_2) is drawn out of the column and transferred to the wine-heater where it flows down and condenses inside the coil. The wine stream fed to the internal partial condenser (F_3) is partially heated (F_4) and sent to the wine-heater to constitute with the stream F_2 the feed of the column (F_5). Finally, the fresh liquid distillate (D_1), is extracted and passes through an alcoholmeter, to measure its temperature and ethanol concentration. The bottom product or vinasse (Vi_3), stripped in ethanol, is continuously withdrawn through a siphon connected to the boiler.

Two accessory circuits in the wine-heater complete the installation. In the first one, for tails extraction (T_1), a fraction of the liquid flow is evacuated from the bottom of the second turn of the coil. The second one, for heads extraction (H_1), operates in the same way but is placed over one of the last turns of the coil before the cooling section, in order to extract a fraction of vapor phase. Tails are due to contain low volatility compounds that condense easily, while heads is expected to be rich in high volatility compounds that condense at the end of the thermal transfer. Currently, these circuits are not used in the process. However they were tested for simulation purposes in this work. Further details about this analysis are developed in section 5.3.2.1.

Given that the distillation unit is not isolated from the environment, internal refluxes are generated by partial condensation of the vapor phase on the column wall. This phenomenon improves the separation capacity of the column and has therefore to be considered for a correct process modeling.

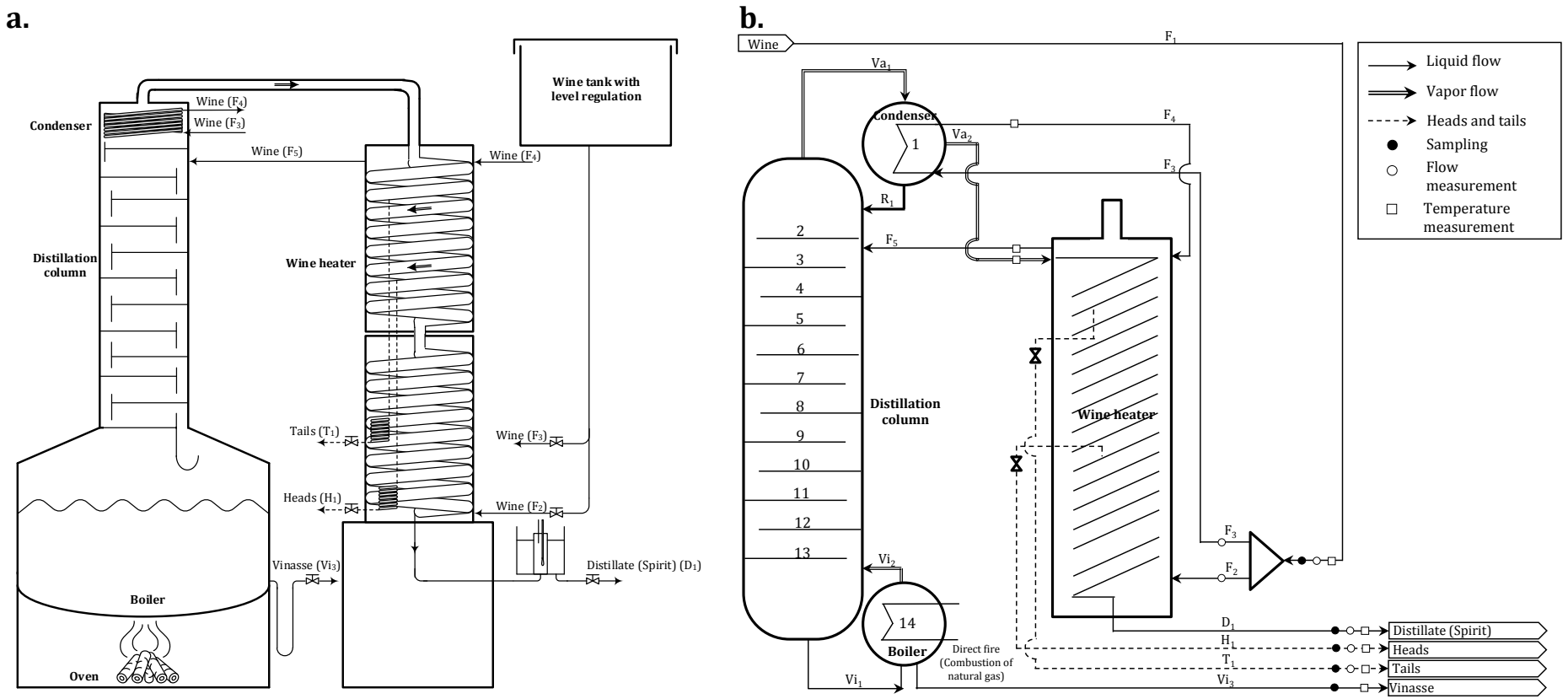

Figure 5-2. ***a.*** *Schema of the distillation unit for Armagnac production.* ***b.*** *Corresponding process diagram.*

5.2.2. DATA ACQUISITION

An experimental campaign was carried out in order to characterize the nominal operation point of the installation and to stablish the corresponding mass and energy balances. The information gathered play a double role of: (i) input data to saturate the freedom degrees of the simulation problem and (ii) validation data to check the reliability of the simulation results. The experimental campaign was performed during six hours, after stabilization of the unit. Every hour, three variables were measured: temperatures, mass flows and distillate ethanol composition (section 5.2.2.1). When possible, several instruments were used to verify the coherence of measurements. At the same time, some streams were sampled and representative global samples were constituted for each one at the end of the campaign, with the aim of quantifying ethanol and volatile aroma compounds composition (section 5.2.2.2).

5.2.2.1. Measurement of flows and temperatures

A previous diagnostic of the installation evidenced a very important limitation in instrumentation. A reduced number of sensors were available before the experimental campaign: three thermocouples (2 placed in the column and one in the wine-heater), one alcohol thermometer for distillate control (D_1), and two flowmeters placed on the cold wine conduits (F_2 and F_3). Those instruments have not been calibrated for a long time and no online measurements or data recording were available.

In this context, new Pt100 probes Fluke-80PK-10 (Fluke, United States) were acquired to perform non-invasive measurements of temperature. They were placed on the following conduits: F_1, F_4 and Vi_3. Wine (F_1) and distillate (D_1) temperatures were also measured by direct contact during the hourly sampling, using a Pt100 probe Checktemp1 (Hanna, country). In the case of wine, the relative deviations of the hourly and average temperatures (from 6 hourly measurements) using the Pt100 probe Fluke-80PK-10 and the Pt100 probe Chekctemp1 were about 9.8%, which can be explained by the different nature of the measurement (surface temperature vs. direct fluid contact). For distillate, the relative deviations between the hourly measurements using the Pt100 probe and the alcohol thermometer (both by direct contact with the liquid) vary between 0.0% and 5.3%, yet the deviation for the average temperature is only of 0.2%.

Thermal profiles of the column and wine-heater were studied by means of an infrared camera Ti9 (Fluke, United States). Some punctual temperatures were also measured with this device, including that of F_1, F_4, F_5 and Va_2. In the case of F_1 and F_4, the relative deviations of the hourly measurements with respect to the Pt100 values were lower than 7.1% for F_1 (deviation of the average temperature 3.4%) and lower than 4.2% for F_4 (deviation of the average temperature 0.2%).

In regards of vinasse temperature, the values measured on the conduit (hourly values between 98.2 °C and 100.6 °C, average value of 99.2 °C) were underestimated, considering that the major component of this stream is water and the boiler operates under a slight overpressure. This problem is due to the direct exposition of the vinasse conduit to the environment, whose temperature is around 20 °C. Thus, only simulation values for this variable will be considered to solve the energy balance.

Concerning stream flows, they were estimated by two ways: for wine (V_1), from the volume variation of the calibrated storage tank, and for distillate (D_1), from the filling time of a container, by means of a weighing-scale and a chronometer. In this latter case, every hourly measurement was made in triplicate, obtaining relative uncertainties lower than 0.7%. Due to evacuation and safety issues, the vinasse mass flow was not measured directly. It was determined from data reconciliation, as explained in section 5.2.2.

Finally, the ethanol volume concentration of the distillate at 20 °C (ABV) was determined with a portable densitymeter DMA35 (Anton Paar, France). The relative deviations between these values and those measured with the alcoholmeter were lower than 0.1 %.

5.2.2.2. Determination of ethanol and volatile aroma compounds compositions

The composition of the process streams were determined by analysis of global samples obtained from mixing of 700 mL hourly samples. Three streams were sampled: feed wine (F_1), distillate (D_1) and vinasse (Vi_3).

The quantitative analysis were carried out at the UNGDA laboratory (*Union Nationale du Groupement de distillateurs d'Alcool*, France), specialized in alcoholic beverages, bioethanol and neutral alcohol. The methodology, illustrated in **figure 5-3**, is based on OIV recommendations [OIV, 1994]. The ABV of distillate was estimated from the mixture density at 20 °C, measured by electronic densitometry with a densitymeter DMA500 (Anton Paar, France), and then converted with the alcoholometric tables [OIML, 1972], integrated in the device calculator. For this estimation, the mixture is considered as a binary mixture of ethanol and water, which leads to an error of 0.5% to 1.0% [UNGDA, 2014].

For wine and vinasse samples, a previous step of steam distillation is necessary to eliminate dry extracts, solid material that modify the liquid density. The separation is carried out at constant volume, to avoid the alteration of ethanol content. The device is regularly controlled by distilling a sample of known ABV. After 5 subsequent distillations, the ABV variation of the product should not exceed 0.1%, which corresponds to a maximal ethanol loss of 0.02% by measurement. For distillate samples, good agreement was obtained with respect to the measurements at the industrial plant, obtaining a relative deviation lower than 0.2%. For mass balance calculations, the selected values were those measured at UNGD with the densitymeter DMA500, more precise than the DMA35.

In regards of volatile aroma compounds, the analysis was performed by gas chromatography coupled to detection by flame ionization (GC-FID). 66 volatile aroma compounds from 7 chemical families were quantified: acetals, alcohols, carbonyl compounds, carboxylic acids, esters, furans and terpenes. Due to the mixture complexity, samples were separated in two groups and their ABV was adjusted to reference values: for the group of low ABV samples, the ABV was adjusted to 10 or 12% v/v and for the group of high ABV samples, the ABV was adjusted to 40 or 50 % v/v. The adjustments were done with anhydrous ethanol or de-ionized water. This treatment aims at minimizing the matrix effects on the chemical analysis.

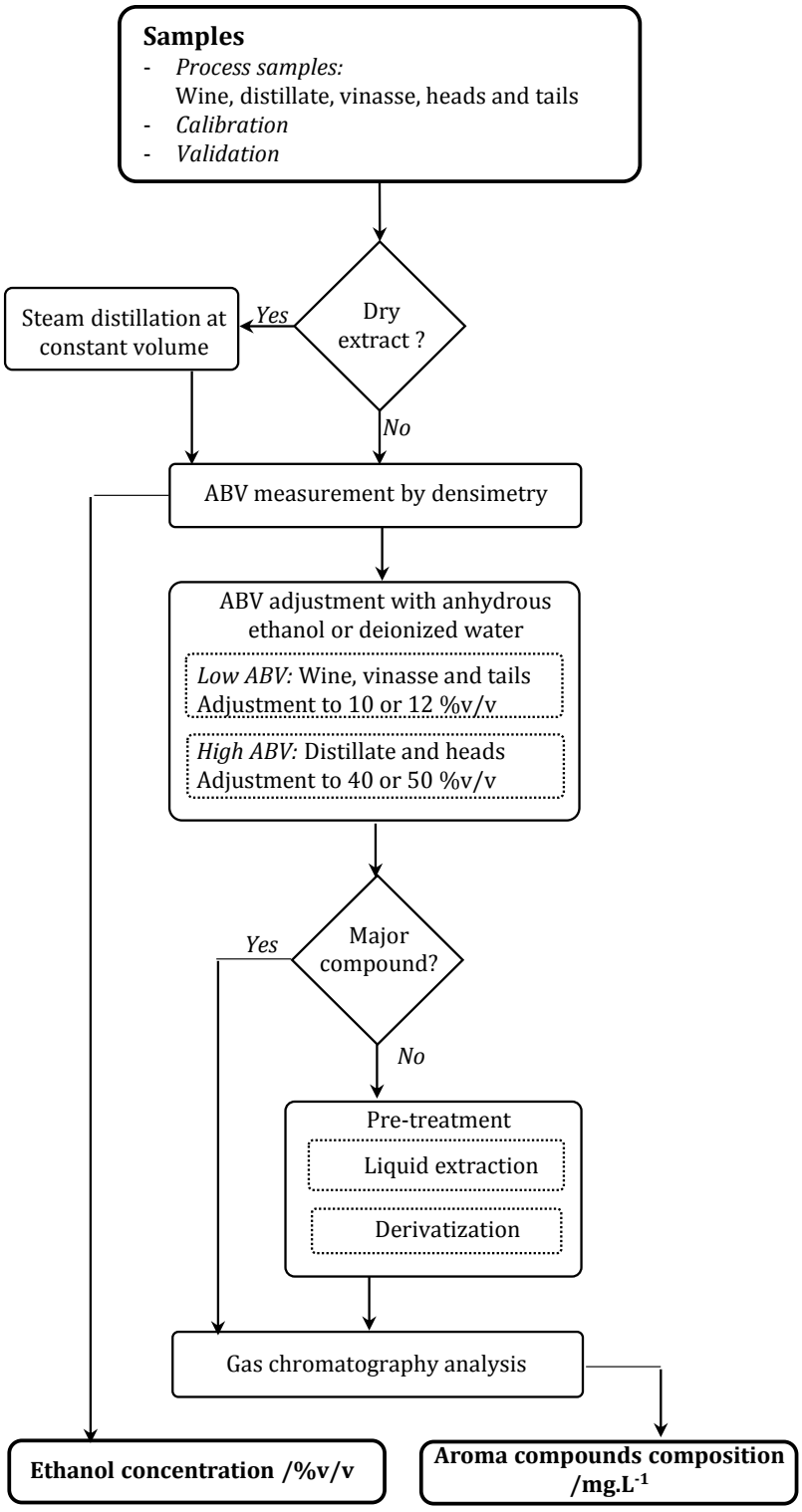

Figure 5-3. *Methodology of chemical analysis of the process stream samples.*

Then, according to the nature and concentration of volatile aroma compounds, three methods were applied:

- Direct injection: for analysis of major compounds, when no pretreatment is required.
- Liquid extraction: pretreatment to concentrate volatile aroma compounds present at very low concentrations, by using organic solvents [UNGDA, 2011a].
- Derivatization: pretreatment to convert the analytes into products with more adapted properties for gas chromatography. In this work, derivatization was applied for the analysis of carboxylic acids, by transforming them into benzylic esters with very specific mass spectra and good response to flame ionization detectors [UNGDA, 2011b].

In **Table 5-3**, further details about each method are presented, including internal standards, pretreatment procedure and conditions of chromatography analysis. **Table 5-4** is a list of the volatile aroma compounds analyzed, classified by chemical family and analysis method. They are presented in an increasing order of molar mass.

Table 5-3. *Analysis methods implemented in this work for the quantification of volatile aroma compounds after ABV adjustment. e : column thickness, V : volume of injection, D_0 : initial volume flow, D_F : final volume flow, T_0 : initial temperature, T_F : final temperature, t : time, R_i : increase i of volume flow or temperature.*

Method	Description	Instrumentation
Direct injection-GC/FID	**Chemical families analyzed** Acetals, alcohols, carbonyl compounds, esters, furans **Internal standard** 4-Methylpentan-2-ol	*Chromatograph:* HP 6890 *Column:* Type : Polar capillary CP WAX 57 CB (Agilent CP97753) Dimensions: 50 m x 0.32 mm, e=0.25 µm *Mobile phase:* Gas: Hydrogen, D_0=2.0 mL.min-1 - t=21.*5 min* R_1=1.0 mL.min^{-2}, D_F=2.5 mL.min^{-1} - t=13.50 min *Injection:* Split: 1/30. V=1 µL *Oven:* T_0=35 °C - t=10 min R_1=5 °C.min^{-1}, T_F=100 °C - t=0 min R_2=15 °C.min^{-1}, T_F=200 °C - t=5 min *Detector:* T=220 °C
Liquid extraction- GC/FID	**Chemical families analyzed** Acetals, alcohols, esters, furans, terpenes **Internal standard** Ethyl tridecanoate, Methyl heptanoate, Methyl heinecosanoate **Pre-treatment** *Low ABV:* Extraction using a mixture of 2,2,4-trimethylpentane/ ethoxyethane (75% / 25% v/v) with sodium chloride in saturated aqueous sodium carbonate solution (250 g.L^{-1}). *High ABV:* Extraction using 2,2,4-trimethylpentane with sodium bicarbonate / sodium chloride (5% / 95% mass).	*Chromatograph:* HP 7890B *Column:* Type: Polar capillary DB WAX (Agilent 122-7062) Dimensions: 60m x 0.25 mm, e=0.25 µm *Mobile phase:* Gas: Hydrogen, D_0=2.1 mL.min^{-1} *Injection:* Split: 1/30, V=2 µL *Oven:* T_0 =35 °C - t=0 min R_1=20 °C.min^{-1}, T_F =60 °C - t=0 min R_2=3 °C.min^{-1}, T_F =120 °C - t=0 min R_2=4 °C.min^{-1}, T_F =220 °C - t=18 min *Detector:* T=220 °C
Derivatization-GC/FID	**Chemical families analyzed** Carboxylic acids **Internal standard** (2E)-But-2-enoic acid **Pre-treatment** *Low ABV:* Isolation of acids by steam distillation at constant volume. Neutralization with tetrabutylammonium hydroxide. Drying with nitrogen and then in an oven for 30 min at 45 °C. Derivatization with benzyl bromide for 1 hour in an oven *High ABV:* Neutralization of acids with tetrabutylammonium hydroxide. Drying with nitrogen and then in an oven for 30 min at 45 °C. Derivatization with benzyl bromide for 1 hour in an oven	*Chromatograph:* HP 7890B *Column:* Type: Polar capillary DB WAX (Agilent 122-7062) Dimensions: 60m x 0.25 mm, e=0.25 µm *Mobile phase:* Gas: Hydrogen, D_0=2.1 mL.min^{-1} *Injection:* Split: 1/30, V=2 µL *Oven:* T_0 =35 °C - t=0 min R_1=20 °C.min^{-1}, T_F =60 °C - t=0 min R_2=3 °C.min^{-1}, T_F =120 °C - t=0 min R_2=4 °C.min^{-1}, T_F =220 °C - t=18 min *Detector:* T=220 °C

Table 5-4. *Aroma compounds quantified by gas chromatography.*

Method	Family	Volatil aroma compound		No. CAS	*MM* /g.mol^{-1}	Quantification limit / mg.L^{-1}		Response factor	
		Common name	IUPAC name			Low ABV	High ABV	Low ABV	High ABV
Direct injection-GC/FID	Acetals	Acetal	1,1-Diethoxyethane	105-57-7	118.2	10.0	10.0	0.5	0.5
	Alcohols	Methanol	Methanol	67-56-1	32.0	10.0	10.0	2.1	1.8
		2-Propenol	Prop-2-en-1-ol	107-18-6	58.1	5.0	5.0	1.0	1.0
		Propanol	Propan-1-ol	71-23-8	60.1	5.0	5.0	1.2	1.2
		Butanol	Butan-1-ol	71-36-3	74.1	5.0	5.0	1.0	1.0
		2-Butanol	Butan-2-ol	78-92-2	74.1	5.0	5.0	1.2	1.2
		Isobutanol	2-Methylpropan-1-ol	78-83-1	74.1	5.0	5.0	1.0	1.0
		2-Methylbutanol	2-Methylbutan-1-ol	137-32-6	88.1	5.0	5.0	1.0	1.0
		Isopentanol	3-Methylbutan-1-ol	123-51-3	88.1	5.0	5.0	1.0	1.0
	Carbonyl compounds	Acetaldehyde	Ethanal	75-07-0	44.1	10.0	10.0	2.6	2.6
	Esters	Ethyl acetate	Ethyl ethanoate	141-78-6	88.1	10.0	10.0	1.8	1.8
		Ethyl lactate	Ethyl 2-hydroxypropanoate	97-64-3	118.1	0.1	5.0	2.0	2.0
	Furanes	Furfural	Furan-2-carbaldehyde	98-01-1	96.1	5.0	5.0	1.6	1.6
Liquid extraction- GC/FID	Acetals	1,1,3-Triethoxypropane	1,1,3-Triethoxypropane	7789-92-6	176.3	0.1	0.1	2.3	2.5
	Alcohols	Cis-3-hexenol	(Z)-Hex-3-en-1-ol	928-96-1	100.2	0.1	0.1	3.4	21.9
		Hexanol	Hexan-1-ol	111-27-3	102.2	0.1	0.1	2.2	12.6
		2-Heptanol	Heptan-2-ol	543-49-7	116.2	0.1	0.1	15.9	5.7
		2-Phenylethanol	2-Phenylethan-1-ol	60-12-8	122.2	0.1	0.1	9.7	70.0
		1-Octanol	Octan-1-ol	111-87-5	130.2	0.1	0.1	2.2	5.2
		1-Decanol	Decan-1-ol	112-30-1	158.3	0.1	0.1	2.1	2.0
		1-Dodecanol	Dodecan-1-ol	112-53-8	186.3	0.1	0.1	2.3	1.3
		1-Tetradecanol	Tetradecan-1-ol	112-72-1	214.4	0.1	0.1	2.0	1.0

Table 5-4. *Aroma compounds quantified by gas chromatography. Continuation.*

Method	Family	Volatil aroma compound		No. CAS	*MM* /g.mol^{-1}	Quantification limit / mg.L^{-1}		Response factor	
		Common name	IUPAC name			Low ABV	High ABV	Low ABV	High ABV
Liquid extraction-GC/FID	Esters	Ethyl butyrate	Ethyl butanoate	105-54-4	116.2	0.1	0.1	9.0	7.5
		Isopentyl acetate	3-Methylbutyl ethanoate	123-92-2	130.2	0.1	0.1	3.5	2.1
		Cis-3-hexenyl acetate	(Z)-3-hexenyl ethanoate	3681-71-8	142.2	0.1	0.1	2.0	1.2
		Ethyl caproate	Ethyl hexanoate	123-66-0	144.2	0.1	0.1	2.1	1.1
		Hexyl acetate	Hexyl ethanoate	142-92-7	144.2	0.1	0.1	2.2	1.0
		2-Phenylethyl acetate	2-Phenylethyl ethanoate	103-45-7	164.2	0.1	0.1	3.0	2.3
		Ethyl caprylate	Ethyl octanoate	106-32-1	172.3	0.1	0.1	2.6	0.8
Liquid extraction- GC/FID		Diethyl succinate	Diethyl butane-1,4-dioate	123-25-1	174.2	0.1	0.2	9.5	16.2
		Ethyl caprate	Ethyl decanoate	110-38-3	200.3	0.1	0.1	4.5	1.2
		Isopentyl caprylate	3-Methylbutyl octanoate	2035-99-6	214.3	0.1	0.1	3.5	1.2
		Ethyl laurate	Ethyl dodecanoate	106-33-2	228.4	0.1	0.1	2.3	1.1
		2-Phenylethyl caprylate	2-Phenylethyl octanoate	5457-70-5	248.4	0.1	0.1	1.9	1.0
		Ethyl myristiate	Ethyl tetradecanoate	124-06-1	256.4	0.1	0.1	2.0	1.0
		Isoamyl laurate	3-methylbutyl dodecanoate	6309-51-9	270.5	0.1	0.1	2.0	1.0
		Ethyl palmitate	Ethyl hexadecanoate	628-97-7	284.5	0.1	0.2	1.9	1.0
		Ethyl linoleate	Ethyl (9Z,12Z)-9,12-octadecadienoate	544-35-4	308.5	0.1	0.1	2.1	1.0
		Ethyl oleate	Ethyl (9Z)-octadec-9-enoate	111-62-6	310.5	0.1	0.2	2.0	1.0
		Ethyl stearate	Ethyl octadecanoate	111-61-5	312.5	0.1	0.2	3.0	1.6
	Furans	Ethyl 2-furoate	Ethyl furan-2-carboxylate	614-99-3	140.1	0.1	0.1	8.0	16.3
	Terpenes	Linalool	3,7-Dimethylocta-1,6-dien-3-ol	78-70-6	154.2	0.1	0.1	1.9	2.5
		α-terpineol	2-(4-Methyl-1-cyclohex-3-enyl)propan-2-ol	98-55-5	154.2	0.1	0.1	2.1	4.0
		Cis-Linalool oxyde	2-[(2R,5S)-5-ethenyl-5-methyloxolan-2-yl]propan-2-ol	5989-33-3	170.2	0.1	0.1	2.4	5.1
		Trans-Linalool oxyde	2-[(2S,5S)-5-ethenyl-5-methyloxolan-2-yl]propan-2-ol	34995-77-2	170.2	0.1	0.1	2.7	6.3
		Cis-Nerolidol	(Z)-3,7,11-Trimethyl-1,6,10-dodecatrien-3-ol	3790-78-1	222.4	0.1	0.1	2.1	1.2
		Trans-Nerolidol	(E)-3,7,11-Trimethyl-1,6,10-dodecatrien-3-ol	40716-66-3	222.4	0.1	0.1	2.1	1.2

Table 5-4. *Aroma compounds quantified by gas chromatography. Continuation.*

Method	Family	Volatil aroma compound		No. CAS	*MM* /g.mol^{-1}	Quantification limit / mg.L^{-1}		Response factor	
		Common name	IUPAC name			Low ABV	High ABV	Low ABV	High ABV
Derivatisation-GC/FID	Carboxylic acids	Formic acid	Methanoic acid	64-18-6	46.0	1.0	1.0	3.7	0.8
		Acetic acid	Ethanoic acid	64-19-7	60.1	1.0	0.1	1.3	0.9
		Propionic acid	Propanoic acid	79-09-4	74.1	1.0	1.0	4.7	1.0
		Butanoic acid	Butanoic acid	107-92-6	88.1	1.0	1.0	1.9	1.0
		Isobutanoic acid	2-Methylpropanoic acid	79-31-2	88.1	1.0	1.0	2.4	1.0
		Lactic acid	2-Hydroxypropanoic acid	50-21-5	90.1	1.0	1.0	4.9	1.3
		2-Methylbutanoic acid	2-Methylbutanoic acid	116-53-0	102.1	1.0	1.0	3.0	1.1
		Isovaleric acid	3-Methylbutanoic acid	503-74-2	102.1	1.0	1.0	3.5	1.0
		Caproic acid	Hexanoic acid	142-62-1	116.2	1.0	1.0	3.9	1.1
		Caprylic acid	Octanoic acid	124-07-2	144.2	1.0	1.0	5.1	1.2
		Capric acid	Decanoic acid	334-48-5	172.3	1.0	1.0	6.4	1.1
		Lauric acid	Dodecanoic acid	143-07-7	200.3	1.0	1.0	-	1.2
		Myristic acid	Tetradecanoic acid	544-63-8	228.4	1.0	1.0	-	1.3
		Palmitoleic acid	(9Z)-Hexadec-9-enoic acid	373-49-9	254.4	1.0	1.0	-	2.0
		Palmitic acid	Hexadecanoic acid	57-10-3	256.4	1.0	1.0	-	1.8
		Linolenic acid	(9Z,12Z,15Z)-9,12,15-Octadecatrienoic acid	463-40-1	278.4	1.0	1.0	-	2.0
		Linoleic acid	(9Z,12Z)-9,12-Octadecadienoic acid	60-33-3	280.4	1.0	1.0	-	1.7
		Oleic acid	(9Z)-Octadec-9-enoic acid	112-80-1	282.5	1.0	1.0	-	1.6
		Stearic acid	Octadecanoic acid	57-11-4	284.5	1.0	1.0	-	3.0

For quantification and reconciliation purposes, two parameters should be introduced: the quantification limit and the response factor. The quantification limit of a volatile aroma compound (QL_{AC}) is the minimal concentration that can be estimated with an acceptable level of accuracy and repeatability at specific separation and detection conditions. This limit can be determined graphically as a function of the background noise in a chromatogram. For its part, the response factor of a volatile aroma compound is defined as the ratio between its concentration and the associated chromatographic peak area. In order to minimize the variability introduced by peak areas, this ratio is compared to the corresponding ratio of an internal standard. The response factor is obtained from the analysis of a calibration solution of known composition. The formula is:

$$RF_{AC/IS} = \frac{A_{IS^\circ} C_{AC^\circ}}{A_{AC^\circ} C_{IS^\circ}} \quad [5.1]$$

Here, $RF_{AC/IS}$ is the response factor (dimensionless) of a volatile aroma compound AC with respect to an internal standard IS, C_{AC° is the concentration (in mg.L^{-1}) of the volatile aroma compound AC in the calibration solution, C_{IS° is the concentration (in mg.L^{-1}) of the internal standard in the same solution, A_{AC° is the peak area (dimensionless) associated to the volatile aroma compound and A_{IS° is the peak area (dimensionless) for the internal standard.

The estimated values of quantification limits in mg.L^{-1} and response factors in both low and high ABV samples are also presented in **Table 5-4**.

The concentrations of volatile aroma compounds in the process samples were estimated using the response factors and the chromatographic data. The equation is:

$$C_{AC,\,j} = \frac{RF_{AC/IS} k_C A_{AC,\,j} C_{IS,\,j}}{A_{IS,\,j}} \quad [5.2]$$

Where $C_{AC,\,j}$ is the concentration (in mg.L^{-1}) of a volatile aroma compound AC in a sample of the process stream j, $RF_{AC/IS}$ is the corresponding response factor (dimensionless) determined at the same analysis conditions, $A_{IS,\,j}$ and $A_{AC,\,j}$ are the peak areas (dimensionless) of internal standard and volatile aroma compound AC in the analyzed sample, $C_{IS,\,j}$ is the concentration (in mg.L^{-1}) of the internal standard in the analyzed sample and k_C is the concentration factor (dimensionless) from the step of ABV adjustment.

In order to validate the accuracy and repeteablity of the analysis, various global samples of the three process streams were separately analyzed: three in the case of wine and vinasse, and two in the case of distillate, whose matrix composition is relatively clean. Every analysis series was accompanied by three supplementary samples of known composition: (i) one calibration sample to determine the response factor of each volatile aroma compound and (ii) two validation samples for quality control. These samples, prepared at the reference ABV, follow the same analysis path of a real sample, including steam distillation and pretreatment steps, when required.

Table 5-5. *Validation of aroma compounds analysis using samples of known composition.*

Method	Volatile aroma compound	Low ABV		High ABV	
		Real concentration /mg.L-1	Relative deviation /%	Real concentration /mg.L-1	Relative deviation /%
Direct injection-GC/FID	1,1-Diethoxyethane	8.1	1%	32.5	1%
	Methanol	50.0	1%	200.0	9%
	Prop-2-en-1-ol	16.1	1%	64.5	0%
	Propan-1-ol	25.7	0%	102.9	0%
	Butan-1-ol	10.1	1%	40.3	1%
	Butan-2-ol	10.1	1%	40.4	0%
	2-Methylpropan-1-ol	37.6	1%	150.4	0%
	2-Methylbutan-1-ol	20.0	0%	79.8	0%
	3-Methylbutan-1-ol	50.0	1%	200.1	0%
	Ethanal	7.8	6%	31.3	6%
	Ethyl ethanoate	60.5	0%	241.8	0%
	Ethyl 2-hydroxypropanoate	20.8	2%	83.3	1%
	Furan-2-carbaldehyde	8.0	1%	32.2	1%
Liquid extraction- GC/FID	1,1,3-Triethoxypropane	5.1	3%	5.1	8%
	(Z)-Hex-3-en-1-ol	5.1	4%	5.1	28%
	Hexan-1-ol	5.3	2%	5.3	16%
	Heptan-2-ol	5.2	4%	5.2	3%
	2-Phenylethan-1-ol	2.8	9%	2.8	23%
	Octan-1-ol	5.3	2%	5.3	6%
	Decan-1-ol	5.1	2%	5.1	14%
	Dodecan-1-ol	2.6	3%	2.6	10%
	Tetradecan-1-ol	2.3	2%	2.3	12%
	Ethyl butanoate	5.4	5%	5.4	3%
	3-Methylbutyl ethanoate	5.0	1%	5.0	2%
	(Z)-3-hexenyl ethanoate	5.2	1%	5.2	7%
	Ethyl hexanoate	5.1	1%	5.1	4%
	Hexyl ethanoate	5.1	3%	5.1	4%
	2-Phenylethyl ethanoate	5.1	2%	5.1	3%
	Ethyl octanoate	5.2	1%	5.2	4%
	Diethyl butane-1,4-dioate	5.4	7%	5.4	13%
	Ethyl decanoate	5.2	1%	5.2	9%
	3-Methylbutyl octanoate	4.9	2%	4.9	12%
	Ethyl dodecanoate	2.6	2%	2.6	2%
	2-Phenylethyl octanoate	2.6	2%	2.6	3%
	Ethyl tetradecanoate	2.7	2%	2.7	7%
	3-methylbutyl dodecanoate	2.5	3%	2.5	9%
	Ethyl hexadecanoate	2.9	0%	2.9	14%
	Ethyl (9Z,12Z)-9,12-octadecadienoate	2.4	2%	2.4	17%
	Ethyl (9Z)-octadec-9-enoate	2.3	1%	2.3	18%
	Ethyl octadecanoate	3.8	2%	3.8	15%
	Ethyl furan-2-carboxylate	5.0	14%	5.0	16%
	3,7-Dimethylocta-1,6-dien-3-ol	5.4	1%	5.4	9%
	2-(4-Methyl-1-cyclohex-3-enyl)propan-2-ol	5.0	2%	5.0	12%
	2-[(2R,5S)-5-ethenyl-5-methyloxolan-2-yl]propan-2-ol	2.8	1%	2.8	31%
	2-[(2S,5S)-5-ethenyl-5-methyloxolan-2-yl]propan-2-ol	2.3	2%	2.3	34%
	(Z)-3,7,11-Trimethyl-1,6,10-dodecatrien-3-ol	0.9	1%	0.9	0%
	(E)-3,7,11-Trimethyl-1,6,10-dodecatrien-3-ol	1.2	1%	1.2	2%

Table 5-5. *Validation of aroma compounds analysis using samples of known composition. Continuation.*

Method	Volatile aroma compound	Low ABV		High ABV	
		Real concentration /mg.L-1	Relative deviation /%	Real concentration /mg.L-1	Relative deviation /%
Derivatization-GC/FID	Methanoic acid	101.8	12%	102.9	11%
	Ethanoic acid	99.0	15%	104.4	6%
	Propanoic acid	97.9	33%	97.5	3%
	Butanoic acid	99.9	15%	99.4	4%
	2-Methylpropanoic acid	99.7	6%	103.2	1%
	2-Hydroxypropanoic acid	98.8	48%	83.5	3%
	2-Methylbutanoic acid	100.5	8%	102.1	4%
	3-Methylbutanoic acid	100.5	11%	104.5	5%
	Hexanoic acid	101.7	23%	103.8	2%
	Octanoic acid	98.5	29%	105.8	1%
	Decanoic acid	98.4	17%	95.0	4%
	Dodecanoic acid	-	-	46.6	9%
	Tetradecanoic acid	-	-	48.9	1%
	(9Z)-Hexadec-9-enoic acid	-	-	56.3	20%
	Hexadecanoic acid	-	-	47.4	7%
	(9Z,12Z,15Z)-9,12,15-Octadecatrienoic acid	-	-	50.3	4%
	(9Z,12Z)-9,12-Octadecadienoic acid	-	-	47.9	6%
	(9Z)-Octadec-9-enoic acid	-	-	58.8	9%
	Octadecanoic acid	-	-	47.5	8%

In **Table 5-5**, the real compositions of validation samples are summarized together with the relative errors of the measured values. The real values were determined by weighing. Concerning the analysis by direct injection, the average errors are small, of the order of 1%, for the both ABV ranges. The maximum errors are 6% at low ABV, associated with ethanal, and 9% at high ABV, associated with methanol. For the method with liquid extraction, average errors become higher: 3% at low ABV and 11% at high ABV. The maximum error at low ABV is the associated with ethyl furan-2-carboxylatefuroate, 14%, and at high ABV, with 2-[(2S, 5S)-5-ethenyl-5-methyloxolan-2-yl] propan-2-ol (trans-linalool oxide), equivalent to 34%. For the derivatization method, the average deviations are 20% at low ABV and 6% at high ABV. The maximum errors are 48% at low ABV, related to 2-hydroxypropanoic acid (lactic acid), and 20% at high ABV, corresponding to (9Z)-hexadec-9-enoic acid (palmitoleic acid).

It should be noted that the maximum tolerances accepted by the UNGDA laboratory on the estimation of volatile aroma compounds composition varies between 20 and 35% for all analysis methods. This is justified by the variability associated with the physicochemical pretreatment, which involves the introduction of solvents and, in derivatization, a chemical reaction whose yield and selectivity may vary. Although these factors increase the uncertainty, the analysis is suitable to determine the correct magnitude order of volatile aroma compounds concentrations, while remaining on a rather quick and simple methodology.

5.2.2.3. Data conversion

For mass balance calculations, all the experimental compositions and flows must be expressed as temperature independent quantities. The average ABV values were converted into mass fractions by means of an empirical correlation established from literature data [OIML, 1972; Oudin, 1980]:

$$x_{mEt,j}=C_1ABV_j+C_2ABV_j^2+C_3ABV_j^3 \quad [5.3]$$

Here, $x_{mEt,j}$ is the ethanol mass fraction of the process stream j and ABV_j is the corresponding ABV. C_1 to C_3 are coefficients determined by data regression. Their values are: C_1=8.172×10^{-3}, C_2=-5.788×10^{-6} and C_3=2.332×10^{-7}.

Concerning the volatile aroma compounds, their mass fractions were obtained as follows:

$$x_{mAC,j}=\frac{C_{AC,j}}{10^6\rho_{j\text{-}20}} \quad [5.4]$$

Here, $x_{mAC,j}$ is the mass fraction of a volatile aroma compound AC in the process stream j, $C_{AC,j}$ is the corresponding concentration (in mg.L^{-1}) and $\rho_{j\text{-}20}$ is the density (in kg.L^{-1}) of the process stream j at 20°C, which corresponds to the analysis temperature.

Finally, water mass fractions ($x_{mW,j}$) were computed by difference:

$$x_{mW,j}=1-x_{mEt,j}-\sum_{AC=1}^{N}x_{mAC,j} \quad [5.5]$$

Here N (≤66) is the number of volatile aroma compounds quantified in the process stream j.

Regarding wine mass flow, this value was estimated from the experimental volume flow and mixture density at the average temperature of the stream ($\rho_{j\text{-}T}$). To simplify the calculation, this latter property was considered as a function of temperature (T in °C) and ethanol mass fraction ($x_{mEt,j}$). An empirical correlation for ethanol–water mixtures is available in the alcoholometric tables [OIML, 1972]:

$$\rho_{j\text{-}T}=A_1+\sum_{k=2}^{12}A_k x_{mEt,j}^{k-1}+\sum_{k=1}^{6}B_k(T\text{-}20)^k+\sum_{i=1}^{n}\sum_{k=1}^{m_i}C_{ik}x_{mEt,j}^{k-1}(T\text{-}20)^k \quad [5.6]$$

Here, A_k, B_k, C_{ik} are empirical coefficients estimated by regression of experimental density data. The values are summarized in **Table 5-6**. As previously stated, the influence of volatile aroma compounds can be neglected because of their low concentrations. In regards of dry extracts, even if they do have an influence on density, they will not be considered for two reasons: (i) the experimental values of ABV, used to compute ethanol mass fractions, were measured after their elimination from the hydroalcoholic matrix and (ii) they cannot be included in the simulation module, as the solution model only considers molecules in liquid or vapor phase. With respect to this latter argument, the direct measurement of a distillate mass flow remains coherent, since this stream do not contain dry extracts.

Table 5-6. *Coefficients for the calculation of density with Equation (5-6). Taken from [OIML, 1972].*

k	A_k	B_k	$C_{1,k}$	$C_{2,k}$	$C_{3,k}$	$C_{4,k}$	$C_{5,k}$
1	9.98×10^{2}	-2.06×10^{-1}	1.69×10^{-1}	-1.19×10^{-2}	-6.80×10^{-4}	4.08×10^{-6}	-2.79×10^{-8}
2	-1.93×10^{2}	-5.27×10^{-3}	-1.05×10	2.52×10^{-1}	1.88×10^{-2}	-8.76×10^{-6}	1.35×10^{-8}
3	3.89×10^{2}	3.61×10^{-5}	7.20×10	-2.17×10^{0}	-2.00×10^{-1}	6.52×10^{-6}	
4	-1.67×10^{3}	-3.90×10^{-7}	-7.05×10^{2}	1.35×10	1.02×10^{0}	-1.52×10^{-6}	
5	1.35×10^{4}	7.17×10^{-9}	3.92×10^{3}	-5.03×10	-2.90×10^{0}		
6	-8.83×10^{4}	-9.97×10^{-11}	-1.21×10^{4}	1.10×10^{2}	4.81×10^{0}		
7	3.06×10^{5}		2.25×10^{4}	-1.42×10^{2}	-4.67×10^{0}		
8	-6.14×10^{5}		-2.61×10^{4}	1.08×10^{2}	2.46×10^{0}		
9	7.47×10^{5}		1.85×10^{4}	-4.41×10	-5.41×10^{-1}		
10	-5.48×10^{5}		-7.42×10^{3}	$7.44E\times10^{0}$			
11	2.23×10^{5}		1.29×10^{3}				
12	-3.90×10^{4}						

5.2.3. Data reconciliation

Direct application of the raw data set to validate mass balance is not possible for two reasons:

- The global mass balance is not redundant, as the experimental vinasse flow is unknown.
- For some volatile aroma compounds, the partial mass flow is bigger in distillate than in wine, which is not only due to errors in the composition analysis, but also to chemical reactions that increase their output mass flow.

Data reconciliation is therefore required to generate a statistically coherent data set, from a minimal correction of the raw values, and to detect possible sensors faults and gross errors [Vrielynick, 2002; Sacher, 2013]. The experimental values are corrected to satisfy some constraints as the conservation equations, mass balance in this case. This procedure can be formulated as an optimization problem of a system with m measured variables, in which the objective function to minimize is [Heyen and Arpentinier, 2017]:

$$FO=\sum_{i=1}^{m}\left(\frac{V_{C,i}-V_{M,i}}{u_i}\right)^2 \qquad [5.7]$$

Where, $V_{M,i}$ is the measured value and $V_{C,i}$ the corrected value of the variable i. The standard deviation or absolute uncertainty, u_i, is included to apply the bigger corrections to the less accurate values.

The reconciliation was initially applied to calculate the vinasse mass flow and to simultaneously verify the ethanol mass balance, acting on total mass flows ($\dot{m}_j$) and ethanol mass fractions ($x_{mEt,j}$) (Esteban-Decloux et al., 2014). In this case, the objective function depends on five variables ($\dot{m}_{F1}$, $x_{mEt,F1}$, $\dot{m}_{D1}$, $x_{mEt,D1}$, $x_{mEt,Vi3}$) and two constraints are taken into account:

Global mass balance: $\dot{m}_{F1}-\dot{m}_{D1}-\dot{m}_{Vi3}=0$ [5.8]

Ethanol mass balance: $\dot{m}_{F1}x_{mEt,F1}-\dot{m}_{D1}x_{mEt,D1}-\dot{m}_{Vi3}x_{mEt,Vi3}=0$ [5.9]

In a second step, the partial mass flow of volatile aroma compounds were corrected to verify the respective mass balance. For each volatile aroma compound, the constraint is written as:

$$\dot{m}_{F1}x_{mAC,\,F1}\text{-}\dot{m}_{D1}x_{mAC,\,D1}\text{-}\dot{m}_{Vi3}x_{mAC,\,Vi3}=0 \qquad [5.10]$$

By fixing the total mass flows, a coherent set of mass fractions ($x_{mAC,\,j}$) can be calculated.

A supplementary constraint is defined when the concentration of a volatile aroma compound is lower than the quantification limit ($C_{AC,\,j}<QL_{AC}$). The measured value as well as its standard uncertainty are fixed at the respective quantification limit. The constraint is written in terms of partial mass flows by means of the Equation 5.4. The following expression is obtained:

$$\dot{m}_{AC,j}\text{-}\frac{QL_{AC}}{10^{6}\rho_{j\text{-}20}}\dot{m}_{j}< 0 \qquad [5.11]$$

The sets of measured and reconciled values, including mass flows and compositions of wine, distillate, and vinasse are presented in **Table 5-7**. The composition values are reported as volume concentrations to facilitate their reading and interpretation. According to this synthesis, the reconciled values of mass flows and ethanol concentrations are in good agreement with the measurements, as the relative deviations are lower than 4.0%.

In regards of volatile aroma compounds, except for methanoic acid and ethanoic acid, high deviations are mainly associated to the species at very low concentrations. Two factors might justify this result: analysis errors and occurrence of chemical reactions. On one hand, although gas chromatography is a technique adapted to the system tackled in this work, aspects such as matrix complexity, sample preparation and overlapping spectra may have a negative impact on quantification. On the other hand, since the measured mass flows were reconciled without taking into account mass generation or consumption, the correction applied for species that were actually involved in chemical reactions may be very important to satisfy the simplified mass constraints.

Despite this problem, from a general point of view, the relative deviations are acceptable, with overall values for each process stream between 10% and 37%. Moreover, as the lowest deviations are associated to distillate (10%), product of interest, the results from reconciliation can be considered as satisfactory for the simulation purposes of this work.

Table 5-7. *Measured and reconciled values for mass flows and compositions.*

Process stream	Feed - F_1			Distillate - D_1			Vinasses -Vi_3		
Variable	Measured value		Reconciled value	Measured value		Reconciled value	Measured value		Reconciled value
	Average	Uncertainty		Average	Uncertainty		Average	Uncertainty	
Mass flow /kg.h^{-1}	856.3	9.8	866.2	126.0	1.5	127.4	-	-	738.7
Ethanol concentration /%v/v	10.8	0.1	10.8	64.8	0.3	64.9	0.33	0.02	0.34
Volatile aroma compounds concentrations /mg.L^{-1}									
Volatile aroma compound									
1,1-Diethoxyethane	-	-	-	<6.5	<6.5	6.5	-	-	-
1,1,3-Triethoxypropane	<0.1	<0.1	0.1	<0.1	<0.1	0.1	<0.1	<0.1	0.1
Methanol	40.7	1.2	41.0	194.6	0.0	194.6	12.7	0.6	11.1
Prop-2-en-1-ol	-	-	-	<6.5	<6.5	6.5	-	-	-
Propan-1-ol	17.3	1.2	17.9	110.3	0.0	110.3	<5.0	<5.0	0.0
Butan-1-ol	<5.0	<5.0	5.0	<6.5	<6.5	6.5	<5.0	<5.0	4.7
Butan-2-ol	<5.0	<5.0	5.0	<6.5	<6.5	6.5	<5.0	<5.0	4.7
2-Methylpropan-1-ol	135.0	1.0	136.8	843.2	0.0	843.2	<5.0	<5.0	0.0
2-Methylbutan-1-ol	74.7	1.2	75.8	470.2	4.6	470.2	<5.0	<5.0	0.0
3-Methylbutan-1-ol	304.0	2.0	305.1	1903.6	22.9	1903.6	<5.0	<5.0	0.0
(Z)-Hex-3-en-1-ol	0.2	0.0	0.4	1.7	0.0	1.7	<0.1	<0.1	0.1
Hexan-1-ol	1.6	0.0	1.6	10.8	0.0	10.8	<0.1	<0.1	0.0
Heptan-2-ol	<0.1	<0.1	0.1	<0.1	<0.1	0.1	<0.1	<0.1	0.1
2-Phenylethan-1-ol	31.5	0.5	29.8	17.3	0.1	17.3	29.4	0.8	32.0
Octan-1-ol	<0.1	<0.1	0.1	0.2	0.0	0.2	<0.1	<0.1	0.1
Decan-1-ol	<0.1	<0.1	0.1	0.1	0.1	0.1	<0.1	<0.1	0.1
Dodecan-1-ol	<0.1	<0.1	0.1	<0.1	<0.1	0.1	<0.1	<0.1	0.1
Tetradecan-1-ol	<0.1	<0.1	0.1	0.2	0.0	0.2	<0.1	<0.1	0.1
Ethanal	<10.0	<10.0	9.4	<6.5	<6.5	6.5	<10.0	<10.0	9.9

Table 5-7. *Measured and reconciled values for mass flows and compositions. Continuation.*

Process stream	**Feed - F_1**			**Distillate - D_1**			**Vinasses -Vi_3**		
Variable	**Measured value**		**Reconciled value**	**Measured value**		**Reconciled value**	**Measured value**		**Reconciled value**
	Average	**Uncertainty**		**Average**	**Uncertainty**		**Average**	**Uncertainty**	
	Volatile aroma compounds concentrations /mg.L^{-1}								
Volatile aroma compound									
Methanoic acid	38.3	44.9	32.7	4.8	0.8	4.8	11.0	2.6	37.7
Ethanoic acid	229.7	156.9	120.3	<0.1	<0.1	0.1	78.0	20.1	142.4
Propanoic acid	8.7	10.7	1.2	0.7	0.1	0.7	1.3	0.6	1.3
Butanoic acid	36.0	56.3	1.6	1.2	0.0	1.2	1.7	0.6	1.7
2-Methylpropanoic acid	1.7	1.2	1.7	1.2	0.0	1.2	4.3	3.2	1.7
2-Hydroxypropanoic acid	-	-	-	9.8	3.7	9.8	-	-	-
2-Methylbutanoic acid	7.3	11.0	0.9	0.5	0.1	0.5	<1.0	<1.0	1.0
3-Methylbutanoic acid	<1.0	<1.0	0.9	0.6	0.0	0.6	<1.0	<1.0	1.0
Hexanoic acid	23.0	19.3	3.2	6.0	0.0	6.0	2.7	1.5	2.6
Octanoic acid	23.7	16.6	4.6	23.1	0.1	23.1	<1.0	<1.0	1.0
Decanoic acid	3.7	4.6	2.8	12.0	0.0	12.0	<1.0	<1.0	1.0
Dodecanoic acid	<1.0	<1.0	1.0	3.2	0.0	3.2	<1.0	<1.0	0.6
Tetradecanoic acid	-	-	-	8.5	2.1	8.5	-	-	-
(9Z)-Hexadec-9-enoic acid	-	-	-	<1.0	<1.0	1.0	-	-	-
Hexadecanoic acid	-	-	-	2.0	0.0	2.0	-	-	-
(9Z,12Z,15Z)-9,12,15-Octadecatrienoic acid	-	-	-	<1.0	<1.0	1.0	-	-	-
(9Z,12Z)-9,12-Octadecadienoic acid	-	-	-	<1.0	<1.0	1.0	-	-	-
(9Z)-Octadec-9-enoic acid	-	-	-	<1.0	<1.0	1.0	-	-	-
Octadecanoic acid	-	-	-	<1.0	<1.0	1.0	-	-	-
Ethyl ethanoate	17.0	1.7	18.9	116.7	0.0	116.7	<10.0	<10.0	0.0
Ethyl butanoate	0.3	0.0	0.4	1.5	0.1	2.1	0.1	0.1	0.1
Ethyl 2-hydroxypropanoate	-	-	-	45.4	0.0	0.0	-	-	-
3-Methylbutyl ethanoate	0.6	0.0	0.7	3.5	0.1	4.1	<0.1	<0.1	0.1
(Z)-3-hexenyl ethanoate	<0.1	<0.1	0.1	<0.1	<0.1	0.1	<0.1	<0.1	0.1

Table 5-7. *Measured and reconciled values for mass flows and compositions. Continuation.*

Process stream	Feed - F_1			Distillate - D_1			Vinasses -Vi_3		
Variable	Measured value		Reconciled value	Measured value		Reconciled value	Measured value		Reconciled value
	Average	Uncertainty		Average	Uncertainty		Average	Uncertainty	
	Volatile aroma compounds concentrations /mg.L^{-1}								
Volatile aroma compound									
Ethyl hexanoate	0.7	0.0	0.9	5.0	0.0	5.2	0.1	0.1	0.1
Hexyl ethanoate	<0.1	<0.1	0.1	0.1	0.0	0.1	<0.1	<0.1	0.1
2-Phenylethyl ethanoate	<0.1	<0.1	0.1	<0.1	<0.1	0.1	<0.1	<0.1	0.1
Ethyl octanoate	0.9	0.1	1.8	11.6	0.0	11.4	0.1	0.1	0.0
Diethyl butane-1,4-dioate	0.2	0.1	0.1	<0.2	<0.2	0.2	0.1	0.1	0.1
Ethyl decanoate	0.2	0.0	1.5	15.3	0.0	9.0	0.1	0.1	0.0
3-Methylbutyl octanoate	<0.1	<0.1	0.1	0.6	0.0	0.6	0.1	0.1	0.0
Ethyl dodecanoate	<0.1	<0.1	0.1	9.4	0.0	0.6	0.1	0.1	0.0
2-Phenylethyl octanoate	<0.1	<0.1	0.1	<0.1	<0.1	0.1	0.1	0.1	0.1
Ethyl tetradecanoate	<0.1	<0.1	0.1	3.5	0.1	0.6	0.1	0.1	0.0
3-Methylbutyl dodecanoate	0.1	0.0	0.2	0.5	0.0	1.0	0.1	0.1	0.1
Ethyl hexadecanoate	<0.1	<0.1	0.1	3.6	0.1	0.6	0.1	0.1	0.0
Ethyl (9Z,12Z)-9,12-octadecadienoate	<0.1	<0.1	0.1	2.2	0.1	0.6	0.1	0.1	0.0
Ethyl (9Z)-octadec-9-enoate	<0.1	<0.1	0.1	0.3	0.0	0.3	0.1	0.1	0.1
Ethyl octadecanoate	<0.1	<0.1	0.1	0.2	0.0	0.2	0.1	0.1	0.1
Furan-2-carbaldehyde	-	-	-	<6.5	<6.5	6.5	-	-	-
Ethyl 2-furoate	<0.1	<0.1	0.1	<0.1	<0.1	0.1	<0.1	<0.1	0.1
3,7-Dimethylocta-1,6-dien-3-ol	<0.1	<0.1	0.1	0.2	0.0	0.2	<0.1	<0.1	0.1
2-(4-Methyl-1-cyclohex-3-enyl)propan-2-ol	<0.1	<0.1	0.1	0.1	0.0	0.1	<0.1	<0.1	0.1
2-[(2R,5S)-5-Ethenyl-5-methyloxolan-2-yl]propan-2-ol	<0.1	<0.1	0.1	<0.1	<0.1	0.1	<0.1	<0.1	0.1
2-[(2S,5S)-5-Ethenyl-5-methyloxolan-2-yl]propan-2-ol	<0.1	<0.1	0.1	<0.1	<0.1	0.1	<0.1	<0.1	0.1
(Z)-3,7,11-Trimethyl-1,6,10-dodecatrien-3-ol	<0.1	<0.1	0.1	<0.1	<0.1	0.1	<0.1	<0.1	0.1
(E)-3,7,11-Trimethyl-1,6,10-dodecatrien-3-ol	<0.1	<0.1	0.1	0.2	0.0	0.2	<0.1	<0.1	0.1

5.2.4. SIMULATION PROCEDURE WITH PROSIMPLUS®

5.2.4.1. Thermodynamic model

A heterogeneous approach, also known as gamma-phi method, was selected to model phase equilibria of the investigated system. Since the distillation unit operates at atmospheric pressure, the vapor phase can be considered as an ideal gas, except for the case of carboxylic acids, which can be associated as dimers due to strong hydrogen bonds [Allen and Caldin, 1953; Vawdrey et al., 2004]. For these compounds, a correction term is included [Detcheberry et al., 2016). This corresponding model is available in Simulis Thermodynamics®, suite for phase equilibria and properties calculations of ProSimPlus®.

The non-ideality of the liquid phases was represented by the NRTL model [Renon and Prausnitz, 1968], used in most simulation works reported in literature on alcohol distillation and recommended by different authors [Valderrama and Faundez, 2003; Faundez and Valderrama, 2004; Faundez et. al, 2006; Faundez and Valderrama, 2009; Athès et al., 2008; Valderrama et al., 2012a]. In this model, the binary interaction parameters required to compute the activity coefficients are determined from phase equilibria data. The non-randomness parameter was set at α=0.3 for all binaries. For binary ethanol–water, the parameters used in this work were those reported by [Kadir, 2009], validated against different sets of literature data [Arce et al., 1996; Yang and Wang, 2002; Kamihama et al., 2012; Lai et al., 2014]. The values are presented in **Table 5-8**.

Table 5-8. *Interaction parameters of the NRTL model for the binary ethanol (2) – water (3). Taken from (Kadir, 2009).*

Solvent	i	j	A_{ij}^0 / cal·mol^{-1}	A_{ji}^0 / cal·mol^{-1}	A_{ij}^T / cal·mol^{-1}·K^{-1}	A_{ij}^T / cal·mol^{-1}·K^{-1}
Ethanol - Water	2	3	34.02	850.12	-1.8	5.65

Concerning the volatile aroma compounds, the parameters were estimated from experimental data at high dilution, closer to the real conditions of spirits distillation. Only the interactions volatile aroma compound–ethanol and volatil aroma compound–water were considered. Besides, the temperature dependence of the interaction parameters was neglected (A_{ij}^T=0, A_{ji}^T=0), as the temperature interval is fixed by the composition of the solvent ethanol-water in boiling conditions. Further details on the estimation and validation methodology are presented in a companion paper [Puentes et al., 2017]. Due to the lack of equilibrium data, only parameters for 26 compounds concerned in this work were obtained. Parameters for 1, 1-diethoxyethane, 2-hydroxypropanoic acid and furan-2-carbaldehyde were also available, but these compounds were not simulated since their compositions in wine and vinasse were not measured. 6 supplementary compounds (octan-1-ol, decan-1-ol, dodecan-1-ol, tetradecan-1-ol, ethyl butanoate and hexyl ethanoate) were then added to complete the group of 32 compounds simulated. In this case, the interaction parameters were estimated from vapor-liquid equilibria predictions, using the UNIFAC model version 1993 [Gmehling, 1993]. The set of parameters is displayed in **table 5-9**.

Table 5-9. *Interaction parameters of the NRTL model for the binaries volatile aroma compounds (1) – ethanol (2) and volatile aroma compounds (1) – water (3). Taken from (Puentes et al., 2017). (*) The interaction parameters were not calculated from experimental data but UNIFAC predictions.*

Aroma compound	i	j	A_{ij}^0 / cal·mol^{-1}	A_{ji}^0 / cal·mol^{-1}	Aroma compound	i	j	A_{ij}^0 / cal·mol^{-1}	A_{ji}^0 / cal·mol^{-1}
Methanol	1	2	501.4	-479.1	Propanoic acid	1	2	3535.6	-589.3
	1	3	44211.4	502.1		1	3	-211.6	1848.5
Propan-1-ol	1	2	-452.9	685.7	Butanoic acid	1	2	-1114.2	2026.4
	1	3	-434.4	2536.2		1	3	-838.0	3724.0
Butan-1-ol	1	2	-1059.5	1792.1	2-Methylpropanoic acid	1	2	1770.5	-702.0
	1	3	-490.7	3423.3		1	3	761.6	1841.7
2-Methylpropan-1-ol	1	2	-935.2	1560.0	3-Methylbutanoic acid	1	2	-1223.8	2147.9
	1	3	-505.1	3358.8		1	3	-566.0	3887.2
2-Methylbutan-1-ol	1	2	25.2	-25.9	Hexanoic acid	1	2	1139.6	960.7
	1	3	412.9	2994.5		1	3	-846.2	5941.1
3-Methylbutan-1-ol	1	2	-1914.3	4567.3	Octanoic acid	1	2	1991.7	1810.6
	1	3	-506.6	4070.5		1	3	10939.2	6231.9
(Z)-Hex-3-en-1-ol	1	2	-1429.0	1893.1	Ethyl ethanoate	1	2	1601.5	-433.2
	1	3	1901.2	3040.5		1	3	715.2	2560.2
Hexan-1-ol	1	2	2396.1	-431.6	Ethyl butanoate(*)	1	2	127.8	706.3
	1	3	2429.5	3342.0		1	3	1561.4	3757.8
2-Phenylethan-1-ol	1	2	-1747.3	3693.2	3-Methylbutyl ethanoate	1	2	-1574.4	2894.8
	1	3	-1363.3	5732.5		1	3	2324.7	4048.3
Octan-1-ol(*)	1	2	-920.2	1668.2	Ethyl hexanoate	1	2	7760.3	1590.9
	1	3	1707.6	4721.9		1	3	6440.1	4451.2
Decan-1-ol(*)	1	2	-1543.4	3321.1	Hexyl ethanoate(*)	1	2	-414.3	1477.2
	1	3	4417.1	6414.4		1	3	1813.6	4846.7
Dodecan-1-ol(*)	1	2	-1822.4	4422.6	2-Phenylethyl ethanoate	1	2	-1662.4	2717.4
	1	3	3043.8	7717.5		1	3	603.8	5060.5
Tetradecan-1-ol(*)	1	2	-2879.4	10827.9	Ethyl octanoate	1	2	-2025.0	4702.3
	1	3	9262.1	9661.8		1	3	1091.0	6332.6
Ethanal	1	2	1125.5	-670.2	Diethyl butane-1,4-dioate	1	2	4366.2	1227.9
	1	3	70.5	1343.1		1	3	-629.7	4389.9
Methanoic acid	1	2	3499.5	-1064.2	Ethyl decanoate	1	2	-2077.9	4754.5
	1	3	926.0	-562.5		1	3	1600.1	8104.5
Ethanoic acid	1	2	1018.8	-397.0	3,7-Dimethylocta-1,6-dien-3-ol	1	2	-2256.0	3773.8
	1	3	-492.8	1590.0		1	3	2698.1	4988.9

5.2.4.2. Configuration of the simulation module

The module for static simulations was built in ProSimPlus® using the standard equipments of distillation, heat transfer and mixing. The distillation was modeled using the rigorous equilibrium approach, based on the MESH equations [Kister, 1992]. As previously stated, the simulation module must take into account the thermal losses, since the column, copper-made, is not isolated from the environment.

For the first simulation level, in which only the binary ethanol – water was considered, input data includes:

- Column configuration: unit of 14 stages, including 12 trays, 1 partial condenser and 1 boiler.
- Feed: Wine ($\dot{m}_{F1}$=866.1 kg.h^{-1}; T_{F1}=76.4 °C; x_{mEt}=0.086) introduced at stage 3 (numbered from top to bottom).
- Temperature data set: for most process streams (F_1, F_2, F_3, F_4, F_5 and D_1) temperatures were fixed at the experimental raw values. For the others streams (R_1, Va_1, Va_2, Vi_1, Vi_2 and Vi_3) the values are estimated by simulation.
- Operating conditions: two operating conditions are required to saturate the two degrees of freedom of the model, the feed being fixed, and then to solve the simulation problem. Physically these two degrees of freedom correspond to the control variables of the distillation unit: heat duty and reflux, via the ratio between F_2 and F_3. Taking into account the reliability of the measurements, the distillate mass flow and the condensation power were selected. The first were measured in triplicate every hour during six hours, obtaining a reconciled value of 127.4 kg.h^{-1} with relative incertitude of 1.2%. The second can be estimated from mass flow and temperature measurements, according to the following equation:

$$\dot{Q}_C = c_{P,F3}\dot{m}_{F3}(T_{F4}-T_{F3}) \quad [5.12]$$

  Here, $c_{P,F3}$ is the specific heat at constant pressure (computed to 4.0 kJ.kg^{-1}.K^{-1} with Simulis Thermodynamic®), $\dot{m}_{F3}$ the mass flow of the stream F_3 (estimated from a correction of the flowmeter value to 187.1 kg.h^{-1}), and T_{F4} and T_{F3} the temperatures after and before condensation (measured values of 66.2 °C and 13.1°C, respectively). The average power obtained was 11.6 kW considering the contribution of thermal losses.
  The condensation power was preferred to the heat power in the boiler because an accurate estimation of this latter requires the knowledge of supplementary parameters (such as temperature and composition of fumes) that were not available during the experimental campaign.
- Complementary specifications: column top pressure fixed at 101.3 kPa and pressure drop of 0.4 kPa by tray. Thermal losses ($\dot{Q}_{TL}$) were estimated by considering two transfer mechanisms: natural convection of air and radiation of copper:

$$\dot{Q}_{TL} = hS(T_S-T_\infty)+\varepsilon\sigma S T_S^4 \quad [5.13]$$

  In this equation, h is an average convective heat transfer coefficient (estimated to 6.0 W.m^{-2}.K^{-1} from empirical correlations for vertical cylinders, proposed by Day (2012), S the transfer surface (total column surface estimated to 5.0 m^2), T_S the average temperature of the column

surface (estimated to 94 °C), T_∞ the air temperature (measured value of 20 °C), ε the emissivity of polished copper (about 0.04, according to Cengel, 2007) and σ the Boltzmann Constant (5.7×10^{-8} W.m^{-2}.K^{-4}). Thus, considering the column geometry and the distance between trays, two average losses were fixed: 0.2 kW in each tray (stages 2 to 13) and 0.4 kW at stage 1, where the internal condenser is located. The thermal losses in the boiler are taken into account indirectly, as the effective heat power is calculated by the simulator to verify the fixed values of quantity (flow) and quality (ethanol concentration) of the distillate.

Finally, the Murphree efficiencies ($\bar{E}$) in the stripping section were adjusted between 0.5 and 1.0, in order to verify the reconciled ethanol mass fractions of the outputs streams. The relationship between both parameters is shown in **Figure 5-4**. According to this result, the Murphree efficiency was fixed at 0.68. For the concentration plate, the efficiency was fixed at a lower value, 0.58, considering that the reflux flow is low (about 19.8 kg.h^{-1}). This may favor preferential flow pathways, reducing the contact with the vapor phase and therefore the concentration efficiency.

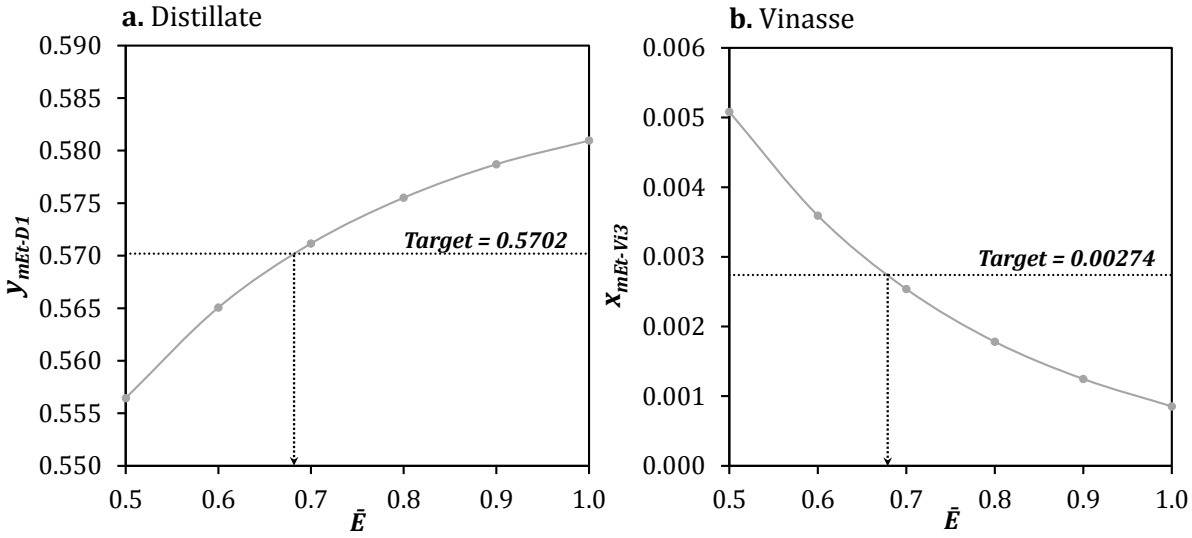

Figure 5-4. *Adjustment of the Murphree tray efficiency of the stripping section to verify the ethanol outputs composition.*

Concerning the second simulation level, all the parameters tuned in the first simulation level are maintained and the 32 volatile aroma compounds are added into the feed at the reconciled mass compositions.

5.3. Analysis of simulation results

This section is focused on the analysis of simulation results for the unit of Armagnac distillation. The first step consists in the representation of the nominal operation point to validate the simulation module. The validation is performed by comparison between experimental and simulation data in two levels: for the first level, binary ethanol – water, it is based on the coherence of the simulated composition and molar flow profiles, and for the second one, multicomponent volatile aroma compounds – ethanol – water mixture, by comparison between experimental and simulated data of partial mass flows and mass recovery from feed to distillate.

Given that the main objective of the study is to better understand the behavior of volatile aroma compounds and process performance, a systematic classification is then proposed, according to their relative volatilities and their composition profiles in the column. Afterwards a simulation of the circuits of heads and tails extractions is proposed and validated against experimental data collected during the experimental campaign. Finally, the influence of some operating parameters (including ethanol concentration in the distillate, thermal losses and distillate temperature after condensation) is evaluated with respect to the composition of volatile aroma compounds in the distillate and energy consumption in the boiler. Analysis on the influence of ethanol concentration and thermal losses is based on different simulations, while for the distillate temperature, only theoretical calculations are considered.

5.3.1. VALIDATION OF THE NOMINAL OPERATION POINT

5.3.1.1. Level 1: Binary ethanol – water

In the first level of simulation, the global and ethanol mass balances were tuned to the experimental reconciled values. The ethanol recovery in the distillate is 97.32% of the amount fed into the column, which corresponds to a maximum concentration of 2700 mg/kg in the vinasse, acceptable for Armagnac production. The reflux ratio calculated by simulation is 0.22, a ratio that justifies the relatively low ABV of distillate, 64.9 %v/v. This value is within the appropriate concentration range stablished by legislation (52.0 %v/v and 72.4 %v/v).

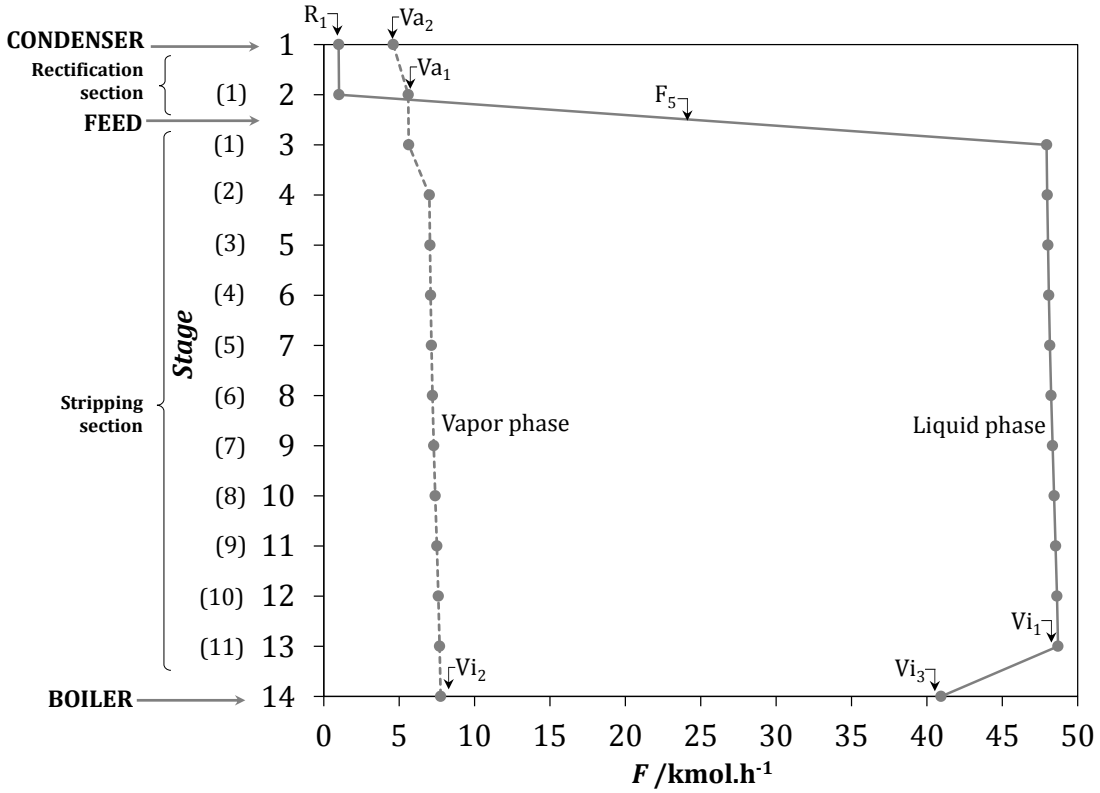

Figure 5-5. *Molar flow profile through the distillation column at the nominal operation point.*

The molar flow profile of liquid and vapor phases in the column is depicted in **Figure 5-5**. The increase of liquid mass flow between stages 2 and 3 corresponds to the introduction of wine. Following the direction of flow (upwards for vapor and downwards for liquid), the simulation predicts a continuous decrease of the vapor flow while the liquid one (before the boiler) increases at the same rate. This phenomenon can be justified by the internal refluxes (partial condensation of the vapor phase) due to thermal losses through the column on each tray. The more pronounced reduction of vapor flow between stages 4 and 3 is associated with a supplementary condensation due to wine feed, whose temperature, despite being preheated, is lower than the temperature at stage 3.

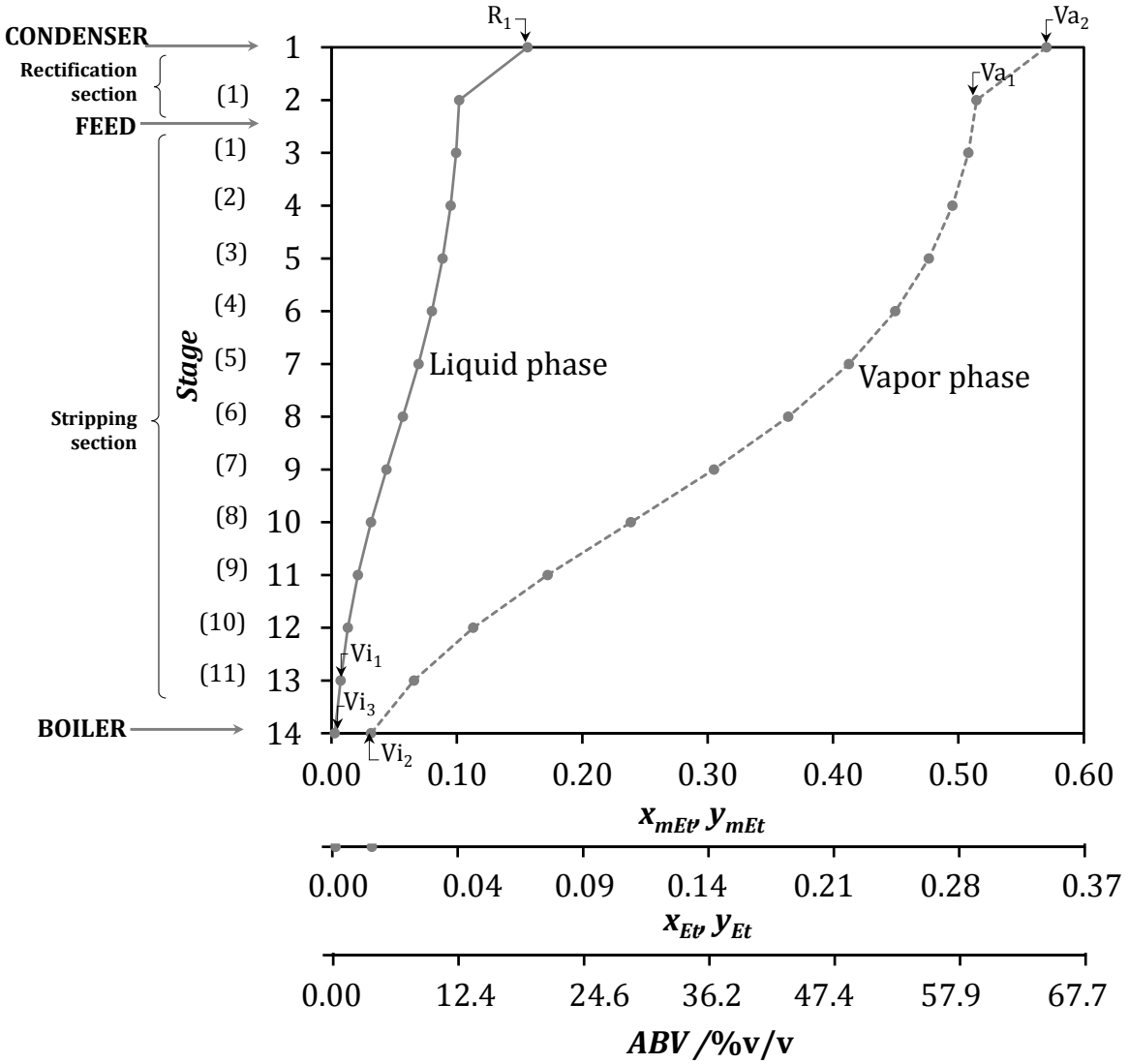

Figure 5-6. *Ethanol composition profile through the distillation column at the nominal operation point.*

The ethanol composition profile is presented in **Figure 5-6**. Even if the absolute variation of liquid composition is less pronounced than that of the vapor phase, the corresponding stripping factor from top to bottom (about 64 in molar basis and 57 in volume) is considerably higher than the concentration factor in the vapor phase (27 in molar basis and 16 in volume). This result is

coherent with the column configuration and indicates that the column plays a preponderant role of ethanol stripping.

The composition profiles here simulated are very different from the profiles in other alcohol distillation units, including those of neutral alcohol and bioethanol production [Decloux and Coustel, 2005; Batista, 2012; Batista, 2013; Esteban-Decloux, 2014], where the distillate has an important ethanol concentration and, as a result, the liquid and vapor compositions at top are very close. Two factors explain this difference: (i) the number of rectification trays is reduced (in bioethanol or neutral alcohol units, this number is around 40-50), and (ii) the distillate is withdrawn as a vapor, since the internal coil operates as a partial condenser.

In matters of energy balance, the net heat power in the boiler calculated by simulation is 88.5 kW. This value is coherent with those reported for other Armagnac units with similar production capacity [AD'3E, 2010]. The heat exchanged in the wine heater was computed by two ways: regarding the cold fluid (F_3), which is preheated to 76.4 °C, and regarding the hot fluid (Va_2), condensed then cooled to 18.8 °C. The average value obtained is 55.2 kW and the relative deviation between the estimations is 15.6%. This difference results from the combined effect of different error sources, including: (i) the estimation of wine mass flow without considering the contribution of solid materials, present in the real feed and (ii) the temperature of streams, most of which were indirectly measured from surface temperatures of a conductor material. Nevertheless, the current deviation in the wine heater energy balance should not affect the analysis of volatile aroma compounds behavior, as the distillation column, where separation takes place, is well represented.

Table 5-10. *Synthesis of the main properties of all the process streams in the distillation unit. R Exp: Reconciled experimental value. NR Exp: Non-reconciled experimental value. Sim: Simulation value.*

Process stream	Mass flow /kg.h^{-1}		Ethanol mass fraction		Temperature /°C	
	Value	Source	Value	Source	Value	Source
F_1	866.2	R Exp	0.086	R Exp	13.1	NR Exp
F_2	678.8	NR Exp	0.086	R Exp	13.1	NR Exp
F_3	187.4	NR Exp	0.086	R Exp	13.1	NR Exp
F_4	187.4	NR Exp	0.086	R Exp	66.2	NR Exp
F_5	866.2	Exp R	0.086	R Exp	76.4	NR Exp
Va_1	147.3	Sim	0.514	Sim	91.6	Sim
Va_2	127.4	R Exp	0.570	R Exp	88.8	Sim
D_1	127.4	R Exp	0.570	R Exp	18.8	NR Exp
R_1	19.8	Sim	0.156	Sim	88.8	Sim
Vi_1	881.3	Sim	0.007	Sim	100.4	Sim
Vi_2	142.5	Sim	0.032	Sim	101.1	Sim
Vi_3	738.7	R Exp	0.003	R Exp	101.1	Sim

A final recapitulation of mass flows, temperatures and ethanol compositions for the distillation unit is presented in **Table 5-10**.

5.3.1.2. Level 2: Binary ethanol – water plus volatile aroma compounds

5.3.1.2.1. Comparison between experimental data and simulation

A comparison between experimental and simulation data for the group of 32 volatile aroma compounds is presented in **Table 5-11**. This synthesis reveals that the consistency of concentrations is variable. For some major (including propan-1-ol, 2-methylpropan-1-ol, 2-methylbutan-1-ol, 3-methylbutan-1-ol and ethyl ethanoate) and minor species (hexan-1-ol, methanoic acid, 2-methylpropanoic acid, ethyl octanoate and ethyl decanoate) the deviations are very low in both distillate and vinasse. For another group of compounds (methanol, 2-phenylethan-1-ol, propanoic acid, butanoic acid, 3-methylbutanoic acid, hexanoic acid, octanoic acid, diethyl butane-1,4-dioate), the deviations become more important but the experimental and simulated values have the same orders of magnitude, even in the case of very low concentrations, around 0.1 $mg.L^{-1}$. For compounds such as (Z)-hex-3-en-1-ol, ethyl butanoate, 3-methylbutyl ethanoate and ethyl hexanoate, although deviations of concentrations in vinasse could be considered high, as simulation predicts zero mass flows, the deviations for distillate are rather low. For ethanoic acid, the simulation prediction is close to the experimental value in vinasse, but in distillate the deviation is rather high, considering that the experimental concentration is about 0. For the remaining volatile aroma compounds (butan-1-ol, octan-1-ol, decan-1-ol, dodecan-1-ol, tetradecan-1-ol, ethanal, hexyl ethanoate, 2-phenylethyl ethanoate and 3,7-dimethylocta-1,6-dien-3-ol), relatively high deviations are obtained in both vinasse and distillate mass flows.

The origin of the deviations is mainly related to an important uncertainty in chemical analysis, but also to the sensitivity of concentrations to small perturbations of the steady state operation [Batista et al., 2012]. In relation to the simulation module, the accuracy of concentration predictions can also be affected by the operating parameters tuned in the first level (for instance the tray efficiency) as well as by the interaction parameters of the NRTL model, most of which were fitted to experimental data with average deviations for vapor mole compositions between 1% and 27%.

Despite this important variability, a global comparison of the data set, depicted in **Figure 5-7**, shows that simulation is rather well correlated to experimental data, with determination coefficients (R^2) of 0.91 for distillate concentrations and 0.94 for vinasse concentrations. From a qualitative point of view, as indicated by [Batista et al. 2012], this result enables us to validate the ability of simulation to represent the distillation process.

Table 5-11. *Experimental and simulated data of mass flow and composition in the main process streams.*

Process stream	**Feed - F_1**	**Distillate - D_1**		**Vinasse - Vi_3**	
Variable	**Simulation = Experimental**	**Experimental**	**Simulation**	**Experimental**	**Simulation**
Mass flow /kg.h^{-1}	866.2	127.4	127.4	738.7	738.7
Partial mass flows /kg.h^{-1}					
Ethanol	74.7	72.7	72.7	2.0	2.0
Water	790.8	54.2	54.2	736.5	736.6
		Concentration /mg.L^{-1}			
Volatil aroma compounds					
Methanol	41.0	194.6	171.1	11.1	15.6
Propan-1-ol	17.9	110.3	109.9	0.0	0.1
Butan-1-ol	5.0	6.5	30.8	4.7	0.0
2-Methylpropan-1-ol	136.8	843.2	843.0	0.0	0.0
2-Methylbutan-1-ol	75.8	470.2	467.3	0.0	0.0
3-Methylbutan-1-ol	305.1	1903.6	1880.1	0.0	0.0
(Z)-Hex-3-en-1-ol	0.4	1.7	2.4	0.1	0.0
Hexan-1-ol	1.6	10.8	9.9	0.0	0.0
2-Phenylethan-1-ol	29.8	17.3	5.9	32.0	34.1
Octan-1-ol	0.1	0.2	0.6	0.1	0.0
Decan-1-ol	0.1	0.1	0.6	0.1	0.0
Dodecan-1-ol	0.1	0.1	0.6	0.1	0.0
Tetradecan-1-ol	0.1	0.2	0.6	0.1	0.0
Ethanal	9.4	6.5	58.2	9.9	0.0
Methanoic acid	32.7	4.8	5.1	37.7	37.6
Ethanoic acid	120.3	0.1	25.3	142.4	137.2
Propanoic acid	1.2	0.7	0.4	1.3	1.4
Butanoic acid	1.6	1.2	0.9	1.7	1.7
2-Methylpropanoic acid	1.7	1.2	1.1	1.7	1.7
3-Methylbutanoic acid	0.9	0.6	1.2	1.0	0.9
Hexanoic acid	3.2	6.0	2.5	2.6	3.3
Octanoic acid	4.6	23.1	24.6	1.0	0.7
Ethyl ethanoate	18.9	116.7	116.8	0.0	0.0
Ethyl butanoate	0.4	2.1	2.6	0.1	0.0
3-Methylbutyl ethanoate	0.7	4.1	4.5	0.1	0.0
Ethyl hexanoate	0.9	5.2	5.5	0.1	0.0
Hexyl ethanoate	0.1	0.1	0.6	0.1	0.0
2-Phenylethyl ethanoate	0.1	0.1	0.6	0.1	0.0
Ethyl octanoate	1.8	11.4	11.4	0.0	0.0
Diethyl butane-1,4-dioate	0.1	0.2	0.1	0.1	0.1
Ethyl decanoate	1.5	9.0	9.0	0.0	0.0
3,7-Dimethylocta-1,6-dien-3-ol	0.1	0.2	0.6	0.1	0.0

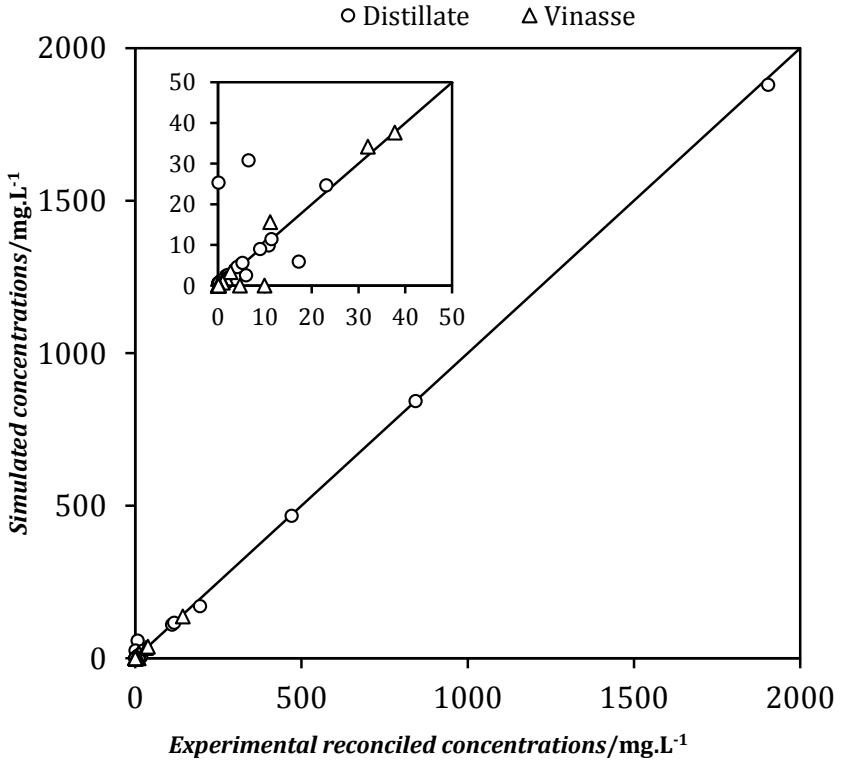

Figure 5-7. *Comparison between experimental and simulation data of aroma compounds concentrations.*

For a better insight into the volatile aroma compounds behavior, a comparison of the mass recovery from feed to distillate is presented in **Figure 5-8**. Global good agreement is obtained between experimental and simulation data. However, for a group of 9 compounds already identified (butan-1-ol, octan-1-ol, decan-1-ol, dodecan-1-ol, tetradecan-1-ol, ethanal, hexyl ethanoate, 2-phenylethyl ethanoate and 3, 7-dimethylocta-1, 6-dien-3-ol), the simulation predicts an integral recovery in the distillate, whereas the experimental recovery is only between 11% and 33%. This results reveals specific issues in data acquisition: for octan-1-ol, decan-1-ol, dodecan-1-ol, tetradecan-1-ol, hexyl ethanoate, 2-phenylethyl ethanoate and 3,7-dimethylocta-1,6-dien-3-ol, the deviations can be associated with a high incertitude of the chemical analysis, due to very low concentrations, smaller than the quantification GC limit in some cases (0.1 mg/L for these species). Concerning ethanal and butan-1-ol, even if the concentrations are not very low, the deviations are also linked to the analysis technique, because their quantification GC limits are particularly high (between 5.0 and 10.0 mg/L). In the case of octan-1-ol, decan-1-ol, dodecan-1-ol, tetradecan-1-ol and hexyl ethanoate, it should be pointed out that the interaction parameters of the NRTL model were estimated from UNIFAC predictions without validation against experimental data. This could be a source of error in simulation, however, the trend displayed in **Figure 5-8** (distillate recovery of 100% for volatile aroma compounds of similar nature) suggests that the origin of deviations are rather associated to experimental data.

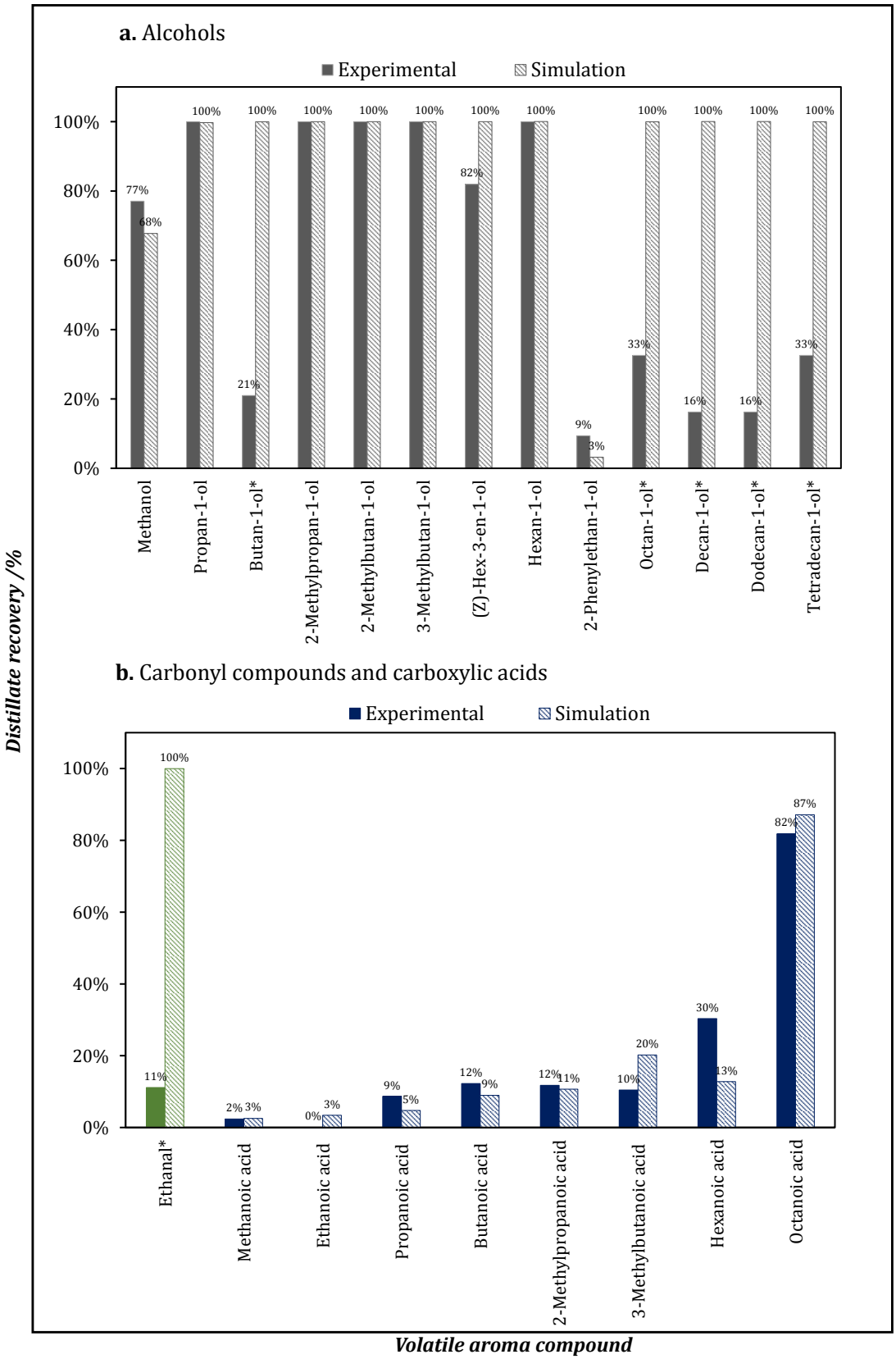

Figure 5-8. *Comparison between reconciled experimental and simulation data of the aroma compounds recovery in distillate at the nominal operation point. (*) Compounds with important deviations between experimental and simulation values.*

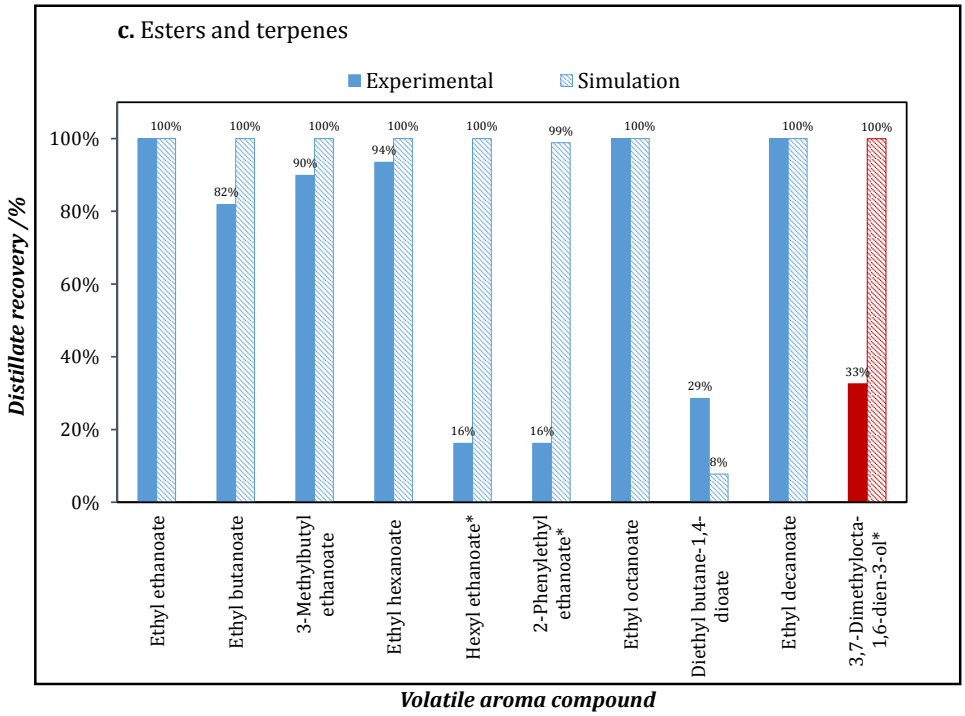

Continuation figure 5-8. *Comparison between reconciled experimental and simulation data of the aroma compounds recovery in distillate at the nominal operation point. (*) Compounds with important deviations between experimental and simulation values.*

A comparison with literature data is presented in **Table 5-12**. These data were acquired from distillation of 58 wine samples in 77 different distillation units. General good agreement is verified with experimental and simulation data from this work. Recoveries higher than 100% in the literature set are due to the combined effect of analysis errors and possible chemical reactions. Indeed, an important proportion of ethyl esters from fatty acids (ethyl hexanoate, ethyl octanoate and ethyl decanoate in this case) is released by heating of yeasts present in wine during distillation [Segur and Bertrand, 1992].

Table 5-12. *Comparison with literature data of the aroma compounds recovery in the distillate. The literature data are average values of 80 Armagnac distillates before aging. Taken from (Segur and Bertrand, 1992).*

Aroma compound	Recovery in distillate /%		
	Reconciled experimental	Simulation	Literature
Methanol	77%	68%	87%
Propan-1-ol	100%	100%	98%
2-Methylpropan-1-ol	100%	100%	105%
2-Methylbutan-1-ol	100%	100%	103%
3-Methylbutan-1-ol	100%	100%	101%
2-Phenylethan-1-ol	9%	3%	10%
Ethyl ethanoate	100%	100%	94%
3-Methylbutyl ethanoate	90%	100%	90%
Ethyl hexanoate	94%	100%	104%
Hexyl ethanoate	16%	100%	100%
2-Phenylethyl ethanoate	16%	99%	84%
Ethyl octanoate	100%	100%	203%
Ethyl decanoate	100%	100%	385%
Ethanoic acid	0%	3%	5%
Hexanoic acid	30%	13%	25%
Octanoic acid	82%	87%	75%

In the light of these results, the simulation module can be validated as a tool to represent the behavior of volatile aroma compounds in continuous Armagnac distillation, with both qualitative and quantitative precision for the estimation of distillate recoveries and good qualitative reproduction of concentrations in distillate and vinasse.

5.3.1.2.2. Classification of volatile aroma compounds

With the aim of identifying general trends on volatile aroma compounds behavior, a systematic classification is proposed. The criterion is based on phase equilibria and composition profiles. The first step was developed by the authors in a companion paper [Puentes et al, 2017]. The knowledge of vapor-liquid equilibria allows us to classify the volatile aroma compounds in three main groups, according to their relative volatilities with respect to ethanol (light key) and water (heavy key). The group I correspond to light compounds, species that are more volatile than ethanol and are therefore mainly recovered in distillate. The group II gathers the intermediary compounds, which are distributed between distillate and vinasse due to their intermediate volatilities. The group III correspond to heavy compounds, less volatile than ethanol and water, thus mainly recovered in the vinasse.

Table 5-13. *Classification of aroma compounds according to their relative volatility in two liquid composition intervals.*

$0.0<x_{Et}<1.0$ (Puentes et al., 2017)		**$0.0<x_{Et}<0.1$ (This work)**	
Group	**Compound**	**Group**	**Compound**
I. Light	Octan-1-ol	I. Light	Octan-1-ol
	Decan-1-ol		Decan-1-ol
	Dodecan-1-ol		Dodecan-1-ol
	Tetradecan-1-ol		Tetradecan-1-ol
	Ethanal		Ethanal
	Ethyl ethanoate		Ethyl ethanoate
	Ethyl butanoate		Ethyl butanoate
	Hexyl ethanoate		Hexyl ethanoate
II. Intermediary	Propan-1-ol		Propan-1-ol
	Butan-1-ol		Butan-1-ol
	2-Methylpropan-1-ol		2-Methylpropan-1-ol
	2-Methylbutan-1-ol		2-Methylbutan-1-ol
	3-Methylbutan-1-ol		3-Methylbutan-1-ol
	(Z)-Hex-3-en-1-ol		(Z)-Hex-3-en-1-ol
	Hexan-1-ol		Hexan-1-ol
	3-Methylbutyl ethanoate		3-Methylbutyl ethanoate
	Ethyl hexanoate		Ethyl hexanoate
	Ethyl octanoate		Ethyl octanoate
	Ethyl decanoate		Ethyl decanoate
	3,7-Dimethylocta-1,6-dien-3-ol		3,7-Dimethylocta-1,6-dien-3-ol
	Methanol	II. Intermediary	Methanol
	2-Phenylethan-1-ol		2-Phenylethan-1-ol
	Propanoic acid		Propanoic acid
	Butanoic acid		Butanoic acid
	2-Methylpropanoic acid		2-Methylpropanoic acid
	3-Methylbutanoic acid		3-Methylbutanoic acid
	Hexanoic acid		Hexanoic acid
	Octanoic acid		Octanoic acid
	2-Phenylethyl ethanoate		2-Phenylethyl ethanoate
	Diethyl butane-1,4-dioate		Diethyl butane-1,4-dioate
III. Heavy	Methanoic acid	III. Heavy	Methanoic acid
	Ethanoic acid		Ethanoic acid

This classification depends on the liquid composition interval. In **Table 5-13**, two classifications are proposed: one over the whole ethanol mole range ($0<x_{Et}<1$), proposed in the original paper, and another over the ethanol mol range of the liquid phase simulated in the distillation column of this work ($0<x_{Et}<0.1$). In the current case, 20 species are classified as light compounds, 10 as intermediary compounds and 2 as heavy compounds. Among light compounds, more than a half were classed as intermediary compounds when considering the whole concentration range, but their behavior changes since the relative volatilities with respect to ethanol are higher in the region of low ethanol concentration.

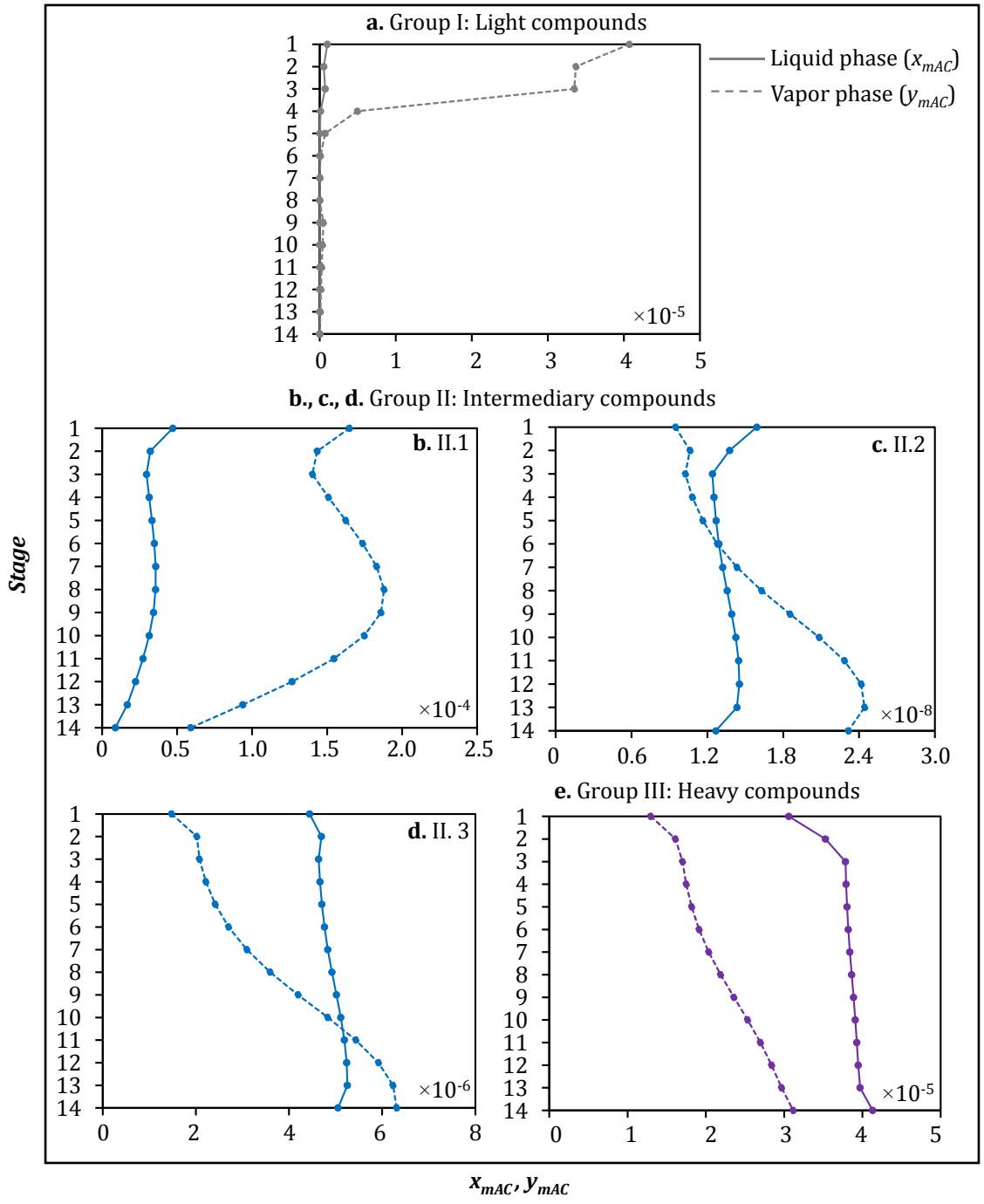

Figure 5-9. *Main types of composition profiles of aroma compounds through the distillation column.*

Now, using the simulation results, it is possible to identify different trends for the composition profiles inside the column. These trends are depicted in **figure 5-9**., where the mass fractions of volatile aroma compounds in the vapor and liquid phases are presented at the different stages of the column, from the partial condenser to the boiler. In the case of light compounds (**figure 5-9a**) and heavy compounds (**figure 5-9e**) the composition profiles are monotonous. A light compound is concentrated in the vapor phase while stripped from the liquid one. A heavy compound exhibits a behavior completely opposed, being concentrated in the liquid phase. On the other hand, a detailed analysis of the composition profiles for intermediary compounds evidences the existence of 3 different profiles: in the first profile, presented in **figure 5-9b**, there is a net concentration of the vapor and stripping of the liquid, but in comparison to the profile of light compounds, the ratio of vapor-liquid mass fraction is lower in every stage. In the second and third profile, depicted in **figure 5-9c** and **figure 5-9d**, the aroma compound is stripped in the vapor phase, to such an extent that the distillate mass fraction becomes smaller than the vinasse one. The differences between those two profiles are related to the profile shape and to the recovery levels of the aroma compound in the distillate.

In this way, a more precise classification of the intermediary compounds can be proposed by considering this difference of composition profiles. The resulting classification is comprised of the 3 groups proposed in the previous classification (I for light compounds, II for intermediary compounds and III for heavy compounds), with 3 new subcategories for intermediary compounds: II.1, II.2 and II.3. The description of each group is completed with some factors that characterize the separation, including: ratio of vapor-liquid mass fractions in every tray, recovery in distillate, profile shape, and variation of composition in both phases throughout the column. A final synthesis of this classification is presented in **table 5-14**.

Table 5-14. *Classification of aroma compounds according to the composition profile in the distillation column.*

Group	Profile type		Volatil roma compound	Ratio y_{mAC}/x_{mAC}		Distillate recovery(%)		Profile shape	Variation of concentration	
				Min	Max	Min	Max		Vapor phase	Liquid phase
Light	I	20	(Table 5-13)	3.8	>100	100%	100%	Monotonous	Concentration	Stripping
Intermediary	II.1	4	Methanol 3-methylbutanoic acid Octanoic acid 2-phenylethyl ethanoate	1.1	18	20%	99%	Concavity change	Net concentration	Net stripping
	II.2	4	Butanoic acid 2-methylpropanoic acid Hexanoic acid Diethyl butane-1,4-dioate	0.5	7.6	8%	13%	Concavity change	Net stripping	Net stripping
	II.3	2	2-Phenylethan-1-ol Propanoic acid	0.3	1.2	3%	5%	Monotonous	Stripping	No variation
Heavy	III	2	Methanoic acid ethanoic acid	0.4	0.8	3%	3%	Monotonous	Stripping	Concentration

5.3.2. VALIDATION OF THE SIMULATION OF HEADS AND TAILS EXTRACTION

The circuits of heads and tails extractions are used in spirits production to modify the distillate composition. As described in section 5.2.1 and shown in **figure 5-2**, both circuits are placed in the coil of the distillate flow inside the wine heater. The tails circuit enables the extraction of a fraction of liquid formed at the beginning of the vapor condensation. The extraction is done from the bottom of the first turn of the coil. In the heads circuit, a fraction of the remaining vapor is withdrawn over the last turn of the coil, before the cooling section. Both circuits are sent to the external compartment of the wine heater, in order to cool the extractions before evacuation from the device.

The simulation module was tested to reproduce the operation of both circuits, using a vapor-liquid flash for their modeling. Two specifications were considered to solve the problem: the ABV of the extraction, used to fix the refrigeration power required to condense a fraction of the vapor distillate, and the mass flow, used to verify the proportion distillate–extraction. The configuration of these theoretical circuits is presented **Figure 5-10**. Since the extractions are placed in the wine heater, mass and energy balances of the column are assumed to be invariable with respect to the nominal operation point.

a. Heads extraction

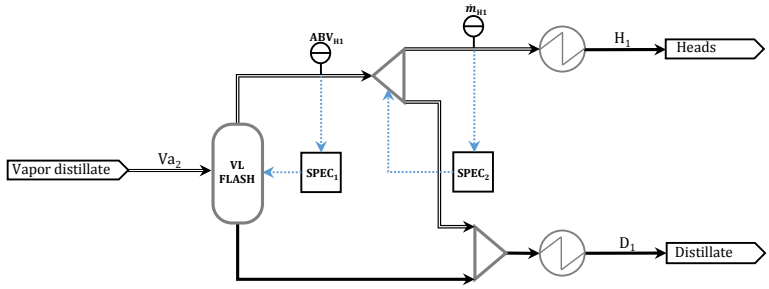

b. Tails extraction

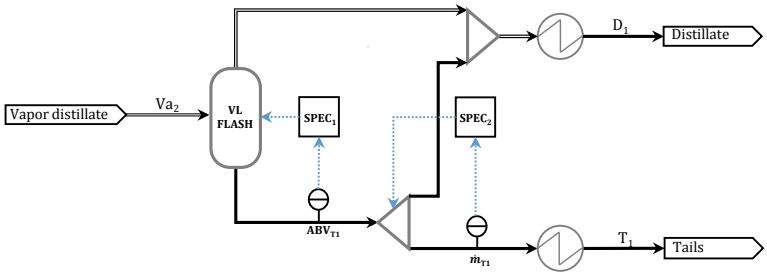

Figure 5-10. *Configuration for the simulation of a. heads and b. tails extractions. $SPEC_1$ and $SPEC_2$ are control loops to verify the respective experimental values of ethanol composition (ABV) and mass flow ($\dot{m}$) of the extraction.*

The data required for this simulation were acquired during the experimental campaign, just after characterization of the nominal operation point. Two independent experiments, one for each extraction, were carried out: the extraction valve was completely opened during 15 min. 5 min after opening, extraction and new distillate mass flows were measured using the same technique described in section 5.2.2.1. Each measurement was made in duplicate. Relative uncertainty for distillate was lower than 0.1% and about 2.3 % for heads and tails extractions. At the end of this period, liquid temperatures were measured, using the Pt100 probe for the extraction and the

mercury thermometer for the distillate after extraction. The ABV was also quantified with the DMA35 densitometer. Finally, a single 700 mL sample of each stream was taken for chemical analysis, following the methodology already described. After reconciliation, the ABV and mass flow were respectively 80.1 %v/v and 14.7 $kg.h^{-1}$ for heads extractions and respectively 40.3%v/v and 19.4 $kg.h^{-1}$ for tails extractions.

To analyze the performance of both circuits, an extraction coefficient is defined with respect to ethanol:

$$\epsilon_{AC/Et,e} = \frac{x_{mAC,\,e}/x_{mEt,\,e}}{y_{mAC,\,Va2}/y_{mEt,\,Va2}} \qquad [5.13]$$

Where $\epsilon_{AC,e}$ is the extraction coefficient of a volatile aroma compound in the circuit *e* (heads H_1 or tails T_1), $x_{mAC,\,e}$ and $x_{mEt,\,e}$ are the respective mass fractions of volatile aroma compound and ethanol in the extraction *e*, and $y_{mAC,\,Va2}$ and $y_{mEt,\,Va2}$ are the respective mass fractions in the stream Va_2, which corresponds to the vapor distillate before extraction. A value of $\epsilon_{AC/Et,\,e}$ higher than 1 indicates that the extraction of the aroma compound is favorable with respect to ethanol.

For the 3 groups of volatile aroma compounds proposed in the previous section, average values of $\epsilon_{AC,\,e}$ with their respective uncertainties are presented in **figure 5-11**. Only the volatile aroma compounds whose behavior was correctly validated against experimental data are considered. Concerning heads extraction, the extraction coefficients follow a decreasing trend from the light compounds (group I) to heavy compounds (group III). This trend is verified with both experimental and simulation data, except for the group III, for which the average experimental extraction coefficients are 0.6, against 0.2 from simulation. The inversed trend is identified for tails extraction. However, the discrepancy between experimental and simulation data is more pronounced. A detailed comparison by volatile aroma compound is presented in **Figure 5-12** for heads extractions and in **Fig 5-13** for tails extraction. The deviations between experimental and simulation data are very variable and may be attributed to sensitivity and accuracy issues of the analysis technique. Moreover, since the calculation of the extraction coefficients depends on two streams, extraction and distillate, the uncertainty of this variable can be amplified.

In relation to the role of each circuit, the trends identified by profile are logic in principle. While a heads circuit is due to extract very volatile species, in a tails circuit low volatile species that condense quickly should be evacuated. Nonetheless, in the heads circuit here simulated, the extraction coefficients for light compounds are close to 1 (group I, average between 1.3 and 1.0), which means that the distillate composition is modified but not in the desired way. A preferential passage of lights compounds with respect to ethanol, reflected in higher extraction coefficients, was expected. The results are more favorable for the tails circuits, particularly regarding simulation data, because the average extraction coefficients for intermediary (group II) and heavy compounds (group III) are considerably higher than 1, between 2.5 and 3.4. In this case, the extraction leads to a real modification of the distillate composition with elimination of the targeted species. For the group of compounds simulated, one can conclude that only the tails circuit works correctly in the installation. The heads circuit is probably not well placed. A different distribution of the volatile aroma compounds would be required to favors the preferential extraction of light compounds with respect to ethanol.

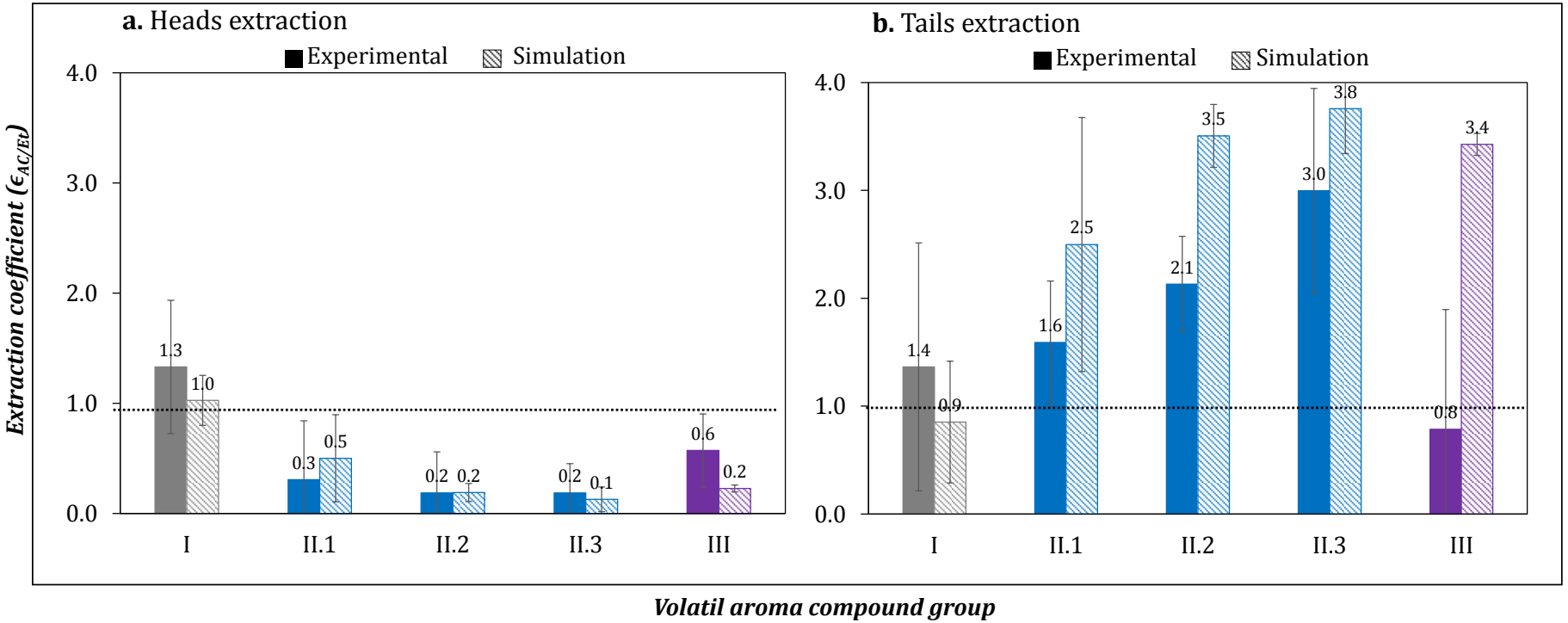

Figure 5-11. *Extraction coefficients of the volatile aroma compounds in a. heads circuit and b. tails circuit. Average experimental and simulation values for the different groups of volatile aroma compounds: light (I), intermediary (II) and heavy (III). In this simulation, the mass and energy balances of the column remains invariable with respect to the nominal operation point.*

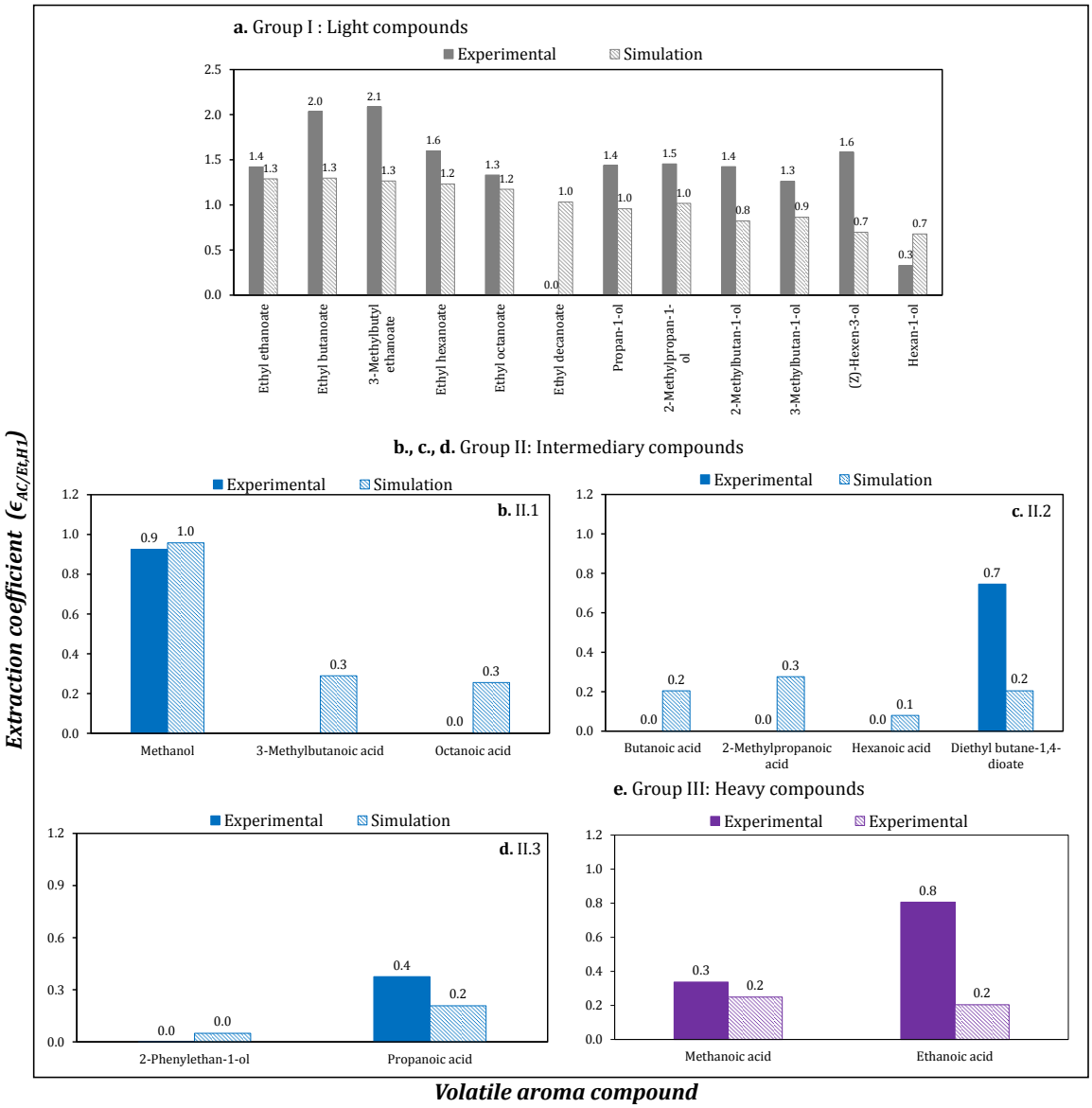

Figure 5-12. *Extraction coefficients of the volatile aroma compounds in heads circuit. Detailed experimental and simulation values for aroma compound, classified by volatility group. In this simulation, the mass and energy balances of the column remains invariable with respect to the nominal operation point.*

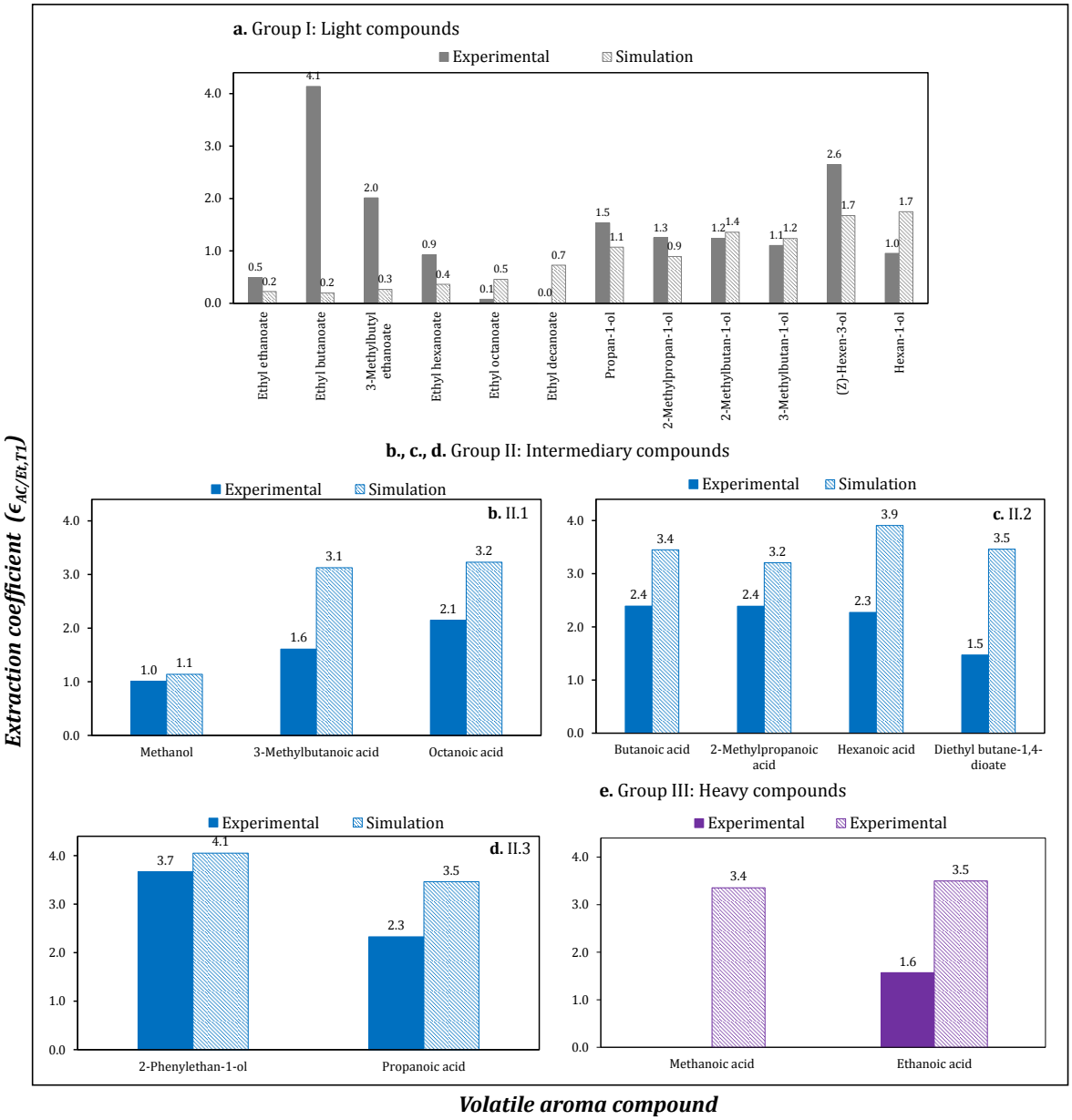

Figure 5-13. *Extraction coefficients of the volatile aroma compounds in tails circuit. Detailed experimental and simulation values for each compound, classified by volatility group. In this simulation, the mass and energy balances of the column remains invariable with respect to the nominal operation point.*

5.3.3. Analysis by simulation of the influence of operating parameters

After validation of the simulation in the nominal operation point, a parametric analysis was performed to study the influence of operating parameters on ethanol and volatile aroma compounds behavior. Again, only volatile aroma compounds whose representation was satisfactory regarding experimental data are considered.

5.3.3.1. Ethanol concentration in the distillate

Several authors have suggested an important influence of the distillate alcoholic strength on the separation of volatile aroma compounds. The simulation module was used to vary the ABV of

distillate between 52%v/v and 72%v/v, by modifying the reflux ratio through the condensation power, (**figure 5-14a**). For comparison purposes, the ethanol mass flow in the distillate was fixed to the nominal value in all the simulations (72.65 $kg.h^{-1}$). Therefore, to verify ethanol mass balance in the column, the net heating power in the boiler was modified using a specification loop. As expected, according to **figure 5-14b**, the evolution of ABV and mass flow with reflux ratio are inverse. The minimum ABV possible in this installation, obtained when the condensation is only generated by thermal losses ($\dot{Q}_C$=0.4 kW), is around 59% v/v. With respect to the nominal operation point, the condensation power must be doubled (from 11.6 kW to 23.4 kW) to increase the ethanol strength to 72%v/v. The net heating power is also increased but the variation is considerably lower, of 2.5% (from 88.5 kW to 90.8 kW).

In the case of volatile aroma compounds, the evolution of distillate partial mass flows with ABV are presented in **Figure 5-15**. Species from the group I (light compounds) are not affected by changes on the alcohol strength, a logic result because they are more volatile than ethanol and are integrally recovered in the distillate. For the other groups, the partial mass flow decreases when the ABV is increased. The variation is slight for intermediary compounds of the subcategory II.1, but the effect is pronounced for the subcategories II.2, and II.3 as well as heavy compounds, group III. The concentrations of volatile aroma compound in the distillate follow exactly the same evolution, as the ethanol mass flow in the distillate does not change. This behavior has already been discussed in the literature and demonstrates that the modification of operating parameters (condensation power in this case) do have an impact on the distillate composition. High concentrations of some intermediary and heavy compounds are favorable for aging purposes, due to their 'winey' character, but for young commercial spirits, without aging, their limitation in the distillate, and therefore operation at high reflux ratio, is recommended[Segur and Bertrand, 1992; Bertrand, 1998; Decloux and Joulia, 2008].

A comparison between simulation and literature data is given in **Figure 5-16**, where the concentration in absolute ethanol is presented as a function of distillate ABV. The trends obtained are the same: no variation for linear C_3-C_6 alcohols (from propan-1-ol to hexan-1-ol) as well as ethyl C_6-C_{10} esters (from ethyl hexanoate to ethyl decanoate) and significant reduction for 2-phenylethan-1-ol. The literature data for ethyl esters are slightly rising, but according to the authors, this is a bias provoked by experimental mass losses of ethanol at high ABV. For this latter group and 2-phenylethan-1-ol, the original concentrations (without the multiplication factors used exclusively for representation purposes) are different from the simulated values, but this can be explained simply by differences in wine composition. Despite those slight differences, this comparison validates simulation and demonstrates its utility in the analysis of operating parameters, with the benefit of both cost and time saving.

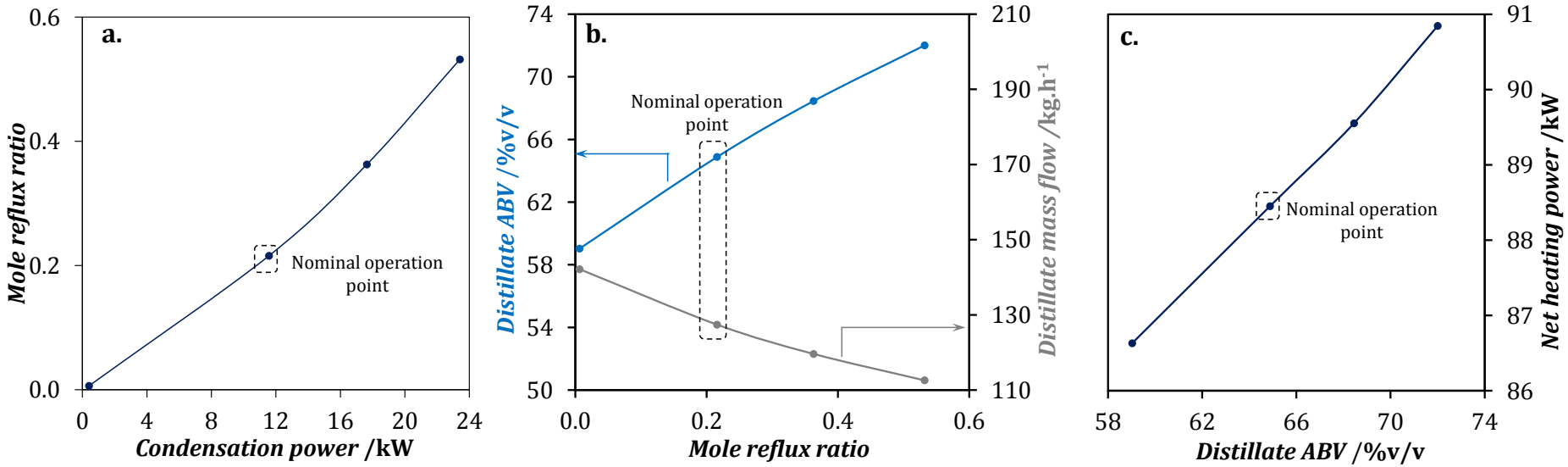

Figure 5-14 *a. Variation of reflux ratio with condensation power. b. Influence of reflux ratio on distillate ethanol concentration and mass flow. c. Influence of ethanol concentration on heat power. In these simulation, the ethanol mass flow in the distillate was fixed to the nominal point value.*

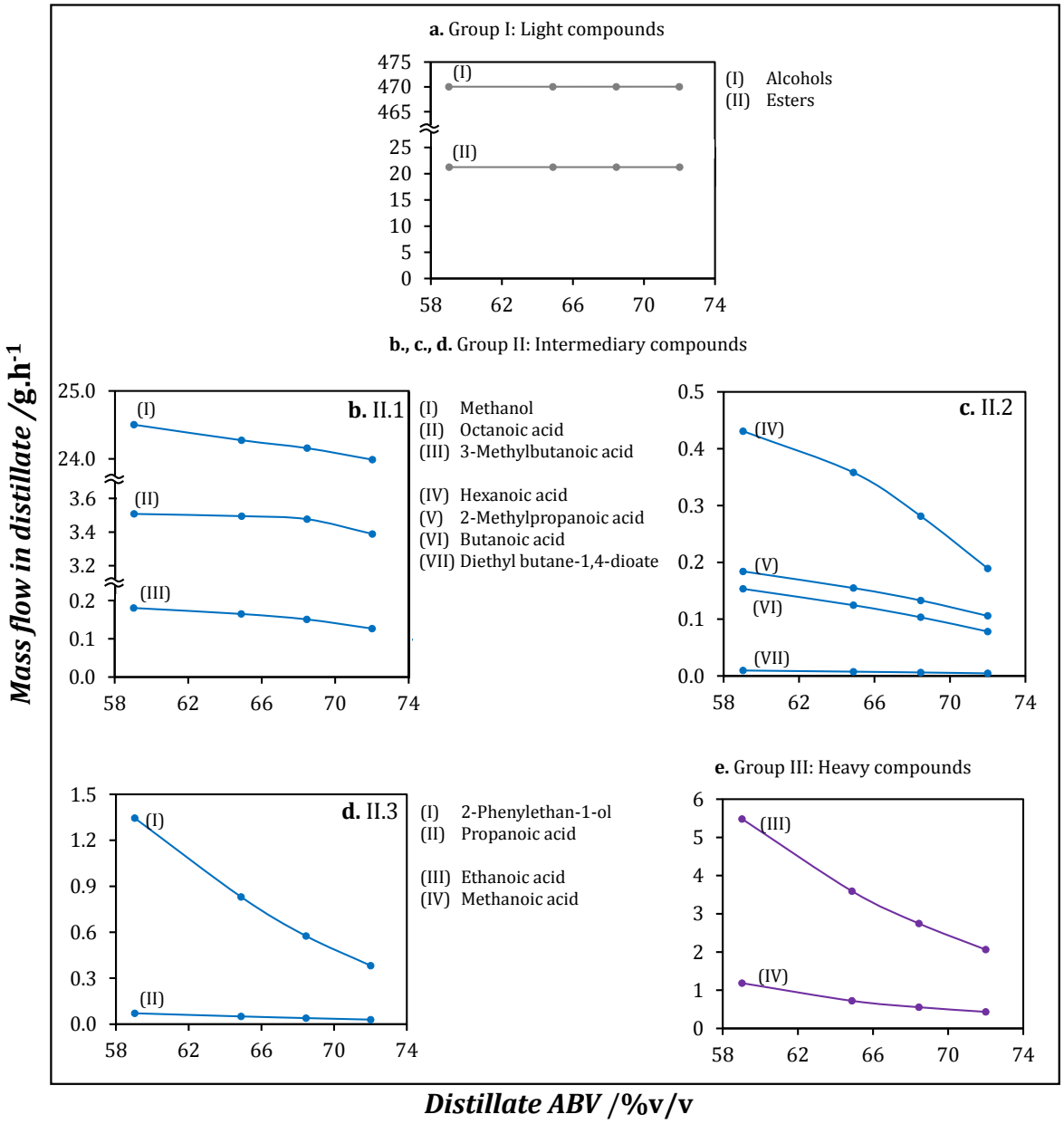

Figure 5-15. *Influence of ethanol concentration in the distillate on aroma compounds partial mass flows. In this simulation, the ethanol composition in distillate was modified with the reflux ratio, which was in turn modified with the condensation power. The ethanol mass flow in the distillate was fixed to the nominal point value.*

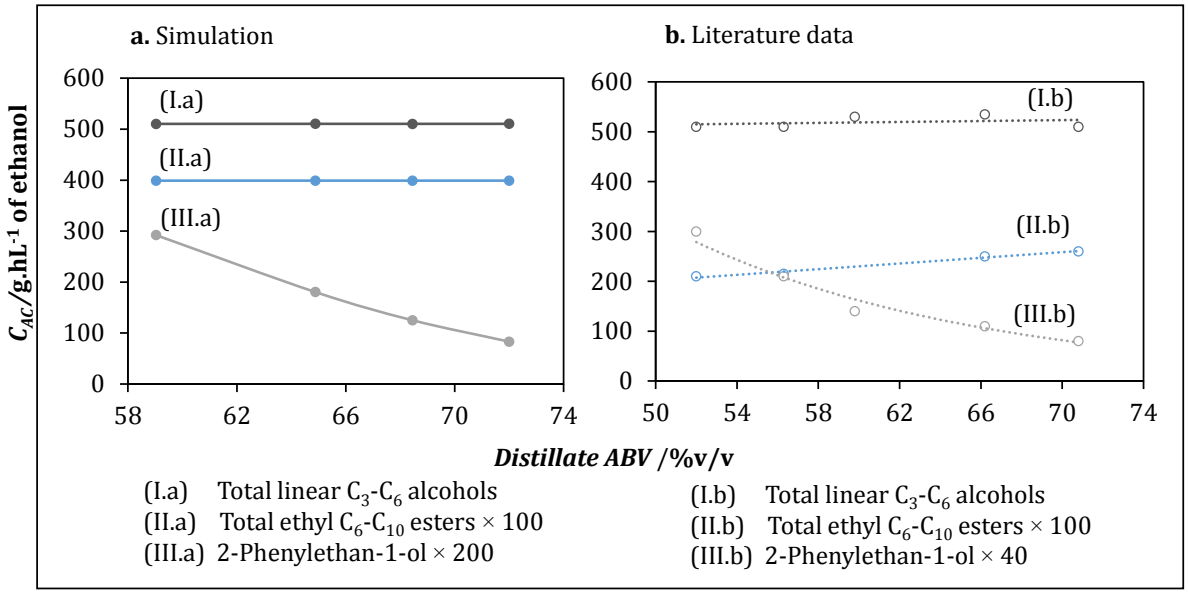

Figure 5-16. *Comparison with literature data of the aroma compounds concentration in the distillate as a function of the ethanol concentration. Literature data taken from (Segur and Bertrand, 1992).*

5.3.3.2. Thermal losses

Thermal losses through the column walls represent between 40% and 50% of total thermal losses in Armagnac distillation units [Ad3, 2010]. To analyze this parameter, three simulation scenarios were considered: the nominal operation as reference point (thermal losses of 2.8 kW), a point with minimal thermal losses, fixed at 0.4 kW (the contribution of thermal losses to condensation power) and a point with doubled losses, 5.6 kW. For these simulations, the ethanol losses in vinasse as well as the condensation power were fixed at the nominal values. The results displayed in **Figure 5-17**, show that the reduction of thermal losses has an antagonist impact, since both net heating power and distillate ABV decrease. The reduction of alcoholic strength confirms the reflux effect of thermal losses on the column. However, the variation are small with respect to the nominal point, 0.5% regarding ABV and 2.3% in the case of heating power.

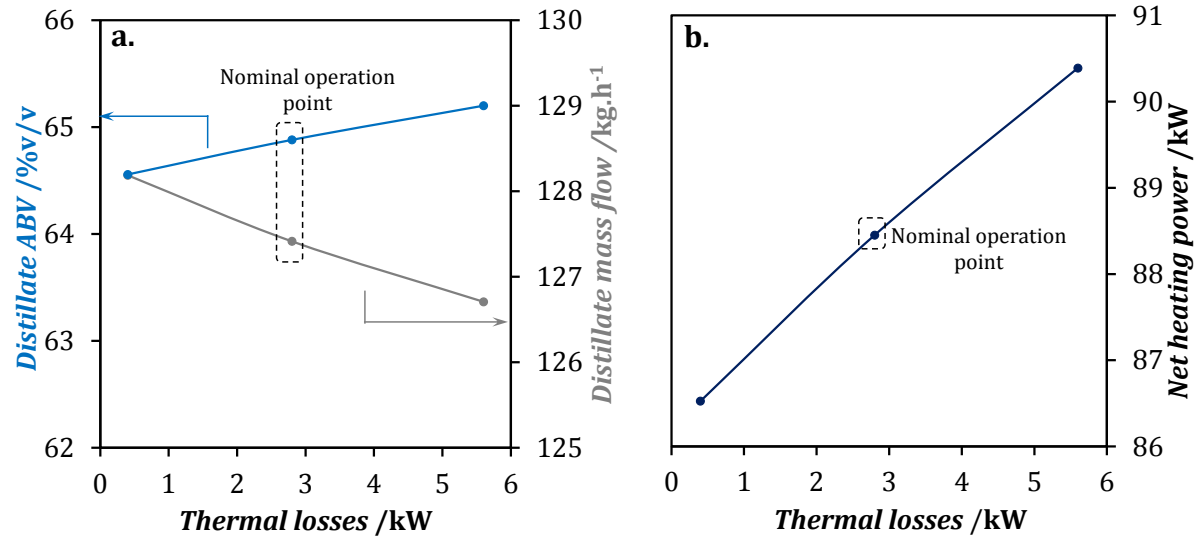

Figure 5-18. *Influence of heat losses on a. distillate ethanol composition and mass flow and, b. heat power. In this simulation, the ethanol losses in the bottoms as well as the condensation power were fixed at the nominal point values.*

Impact on distillate composition was also studied, but no significant variation of concentrations was detected for any of the aroma compounds groups. This result can be explained by the little variation of the distillate ABV and suggests, at least for the compounds here simulated, that the isolation of the distillation unit would not modify the spirit composition. In these conditions, isolation would be an advantaging solution to reduce energy consumption (about 2 kW) while maintaining both ethanol recovery and spirit composition. However, experimental validation would be still necessary to verify the real impact on product quality.

5.3.3.3. Distillate temperature after condensation

To conclude the analysis, a theoretical effect of the distillate temperature on the spirits composition was analyzed by means of the Simulis Thermodynamics® calculator. This parameter has a practical interest because the condensed distillate is directly exposed to the atmosphere during its evacuation, before storage. Using the NRTL model and the corresponding interaction parameters, the partial pressure of all the species were calculated at four temperatures, T=12 °C, T=15 °C, T=25 °C and T=28 °C. The composition of the liquid phase was fixed at the reconciled experimental set reported in this work. By defining the reference temperature as the lowest value (T=12 °C), the variations of partial pressure of the volatile aroma compounds due to temperature increases (25%, 108% and 133%) were calculated and compared to those of ethanol, equivalent to 21%, 119% and 159%.

The results are presented in **Table 5-15**. Two types of behavior can be identified, independent of the compounds classification: (i) increases of partial pressure with the same order of magnitude of ethanol increase (between 0.8 and 1.4 times in the case of methanol, propan-1-ol, 2-methylpropan-1-ol, methanoic acid, ethanoic acid, propanoic acid, ethyl ethanoate, ethyl butanoate, 3-methylbutyl ethanoate, ethyl hexanoate), and (ii) increases of partial pressure considerably higher than that of ethanol, between 1.4 and 2.8 times (case of 2-methylbutan-1-ol, 3-methylbutan-1-ol, (Z)-hex-3-en-1-ol, hexan-1-ol, 2-phenylethan-1-ol, 2-methylpropanoic acid, butanoic acid, 3-methylbutanoic acid, hexanoic acid, octanoic acid, ethyl octanoate, ethyl decanoate, diethyl butane-1,4-dioate). The second behavior, associated with non-linear (2-phenylethan-1-ol for instance) or high molar mass molecules, suggests that it is possible to entail a preferential evacuation of these molecules to the atmosphere, whose effect is all the more relevant when the distillate temperature is higher.

Table 5-15. *Theoretical variation of the partial pressure of aroma compounds with the cooling temperature of distillate.*

Group	Compound	Mass fractions in liquid distillate	Partial pressure at T_0=12 °C /kPa	Increase of partial pressure /%		
				T_f=15 °C	T_f=25 °C	T_f=28 °C
				ΔT=3°C (25%)	ΔT=13°C (108%)	ΔT=16°C (133%)
	Ethanol	0.57	3.32	21%	119%	159%
	Water	0.43	0.74	22%	127%	171%
I	Ethyl ethanoate	1.3×10^{-4}	4.43×10^{-3}	18%	99%	130%
	Ethyl butanoate	2.4×10^{-6}	6.50×10^{-5}	18%	97%	128%
	Propan-1-ol	1.2×10^{-4}	3.51×10^{-4}	23%	139%	189%
	2-Methylpropan-1-ol	9.4×10^{-4}	1.92×10^{-3}	26%	163%	223%
	2-Methylbutan-1-ol	5.2×10^{-4}	1.48×10^{-4}	33%	231%	329%
	3-Methylbutan-1-ol	2.1×10^{-3}	9.71×10^{-4}	32%	216%	303%
	(Z)-Hex-3-en-1-ol	2.2×10^{-6}	6.26×10^{-7}	29%	191%	266%
	Hexan-1-ol	1.1×10^{-5}	1.93×10^{-6}	36%	253%	362%
	3-Methylbutyl ethanoate	4.5×10^{-6}	3.39×10^{-5}	22%	128%	172%
	Ethyl hexanoate	5.8×10^{-6}	4.71×10^{-5}	23%	137%	185%
	Ethyl octanoate	1.3×10^{-5}	7.56×10^{-6}	31%	207%	290%
	Ethyl decanoate	1.0×10^{-5}	5.65×10^{-7}	40%	298%	434%
II.1	Methanol	2.2×10^{-4}	1.84×10^{-3}	19%	103%	137%
	3-Methylbutanoic acid	6.7×10^{-7}	5.19×10^{-8}	31%	205%	287%
	Octanoic acid	2.6×10^{-5}	5.50×10^{-7}	39%	299%	438%
II.2	2-Methylpropanoic acid	1.3×10^{-6}	2.84×10^{-7}	30%	198%	276%
	Butanoic acid	1.3×10^{-6}	1.76×10^{-7}	29%	185%	257%
	Hexanoic acid	6.7×10^{-6}	5.55×10^{-8}	39%	294%	430%
	Diethyl butane-1,4-dioate	2.2×10^{-7}	7.64E-09	39%	287%	416%
II.3	2-Phenylethan-1-ol	1.9×10^{-5}	6.71×10^{-8}	39%	295%	430%
	Propanoic acid	7.2×10^{-7}	2.51×10^{-7}	26%	165%	227%
III	Methanoic acid	5.3×10^{-6}	1.15×10^{-5}	19%	106%	141%
	Ethanoic acid	1.1×10^{-7}	1.31×10^{-7}	22%	126%	170%

This result should not be overestimated as it is derived only from theoretical calculations. In general, to define the real impact of distillate temperature and other operating parameters on product quality, it would be necessary to integrate simulation with sensory and olfactometric analysis, which would allow a better understanding of the specific role of each compound, and its concentration, on the organoleptic properties of spirits.

5.4. Conclusions

In this work, a module for the simulation of spirits distillation at steady state was developed and validated using the commercial software ProSimPlus®. A thorough analysis of an industrial unit for Armagnac production was performed, considering a model solution composed by ethanol, water and 32 volatile aroma compounds that have an impact on product quality.

Comparison with experimental data confirmed that the simulation is able to reproduce the right orders of magnitude of the volatile aroma compound concentrations and to predict with good precision the recovery from wine to distillate. High deviations for this latter parameter were identified in a group of nine compounds, which is attributed to errors in chemical analysis that conducted to incoherent mass flows, even after data reconciliation. The technique employed, gas chromatography, is very sensitive and has a limited accuracy due to the system complexity and the great variety of factors involved, including sample preparation and instrumentation. More powerful methods should be used to get better estimations. However, the gain in accuracy may

imply an important increase of technical complexity, which is not strictly desirable for a simulation approach, aimed for better yet faster process design.

Simulation of the extraction circuits proves that only the tails circuit favors the elimination of intermediary and heavy species with respect to ethanol. Through the heads circuit is possible to evacuate light compounds. However, for the group of compounds simulated in this work, the performance of the circuit is not adequate, since the average extraction coefficient for the group of light compounds is close to 1. If possible, this circuit should be placed in another position, in order to have a different distribution of light compounds between the coexisting vapor and liquid phases.

The analysis of operating parameters proved that the distillation process can modify the distillate composition. Two parameters were identified to have a real impact: ethanol concentration and distillate temperature after condensation. The increase of alcoholic strength, by modification of the condensation power, leads to a reduction of the concentration of intermediary and heavy compounds in the distillate. Concerning the temperature after condensation, the composition modification is based on a preferential elimination of non-linear and high mass molar species towards the environment. On the other hand, thermal losses have a slight effect on distillate ethanol concentration. However, at the concentration levels here evaluated, the effect on volatile aroma compounds can be neglected.

These results demonstrate that simulation is a powerful tool to better understand and predict the behavior of volatile aroma compounds in spirits distillation. The real aim is not to reproduce with high accuracy the experimental data (whose uncertainties may be important) but to represent correctly the distillation trends and, in this way, analyze the impact of operating parameters on product quality and process performance. Further results of our ongoing research on Armagnac and Calvados distillation will be reported in a future work.

However, it is important to conclude that the concrete improvement of product quality goes beyond process engineering, and requires the coupling of simulation with complementary scientific tools such as reaction chemistry, sensory and olfactometric analysis.

ACKNOWLEDGMENTS

This work was supported by the ABIES Doctoral School (AgroParisTech, Université Paris-Saclay) and was implemented within the framework of the RMT FIDELE (Réseau Mixte Technologique Produits fermentés et distillés), with funding from the French Association ACTIA (Association de coordination technique pour l'industrie agroalimentaire). The authors are grateful to Marie-Claude Segur, for advisory and support during the experimental campaign in Armagnac, and to the UNGDA staff, particularly Stephane Couturier, for the technical support during the samples analysis. They also wish to thank Silvère Massebeuf from ProSim, for his assistance with ProSimPlus®.

CHAPITRE 6. SYNTHESE DES RESULTATS ET PERSPECTIVES

Cette thèse de doctorat a été dédiée à l'application de la simulation numérique dans l'étude du comportement des composés volatils d'arôme lors de la distillation continue des eaux-de-vie. Dans ce dernier chapitre, un rappel des objectifs du doctorat et de la démarche mise en œuvre est proposé, suivi d'une synthèse des résultats développés dans les chapitres 2 à 5, concernant l'acquisition de données d'équilibre liquide–vapeur et la simulation d'une unité de distillation en régime stationnaire. Les contributions et les perspectives qui émergent de ces travaux sont synthétisées à la fin de ce chapitre.

6.1. Rappel des objectifs du doctorat et de la demarche mise en œuvre

Cette thèse de doctorat a été menée dans le cadre d'une allocation de recherche attribuée par l'école doctorale ABIES de l'Université Paris-Saclay. L'ensemble du travail est le résultat d'une étroite collaboration entre différents centres de recherche (UMR GENIAL - Massy, LGC - Toulouse, UCP – Palaiseau, UMR GMPA - Grignon), la société de logiciels de simulation ProSim, le laboratoire d'analyse UNGDA et des producteurs du domaine des eaux-de-vie, représentés par les centres techniques des filières Armagnac, Calvados et Cognac.

Les composés volatils d'arôme sont responsables de la qualité des eaux-de-vie. Leur présence et concentration dépendent de la nature de la matière première et évoluent au cours des différentes phases de fermentation, distillation et vieillissement. Les objectifs du doctorat étaient de contribuer à la compréhension du comportement des composés volatils d'arôme lors de la phase de distillation et de fournir des bases scientifiques à la conduite des unités par le biais de modules de simulation.

La démarche de recherche mise en œuvre a compris : la sélection des composés volatils d'arôme à suivre, l'acquisition des données d'équilibre liquide–vapeur de ces composés en milieu hydroalcoolique, la sélection et caractérisation précise des conditions de fonctionnement des unités de distillation, la création et validation des modules de simulation et enfin, l'analyse de l'influence de paramètres opératoires sur le comportement des composés volatils d'arôme. Dans ces travaux, l'attention a été portée sur la distillation d'Armagnac et de Calvados dans des colonnes multiétagées en régime stationnaire. Les modules de simulation ont été construits avec le logiciel ProSimPlus®.

Après la présentation du cadre théorique et de la description détaillée de la démarche de recherche dans le **chapitre 1**, le cœur des travaux a été divisé en deux grandes parties :

- Acquisition de données d'équilibre liquide-vapeur pour l'identification du modèle thermodynamique permettant leur représentation analytique dans le logiciel de simulation. Cette partie comprend les **chapitres 2**, **3** et **4**, dans lesquels sont décrites les trois approches d'acquisition proposées : recherche dans la littérature, détermination expérimentale et prédiction théorique.
- Construction et validation des modules de simulation en régime stationnaire, à partir des informations issues de la caractérisation expérimentale des unités de distillation et de l'identification du modèle thermodynamique. Cette partie est développée dans le **chapitre 5** pour une unité de production d'Armagnac.

Une synthèse générale des résultats obtenus dans chaque partie et des perspectives identifiées est développée ci-après.

6.2. SYNTHESE DES RESULTATS

6.2.1. ACQUISITION DES DONNEES D'EQUILIBRE POUR L'IDENTIFICATION DU MODELE NRTL

Quatre-vingt-cinq (85) composés volatils d'arôme appartenant à différentes familles chimiques (acétals, alcools, composés carbonylés, acides carboxyliques, esters, furanes, terpènes et norisoprénoïdes) ont été répertoriés. Ces composés sont présents dans toutes les matrices d'eaux-de-vie françaises (Armagnac, Calvados et Cognac) et ont un impact sur la qualité du produit.

En considérant les conditions de distillation et la nature chimique du système étudié, une approche hétérogène a été sélectionnée pour le calcul des équilibres entre phases. La phase vapeur est considérée comme un gaz parfait, tandis que le comportement non idéal de la phase liquide est représenté au moyen du modèle NRTL pour le calcul des coefficients d'activité. Ce modèle est recommandé dans la littérature pour l'étude des mélanges hydroalcooliques. Concernant les acides carboxyliques, une correction a été appliquée pour tenir compte des phénomènes d'association chimique dans la phase vapeur.

Dans ce contexte, l'identification du modèle thermodynamique revient à l'estimation des paramètres d'interaction binaire du modèle NRTL à partir de données d'équilibre liquide–vapeur à pression atmosphérique. Trois types d'interaction binaire ont été considérés : éthanol–eau, composé volatil d'arôme–éthanol et composé volatil d'arôme–eau. Les interactions entre composés volatils d'arôme ont été négligées car ces espèces sont présentes en faibles concentrations dans la matrice éthanol–eau. Par ailleurs, les paramètres d'interaction du binaire éthanol–eau ont été pris de la littérature et validés sur plusieurs jeux de données d'équilibre de référence. Pour sa part, la détermination des paramètres associés aux binaires composé volatil d'arôme–éthanol et composé volatil d'arôme–eau, a nécessité la connaissance de données d'équilibre des composés d'arôme en milieu hydroalcoolique à faible concentration.

Trois approches complémentaires ont été mises en œuvre pour l'acquisition de ces données : recherche dans la littérature, détermination expérimentale et enfin prédiction au moyen des modèles d'activité UNIFAC et COSMO.

En premier lieu, l'approche de recherche dans la littérature, traitée dans le **chapitre 2**, a permis l'acquisition des données d'équilibre liquide–vapeur pour 43 composés volatils d'arôme, provenant de 9 références publiées entre 1960 et 2012. La synthèse est complétée avec les données d'équilibre du 2-hydroxypropanoate d'éthyle (lactate d'éthyle), déterminées expérimentalement dans cette thèse selon la méthodologie présentée dans le chapitre 3. Les informations compilées sont de nature très variable, incluant : des données de composition et de température à l'équilibre, des données de volatilités absolue et relative et enfin des modèles empiriques de volatilité relative en fonction de la fraction molaire en éthanol dans la phase liquide. Dans tous les cas, les mesures reposent sur deux méthodes dynamiques de mise à l'équilibre : avec recirculation unique de la phase vapeur ou avec recirculation des phases liquide et vapeur. Pour la plupart des composés étudiés, les volatilités absolues et relatives diminuent avec la concentration en éthanol dans la phase liquide en équilibre. Sauf pour certaines espèces, dont le méthanol, l'éthanal, l'acide méthanoïque et l'acide éthanoïque, l'évolution de la volatilité

relative par rapport à l'éthanol est légèrement croissante sur tout l'intervalle de composition en éthanol.

Dans la procédure d'identification, la fonction objectif a été écrite en termes de volatilité relative par rapport à l'éthanol. Ce choix se justifie pour deux raisons : (i) la volatilité relative synthétise toutes les informations sur la distribution des composés volatils d'arôme entre les phases liquide et vapeur et (ii) l'éthanol est le composé majoritaire du distillat par rapport auquel la séparation des composés minoritaires est évaluée. Les jeux de paramètres obtenus sont rassemblés dans le **Tableau 2-4**. Les écarts entre les données expérimentales et calculées par le modèle varient entre 1% et 30% pour les volatilités absolues et relatives. Seulement dans le cas de l'hexan-1-ol les écarts des volatilités absolue et relative par rapport à l'eau sont légèrement supérieurs, de l'ordre de 33%. Ces écarts d'erreur restent acceptables en considérant la variabilité de sources d'information utilisées ainsi que la complexité dans la détermination des grandeurs à l'équilibre, du fait de la faible concentration des composés volatils dans la matrice hydroalcoolique.

A partir du modèle NRTL, un classement des composés volatils suivant leurs volatilités relatives par rapport à l'éthanol et l'eau a été proposé sur tout l'intervalle de composition en éthanol dans la phase liquide ($0<x_{Et}<1$). Le résultat est présenté dans le **Tableau 2-5**. Selon cette classification, 10 composés sont toujours plus volatils que l'éthanol (composés légers), 2 sont toujours moins volatils que l'eau (composés lourds) et 32 présentent des volatilités intermédiaires entre l'éthanol et l'eau (composés intermédiaires). Les composés intermédiaires constituent la catégorie la plus importante en distillation, en raison de leur distribution entre le distillat et le résidu. Une description précise des équilibres entre phases devient particulièrement importante pour représenter correctement leur séparation par simulation numérique.

L'analyse des données d'équilibre issues de la littérature a été conclue par une comparaison de la qualité de leur représentation par le modèle NRTL avec trois types jeux de paramètres : (i) les paramètres estimés directement à partir de ces données, où le composé volatil d'arôme est à faible concentration (jeu identifié dans le chapitre 2 comme NRTL-0), (ii) les paramètres estimés au moyen des données d'équilibre des systèmes binaires indépendants composé volatil d'arôme–éthanol et composé volatil d'arôme–eau (identifiés comme le jeu NRTL-B) et (iii) les paramètres estimés à partir des données des systèmes ternaires composé volatil d'arôme–éthanol–eau (jeu identifié comme NRTL-T), dans lesquels le composé volatil d'arôme peut couvrir toute la gamme de concentration, de 0 à 1. Les résultats de la comparaison, appliquée à 9 composés est présentée dans le **Tableau 2-10**. Comme il pouvait être attendu, la meilleure représentation des données à faible concentration est obtenue avec le jeu de paramètres NRTL-0. Toutefois, l'intérêt de cette comparaison a été de montrer qu'une première identification du modèle thermodynamique peut être faite à partir de données qui se trouvent plus facilement dans la littérature. Ainsi, en l'absence de données d'équilibre d'un composé volatil d'arôme à faible concentration en milieu hydroalcoolique, la première option conseillée pour l'estimation des paramètres d'interaction du modèle NRTL est d'utiliser, si elles existent, des données publiées pour les binaires composé volatil d'arôme–éthanol et composé volatil d'arôme–eau, cas où le composé volatil d'arôme couvre toute la gamme de concentration. La validité de ces paramètres peut être jugée en fonction de la qualité de la simulation par rapport aux données expérimentales récoltées dans les unités de distillation.

Il convient d'indiquer que la sélection des données d'équilibre rapportées dans le chapitre 2 a été réalisée sans suivre une méthodologie précise de cohérence thermodynamique. Les paramètres d'interaction ont été estimés après l'élimination des données considérées comme aberrantes. Néanmoins, le critère d'élimination n'a été basé que sur la tendance globale des données par rapport aux compositions molaires d'éthanol dans la phase liquide. A notre connaissance, des tests particuliers de cohérence thermodynamique adaptés à la nature et à la complexité du système étudié (mélange multiconstituants avec différentes espèces à faible concentration) n'ont pas encore été développés. Pour les objectifs de cette étude, la cohérence intrinsèque du modèle NRTL s'est avérée satisfaisante pour la validation des données. Par la suite de ces travaux, il serait intéressant d'approfondir cette notion de cohérence thermodynamique et de concevoir des tests spécifiques reposant sur la relation de Gibbs-Duhem, dans le but d'éviter la validation de données erronées mais également l'invalidation de données cohérentes.

En deuxième lieu, l'approche de détermination expérimentale des données d'équilibre a fait l'objet du **chapitre 3.** La méthodologie a été illustrée pour le lactate d'éthyle, ester majoritaire qui agit comme stabilisateur et masqueur d'arômes, mais dont l'impact peut devenir négatif à des concentrations élevées. Les données ont été mesurées à l'aide du Labodest VLE 602™, appareil déjà utilisé dans d'autres études concernant des composés volatils d'arôme en milieu hydroalcoolique. Le dispositif opère selon une méthode dynamique avec recirculation des phases vapeur et liquide, stratégie qui réduit le temps de mise à l'équilibre par rapport à la recirculation unique de la phase vapeur. Deux critères ont été utilisés pour garantir l'équilibre : stabilité de la température, atteinte au bout de 30 min de recirculation, et stabilité de la composition du composé volatil d'arôme, obtenue deux heures après stabilisation de la température. Des échantillons de liquide et de vapeur condensée ont été prélevés pour quantifier la distribution du lactate d'éthyle. La composition en éthanol a été estimée au travers des mesures de températures, toujours en supposant que l'effet du lactate d'éthyle (à faible concentration) sur l'équilibre thermique du système est négligeable. Pour sa part, la composition en lactate d'éthyle a été déterminée par chromatographie en phase gazeuse couplée à un détecteur par ionisation de flamme, avec comme étalon interne le butan-1-ol.

Dix-sept points expérimentaux ont été déterminés en suivant cette méthodologie. Les résultats indiquent que la volatilité du lactate d'éthyle est décroissante avec la teneur en éthanol dans la phase liquide. Bien que ce composé soit toujours moins volatil que l'éthanol, la phase vapeur est plus concentrée en lactate d'éthyle que la phase liquide dans la région riche en eau ($0<x_{Et}<0.1$). Pour l'estimation des paramètres d'interaction binaire, deux formulations de fonction objectif ont été testées, une écrite en termes de volatilités absolues et une deuxième en termes de volatilités relatives par rapport à l'éthanol. Dans les deux cas, des facteurs de pondération inversement proportionnels aux incertitudes des mesures expérimentales ont été considérés. D'autre part, deux modèles de calcul de coefficients d'activité ont été étudiés, NRTL et UNIQUAC. Reposant sur le même principe de composition locale non aléatoire, le but était de vérifier que la représentation obtenue avec les deux était globalement de même qualité. Les jeux de paramètres calculés sont rassemblés dans le **Tableau 3-8**. Par rapport aux données expérimentales, la qualité de la représentation est globalement meilleure à partir des paramètres estimés avec la fonction objectif écrite en termes de volatilités relatives par rapport à l'éthanol. Avec ces jeux de paramètres, une

comparaison plus fine montre que la représentation du modèle NRTL, avec écarts de l'ordre de 10,1%, est légèrement plus précise que celle du modèle UNIQUAC, avec des écarts de l'ordre de 10,7%.

L'étude a été conclue par une comparaison avec des paramètres issus de données des systèmes binaires lactate d'éthyle–éthanol et lactate d'éthyle–eau. Ces informations sont disponibles dans la littérature pour le modèle UNIQUAC. La représentation obtenue suit le même comportement que les données expérimentales pour toutes les variables analysées (coefficient d'activité, volatilités et constante d'Henry). Néanmoins les écarts sont plus importants que ceux obtenus avec les paramètres identifiés directement à partir de nos données expérimentales. Ce résultat est cohérent avec les conclusions du chapitre 2**.** Le jeu de paramètres du modèle NRTL déterminé à partir de la fonction objectif basée sur les volatilités relatives par rapport à l'éthanol, est finalement conseillé pour la simulation du comportement du lactate d'éthyle en distillation. Ce jeu a été intégré dans la synthèse bibliographique du chapitre 2.

En troisième lieu, l'approche prédictive, présentée dans le **chapitre 4**, a été proposée comme une alternative à l'acquisition de données expérimentales d'équilibre, couteuse en temps et ressources matérielles et humaines. En effet, la distribution d'un composé volatil d'arôme entre les phases liquide et vapeur peut être prédite sans passer par l'étape expérimentale à partir des modèles thermodynamiques comportant des paramètres universels, de telle sorte qu'aucune identification spécifique ne soit nécessaire.

La méthodologie de calcul a été appliquée à l'étude du lactate d'éthyle. Deux modèles d'estimation de coefficients d'activité ont été évalués : le modèle UNIFAC dans ses versions 1975 et 1993, et le modèle COSMO-SAC dans ses versions 2002, 2006, 2010 et 2014. Le but était de valider la capacité prédictive des modèles par comparaison à des données expérimentales d'incertitude connue. Afin de se focaliser sur la prédiction des propriétés du composé volatil d'arôme à l'équilibre, le comportement du binaire éthanol–eau a été fixé à sa représentation par modèle NRTL. Ainsi, sous l'hypothèse de dilution infinie, aussi vérifiée avec les modèles prédictifs, les coefficients d'activité ont été estimés à la composition expérimentale du binaire éthanol – eau dans la phase liquide et à la température de bulle correspondante, calculée par le modèle NRTL.

Les résultats obtenus montrent que les écarts entre les valeurs prédites par le modèle COSMO-SAC et les données expérimentales sont globalement plus faibles (entre 11% et 39%) que ceux associés au modèle UNIFAC (entre 33% et 329%). Ce résultat est cohérent en considérant la nature chimique du lactate d'éthyle ainsi que la formulation plus rigoureuse des modèles de type COSMO. La version COSMO-SAC 2014 présente la meilleure capacité prédictive, avec des écarts entre 11% et 16% pour les coefficients d'activité et les volatilités du lactate d'éthyle. Ce modèle est donc conseillé pour la prédiction des équilibres liquide–vapeur des composés d'arôme de nature similaire (hydroxyle esters) en milieu hydroalcoolique.

Deux perspectives découlent des travaux sur l'acquisition des données d'équilibre liquide–vapeur avec les trois approches présentées. La première, portant sur la troisième approche, consiste à mener une validation des modèles prédictifs avec un nombre plus important de molécules. Le but est d'évaluer leur capacité prédictive pour ensuite établir des recommandations permettant un choix adapté du modèle, basé par exemple sur la nature chimique des molécules ou sur leurs

volatilités. Une partie importante de ce travail a déjà été réalisé pour un groupe supplémentaire de 34 composés, identifié dans le **Tableau 1-1** (comportant 1 acétal, 10 alcools, 6 composés carbonylés, 7 acides carboxyliques, 6 esters, 1 furane et 2 terpènes). Les résultats seront présentés dans un article supplémentaire en cours de préparation.

La deuxième perspective concerne la génération de données pour les composés répertoriés dans cette thèse, mais dont aucune information d'équilibre n'est disponible. L'approche préconisée pour leur génération est au travers de l'utilisation de modèles prédictifs. La validation des données prédites sera basée directement sur les résultats de la simulation, après estimation des paramètres d'interaction respectifs. Si les données d'équilibre des systèmes binaires composé volatil d'arôme – éthanol et composé volatil d'arôme–eau sont disponibles, il convient également de les utiliser pour une première estimation des paramètres d'interaction et de valider ceux-ci par simulation. En dernier lieu, si la validation par simulation n'est pas satisfaisante dans les étapes précédentes, il faudra avoir recours à la détermination expérimentale des données d'équilibre. Les modèles prédictifs peuvent être utilisés dans ce cas pour définir les limites maximales de dilution infinie, afin de faciliter le dosage du composé volatil d'arôme dans les phases en équilibre.

Les composés volatils d'arôme concernés par cette deuxième perspective sont rassemblés dans le **Tableau 6-1.** Il s'agit de 41 espèces appartenant à toutes les familles étudiées. Pour la génération des données d'équilibre, il conviendrait de suivre l'ordre de priorité suivante :

- en premier lieu les composés dosés à l'UNGDA et présents dans la base de données de ProSimPlus® (20 composés),
- ensuite les composés dosés mais devant être ajoutés à la base de données, après recherche des paramètres des composés purs et établissement d'une loi de pression de vapeur (17 composés),
- enfin les composés non dosés à l'UNGDA mais disponibles dans la base de données (4 composés).

L'étude du dernier groupe de 4 composés (comprenant le pentan-1-ol, le méthanal, l'acide pentanoïque et le méthanoate d'éthyle) reste optionnelle, car leur suivi dans les courants de procédé à simuler impliquerait soit un travail analytique supplémentaire (ajout dans les protocoles d'analyse de l'UNGDA ou développement de nouvelles méthodes de quantification) soit la réalisation des analyses dans un autre laboratoire.

Tableau 6-1. *Classement de composés volatils d'arôme pour la génération de nouvelles données d'équilibre liquide–vapeur.*

Priorité	Famille chimique	Composé volatil d'arôme
1. Composés dosés à l'UNGDA et disponibles dans la base de données de ProSim®	Alcools	Butan-2-ol
		Heptan-2-ol
		Octan-1-ol
		Decan-1-ol
		Dodecan-1-ol
		Tetradecan-1-ol
	Acides carboxyliques	Acide 2-hydroxypropanoïque
		Acide decanoïque
		Acide dodecanoïque
		Acide tetradecanoïque
		Acide hexadecanoïque
		Acide (9Z,12Z,15Z)-9,12,15-octadecatrienoïque
		Acide (9Z,12Z)-9,12-octadecadienoïque
		Acide (9Z)-octadec-9-enoïque
		Acide octadecanoïque
	Esters	Butanoate d'éthyle
		Ethanoate de hexyle
	Furanes	Furan-2-carboxylate d'éthyle
	Terpènes	2-(4-methyl-1-cyclohex-3-enyl)propan-2-ol
2. Composés dosés à l'UNGDA mais non disponibles dans la base de données de ProSim®	Acetals	1,1,3-Triethoxypropane
	Acides carboxyliques	Acide (9Z)-hexadec-9-enoïque
	Esters	Ethanoate de (Z)-hexen-3-yle
		Octanoate de 3-methylbutyle
		Dodecanoate d'éthyle
		Octanoate de 2-phenylethyle
		Tetradecanoate d'éthyle
		Dodecanoate de 3-methylbutyle
		Hexadecanoate d'éthyle
		(9Z,12Z,15Z)-9,12,15-octadecatrienoate d'éthyle
		(9Z,12Z)-9,12-octadecadienoate d'éthyle
		(9Z)-octadec-9-enoate d'éthyle
		Octadecanoate d'éthyle
	Terpènes	(Z)-3,7,11-Trimethyl-1,6,10-dodecatrien-3-ol
		(E)-3,7,11-Trimethyl-1,6,10-dodecatrien-3-ol
	Norisoprénoïdes	1,1,6-trimethyl-1,2-dihydronaphthalene
		(E)-1-(2,6,6-trimethyl-1-cyclohexa-1,3-dienyl)but-2-en-1-one
3. Composés non dosés à l'UNGDA mais disponibles dans la base de données de ProSim®	Alcools	Pentan-1-ol
	Composés carbonylés	Méthanal
	Acides carboxyliques	Acide pentanoïque
	Esters	Méthanoate d'éthyle

6.2.2. VALIDATION DES MODULES DE SIMULATION DES UNITES DE DISTILLATION CONTINUE

La deuxième partie des travaux de recherche a porté sur la construction et la validation des modules de simulation. Pour cela, quatre éléments sont indispensables : (i) le diagramme de procédé de l'unité, (ii) les propriétés physicochimiques des composés purs, (iii) les paramètres du modèle thermodynamique et (iv) les spécifications de fonctionnement de l'unité. Le **chapitre 5** est consacré aux travaux de simulation pour l'unité de distillation d'Armagnac de l'atelier Janneau. Le module de simulation a été utilisé pour analyser l'influence de divers paramètres opératoires sur la composition du distillat.

D'une manière générale la démarche suivie pour la construction du module de simulation intègre les étapes suivantes :

- Sélection et description de l'unité de distillation : pour le repérage des circuits et l'établissement du diagramme de procédé.
- Acquisition et réconciliation des données : pour la validation des bilans matière et énergie, ainsi que la détermination des spécifications de fonctionnement, données d'entrée du module de simulation.

  Les données sont récoltées lors d'une campagne expérimentale dans l'unité sélectionnée et comprennent : (i) mesures des débits (massiques ou volumiques) et des températures des différents courants du procédé à l'aide de capteurs non-intrusifs, (ii) prélèvement des échantillons pour le dosage de l'éthanol, par densimétrie électronique (après distillation par entrainement à la vapeur dans le cas des échantillons d'alimentation et résidu) puis des composés volatils d'arôme par chromatographie en phase gazeuse couplée à une détecteur par ionisation de flamme. 66 espèces, appartenant à 7 familles chimiques, sont suivies dans cette étude.

  Une technique de réconciliation statistique des données a été appliquée pour l'établissement des bilans, permettant la définition d'un point nominal d'opération cohérent. Pour l'unité étudiée, les valeurs réconciliées des débits massiques et de la concentration en éthanol se sont avérées cohérentes avec les mesures expérimentales. Les corrections appliquées aux compositions des composés volatils d'arôme ont été plus importantes mais elles restent acceptables, compte tenu des incertitudes liées aux techniques analytiques et l'occurrence de réactions chimiques, non prises en compte dans le module de simulation.
- Sélection et identification du modèle thermodynamique : cette étape correspond à la première partie des travaux de recherche, focalisée sur l'estimation des paramètres d'interaction binaire du modèle NRTL.
- Configuration du module de simulation : ce qui comprend la sélection du modèle de distillation, l'introduction des paramètres du modèle NRTL et des spécifications de fonctionnement, requises pour saturer les degrés de liberté du problème de simulation. En régime stationnaire, les paramètres de fonctionnement sélectionnés incluent : caractéristiques géométriques de la colonne (nombre de plateaux, position du plateau d'alimentation et pertes de charge), alimentation (débit, température, pression et composition), pertes thermiques par plateau, puissance de condensation et débit de distillat. L'efficacité de plateau a été ajustée afin de vérifier les compositions en éthanol des courants de sortie (distillat et résidu), mesurées expérimentalement.

Deux niveaux de simulation ont été réalisés, un premier niveau pour le binaire éthanol-eau et un deuxième intégrant les composés volatils d'arôme. 32 des 66 composés d'arôme, dosés à l'UNGDA et dont les données d'équilibres liquide-vapeur étaient disponibles, ont été simulés. Ce groupe contient 13 alcools, 1 composé carbonylé, 8 acides, 9 esters et 1 terpène.

Pour le point nominal d'opération, les résultats de la simulation de l'unité d'Armagnac montrent que le profil de concentration en éthanol est très différent de celui d'autres installations (par exemple, de production de Vodka et d'alcool surfin), puisque le distillat est extrait sous forme de vapeur et le nombre de plateaux de concentration est réduit (deux au maximum). La simulation met également en évidence que les pertes thermiques à travers les parois augmentent le reflux interne dans la colonne, généré sur chaque plateau par condensation d'une fraction de la phase vapeur.

Concernant les composés volatils d'arôme, leur comportement est dans l'ensemble bien représenté et pour la plupart, le taux de récupération dans le distillat obtenu par simulation est cohérent avec l'information expérimentale. Cependant, des écarts non négligeables avec les données expérimentales ont été constatés pour 9 composés, à savoir : butan-1-ol, octan-1-ol, decan-1-ol, dodecan-1-ol, tetradecan-1-ol, éthanal, ethanoate d'hexyle, ethanoate de 2-phenyléthyle et 3,7-dimethylocta-1,6-dien-3-ol (linalool). Ces différences peuvent être dues à des problèmes de dosage ou à la fiabilité contestable des paramètres d'interaction binaire. Le dernier cas concerne notamment les composés octan-1-ol, decan-1-ol, dodecan-1-ol, tetradecan-1-ol et ethanoate d'hexyle, dont les paramètres ont été identifiés à l'aide des prédictions du modèle UNIFAC, sans validation préalable avec des informations expérimentales. Plusieurs solutions peuvent être proposées pour pallier ce problème : en premier lieu, la répétition des analyses des 9 composés concernés, afin de vérifier qu'il n'y a pas eu un problème ponctuel de dosage. Si les résultats de la simulation restaient insatisfaisants, il serait alors nécessaire soit de changer de méthode d'analyse soit de vérifier leur dosage dans un autre laboratoire. Enfin, si ces actions sur le plan analytique n'étaient pas probantes, il faudrait envisager l'acquisition de nouvelles données d'équilibre, par voie prédictive ou par voie expérimentale comme dernière alternative. Dans ce dernier cas, le design expérimental (concrètement la définition de la limite maximale de dilution infinie) pourrait être optimisé avec les prédictions des modèles UNIFAC et COSMO.

Grâce à la connaissance acquise sur les volatilités relatives par rapport à l'éthanol et à l'eau, les composés volatils d'arôme ont pu être classifiés en trois groupes : (i) composés légers, récupérés dans le distillat, (ii) composés intermédiaires, se répartissant entre le distillat et le résidu et (iii) composés lourds, récupérés pour l'essentiel dans le résidu. Cette classification dépend de l'intervalle de concentration en éthanol dans la phase liquide. Le **Tableau 5-11**, reprend la classification présenté dans la chapitre 2, appliquée à tout l'intervalle de concentration en éthanol dans la phase liquide ($0<x_{Et}<1$), et propose une nouvelle classification dans le domaine de la distillation de l'Armagnac, cas où cet intervalle est plus de réduit ($0<x_{Et}<0,1$).

L'étude du comportement en distillation a permis d'affiner le classement des composés intermédiaires en trois catégories supplémentaires selon leur profil de concentration dans la

colonne et leurs taux de récupération dans le distillat. Le **Tableau 5-12** présente les caractéristiques des différents groupes de composés volatils d'arôme.

Dans le but de disposer d'un outil de compréhension du comportement des composés volatils d'arôme en fonction des conditions de distillation, une analyse de l'influence de divers paramètres opératoires a été menée pour conclure cette étude. Les paramètres ont été choisis en fonction des besoins des industriels et comprennent : la mise en place des extractions de têtes et de queues, la teneur en éthanol dans le distillat, les pertes thermiques et la température de coulage du distillat après condensation. En distillation d'Armagnac, la simulation a mis en évidence que la modification de certaines conditions opératoires a une véritable influence sur composition du distillat. Parmi les paramètres étudiés, l'augmentation de la teneur en éthanol dans le distillat, ainsi que l'extraction de queues, favorisent la séparation préférentielle de composés d'arôme de volatilité faible ou intermédiaire. Un calcul théorique a également permis de constater l'influence de la température de coulage sur l'élimination de composés volatils d'arôme non linéaires ou de masse molaire plus élevée que celle de l'éthanol.

La simulation a montré que les pertes thermiques par les parois de la colonne modifient la teneur en éthanol du distillat, mais l'effet sur le groupe de composés volatils d'arôme étudié est plutôt négligeable. D'autre part, il a été constaté que le circuit d'extraction de têtes permet d'évacuer des composés volatils légers. Toutefois, pour le groupe de composés simulés, cette séparation n'est pas sélective par rapport à l'éthanol. Pour un meilleur fonctionnement, il faudrait modifier l'emplacement de l'extraction afin d'avoir une distribution différente des composés volatils présents dans la vapeur en cours de condensation.

L'ensemble des résultats sur la simulation de la distillation ouvrent de nombreuses perspectives. En premier lieu, la construction des modules de simulation pour d'autres unités de distillation continue, avec des configurations et/ou des matières premières différentes. Ces travaux sont déjà avancés pour les deux unités supplémentaires traitées au cours de cette thèse, à savoir l'unité d'Armagnac de la distillerie CPR et l'unité de Calvados de la distillerie Préaux. Les résultats seront présentés dans un article qui sera préparé prochainement. D'autre part, l'étude par simulation pourrait être complétée par l'analyse de l'influence d'autres paramètres opératoires sur la composition du distillat. Ces paramètres devront être définis selon les besoins des industriels et comprennent, entre autres, la puissance de chauffe, le débit de l'alimentation et sa composition. Le débit définit la capacité de la colonne. Une augmentation importante pourrait détériorer l'efficacité des plateaux et donc affecter le rendement de la distillation. La composition de l'alimentation influe également sur les limites de la séparation dans une unité de structure fixée.

L'approche de simulation pourrait être étendue à la distillation discontinue. Bien que la construction et la résolution des modules soient plus complexes, du fait de l'évolution des propriétés au cours du temps, leur application s'avérerait extrêmement utile, non seulement pour maîtriser les coupes et les éventuels recyclages, mais plus largement pour comprendre les différences avec la distillation continue, en termes de séparation des composés volatils d'arôme. Un projet parallèle portant sur le suivi de la distillation de Cognac par simulation est en cours dans l'UMR GENIAL. Ce projet reprend les paramètres d'interaction binaire du modèle NRTL issus

de cette thèse, ainsi que la méthodologie expérimentale de traitement et d'analyse des échantillons du procédé. Les résultats seront présentés dans un article en cours de préparation.

Sur les aspects méthodologiques de la simulation, il pourrait être intéressant d'effectuer une analyse de sensibilité des résultats de la simulation par rapport aux paramètres d'interaction binaire du modèle NRTL. Cela permettrait de chiffrer le degré de confiance à accorder aux grandeurs clefs de la distillation (dont la composition du distillat, le profil de température et la consommation énergétique) et par conséquent de vérifier la validité des paramètres d'interaction pour le suivi de l'impact sur ces grandeurs sur les conditions opératoires de la distillation. Une autre proposition serait d'ajouter la contrainte du bilan énergie dans la réconciliation des données. Au vu des limitations en instrumentation, cette alternative s'avère pertinente pour tenir compte des erreurs associées aux mesures de température sur les surfaces des canalisations. La seule limitation est que la réconciliation deviendrait plus complexe sur le plan numérique. Finalement, il pourrait être utile de valider expérimentalement les profils de concentration des composés volatils d'arôme dans les colonnes de distillation. Ce travail apporterait des informations essentielles pour un ajustement plus fin de l'efficacité de Murphree, laquelle peut varier non seulement entre plateaux mais également entre les constituants du mélange. Néanmoins l'exécution d'un tel travail est compliquée dans ce domaine, car la plupart des colonnes ne disposent pas de points de prélèvement pour l'analyse de l'éthanol et des composés d'arôme.

Concernant l'identification du modèle NRTL, il serait pertinent d'introduire la volatilité relative par rapport à l'eau dans la formulation de la fonction objectif utilisée pour l'estimation des paramètres d'interaction binaire. Jusqu'à présent, seule la volatilité relative par rapport à l'éthanol a été considérée. Cependant, une représentation plus précise des données d'équilibre aux fins de simulation dans le domaine des eaux-de-vie nécessiterait la prise en compte directe de l'eau. Cela se justifie d'une part car dans le classement des composés volatils d'arôme, l'eau est un composé de référence (la clef lourde) et d'autre part, car la simulation a mis en évidence que l'eau est toujours le composé majoritaire dans la phase liquide à l'intérieur de la colonne d'Armagnac, avec des fractions molaires comprises entre à 0,9 et 1,0.

Des perspectives encore plus ambitieuses pourraient aussi être envisagées sur le long terme. Cela comprend la prise en compte des réactions chimiques pour la construction des modules de simulation couplant distillation et réaction. Des travaux sur la réactivité chimique en distillation de Cognac sont en cours dans les UMR GENIAL et GMPA. Les résultats sont principalement de type qualitatif, mais ils apportent des pistes pour une étude plus approfondie des cinétiques de réaction. En outre, il serait intéressant d'intégrer l'étude de nouvelles familles ayant un impact organoleptique sur les eaux-de-vie. Cela comprend entre autres les composés soufrés et les pyrazines. Les limitations principales d'un tel travail restent liées à la disponibilité des données d'équilibre liquide–vapeur et aux méthodes d'analyse quantitative.

D'autres propositions comprennent le développement de modules de simulation dynamique pour l'élaboration rationnelle de stratégies de contrôle-commande ainsi que l'utilisation en ligne des modules en régime stationnaire pour l'optimisation des conditions opératoires du procédé. Sur

ce dernier point, le logiciel ProSimPlus® dispose des algorithmes destinés à la solution des problèmes d'optimisation pour des systèmes de structure fixée. Un meilleur fonctionnement des unités de distillation pourrait être ainsi conçu afin d'assurer la stabilité en termes de qualité et débit de l'eau-de-vie, d'augmenter le rendement et de minimiser les coûts opératoires.

Finalement, les modules de simulation constitueraient un moyen efficace et rapide pour tester des voies de fonctionnement réduisant la consommation de ressources, dont l'eau de refroidissement du distillat et l'énergie fournie aux bouilleurs. Un tel développement ferait de la simulation un véritable outil d'ingénierie dans le domaine des eaux-de-vie, permettant aux producteurs de faire face aux enjeux du développement durable du XXI^{ème} siècle, avec une réduction de l'impact environnemental du procédé de fabrication.

6.3. SYNTHESE DES CONTRIBUTIONS ET PERSPECTIVES

Ce doctorat a permis de revisiter l'opération de distillation des eaux-de-vie dans une optique de simulation des procédés. Les résultats démontrent que les modules de simulation constituent un outil performant pour une meilleure compréhension et maîtrise du comportement des composés volatils d'arôme. Dans ce domaine, il n'est pas nécessaire de reproduire parfaitement les données expérimentales, celles-ci portant un niveau d'incertitude non négligeable, mais de représenter correctement les tendances de la séparation, pour pouvoir ainsi analyser l'impact des paramètres opératoires sur la composition du produit et sur la performance du procédé.

Les contributions concrètes des travaux de recherche sont les suivantes :

- *Compilation des données d'équilibre liquide–vapeur rapportées dans la littérature pour les composés volatils d'arôme à faible concentration en milieu hydroalcoolique*. Génération d'un jeu cohérent de paramètres d'interaction du modèle NRTL pour 44 composés, adapté aux fins de simulation numérique. Les résultats de cette synthèse montrent également qu'en absence de données d'équilibre à faible concentration, celles des binaires composé volatil d'arôme–éthanol et composé volatil d'arôme–eau pourraient être utilisées pour une première estimation des paramètres d'interaction. Leur fiabilité pourra être jugée par rapport aux résultats de la simulation.
- *Mesures expérimentales des données d'équilibre liquide–vapeur du lactate d'éthyle*. Les mesures ont été réalisées à l'aide de l'appareil Labodest VLE 602™, reposant sur une méthode dynamique de recirculation des phases liquide et vapeur. Le dosage du composé d'arôme a été assuré par chromatographie en phase gazeuse. Outre que la méthodologie développée est fiable et rigoureuse, elle est extensible à tout composé volatil d'arôme d'intérêt dans les eaux-de-vie. Les aspects à adapter concernent les niveaux de concentration des solutions mises à l'équilibre, le choix de l'étalon interne et le système de détection couplé à la chromatographie.
- *Evaluation des modèles UNIFAC et COSMO pour la prédiction des données d'équilibre liquide–vapeur du lactate d'éthyle*. La comparaison des modèles montre que les modèles COSMO-SAC sont mieux adaptés à la description de l'équilibre du lactate d'éthyle en milieu hydroalcoolique. La méthodologie proposée est extensible à tout composé volatil d'arôme dans le domaine des pressions proches de la pression atmosphérique. Elle permet également

de vérifier l'hypothèse de dilution infinie, utilisée dans l'identification des paramètres du modèle NRTL.

- *Construction et validation de modules de simulation d'unités de distillation en régime stationnaire.* Le module de simulation a été appliqué avec succès à l'étude du comportement de 32 composés volatils d'arôme dans une unité de distillation d'Armagnac. Une première classification de ces composés a été proposée en fonction de leurs volatilités relatives. Pour les composés de volatilité intermédiaire, trois catégories supplémentaires ont été identifiées selon les profils de concentration dans la colonne et les taux de récupération dans le distillat. De plus, la simulation a permis d'identifier trois paramètres opératoires permettant une séparation sélective de certains composés de volatilité intermédiaire et faible, par rapport à l'éthanol. Ces paramètres sont : la teneur en éthanol dans le distillat, l'extraction de queues et la température de coulage du distillat. L'approche développée est applicable à toute unité de distillation continue et l'analyse paramétrique peut être adaptée aux spécificités de chaque procédé.

Les perspectives ouvertes à ce travail ont été déjà présentées en détail dans ce chapitre. Ici elles sont hiérarchisées en fonction de leur priorité et/ou faisabilité :

- Evaluation de la capacité prédictive des modèles UNIFAC et COSMO pour un groupe représentatif de composés volatils d'arôme. Etablissement des recommandations pour un choix de modèle adapté, en s'appuyant sur la nature des composés ou leur volatilité.
- Comparaison de différentes unités de distillation en régime stationnaire, avec des configurations ou matières premières différentes.
- Analyse de l'influence d'autres paramètres opératoires, dont la puissance de chauffe, le débit de l'alimentation et sa composition.
- Développement des modules de simulation pour la distillation discontinue, appliqués à la production de Cognac.
- Génération de nouvelles données d'équilibre liquide–vapeur par voie prédictive ou expérimentale pour le groupe de composés répertoriés.
- Développement d'une méthodologie spécifique de validation de la cohérence thermodynamique des données expérimentales d'équilibre des composés volatils d'arôme à faible concentration en milieu hydroalcoolique.
- Estimation de paramètres d'interaction binaire du modèle NRTL en utilisant une fonction objectif écrite en termes de volatilités relatives par rapport à l'éthanol et à l'eau.
- Analyse de sensibilité des paramètres d'interaction NRTL sur la performance de la simulation.
- Réconciliation des données expérimentales avec inclusion de la contrainte du bilan énergie.
- Validation expérimentale des profils de composition dans la colonne.
- Prise en compte des réactions chimiques pour la construction de modules avec couplage distillation–réaction.
- Etude de nouvelles familles de composés volatils d'arôme ayant un impact organoleptique, notamment les composés soufrés et les pyrazines.
- Simulation dynamique du procédé pour l'élaboration de stratégies de contrôle-commande.

- Optimisation en ligne du fonctionnement des unités afin de maximiser le bénéfice, tout en respectant les contraintes de qualité et débit des eaux-de-vie.
- Optimisation énergétique pour la réduction de l'impact environnemental de la distillation.

Une partie importante des travaux associés aux deux premières perspectives a déjà été effectuée, mais le temps a manqué pour les synthétiser dans ce manuscrit. Cependant, ils seront valorisés ultérieurement sous la forme d'articles. Concernant la distillation discontinue, des travaux sur la distillation de Cognac sont en cours dans l'UMR GENIAL et seront aussi divulgués dans un article en cours de préparation. Les connaissances développées permettraient aux différentes filières des eaux-de-vie de confronter leur maîtrise des méthodes de production utilisées.

A l'issue de ces travaux de recherche, il convient de conclure que le génie des procédés ne peut dévoiler tous les *secrets* de la distillation des eaux-de-vie. Néanmoins, il constitue un outil performant pour mieux comprendre le comportement des composés volatils d'arôme et pour améliorer la conduite des unités de distillation. Une réelle maîtrise de la qualité des eaux-de-vie nécessite l'intégration de la simulation des procédés avec d'autres outils scientifiques comme la chimie réactionnelle, nécessaire pour mieux décrire toutes les transformations chimiques au cours de la distillation, ainsi que les analyses sensorielle et olfactométrique, clefs pour élucider la synergie entre la composition du produit, ses propriétés organoleptiques et les préférences des consommateurs.

REFERENCES BIBLIOGRAPHIQUES

Abrams, D.S., Prausnitz, J.M., 1975. Statistical thermodynamics of liquid mixtures: A new expression for the excess Gibbs energy of partly or completely miscible systems, *AIChE J.* 21, 116-128.

AD'3E, 2010. Diagnostic énergétique dans l'Armagnac. Synthèse audit énergétique.

Alessi, P., Fermeglia, M., Kikic, I., 1991. Signficance of dilute regions. *Fluid Phase Equilib.* 70, 239-250.

Allen, G., Caldin, E.F., 1953. The association of carboxylic acids. Q. Rev. Chem. Soc. 7, 255-278.

Amer, H.H., Paxton, R.R., Van Winkle, M., 1956. Methanol-Ethanol-Acetone. *Ind. Eng. Chem.* 48 (1), 142–146. In: Ohe, S., 1989. Vapor-liquid equilibrium data. Kodansha, Tokyo.

Anderson, T.F., Prausnitz, J.M., 1978. Application of the UNIQUAC Equation to Calculation of Multicomponent Phase Equilibria. 1. Vapor-Liquid Equilibria. *Ind. Eng. Chem. Process Des. Dev.* 17, 552-561.

Andiappan, A. N., McLean, A. Y., 1972. Prediction of isobaric vapor-liquid equilibrium data for mixtures of water and simple alcohols. *Adv. Chem. Ser.* 115, 93. In: ThermoData (TDE) Version 3.0, 2008. NIST Standard Reference Database.

Aparicio, S., Alcalde, R., 2009a. The green solvent ethyl lactate: an experimental and theoretical characterization, *Green Chem.* 11, 65-78.

Aparicio, S., Alcalde, R., 2009b. Insights into the Ethyl Lactate + Water Mixed Solvent, *J. Phys. Chem.* B 113, 14257-14269.

Aparicio, S., Halajian, S., Alcalde, R. García, B. Leal, J.M., 2008. Liquid structure of ethyl lactate, pure and water mixed, as seen by dielectric spectroscopy, solvatochromic and thermophysical studies, *Chem. Phys. Lett.* 454 49-55.

Apostolopoulou, A.A., Flouros, A.I., Demertzis, P.G., Akrida-Demertzi, K., 2005. Differences in concentration of principal volatile constituents in traditional Greek distillates. *Food Control*, 16, 157-164.

Arce, A., Martinez-Ageitos, J., Soto, A., 1996. VLE for water + ethanol + 1-octanol mixtures. Experimental measurements and correlations. *Fluid Phase Equilib.* 122, 117-129.

Ashour, I., Aly, G., 1996. Effect of computation techniques for equation of state binary interaction parameters on the prediction of binary VLE data. *Computers Chem. Eng.* 20 (1), 79-91.

Athes, V., Lillo, M.P.I., Bernard, C., Perrez-Correa, R., Souchon, I., 2004. Comparison of Experimental Methods for Measuring Infinite Dilution Volatilities of Aroma Compounds in Water/Ethanol Mixtures. *J. Agric. Food Chem*. 52, 2021–2027.

Athès, V.; Paricaud, P.; Ellaite, M.; Souchon, I.; Fürst, W. Vapour–liquid equilibria of aroma compounds in hydroalcoholic solutions: Measurements with a recirculation method and modelling with the NRTL and COSMO-SAC approaches. 2008. *Fluid Phase Equilib.* 265, 139-154.

Baburao, B., Visco, D.P., 2011. Methodology for the Development of Thermodynamic Models Describing Substances that Exhibit Complex Association Interactions. *J. Chem. Eng. Data* 56, 1506-1525.

Bankfort, C.W., Ward, R. E., 2014. The oxford handbook of food fermentations. Oxford University Press, Oxford.

Barrera R., Villa A., Montes de Correa, C., 2009. Measurement of activity coefficients at infinite dilution for acetonitrile, water, limonene, limonene epoxide and their binary pairs. *Fluid Phase Equilib.* 275, 46–51.

Bastidas, P., Parra, J., Gil I., Rodriguez, G., 2012. Alcohol distillation plant simulation: thermal and hydraulic studies. *Procedia Eng.* 42, 80–89.

Bastos, J.C., Soares, M.E., Medina, A.G., 1988. Infinite dilution activity coefficients predicted by UNIFAC group contribution, *Ind. Eng. Chem. Res.* 27 1269-1277.

Batista, R.M., Meirelles, A.J.A., 2009. A Strategy for Controlling Acetaldehyde Content in an Industrial Plant of Bioethanol. IFAC Proc. Vol. 42 (11), 928-933.

Batista, F.R.M., Meirelles, A.J.A., 2011. Computer simulation applied to studying continuous spirit distillation and product quality control. *Food Control* 22, 1592-1603.

Batista, F.R.M., Follegatti-Romero, L.A., Bessa, L.C.B.A., Meirelles, A.J.A., 2012. Computational simulation applied to the investigation of industrial plants for bioethanol distillation. *Comp. Chem. Eng.* 46, 1-16.

Batista, F.R.M., Follegatti-Romero, L.A., Meirelles, A.J.A., 2013. A new distillation plant for natural alcohol production. *Sep. Purif. Technol.* 118, 784-793.

Becke, A.D., 1986. Density functional calculations of molecular bond energies, *J. Chem. Phys.* 84, 4524-4529.

Benziane, M., Khimeche, K., Mokbel, l., Sawaya, T., Dahmani, A., Jose, J., 2011. Experimental Vapor Pressures of Five Saturated Fatty Acid Ethyl Ester (FAEE) Components of Biodiesel. *J. Chem. Eng. Data.* 56, 4736–4740.

Bertrand, A., 2003. Armagnac and Wine-Spirits, in: Lea, A.G.H., Piggott, J.R. (Eds.), Fermented Beverage Production, Second ed. Kluwer Academic/ Plenum Publishers, New York, pp. 213-238.

Bon, J., Clemente, G., Vaquiro, H., Mulet, A., 2009. Simulation and optimization of milk pasteurization processes using general process simulator (ProSimPlus). *Comp. Chem. Eng.* 34, 414–420.

Borho, N., Suhm, M.A., Le Barbu-Debus, K., Zehnacker, A., 2006. Intra- vs. intermolecular hydrogen bonding: dimers of alpha-hydroxyesters with methanol, *Phys. Chem. Chem. Phys.* 8, 4449-4460.

Brown, I., Ewaldq, A.H. Austra. J. Sci. Res. A. 1950, 3, 306. In: Gmehling, J., Onken, U., 1977. Vapor-Liquid Equilibrium Data Collection. Aqueous-Organic Systems. Dechema, Frankfurt.

Cacho, J., Moncayo, L., Palma, J.C., Ferreira, V., Culleré, L., 2013. The influence of Different Production Processes on the Aromatic composition of Peruvian Piscos. *J. Nutr. Food Sci.* 3 (6), 1-10.

Cadoret, L., Yu, C.-C. Huang, H.-P., Lee, M.-J., 2009. Effects of physical properties estimation on process design: a case study using AspenPlus, *Asia Pac. J. Chem. Eng.* 4, 729-734.

Câmara, J.S., Alves, M.A., Marques, J.C., 2006. Multivariate analysis for the classification and differentiation of Madeira wines according to main grape varieties. *Talanta* 68, 1512-1521.

Cantagrel, R., Lurton, L., Vidal, J.-P., Galy B., 1990. La distillation charentaise pour l'obtention des eaux-de-vie de Cognac. In 1er symposium international sur les eaux-de-vie traditionnelles d'origine viticole, Bordeaux.

Carrau, F., Medina, K., Farina, L., Boido, E., Henschke, P., Dellacassa, E., 2008. Production of fermentation aroma compounds by Saccharomyces cerevisiae wine yeasts: effects of yeast assimilable nitrogen on two model strains. FEMS Yeast Res. 8, 1196-1207.

Carvallo, J., Labbe, M., Pérez-Correa, J.R., Zaror, C., Wisniak, J., 2011. Modeling methanol recovery in wine distillation stills with packing columns. *Food Control* 22, 1322-1332.

Çengel, Y., 2007. Heat and Mass Transfer. 3rd edition. McGraw Hill, Mexico.

Christensen, S.P., 1998. Measurement of dilute mixture vapor–liquid equilibrium data for aqueous solutions of methanol and ethanol with a recirculating still. *Fluid Phase Equilib.* 150–151, 763-773.

Chu, J.C., Getty, R.J., Brennecke, L.F., Paul, R., 1950. Distillation Equilibrium Data, Reinhold Publishing Corporation, New York.

Claus, M.J., Berglund, K.A., 2009. Defining still parameters using ChemCAD batch distillation model for modeling fruit spirits distillations. *J. Food Process Eng.* 32, 881-892.

Coelho, T.C., Souza, O., Sellin N., Medeiros, S.H.W., Marangoni, C., 2012. Analysis of the reflux ratio on the batch distillation of bioethanol obtained from lignocellulosic residue. *Procedia Eng.* 42, 131–139.

Conti, J.J, Othmer, D.F, Gilmont, R., 1960. Composition of Vapors from Boiling Binary Solutions. Systems Containing Formic Acid, Acetic Acid, Water, and Chloroform. J. Chem. Eng. Data, 5 (3), 301–307. In: Gmehling, J., Onken, U., 1977. Vapor-Liquid Equilibrium Data Collection. Aqueous-Organic Systems. Dechema, Frankfurt.

Copigneaux, P., 1993. Distillation – Absorption. Colonnes garnies. in: Techniques de l'ingénieur, Chapitre J2626, V3. 1–21.

Coquelet, C., Laurens, S. Richon, D., 2008. Measurement through a Gas Stripping Technique of Henry's Law Constants and Infinite Dilution Activity Coefficients of Propyl Mercaptan, Butyl Mercaptan, and Dimethyl Sulfide in Methyldiethanolamine (1) + Water (2) with w_1 = 0.25 and 0.35. *J. Chem. Eng. Data* 53, 2540-2543.

Covarrubias-Cervantes, M., Mokbel, I., Champion, D., Jose, J. Voilley, A., 2004. Saturated vapor pressure of aroma compounds at various temperatures. *Food Chem.* 85, 221–229.

Dahm, K.D., Visco Jr, D. P., 2015. Fundamentals of Chemical Engineering Thermodynamics, Cencage Learning: Stamford.

Darton R.C., 1992. Distillation and absorption technology: Current market and new developments. Distillation and absorption '92. Volume 1. Birmingham, United Kingdom. Icheme Symposium Series 128, A385-A390.

Day, J., 2012. Laminar natural convection from isothermal vertical cylinders. MSc. Thesis. University of North Texas.

Decloux, M., Coustel, J., 2004. Alcool surfin : simulation d'une unité de distillation. *Ind. Alim. Agric.* 121 (7/8), 9-20.

Decloux, M., Coustel, J., 2005. Simulation of a neutral spirit production plant using beer distillation. *Int. Sugar J.* 107-1283, 628-643.

Decloux, M. 2009. Simulation of Cognac distillation. Confidential document. AgroParisTech, Paris, 2009.

Decloux, M., Fabien, T., 2007. La distillation du calvados pratiques et savoir-faire.

Decloux, M., Joulia, X., 2009. Distillation of AOC French spirits: Cognac, Armagnac, calvados and Martinique agricultural rum, in: Ingledew, W.M., Kelsall, D.R., Austin G.D., Kluhspies C. (Eds.), The Alcohol Textbook, fifth ed. Nottingham University Press, Nottingha m, pp. 491–506.

Delgado, P., Sanz, M.T., Beltrán, S., 2007. Isobaric vapor–liquid equilibria for the quaternary reactive system: Ethanol + water + ethyl lactate + lactic acid at 101.33 kPa. *Fluid Phase Equilib.* 255, 17-23.

Delzenne, A., 1958. Vapor Liquid Equilibrium Data for Ternary System Methanol-Ethanol-Water. Ind. Eng. Chem. Chem. Eng. Data Series. 3 (2), 224–230. In: Gmehling, J., Onken, U., 1977. Vapor-Liquid Equilibrium Data Collection. Organic Hydroxy compounds: Alcohols. Dechema, Frankfurt.

Detcheberry, M., Destrac, P., Massebeuf, S., Baudouin, O., Gerbaud, V., Condoret, J.-S., Meyer, X.-M., 2016. Thermodynamic modeling of the condensable fraction of a gaseous effluent from lignocellulosic biomass torrefaction. *Fluid Phase Equilib.* 409, 242-255.

Deterre, S., Albet, J., Joulia, X., Baudouin, O., Giampaoli, P., M. Decloux, V. Athès., 2012. Vapor–Liquid Equilibria Measurements of Bitter Orange Aroma Compounds Highly Diluted in Boiling Hydro-Alcoholic Solutions at 101.3 kPa. *J. Chem. Eng. Data* 57, 3344-3356.

Dias, T.P.V.B., Fonseca, L.A.A.P., Ruiz, M.C., Batista, F.R.M., Batista, E.A.C., Meirelles A.J.A., 2014. Vapor–Liquid Equilibrium of Mixtures Containing the Following Higher Alcohols: 2-Propanol, 2-Methyl-1-propanol, and 3-Methyl-1-butanol. *J. Chem. Eng. Data* 59, 659-665.

Dobroserdov, L.L., Ilina, V.P., 1961. Zh. Prikl. Khim. 34, 386. Cited in Vapor-Liquid Equilibrium Data Collection. Aqueous-Organic Systems, Gmehling, J, Onken, U., Dechema: Frankfurt, 1977.

Dragone, G., Mussatto, S., Oliveira, J., Teixeira, J., 2009. Characterisation of volatile compounds in an alcoholic beverage produced by whey fermentation. *Food Chem.* 112, 929-935.

Dreisbach, R.R., Shrader, S.A. Vapor Pressure Temperature Data on Some Organic Compounds. *Ind. Eng. Chem.* 1949, 41 (12), 2879-2880.

Dunlop, J.G. M.Sc. Thesis, Brooklyn Polytechnic Institute, New York, 1948. In: Gmehling, J., Onken, U., 1977. Vapor-Liquid Equilibrium Data Collection. Aqueous-Organic Systems. Dechema, Frankfurt.

Durand, M., Moliner, V. Kunz, W. Aubry, J.-M., 2011. Classification of Organic Solvents Revisited by using the COSMO-RS approach, *Chem. Eur. J.* 17, 5155-5164.

Ebeler, S.E., 2001. Analytical Chemistry: Unlocking the Secrets of Wine. *Food Rev. Int.* 17, 45-64.

Emtir M., Etoumi A., 2009. Enhancement of conventional distillation configurations for ternary mixtures separation. *Clean Techn. Environ. Policy* 11, 123–131.

Esteban-Decloux M. 2013. Eco-efficiency of distillation of spirit beverages : identification and proposals to save resources. AlaDIn Stimuler le renouveau industriel (3.3), axe produits (3.3.3) produire de façon éco-efficiente.

Esteban-Decloux, M., Deterre, S., Kadir, S., Giampaoli, P., Albet, J., Joulia, X., Baudouin, O., 2014. Two industrial examples of coupling experiments and simulations for increasing quality and yield of distilled beverages. *Food Bioprod. Process.* 92, 343-354.

Fan, D., Li, J., Shi, J., Peng, C., Liu, H., Hu, Y., Paricaud, P. 2011. Vapor−Liquid Equilibria in the Propyl Acetate + Ethanoic Acid Binary System from (323.15 to 353.15) K: Measurement with a Static Method and Modeling with the NRTL, Wilson, UNIQUAC, and COSMO−SAC Approaches, J. *Chem. Eng. Data* 56, 1323-1329.

Faúndez, C.A., Valderrama J.O., 2004. Phase equilibrium modeling in binary mixtures found in wine and must distillation. *J. Food Eng.* 65, 577-583.

Faúndez, C.A., Alvarez, V.H., Valderrama, J.O., 2006. Predictive models to describe VLE in ternary mixtures water + ethanol + congener for wine distillation. *Thermochim. Acta* 450, 110-117.

Faúndez, C.A., Valderrama, J.O., 2009. Activity Coefficient Models to Describe Vapor-Liquid Equilibrium in Ternary Hydro-Alcoholic Solutions. *Chin. J. Chem. Eng.* 17, 259-267.

Ferrari, G., Lablanquie, O., Cantagrel, R., Ledauphin, J., Payot, T., Fournier, N., Guichard, E., 2004. Determination of Key odorant compounds in freshly distilled Cognac using GC-O, GC-MS, and sensory evaluation. *J. Agric. Food Chem.* 52, 5670-5676.

FFS, 2017. Les spiritueux. Repères 2016. URL: http://www.spiritueux.fr/index.php.

Foo D.C.Y. and Elyas R., 2017. Introduction to Process Simulation. In Chemical Engineering Process Simulation. Foo D.C.Y., Chemmangattuvalappil N., D.K.S Ng, Elyas R., Chen C.-L., Elms R.D., Lee H.-Y., Chien I.-L. Chong S., Chong C.H. Elsevier, Amsterdam.

Franitza, L., Granvogl, M., Schieberle, P., 2016. Influence of the Production Process on the Key volatile aroma compounds of Rum: From Molasses to the Spirit. *J. Agric. Food Chem.* 64, 9041-9053.

Fredenslund, A., Jones R., Prausnitz J., 1975. Group-contribution estimation of activity coefficients in nonideal liquid mixtures. *AIChE J.* 21(6), 1086–1099.

Gaiser, M., Bell, G.M., Lim, A.W., Roberts, N.A., Faraday, D.B.F., Schulz, R.A., Grob, R., 2002. Computer simulation of a continuous whisky still. *J. Food Eng.* 51, 27-31.

Gay, L., 1927. Chim. Ind. 18, 187. In: Ohe, S., 1989. Vapor-liquid equilibrium data. Kodansha, Tokyo.

GESTIS Substance Database, German Social Accident Insurance, 2016.
URL: www.dguv.de/ifa/gestis-database.

Gil, I.D., Guevara, J.R., García, J.L., Leguizamón, A., 2011. Análisis y simulación de procesos en Ingeniería Química, first ed. Editorial Universidad Nacional de Colombia. Bogotá.

Gillespie, D.T.C., 1946. Vapor-Liquid Equilibrium Still for Miscible Liquids. *Ind. Eng. Chem. Anal.* Ed.18, 575-577.

Gmehling, J., Li, J., Schiller, M., 1993. A modified UNIFAC model. 2. Present parameter matrix and results for different thermodynamic properties. *Ind. Eng. Chem. Res.* 32,178-193.

Gmehling, J., Onken, U., Arlt, W., Grenzheuser, P., Weidlich, U., Kolbe, B., Rarey. J., 2001. Vapor-liquid Equilibrium Data Collection Part 5: Carboxylic Acids, Anhydrides, Esters, Chemistry Data Series, Vol. 1, Dechema.

Gmehling, J. 2003. Potential of thermodynamic tools (group contribution methods, factual data banks) for the development of chemical processes. *Fluid Phase Equilib.* 210(2), 161–173.

Griswold, J., Dinwiddie, J.A., 1942. Vapor-Liquid Equilibrium of Methanol-Ethanol-Water - Mechanism of Ethanol Dehydration. *Ind. Eng. Chem.* 34 (10), 1188–1191.

Griswold, J., Chu P.L., Winsauer, W.O., 1949. Phase Equilibria in Ethyl Alcohol – Ethyl Acetate – Water System. Ind. Eng. Chem. 41 (10), 2352–2358.

Guichard, H., Lemesle, S., Ledauphin, J., Barillier, D., Picoche, B., 2003. Chemical and sensorial aroma characterization of freshly distilled calvados. 1. Evaluation of quality and defects on the basis of key Odorants by olfactometry and sensory analysis. *J. Agric. Food Chem.* 51, 424-432.

Guymon, J., 1974. Chemical aspects of distilling wine into brandy. In : Chemistry of Winemaking, Webb, A., Advances in Chemistry. American Chemical Society, Washington, 232-253.

Harwardt A., Marquardt W., 2012. Heat-Integrated Distillation Columns: Vapor Recompression or Internal Heat Integration? *AIChE J.* 58, 3740–3750.

Heitz, J.E., 1960. Measurement of vapor-liquid equilibria for acetaldehyde-ethanol-water mixtures. *Amer. J. Enol. Viticult.* 11, 19.

Heyen, G., Arpentinier, P., 2017. Validation et réconciliation de données mesurées sur une installation industrielle. Tutoriel 11. Congrès SFGP.

Hsieh, C.-M., Sandler, S.I., Lin S.-T., 2010. Improvements of COSMO-SAC for vapor–liquid and liquid–liquid equilibrium predictions. *Fluid Phase Equilib.* 297, 90-97.

Hsieh, C.-M., Lin, S.-T., Vrabec, J., 2014a. Considering the dispersive interactions in the COSMO-SAC model for more accurate predictions of fluid phase behavior, *Fluid Phase Equilib.* 367, 109-116.

Hsieh, C.-M., Lin, S.-T., Vrabec, J., 2014b. Corrigendum to: Considering the dispersive interactions in the COSMO-SAC model for more accurate predictions of fluid phase behavior [Fluid Phase Equilib. 367, 109–116], *Fluid Phase Equilib.* 384, 14-15.

Hughes, H.E., Maloney, J.O., 1952. Binary and Ternary Equilibrium Data. Chem. Eng. Prog. 48, 192-200. In: Gmehling, J., Onken, U., 1977. Vapor-Liquid Equilibrium Data Collection. Aqueous-Organic Systems. Dechema, Frankfurt.

Ikari, A., Kubo, R., 1975. Behaviour of simple impurities in simple distillation of aqueous solution of ethanol. *J. Chem. Eng. Japan* 8 (4), 294-299.

Ikari, A., Hatate, Y., Sakaue, S., Kubota, Y., 1984. Behavior of a minute amount of Furfural in Distillation of Aqueous Ethanol solution under reduced pressure, *J. Chem. Eng. Japan* 17, 486-490.

Ikari, A., Hatate, Y., Yanagida, K., Eta, M., 1990. Vapor-Liquid Equilibria of a Minute Amount of n-Propyl, Isobutyl, and Isoamyl Alcohols in Aqueous Ethanol Solution under Reduced Pressure, *Kagaku Kogaku Ronbun.* 16, 1101-1104.

Ikari, A., Hatate, Y., Fukumoto, T., 1998. Vapor-Liquid Equilibria of a Minute Amount of Methanol, Isovaleraldehyde and Diacetyl in Aqueous Ethanol Solution under Reduced Pressure, *Kagaku Kogaku Ronbun.* 24, 111-115.

Institute of Alcohol Studies, 2016. The alcohol Industry. URL: http://www.ias.org.uk.

International Center for Alcohol Policies, 2006. The structure of the beverage alcohol industry. ICAP reports 17.

Jiang, B., Zhang, Z., 2010. Volatile Compounds of Young Wines from Cabernet Sauvignon, Cabernet Gernischet and Chardonnay Varieties Grown in the Loess Plateau Region of China. Mol. 15, 9184.

JOCE, 2000. Règlement (CE) n°2870/2000 de la commission du 19 décembre 2000 établissant des méthodes d'analyse communautaires de références applicables dans le secteur des boissons spiritueuses. Rapport technique, Journal officiel des communautés européennes.

JORF, 2014. Cahier des charges de l'appellation d'origine contrôlée Armagnac homologué par le décret n°2014-1642 du 26 décembre 2014.

Joulia, X., 2008. Simulateurs de procédés, in: Techniques de l'ingénieur, Chapitre J1022, 1–25.

Kadir, S., 2009. Optimisation du procédé de production d'Alcool surfin, PhD Thesis, AgroParisTech, Paris,

Kamihama, N., Matsuda, H., Kurihara, K., Tochigi, K., Oba, S., 2012. Isobaric Vapor–Liquid Equilibria for Ethanol + Water + Ethylene Glycol and Its Constituent Three Binary Systems. *J. Chem. Eng. Data* 57, 339-344.

Kang, J.W., Diky, V., Chirico, R.D., Magee, J.W., Muzny, C.D., Abdulagatov, I., Kazakov, A.F., Frenkel, M., 2010. Quality Assessment Algorithm for Vapor-Liquid Equilibrium Data. *J. Chem. Eng. Data* 55, 3631-3640.

Kharin, S.E., Perelygin, V.M., Polyansky, K.K., 1970a. Gidroliz. Lesokhim. Prom. 23, 15. In: Gmehling, J., Onken, U., 1977. Vapor-Liquid Equilibrium Data Collection. Organic Hydroxy compounds: Alcohols. Dechema, Frankfurt.

Kharin, S.E., Perelygin, V.M., Remizov, G.P., 1970b. J. Appl. Chem. 43, 2036. In: Gmehling, J., Onken, U., 1977. Vapor-Liquid Equilibrium Data Collection. Aqueous-Organic Systems. Dechema, Frankfurt.

Kharin, S.E., Perelygin, V.M., Smirnov, V.S., 1971a. Khim. Prom. 47, 510. In: Gmehling, J., Onken, U., 1977. Vapor-Liquid Equilibrium Data Collection. Aqueous-Organic Systems. Dechema, Frankfurt.

Kharin, S.E., Perelygin, V.M., Remizov, G.P., 1971b. J. Appl. Chem., 44, 127. In: Gmehling, J., Onken, U., 1977. Vapor-Liquid Equilibrium Data Collection. Aqueous-Organic Systems. Dechema, Frankfurt.

Kharin, S.E., Perelygin, V.M., Polyansky, K.K., 1971c. Gidroliz. Lesokhim. Prom. 24, 10. In: Gmehling, J., Onken, U., 1977. Vapor-Liquid Equilibrium Data Collection. Aqueous-Organic Systems. Dechema, Frankfurt.

Kharin, S.E., Perelygin, V.M., Pisarevsky, V.G., 1972. Zh. Prikl. Khim. 45, 466. In: Gmehling, J., Onken, U., 1977. Vapor-Liquid Equilibrium Data Collection. Aqueous-Organic Systems. Dechema, Frankfurt.

Kister, H. Z., 1992. Distillation design. First ed. McGraw-Hill Education, New York.

Klamt, A., Eckert, F., 2000. COSMO-RS: a novel and efficient method for the a priori prediction of thermophysical data of liquids, *Fluid Phase Equilib.* 172, 43-72.

Koch, W., Holthausen, M. C., 2001. Chemist's Guide to Density Functional Theory, second ed., Wiley-VCH, Weinheim.

Kohoutova, J., Suska, J., Novak, J.P., Pick, J., 1970. Liquid-Vapor Equilibrium XLV. System Methanol-2-Propanol Water. Collect. Czech. Chem. Commun. 35, 3210-3222. In: Gmehling, J., Onken, U., 1977. Vapor-Liquid Equilibrium Data Collection. Aqueous-Organic Systems. Dechema, Frankfurt.

Kojima, K., Ochi, K., Nakazawa, Y., 1969. Int. Chem. Eng. 9, 342. In: Gmehling, J., Onken, U., 1977. Vapor-Liquid Equilibrium Data Collection. Aqueous-Organic Systems. Dechema, Frankfurt.

Kozlovskiy, M, Gobble, C. Chickos, J., 2015. Vapor pressures and vaporization enthalpies of a series of esters used in flavors by correlation gas chromatography. *J. Chem. Thermodyn.* 86, 65–74.

Lai, H.-S., Lin, Y.-F., Tu, C.-H., 2014. Isobaric (vapor + liquid) equilibria for the ternary system of (ethanol + water + 1,3-propanediol) and three constituent binary systems at P = 101.3 kPa. *J. Chem. Thermodyn.* 68, 13-19.

Lambert, C., 2015. Simulation et optimisation énergétique des procédés agroalimentaires dans un logiciel de génie chimique. Modélisation du séchage convectif d'aliments solides et application à une sucrerie de betteraves. Thèse de doctorat. AgroParisTech., Paris.

Lasdon, L.S., Fox, R.L., Ratner, M.W., 1974. Nonlinear optimization using the generalized reduced gradient method. Revue française d'automatique, d'informatique et de recherche opérationnelle 8, 73-103.

Ledauphin J., Basset B., Cohen S., Thierry P., Barillier D. 2006. Identification of trace volatile compounds in freshly distilled Calvados and Cognac: Carbonyl and sulphur compounds. *J. Food Comp. Anal.* 19, 28-40.

Ledauphin, J., Le Milbeau, C., Barillier, D., Hennequin, D., 2010. Differences in the Volatile Compositions of French Labeled Brandies (Armagnac, Calvados, Cognac, and Mirabelle) Using GC-MS and PLS-DA. *J. Agric. Food Chem.* 58, 7782-7793.

Lei Z., Chen B., Ding Z., 2005. Special distillation processes. First Edition. Elsevier, Amsterdam.

Letcher, T. M., 2007. Developments and Applications in Solubility, The Royal Society of Chemistry: Cambridge.

Lewis, G., Randall M., 1923. Thermodynamics and the free energy of chemical substances. McGraw-Hill Book Co. Inc., New York.

Li, J., Paricaud, P., 2012. Application of the Conduct-like Screening Models for Real Solvent and Segment Activity Coefficient for the Predictions of Partition Coefficients and Vapor–Liquid and Liquid–Liquid Equilibria of Bio-oil-Related Mixtures. *Energy Fuels* 26, 3756-3768.

Lin, S.-T., Sandler, S.I., 2002, A Priori Phase Equilibrium Prediction from a Segment Contribution Solvation Model, *Ind. Eng. Chem. Res.* 41, 899-913.

Maarse, H., Van Den Berg, F., 1994. Flavour of distilled beverages. In Understanding of natural flavors, Piggott, J.R., Paterson, A., First ed., Springer Science+Business Media Dordetch: London, pp 243-267.

MacNamara, K., Hoffmann, A., 1998. Gas chromatography technology in analysis of distilled spirits. In : Wetzel, D., Charalambous, G. (Ed.), Instrumental Methods in Food and Beverage Analysis. Elsevier, Amsterdam, pp. 303-346.

MacNamara, K., Lee, M., Robbat A., 2010. Rapid gas chromatographic analysis of less abundant compounds in distilled spirits by direct injection with ethanol–water venting and mass spectrometric data deconvolution. *J. Chromatog. A* 1217, 136-142.

Mains, G.H., 1922. Chem. Met. Eng. 26, 779. In: Gmehling, J., Onken, U., 1977. Vapor-Liquid Equilibrium Data Collection. Aqueous-Organic Systems. Dechema, Frankfurt.

Malanowski, S., 1982. Experimental methods for vapor liquid equilibria. Part I. Circulation methods, *Fluid Phase Equilib.* 8, 197-219.

Martí, M.P, Mestres, M., Sala, C., Busto, O., Guasch J., 2003. Solid-Phase Microextraction and Gas Chromatography Olfactometry Analysis of Successively Diluted Samples. A New Approach of the Aroma Extract Dilution Analysis Applied to the Characterization of Wine Aroma, *J. Agric. Food Chem.* 51, 7861-7865.

Martin, A., Carillo, F., Trillo, L., Rossello, A., 2009. A quick method for obtaining partition factor of congeners in spirits. *Eur. Food. Res. Technol.* 229, 697–703.

Miyamoto, S., Nakamura, S., Iwai, Y., Arai, Y., 2001. Measurement of Isothermal Vapor-Liquid Equilibria for Binary and Ternary Systems Containing Monocarboxylic Acid*. J. Chem. Eng. Data* 46, 1225–1230.

Morakul, S., Mouret, J.-R., Nicolle, P., Trelea I., Sablayrolles, J.-M., Athès, V., 2011. *Process Biochem.* 46, 1125-1131.

Mullins, E., Oldland, R., Liu, Y.A., Wang, S., Sandler, S.I., Chen, C.-C., Zwolak, M., Seavey, K.C., 2006. Sigma-Profile Database for Using COSMO-Based Thermodynamic Methods, *Ind. Eng. Chem. Res.* 45, 4389-4415.

Murphree, E., 1925. Rectifying column calculations. *Ind. Eng. Chem.* 17(7), 747-750.

Nala, M., Auger, E., Gedik, I., Ferrando, N., Dicko, M., Paricaud, P., Volle, F., Passarello, J.P., de Hemptinne, J.-C., Tobaly, P., Stringari, P., Coquelet, C., Ramjugernath, D., Naidoo, P., Lugo, R., 2013. Vapor–liquid equilibrium (VLE) for the systems furan + n-hexane and furan + toluene. Measurements, data treatment and modeling using molecular models. *Fluid Phase Equilib.* 337, 234-245.

Ng, L.-K., 2002. Analysis by gas chromatography/mass spectrometry of fatty acids and esters in alcoholic beverages and tobaccos. *Analytica Chim. Acta* 465, 309-318.

Nieto-Draghi, C., Fayet, G., Creton, B., Rozanska, X., Rotureau, P., de Hemptinne, J.-C., Ungerer, P., Rousseau, B., Adamo, C., 2015. A General Guidebook for the Theoretical Prediction of Physicochemical Properties of Chemicals for Regulatory Purposes, *Chem. Rev.* 115, 13093-13164.

NIST, 2016. Chemistry Webbook, U.S. Secretary of Commerce, SRD 69.
URL: http://webbook.nist.gov/chemistry/

Nykänen, L., 1986. Formation and occurrence of flavor compounds in wine and distilled alcoholic beverages. *Am. J. Enol. and Vit.* 37(1), 84-96.

Nykänien, L., Suomalainen, H., 1983. Aroma of Beer, Wine and Distilled Alcoholic Beverages, D. Reidel Publishing Company, Dordretch.

Ochi, K., Kojima, K., 1969. Kagaku Kogaku. 33, 352–357. In: Gmehling, J., Onken, U., 1977. Vapor-Liquid Equilibrium Data Collection. Organic Hydroxy compounds: Alcohols. Dechema, Frankfurt.

Ocon, J., Rebolleda, F., 1958. An. Real. Soc. Espan. Fis. Quim. 54 B (7-8), 525. In: Gmehling, J., Onken, U., 1977. Vapor-Liquid Equilibrium Data Collection. Aqueous-Organic Systems. Dechema, Frankfurt.

OIML, 1972. International alcoholometric tables, Paris.

OIV, 1994. Recueil des méthodes internationales d'analyse des boissons spiritueuses, des alcools et de la fraction aromatiquedes boissons, Paris.

Ortega, C., López, R., Cacho, J., Ferreira, V., 2001. Fast analysis of important wine volatile compounds: Development and validation of a new method based on gas chromatographic–flame ionisation detection analysis of dichloromethane microextracts*. J. Chromatog. A* 923, 205-214.

Osorio, D., Pérez-Correa, R., Belancic, A., Agosin, E., 2004. Rigorous dynamic modeling and simulation of wine distillations. *Food Control* 15, 515-521.

Othmer, D., 1943. Composition of Vapors from boiling binary solutions. *Ind. Eng. Chem.* 35 (5), 614-620.

Othmer, D., 1948. Composition of Vapors from boiling binary solutions. Improved equilibrium still. *Ana. Chem.* 20 (8), 763-766.

Oudin, P., 1980. Guide pratique d'alcoométrie. Ed Oudin, Poitiers.

Owens B., Dikty A., 2011. The Art of Distilling Whiskey and Other Spirits: An Enthusiast's Guide to the Artisan Distilling of Potent Potables. Quarto Publishing Group. New York.

Paine, A., Dayan, A., 2001. Defining a tolerable concentration of methanol in alcoholic drinks. *Human & Experimental Toxicology* 20, 563-568.

Palomar, J., Torrecilla, J.S., Lemus, J., Ferro, V.R., Rodríguez, F., 2008. Prediction of non-ideal behavior of polarity/polarizability scales of solvent mixtures by integration of a novel COSMO-RS molecular descriptor and neural networks, *Phys. Chem. Chem. Phys.* 10, 5967–5975.

Peña-Tejedor, S., Murga, R., Sanz, M.T., Beltrán, S., 2005. Vapor–liquid equilibria and excess volumes of the binary systems ethanol + ethyl lactate, isopropanol + isopropyl lactate and n-butanol + n-butyl lactate at 101.325 kPa. *Fluid Phase Equilib.* 230, 197-203.

Perdew, J.P., 1986. Density-functional approximation for the correlation energy of the inhomogeneous electron gas, *Phys. Rev.* B 33, 8822-8824.

Perry, J.H. , 1950. Chemical Engineers Handbook, McGraw-Hill Book Co, New York.

Piggott J., 2009. Distillation of brandies, in: Ingledew, W.M., Kelsall, D.R., Austin G.D., Kluhspies C. (Eds.), The Alcohol Textbook, fifth ed. Nottingham University Press, Nottingham, pp. 491–506.

Prausnitz, J.M., Lichtenthaler, R.N., de Azevedo, E.G., 1999. Molecular Thermodynamics of Fluid-Phase Equilibria, third ed., Prentice Hall PTR, New Jersey.

ProSim, 2014. Simulis® Thermodynamics Serveur de calculs de propriétés thermodynamiques et d'équilibres entre phases. Modèles Thermodynamiques. Version 2.0. Labège.

Puentes, C., Joulia, X., Athès, V., Esteban-Decloux, M., 2018a. Review and thermodynamic modeling with NRTL model of vapor-liquid equilibria (VLE) of volatile aroma compounds highly diluted in ethanol - water mixtures at 101.3 kPa. *Ind. Eng. Chem. Res.* Accepted.

Puentes, C., Joulia X., Paricaud, P., Giampaoli, P., Athès, V., Esteban-Decloux, M., 2018b. Vapor-liquid equilibrium (VLE) of ethyl lactate highly diluted in ethanol-water solutions at 101.3 kPa: experimental measurements and thermodynamic modeling with semi-empiric models. *J. Chem. Eng. Data* 63, 2, 365-379.

Rall, J.D., Mühlbauer, A.L., 1998. Phase equilibria: Measurement and computation, Taylor & Francis, Washington.

Renon, H. Prausnitz, J.M., 1968. Local compositions in thermodynamic excess functions for liquid mixtures. *AIChE J.* 14, 135-144.

Renon, H., Asselineau L., Cohen G., Raimbault C., 1971. Calcul sur ordinateur des équilibres liquide-vapeur et liquide-liquide. Application à la distillation des mélanges non idéaux et à l'extraction par solvants. Editions Technip.

Rhodes, C.L., 1996. The Process Simulation Revolution: Thermophysical Property Needs and Concerns. *J. Chem. Eng. Data* 41, 947-950.

Riddick, J.A., Bunger, W.B., Sakano, T.K., , 1986. Organic Solvents Physical Properties and Methods of Purification. Techniques of Chemistry, fourth ed., Wiley, New York.

Rios, K., 2009. Lecture notes on chemical thermodynamics, National University of Colombia, Bogota.

Rius, A., Otero, J.L., Macarron, A., 1959. Chem. Eng. Sci. 10, 105. In: Gmehling, J., Onken, U., 1977. Vapor-Liquid Equilibrium Data Collection. Organic Hydroxy compounds: Alcohols. Dechema, Frankfurt.

Rodriguez, R., Blanco, D., Mangas, J., 2003. Influence of distillation system, oak wood type, and aging time on volatile compounds of cider brandy. *J. Agric. Food Chem.* 51, 5709-5714.

Rowley, R., Wilding, W., Oscarson, J., Yang, Y., Zundel, N., Daubert, T., Danner, R., DIPPR data compilation of pure chemical properties, design institute for physical properties, *AIChE J.* URL: http://www/aiche.org/dippr

Sacher, J., García-Llobodanin, L., López, F., Segura, H., Pérez-Correa, J.R. 2013. Dynamic modeling and simulation of an alembic pear wine distillation. *Food Bioprod. Process.* 91, 447–456.

Scanavini, H.F.A., Ceriani, R., Cassini, C.E.B., Souza, E.L.R., Maugeri-Falco, F., Meirelles, A.J.A., 2010. Cachaça Production in a Lab-Scale Alembic: Modeling and Computational Simulation. *J. Food Process Eng.* 33, 226–252.

Scanavini, H.F.A., Ceriani, R., Meirelles, A.J.A., 2012. Cachaça Distillation Investigated on the Basis of Model Systems. Braz. *J. Chem. Eng.* 29-02, 429–440.

Schneider, H.-J., 2015. Dispersive Interactions in Solution Complexes, *Acc. Chem. Res.* 48, 1815-1822.

Sebastiani, E., Lacquaniti, L., 1967. Acetic acid—water system thermodynamical correlation of vapor—liquid equilibrium data. Chem. Eng. Sci. 22 (9), 1155-1162. In: Gmehling, J., Onken, U., 1977. Vapor-Liquid Equilibrium Data Collection. Aqueous-Organic Systems. Dechema, Frankfurt.

Segur, M.C., Bertrand, A., 1992. La distillation continue armagnacais (Continous Armagnac distillation), in: Cantagrel, R. (Ed.), Elaboration et connaissances des Spiritieux (Elaboration and knowledge of spirit beverages). Lavoisir Tec et Doc, Paris, pp. 257-266.

Sinha A.P, De P., 2012. Mass Transfer: Principles and Operations. PHI Learning Private Limited, New Delhi.

Slobodyanik, I.P., Babuskhina, E.M., 1966. Zh. Prikl. Khim. 39, 1555. In: Gmehling, J., Onken, U., 1977. Vapor-Liquid Equilibrium Data Collection. Organic Hydroxy compounds: Alcohols. Dechema, Frankfurt.

Smirnova, N.A., 1959. Vestn. Leningr. Univ. Fiz. Khim. 81. In: Gmehling, J., Onken, U., 1977. Vapor-Liquid Equilibrium Data Collection. Aqueous-Organic Systems. Dechema, Frankfurt.

Soni, M., 2003. Vapor-liquid equilibria and infinite dilution activity coefficient measurements of systems involving diketones, MSc Thesis, University of Nartal, Durban.

Sourisseau, J., 2002. Etude chimique de la distillation du cognac. *Bulletin de l'Union des Physiciens,* 96, 881-892.

Stejfa, V., Fulem, M., Ruzicka, K, Matejka, P., 2015. Vapor pressures and thermophysical properties of selected hexenols and recommended vapor pressure for hexan-1-ol. *Fluid Phase Equilib.* 402, 18–29.

Suomalainen, H., Lehtonen, M., 1979. The production of Aroma Compounds by Yeast. *J. Inst. Brew.* 85, 149-156.

Suska, J., 1979. Collect. Czech. Chem. Commun. 44, 1852. In: Ohe, S., 1989. Vapor-liquid equilibrium data. Kodansha, Tokyo.

Suska, J., Holub, R., Vonka, P., Pick, J., 1970. Collect. Czech. Chem. Commun. 35,385. In: Gmehling, J., Onken, U., 1977. Vapor-Liquid Equilibrium Data Collection. Aqueous-Organic Systems. Dechema, Frankfurt.

Tan, T.C., Chai, C.M., Tok, A.T., Ho, K.W., 2004. Prediction and experimental verification of the salt effect on the vapor–liquid equilibrium of water–ethanol–2-propanol mixture. *Fluid Phase Equilib.* 218, 113–121.

Tan, T.C., Tan, Rowell, Soon, L.H., Ong, S.H.P., 2005. Prediction and experimental verification of the effect of salt on the vapor–liquid equilibrium of ethanol/1-propanol/water mixture. *Fluid Phase Equilib.* 234, 84–93.

Taylor R., Krishna R., Kooijman H., 2003. Real-World Modeling of Distillation. *Cep Magazine* 28-39.

Taylor, B. N., Kuyatt, C. E., 1994. Guidelines for Evaluating and Expressing the Uncertainty of NIST Measurement Results, NIST Technical Note 1297. Gaithersburg, pp. 1-20.

Tgarguifa, A., Abderafi, S., Bounahmidi, T., 2017. Energetic optimization of Moroccan distillery using simulation and response surface methodology. *Renew. Sust. Energy Rev.* 76, 415-425.

Thakore S.B., Bhatt B.I., 2007. Introduction to Process Engineering Design. Tata McGraw-Gill, New Dehli.

Truong H.S., Ismail I., Razali R., 2010. Fundamental Modeling and Simulation of a Binary Continuous Distillation Column. 2010 International Conference on Intelligent and Advanced Systems, Kuala Lumpur, 1-5.

UNGDA, 2011a. Document interne MO 504.1.009. Dosage des composés volatils des alcools et des boissons spiritueuses par chromatographie en phase gazeuse.

UNGDA, 2011b. Document interne MO 504.1.097. Dosage des acides gras volatils et des acides fermentaires par chromatographie en phase gazeuse.

UNGDA, 2014. Document interne MO 504.1.002. Masse volumique à 20 °C et titres alcoométriques volumiques brut et réel à 20 °C des alcools neutres, alcools bruts et des boissons spiritueuses par densimètre électronique.

Valderrama, J.O., Faúndez, C.A., 2003. Modeling of vapor–liquid equilibrium in binary and ternary mixtures of interest in alcoholic distillation. *Información Tecnológica* 14 (1), 83–92.

Valderrama, J.O., Faúndez, C.A., Toselli, L.A., 2012a. Advances on modeling and simulation of alcoholic distillation. Part 1: Thermodynamic modeling. *Food Bioprod. Process.* 90, 819-831.

Valderrama, J.O., Toselli, L.A., Faúndez, C.A., 2012b. Advances on modeling and simulation of alcoholic distillation. Part 2: Process simulation. *Food Bioprod. Process*. 90, 832-840.

Van Zandijcke, F., Verhoeye, L., 1974. J. Appl. Chem. Biotechnol. 24, 709. In: Gmehling, J., Onken, U., 1977. Vapor-Liquid Equilibrium Data Collection. Aqueous-Organic Systems. Dechema, Frankfurt.

Vawdrey, A.C., Oscarson, J.L, Rowley, R.L., Wilding, W.V., 2004. Vapor-phase association of n-aliphatic carboxylic acids. *Fluid Phase Equilib*. 222-223, 239-245.

Verevkin, S.P., Heintz, A., 1999. Determination of Vaporization Enthalpies of the Branched Esters from Correlation Gas Chromatography and Transpiration Methods. *J. Chem. Eng. Data*. 44, 1240-1244.

Vetere, A., 1991. The Riedel equation. *Ind. Eng. Chem. Res*. 30, 2487-2492.

Vidal, J., 2003. Thermodynamics. Applications in chemical engineering and petroleum industry, Editions Technip: Paris.

Vosko, S.H., Wilk, L., Nusair, M., 1980. Accurate spin-dependent electron liquid correlation energies for local spin density calculations: a critical analysis, *Can. J. Phys.* 58, 1200-1211.

Voutsas, E.C., Pamouktsis, C., Argyris, D., Pappa, G.D., 2011. Measurements and thermodynamic modeling of the ethanol–water system with emphasis to the azeotropic region, *Fluid Phase Equilib.* 308, 135-141.

Vrielynck, B., 2002. Les procédés mieux maîtrisés grâce à la réconciliation de données. *Mesures* 741, 30–34.

Vu, D.T., Lira, C.T., Asthana, N.S., Kolah, A.K. , Miller, D.J., 2006. Vapor–Liquid Equilibria in the Systems Ethyl Lactate + Ethanol and Ethyl Lactate + Water. *J. Chem. Eng. Data* 51, 1220-1225.

Wang J.C., Wang Y.L., 1981. A review of the modeling and simulation of multi-stage separation processes. (2nd edn.) R.S.H. Mah, W.D. Seider (Eds.), Foundations of Computer-Aided Chemical Process Design, Engineering Foundation 121-170.

Wang, S., Sandler, S.I., Chen, C.-C., 2007. Refinement of COSMO–SAC and the Applications, *Ind. Eng. Chem. Res.* 46, 7275-7288.

Wauquier J.P., 1998. Le raffinage du pétrole. Procédés de séparation. Editions Technip, Paris.

Weidlich, U., Gmehling, J., 1987. A modified UNIFAC model. 1. Prediction of VLE, h^E, and Gamma at Infinite Dilution. *Ind. Eng. Chem. Res.* 26, 1372-1381.

Welke, J., Sanes M., Lazzarotto, M., Alcaraz, C., 2014. Quantitative analysis of headspace volatile compounds using comprehensive two-dimensional gas chromatography and their contribution to the aroma of Chardonnay wine. *Food Res. Int.* 59, 85-99.

Williams, G.C., 1962. Vapor-Liquid Equilibria of Organic Homologues in Ethanol-Water Solutions, *Am. J. Enol. Vitic.* 13, 169-180.

Wilson, G.M., 1964. Vapor-Liquid Equilibrium. XI. A New Expression for the Excess Free Energy of Mixing. J. Am. Chem. Soc. 86, 127-130.

Wu Y.C., Lee H.-Y., Huang H.-P., Chien I.-L., 2014. Energy-Saving Dividing-Wall Column Design and Control for Heterogeneous Azeotropic Distillation Systems. *Ind. Eng. Chem. Res.* 53, 1537–1552.

Yang, B., Wang, H., 2002. Vapor-Liquid Equilibrium for Mixtures of Water, Alcohols, and Ethers. *J. Chem. Eng. Data* 47, 1324-1329.

Zaitsau, D.H., Paulechka, Y.U., Blokhin, A.V., Yermalayeu, A.V., Kabo, A.G., Ivanets, M.R, 2009. Thermodynamics of Ethyl Decanoate. *J. Chem. Eng. Data.* 54, 3026–3033.

Zhu, D., Gao, D., Zhang, H., Winter, B., Lücking, P., Sun, H., Guan, H., Chen, H., Shi, J., 2013. Geometric Structures of Associating Component Optimized toward Correlation and Prediction of Isobaric Vapor–Liquid Equilibria for Binary and Ternary Mixtures of Ethanal, Ethanol, and Ethanoic Acid. *J. Chem. Eng. Data* 58, 7–17.

ANNEXES

A1. PRESSION DE VAPEUR DES COMPOSES AJOUTES DANS SIMULIS THERMODYNAMICS®.

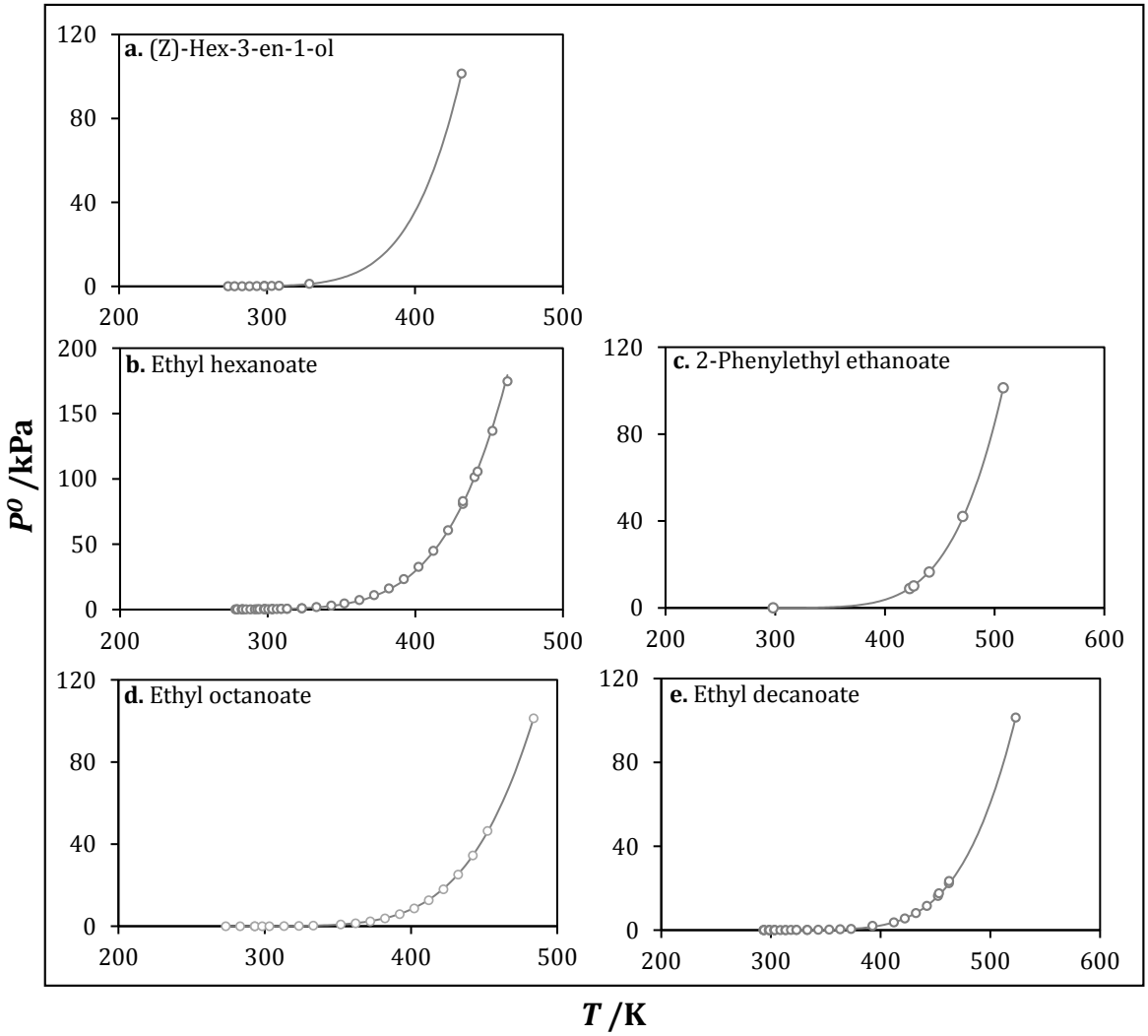

Figure A1-1. *Evolution of the vapour pressure with temperature for a. (Z)-Hex-3-en-1-ol; b. Ethyl hexanoate; c. 2-Phenylethyl ethanoate; d. Ethyl octanoate; e. Ethyl decanoate. (○) Experimental data. (——) Regression with the Riedel equation.*

Table A1-1. *Vapour pressure data for (Z)-hex-3-en-1-ol.*

T /K	P^O_{Exp}/kPa	Reference	*%AAD*	*2%*
			P^O_{calc} /kPa	$\%AD = \lvert P^O_{calc} - P^O_{Exp} \rvert / P^O_{Exp}$
273.7	0.02	Stejfa et al., 2015	0.02	1%
278.2	0.03	Stejfa et al., 2015	0.03	1%
283.2	0.04	Stejfa et al., 2015	0.04	1%
288.2	0.06	Stejfa et al., 2015	0.06	1%
293.2	0.09	Stejfa et al., 2015	0.09	1%
298.2	0.13	GESTIS Substance Database	0.14	12%
298.2	0.14	GESTIS Substance Database	0.14	1%
298.2	0.14	Stejfa et al., 2015	0.14	2%
303.2	0.21	Stejfa et al., 2015	0.21	2%
308.2	0.30	Stejfa et al., 2015	0.30	2%
328.7	1.20	GESTIS Substance Database	1.17	3%
431.5	101.3	GESTIS Substance Database, NIST Webbook	101.3	0%

Table A1-2. *Vapour pressure data for 2-phenylethyl ethanoate.*

T /K	P^O_{Exp}/kPa	Reference	*%AAE*	**1%**
			P^O_{calc} /kPa	$\%AD = \lvert P^O_{calc} - P^O_{Exp} \rvert / P^O_{Exp}$
298.2	0.01	GESTIS Substance Database	0.01	0%
422.6	8.85	Dreisbach & Shrader, 1949	9.05	2%
426.3	10.11	Dreisbach & Shrader, 1949	10.33	2%
440.4	16.50	Dreisbach & Shrader, 1949	16.70	1%
471.1	42.07	Dreisbach & Shrader, 1949	41.45	1%
507.9	101.3	Dreisbach & Shrader, 1949, NIST Webbook, GESTIS Substance Database	101.3	0%

Table A1-3. *Vapour pressure data for ethyl hexanoate.*

T /K	P^o_{Exp}/kPa	Reference	*%AAE*	5%
			P^o_{calc} /kPa	$\%AD = \lvert P^o_{calc} - P^o_{Exp} \rvert / P^o_{Exp}$
278.2	0.05	Covarrubias-Cervantes et.al, 2004	0.05	4%
279.4	0.05	Kozlovskiy et. al, 2015	0.05	2%
279.4	0.05	Verevkin & Heintz, 1999	0.05	4%
282.4	0.06	Verevkin & Heintz, 1999	0.06	2%
283.1	0.07	Benziane et. al, 2011	0.07	0%
283.2	0.07	Covarrubias-Cervantes et.al, 2004	0.07	5%
285.4	0.08	Verevkin & Heintz, 1999	0.08	2%
288.4	0.10	Verevkin & Heintz, 1999	0.10	1%
291.4	0.12	Verevkin & Heintz, 1999	0.12	0%
293.1	0.14	Benziane et. al, 2011	0.14	3%
294.4	0.15	Verevkin & Heintz, 1999	0.15	1%
297.4	0.19	Verevkin & Heintz, 1999	0.19	2%
298.2	0.22	GESTIS Substance Database	0.20	10%
298.2	0.20	Kozlovskiy et. al, 2015	0.20	0%
298.2	0.22	Covarrubias-Cervantes et.al, 2004	0.20	7%
300.4	0.24	Verevkin & Heintz, 1999	0.23	2%
303.0	0.29	Benziane et. al, 2011	0.28	5%
303.2	0.22	GESTIS Substance Database	0.28	26%
303.2	0.28	Verevkin & Heintz, 1999	0.28	1%
306.2	0.35	Verevkin & Heintz, 1999	0.34	3%
309.2	0.42	Kozlovskiy et. al, 2015	0.41	1%
309.2	0.43	Verevkin & Heintz, 1999	0.41	3%
313.2	0.43	GESTIS Substance Database	0.53	23%
313.2	0.56	Benziane et. al, 2011	0.53	6%
323.2	0.79	GESTIS Substance Database	0.96	21%
323.2	1.02	Benziane et. al, 2011	0.96	6%
333.1	1.78	Benziane et. al, 2011	1.66	7%
343.1	2.98	Benziane et. al, 2011	2.78	7%
352.0	4.55	Benziane et. al, 2011	4.26	6%
362.1	7.18	Benziane et. al, 2011	6.74	6%
372.1	10.93	Benziane et. al, 2011	10.32	6%
382.2	16.07	Benziane et. al, 2011	15.37	4%
392.2	23.19	Benziane et. al, 2011	22.40	3%
402.2	32.56	Benziane et. al, 2011	31.78	2%
412.2	44.90	Benziane et. al, 2011	44.26	1%
422.2	60.62	Benziane et. al, 2011	60.40	0%
432.3	80.76	Benziane et. al, 2011	81.26	1%
432.3	82.90	Kozlovskiy et. al, 2015	81.30	2%
440.2	101.3	ESTIS Substance Database, NIST Webbook	101.3	0%
442.3	105.57	Benziane et. al, 2011	107.27	2%
452.3	136.73	Benziane et. al, 2011	139.63	2%
462.4	174.60	Benziane et. al, 2011	179.33	3%

Table A1-4. *Vapour pressure data for ethyl octanoate.*

T /K	$P_{exp}°$ /kPa	Reference	*%AAE*	4%
			P^{O}_{calc} /kPa	$\%AD = \lvert P^{O}_{calc} - P^{O}_{Exp} \rvert / P^{O}_{Exp}$
273.3	0.00	Benziane et. al, 2011	0.00	13%
283.1	0.01	Benziane et. al, 2011	0.01	3%
293.1	0.02	Benziane et. al, 2011	0.02	1%
293.2	0.02	GESTIS Substance Database	0.02	21%
298.2	0.03	GESTIS Substance Database	0.02	19%
303.1	0.03	Benziane et. al, 2011	0.04	3%
313.2	0.08	Benziane et. al, 2011	0.08	2%
323.3	0.15	Benziane et. al, 2011	0.16	3%
333.2	0.32	GESTIS Substance Database	0.30	6%
351.9	0.87	Benziane et. al, 2011	0.89	3%
362.1	1.49	Benziane et. al, 2011	1.52	2%
372.1	2.43	Benziane et. al, 2011	2.48	2%
382.1	3.87	Benziane et. al, 2011	3.92	1%
392.2	5.90	Benziane et. al, 2011	6.01	2%
402.1	8.72	Benziane et. al, 2011	8.92	2%
412.1	12.67	Benziane et. al, 2011	12.92	2%
422.1	18.04	Benziane et. al, 2011	18.29	1%
432.2	25.22	Benziane et. al, 2011	25.40	1%
442.3	34.49	Benziane et. al, 2011	34.50	0%
452.3	46.42	Benziane et. al, 2011	45.98	1%
483.7	101.3	GESTIS Substance Database, NIST Webbook	101.3	0%

Table A1-5. *Vapour pressure data for ethyl decanoate.*

T /K	$P_{exp}°$ /kPa	Reference	*%AAE*	6%
			P^{O}_{calc}/kPa	$\%AD = \lvert P^{O}_{calc}-P^{O}_{Exp}\rvert/P^{O}_{Exp}$
293.2	0.00	GESTIS Substance Database	0.00	20%
293.8	0.00	Zaitsau et. al, 2009	0.00	1%
293.8	0.00	Kozlovskiy et. al, 2015	0.00	7%
298.2	0.00	GESTIS Substance Database	0.00	42%
298.7	0.00	Zaitsau et. al, 2009	0.00	3%
298.7	0.00	Zaitsau et. al, 2009	0.00	3%
303.1	0.00	Kozlovskiy et. al, 2015	0.00	9%
303.1	0.00	Benziane et. al, 2011	0.00	7%
303.7	0.00	Zaitsau et. al, 2009	0.00	6%
308.6	0.01	Zaitsau et. al, 2009	0.01	5%
313.2	0.01	Benziane et. al, 2011	0.01	4%
313.6	0.01	Zaitsau et. al, 2009	0.01	4%
318.3	0.02	Zaitsau et. al, 2009	0.02	1%
323.2	0.02	Zaitsau et. al, 2009	0.02	4%
323.4	0.02	Kozlovskiy et. al, 2015	0.02	10%
333.2	0.05	GESTIS Substance Database	0.05	4%
333.2	0.05	Benziane et. al, 2011	0.05	1%
343.2	0.10	Benziane et. al, 2011	0.10	2%
353.2	0.18	Benziane et. al, 2011	0.18	2%
363.1	0.33	Benziane et. al, 2011	0.34	2%
373.2	0.56	Kozlovskiy et. al, 2015	0.59	5%
392.7	2.00	GoodScents Company	1.58	21%
412.2	3.65	Benziane et. al, 2011	3.75	3%
422.1	5.47	Benziane et. al, 2011	5.60	2%
432.2	8.07	Benziane et. al, 2011	8.19	1%
442.2	11.55	Benziane et. al, 2011	11.64	1%
452.3	16.28	Benziane et. al, 2011	16.21	0%
453.2	17.50	Kozlovskiy et. al, 2015	16.67	5%
462.4	22.35	Benziane et. al, 2011	22.16	1%
462.4	23.40	Kozlovskiy et. al, 2015	22.18	5%
523.2	101.3	GESTIS Substance Database, NIST Webbook	101.3	0%

A2. CALCUL DES INCERTITUDES STANDARD DES VARIABLES D'EQUILIBRE

The combined standard uncertainty represents the estimated standard deviation of an indirect measurement and is calculated as the positive square root of the estimated variance u_c^2. The combined expanded uncertainty, U_c, is obtained by multiplying u_c by the selected coverage factor k.

A2.1. Mass compositions

Ethyl Lactate

Uncertainty associated with the mass measurements as well as the three replicates of sample injections during the chromatographic analysis:

$$u_c^2(z_{mEL})=\sum_{i=1}\left(\frac{\partial z_{mEL}}{\partial m_i}\right)^2 u^2(m_i)+\left(\frac{\partial z_{mEL}}{\partial R_{A_{EL\text{-}IS}}}\right)^2 u^2\left(R_{A_{EL\text{-}IS}}\right)$$

Relationship between mass composition, area ratio of Ethyl Lactate - internal standard peaks and reagents masses:

$$z_{mEL}=\left(\frac{R_{A_{EL\text{-}IS}}}{k_{Calibration}}\right)\left(\frac{m_{IS\text{-}SM_0}}{m_{SM\text{-}IS_0}}\frac{m_{SM\text{-}IS_f}}{m_{Sample}}\right)$$

Hence:

$$u_c^2(z_{mEL})=\left(\frac{R_{A_{EL\text{-}IS}}}{k_{Calibration}}\right)^2\left[\left(\frac{1}{m_{SM\text{-}IS_0}}\frac{m_{SM\text{-}IS_f}}{m_{Sample}}\right)^2 u^2(m_{IS\text{-}SM_0})+\left(\frac{m_{SM\text{-}IS_0}}{m_{SM\text{-}IS_0}^2}\frac{m_{SM\text{-}IS_f}}{m_{Sample}}\right)^2 u^2(m_{SM\text{-}IS_0})+\left(\frac{m_{IS\text{-}SM_0}}{m_{SM\text{-}IS_0}}\frac{1}{m_{Sample}}\right)^2 u^2(m_{SM\text{-}IS})\right]$$
$$+\left(\frac{m_{IS\text{-}SM_0}}{m_{SM\text{-}IS_0}}\frac{m_{SM\text{-}IS_f}}{m_{Sample}^2}\right)^2 \mathrm{u}^2(m_{Sample})+\left(\frac{1}{k_{Calibration}}\right)^2\left(\frac{m_{IE\text{-}SM_0}}{m_{SM\text{-}IE_0}}\frac{m_{SM\text{-}IE}}{m_{Sample}}\right)^2 u^2\left(R_{A_{EL\text{-}IS}}\right)$$

Here:

$$u(m_{IS\text{-}SM_0})=u(m_{SM\text{-}IS_f})=u(m_{Sample})=u(m_1)=0.00006\ \mathrm{g}$$
$$u(m_{SM\text{-}IS_0})=u(m_2)=0.006\ \mathrm{g}$$

Therefore:

$$u_c^2(z_{mEL})=\left(\frac{R_{A_{EL\text{-}IS}}}{k_{Calibration}}\right)^2\left[\left(\frac{1}{m_{SM\text{-}IS_0}}\frac{m_{SM\text{-}IS_f}}{m_{Sample}}\right)^2+\left(\frac{m_{IS\text{-}SM_0}}{m_{SM\text{-}IS_0}}\frac{1}{m_{Sample}}\right)^2+\left(\frac{m_{IS\text{-}SM_0}}{m_{SM\text{-}IS_0}}\frac{m_{SM\text{-}IS_f}}{m_{Sample}^2}\right)^2\right]u^2(m_1)$$
$$+\left(\frac{R_{A_{EL\text{-}IS}}}{k_{Calibration}}\right)^2\left(\frac{m_{SM\text{-}IS_0}}{m_{SM\text{-}IS_0}^2}\frac{m_{SM\text{-}IS_f}}{m_{Sample}}\right)^2 u^2(m_2)+\left(\frac{1}{k_{Calibration}}\right)^2\left(\frac{m_{IS\text{-}SM_0}}{m_{SM\text{-}IS_0}}\frac{m_{SM\text{-}IS_f}}{m_{Sample}}\right)^2 u^2\left(R_{A_{EL\text{-}IS}}\right)\ [\mathrm{A}$$

Ethanol

Uncertainty associated with the temperature and pressure measurements in the equilibrium experiments:

$$u_c^2(z_{mEt})=\left(\frac{\partial z_{mEt}}{\partial T}\right)^2 u^2(T)+\left(\frac{\partial z_{mEt}}{\partial P}\right)^2 u^2(P)=\left(\frac{\partial z_{mEt}}{\partial z_{Et}}\right)^2\left[\left(\frac{\partial z_{Et}}{\partial T}\right)^2 u^2(T)+\left(\frac{\partial z_{Et}}{\partial P}\right)^2 u^2(P)\right]$$

Relationship between composition, temperature and pressure given by the equilibrium relation for the binary system Ethanol - Water the, namely:

$$y_{Et}P=\gamma_{Et}(T,\boldsymbol{x})x_{Et}P_{Et}^0(T)$$

Where $\gamma_{Et}(T,\boldsymbol{x})$ is determined with the NRTL model and $P_{Et}^0(T)$ calculated by means of the Riedel equation.

Therefore, for the liquid phase:

$$x_{Et}=\frac{y_{Et}P}{\gamma_{Et}P_{Et}^0}$$

$$u_c^2(x_{mEt})=\left[\frac{MM_{Et}MM_W}{(MM_{Et}x_{Et}-MM_Wx_{Et}+MM_W)^2}\right]^2\left[\left(\frac{y_{Et}P\gamma_{Et}}{\gamma_{Et}^2P_{Et}^{02}}\right)^2\left(P_{Et}^{0L}\frac{\partial \ln\gamma_{Et}}{\partial T}+\frac{\partial P_{Et}^0}{\partial T}\right)^2u^2(T)+\left(\frac{y_{Et}}{\gamma_{Et}P_{Et}^0}\right)^2u^2(P)\right]$$

And for the vapor phase:

$$y_{Et}=\frac{x_{Et}\gamma_{Et}P_{Et}^0}{P}$$

$$u_c^2(y_{mEt})=\left[\frac{MM_{Et}MM_W}{(MM_{Et}y_{Et}-MM_Wy_{Et}+MM_W)^2}\right]^2\left[\left(\frac{x_{Et}\gamma_{Et}}{P}\right)^2\left(P_{Et}^0\frac{\partial \ln\gamma_{Et}}{\partial T}+\frac{\partial P_{Et}^0}{\partial T}\right)^2u^2(T)+\left(\frac{x_{Et}\gamma_{Et}P_{Et}^0}{P^2}\right)^2u^2(P)\right]$$

$\frac{\partial P_{Et}^0(T)}{\partial T}$ and $\frac{\partial \ln\gamma_{Et}(T,x)}{\partial T}$ are obtained analytically. The final expressions are:

For $P_{Et}^0(T)$:

$$\frac{\partial P_{Et}^0(T)}{\partial T}=P_{Et}^0(T)\left(-\frac{B}{T^2}+\frac{C}{T}+EDT^{E-1}\right)$$

For $ln\,\gamma_{Et}(T,\boldsymbol{x})$: The function differentiated is the simplified version of the NRTL model for a binary system, that is,

$$ln\,\gamma_{Et}(T,\boldsymbol{x})=x_W^2\left[\tau_{W\text{-}Et}\left(\frac{G_{W\text{-}Et}}{x_{Et}+x_WG_{W\text{-}Et}}\right)^2+\frac{\tau_{Et\text{-}W}G_{Et\text{-}W}}{(x_W+x_{Et}G_{Et\text{-}W})^2}\right]$$

Hence:

$$\frac{\partial \ln\gamma_{Et}(T,x)}{\partial T}=x_W^2\left[\left(\frac{G_{W\text{-}Et}}{x_{Et}+x_WG_{W\text{-}Et}}\right)^2\frac{\partial\tau_{W\text{-}Et}}{\partial T}+2\tau_{W\text{-}Et}\left(\frac{G_{W\text{-}Et}}{x_{Et}+x_WG_{W\text{-}Et}}\right)\left(\frac{x_{Et}}{(x_{Et}+x_WG_{W\text{-}Et})^2}\frac{\partial G_{W\text{-}Et}}{\partial T}\right)\right]$$
$$+x_W^2\left[\frac{\left(G_{Et\text{-}W}\frac{\partial\tau_{Et\text{-}W}}{\partial T}+\tau_{Et\text{-}W}\frac{\partial G_{Et\text{-}W}}{\partial T}\right)(x_W+x_{Et}G_{Et\text{-}W})^2-2\tau_{Et\text{-}W}x_{Et}G_{Et\text{-}W}(x_W+x_{Et}G_{Et\text{-}W})\frac{\partial G_{Et\text{-}W}}{\partial T}}{(x_W+x_{Et}G_{Et\text{-}W})^4}\right]$$

With:

$$\frac{\partial G_{Et\text{-}W}}{\partial T}=-c^0\exp(-c^0\tau_{Et\text{-}W})\frac{\partial\tau_{Et\text{-}W}}{\partial T}$$
$$\frac{\partial\tau_{Et\text{-}W}}{\partial T}=\frac{-R\left(A_{Et\text{-}W}^0+273.15A_{Et\text{-}W}^T\right)}{R^2T^2}$$
$$\frac{\partial G_{W\text{-}Et}}{\partial T}=-c^0\exp(-c^0\tau_{W\text{-}Et})\frac{\partial\tau_{W\text{-}Et}}{\partial T}$$
$$\frac{\partial\tau_{W\text{-}Et}}{\partial T}=\frac{-R\left(A_{W\text{-}Et}^0+273.15A_{W\text{-}Et}^T\right)}{R^2T^2}$$

Water

Propagation of the combined uncertainties of the mass fractions of Ethyl Lactate and Ethanol:

$$u_c^2(z_{mW})=\left(\frac{\partial z_{mW}}{\partial z_{mEL}}\right)^2u_c^2(z_{mEL})+\left(\frac{\partial z_{mW}}{\partial z_{mEt}}\right)^2u_c^2(z_{mEt})$$

Relationship between z_{mW}, z_{mEL} and z_{mEt}

$$z_{mW}=1-z_{mEL}-z_{mEt}$$

Therefore:

$$u_c^2(z_{mW})=u_c^2(z_{mEL})+u_c^2(z_{mEt})$$

A2.2. Mole compositions

Ethyl Lactate

Propagation of the standard uncertainties of the mass fractions of ethyl lactate, ethanol and water:

$$u_c^2(z_{EL})=\left(\frac{\partial z_{EL}}{\partial z_{mEL}}\right)^2u_c^2(z_{mEL})+\left(\frac{\partial z_{EL}}{\partial z_{mEt}}\right)^2u_c^2(z_{mEt})+\left(\frac{\partial z_{EL}}{\partial z_{mW}}\right)^2u_c^2(z_{mW})$$

Relationship between z_{EL}, z_{mEL}, z_{mEt} and z_{mW} given by:

$$z_{EL}=\frac{\frac{z_{mEL}}{MM_{EL}}}{\frac{z_{mEL}}{MM_{EL}}+\frac{z_{mEt}}{MM_{Et}}+\frac{z_{mW}}{MM_{W}}}=\frac{z_{mEL}MM_{EL}MM_{Et}MM_{W}}{z_{mEL}MM_{Et}MM_{W}+z_{mEt}MM_{EL}MM_{W}+z_{mW}MM_{EL}MM_{Et}}$$

Resulting expression:

$$\boldsymbol{u_c^2(z_{EL})=\frac{\left(MM_{EL}MM_{Et}MM_{W}(z_{mEt}MM_{EL}MM_{W}+z_{mW}MM_{EL}MM_{Et})\right)^2u_c^2(z_{mEL})+\left(z_{mEL}MM_{EL}{}^2MM_{Et}MM_{W}{}^2\right)^2u_c^2(z_{mEt})+\left(z_{mEL}MM_{EL}{}^2MM_{Et}{}^2MM_{W}\right)^2u_c^2(z_{mW})}{[(z_{mEL}MM_{Et}MM_{W}+z_{mEt}MM_{EL}MM_{W}+z_{mW}MM_{EL}MM_{Et})^2]^2}}$$

Ethanol

Analogous calculation to that for Ethyl Lactate:

$$u_c^2(z_{Et})=\left(\frac{\partial z_{Et}}{\partial z_{mEL}}\right)^2u_c^2(z_{mEL})+\left(\frac{\partial z_{Et}}{\partial z_{mEt}}\right)^2u_c^2(z_{mEt})+\left(\frac{\partial z_{Et}}{\partial z_{mW}}\right)^2u_c^2(z_{mW})$$

$$\boldsymbol{u_c^2(z_{EL})=\frac{\left(MM_{EL}MM_{Et}MM_{W}(z_{mEL}MM_{Et}MM_{W}+z_{mW}MM_{EL}MM_{Et})\right)^2u_c^2(z_{mEt})+\left(z_{mEt}MM_{EL}MM_{Et}{}^2MM_{W}{}^2\right)^2u_c^2(z_{mEL})+\left(z_{mEt}MM_{EL}{}^2MM_{Et}{}^2MM_{W}\right)^2u_c^2(z_{mW})}{[(z_{mEL}MM_{Et}MM_{W}+z_{mEt}MM_{EL}MM_{W}+z_{mW}MM_{EL}MM_{Et})^2]^2}}$$

Water

Analogous calculation to that for water mass fraction:

$$u_c^2(z_W)=\left(\frac{\partial z_W}{\partial z_{EL}}\right)^2u_c^2(z_{EL})+\left(\frac{\partial z_W}{\partial z_{Et}}\right)^2u_c^2(z_{Et})$$

$$u_c^2(z_W)=u_c^2(z_{EL})+u_c^2(z_{Et})$$

A2.3. Activity coefficient of ethyl lactate

$$\gamma_{EL}^{\infty}(T,\boldsymbol{x_s})=\frac{y_{EL}P}{x_{EL}P_{EL}^{O}(T)}$$

$$u_c^2(\gamma_{EL}^{\infty})=\left(\frac{\partial\gamma_{EL}^{\infty}}{\partial y_{EL}}\right)^2u_c^2(y_{EL})+\left(\frac{\partial\gamma_{EL}^{\infty}}{\partial x_{EL}}\right)^2u_c^2(x_{EL})+\left(\frac{\partial\gamma_{EL}^{\infty}}{\partial P_{EL}^{O}}\right)^2\left(\frac{\partial P_{EL}^{O}}{\partial T}\right)^2u^2(T)+\left(\frac{\partial\gamma_{EL}^{\infty}}{\partial P}\right)^2u^2(P)$$

$$\boldsymbol{u_c^2(\gamma_{EL}^{\infty})=\left(\frac{P}{x_{EL}P_{EL}^{0}}\right)^2u_c^2(y_{EL})+\left(\frac{y_{EL}P}{x_{EL}{}^2P_{EL}^{0}}\right)^2u_c^2(x_{EL})+\left(\frac{y_{EL}P}{x_{EL}P_{EL}^{0}{}^2}\right)^2\left[P_{Et}^{0}(T)\left(-\frac{B}{T^2}+\frac{C}{T}+EDT^{E-1}\right)\right]^2u^2(T)+\left(\frac{y_{EL}}{x_{EL}P_{EL}^{0}(T)}\right)^2u^2(P)}$$

A2.4. Henry constant of ethyl lactate

$$\mathcal{H}_{EL}(T,\boldsymbol{x_s})=\gamma_{EL}^{\infty}(T,\boldsymbol{x_s})P_{EL}^{O}(T)$$

$$u_c^2(\mathcal{H}_{EL})=\left(\frac{\partial\mathcal{H}_{EL}}{\partial\gamma_{EL}^{\infty}}\right)^2u_c^2(\gamma_{EL}^{\infty})+\left(\frac{\partial\mathcal{H}_{EL}}{\partial P_{EL}^{O}}\right)^2\left(\frac{\partial P_{EL}^{O}}{\partial T}\right)^2u^2(T)$$

$$\boldsymbol{u_c^2(\mathcal{H}_{EL})=P_{EL}^{0}{}^2u_c^2(\gamma_{EL}^{\infty})+\gamma_{EL}^{\infty}{}^2\left[P_{EL}^{0}\left(-\frac{B}{T^2}+\frac{C}{T}+EDT^{E-1}\right)\right]^2u^2(T)}$$

A2.5. Volatility of ethyl lactate

Absolute volatility

$$K_{EL}=\frac{y_{EL}}{x_{EL}}$$

$$u_c^2(K_{EL})=\left(\frac{\partial K_{EL}}{\partial y_{EL}}\right)^2u_c^2(y_{EL})+\left(\frac{\partial K_{EL}}{\partial x_{EL}}\right)^2u_c^2(x_{EL})$$

$$\boldsymbol{u_c^2(K_{EL})=\left(\frac{1}{x_{EL}}\right)^2u_c^2(y_{EL})+\left(\frac{y_{EL}}{x_{EL}{}^2}\right)^2u_c^2(x_{EL})}$$

Relative volatility with respect to ethanol

$$\alpha_{EL/Et}=\frac{K_{EL}}{K_{Et}}=\frac{y_{EL}/x_{EL}}{y_{Et}/x_{Et}}=\frac{y_{mEL}/x_{mEL}}{y_{mEt}/x_{mEt}}=\frac{y_{mEL}x_{mEt}}{y_{mEt}x_{mEL}}$$

$$u_c^2(\alpha_{EL/Et})=\left(\frac{\partial\alpha_{EL/Et}}{\partial y_{mEL}}\right)^2u_c^2(y_{mEL})+\left(\frac{\partial\alpha_{EL/Et}}{\partial x_{mEL}}\right)^2u_c^2(x_{mEL})+\left(\frac{\partial\alpha_{EL/Et}}{\partial y_{mEt}}\right)^2u_c^2(y_{mEt})+\left(\frac{\partial\alpha_{EL/Et}}{\partial x_{mEt}}\right)^2u_c^2(x_{mEt})$$

$$\boldsymbol{u_c^2(\alpha_{EL/Et})=\left(\frac{x_{mEt}}{y_{mEt}x_{mEL}}\right)^2u_c^2(y_{mEL})+\left(\frac{y_{mEL}x_{mEt}}{y_{mEt}x_{mEL}{}^2}\right)^2u_c^2(x_{mEL})+\left(\frac{y_{mEL}x_{mEt}}{y_{mEt}{}^2x_{mEL}}\right)^2u_c^2(y_{mEt})+\left(\frac{y_{mEL}}{y_{mEt}x_{mEL}}\right)^2u_c^2(x_{mEt})}$$

A3. EQUATIONS ET PARAMETRES DES MODELES UNIFAC ET COSMO-SAC

Table A3-1. *UNIFAC Activity coefficient equations.*

Model	Equations	Parameters
UNIFAC 1975	$$\ln \gamma_i (T,x) = \ln \gamma_i^C + \ln \gamma_i^R$$ Combinatorial contribution, $\ln \gamma_i^C$ Staverman-Guggenheim term $$\ln \gamma_i^C = \ln\frac{\varphi_i}{x_i} + \frac{Z}{2} q_i \ln\frac{\theta_i}{\varphi_i} + l_i - \frac{\varphi_i}{x_i}\sum_{j=1}^{n} x_j l_j$$ $$l_i = \frac{Z}{2}(r_i - q_i) - (r_i - 1)$$ $$\varphi_i = \frac{r_i x_i}{\sum_{j=1}^{n} r_j x_j}$$ $$\theta_i = \frac{q_i x_i}{\sum_{j=1}^{n} q_j x_j}$$ Definition of r_i and q_i for groups $$r_i = \sum_{k=1}^{ng} v_k^i R_k$$ $$q_i = \sum_{k=1}^{ng} v_k^i Q_k$$ Residual contribution, $\ln \gamma_i^R$ $$\ln \gamma_i^R = \sum_{k=1}^{ng} v_k^i \left(\ln \Gamma_k - \ln \Gamma_k^i\right)$$ $$\ln \Gamma_k = Q_k \left[1 - \ln\left(\sum_{m=1}^{ng} \Theta_m \tau_{m,k}\right) - \sum_{m=1}^{ng} \frac{\Theta_m \tau_{k,m}}{\sum_{p=1}^{ng} \Theta_p \tau_{p,m}}\right]$$ $$\Theta_m = \frac{Q_m X_m}{\sum_{p=1}^{ng} Q_p X_p}$$ $$X_m = \frac{\sum_{j=1}^{n} v_m^j x_j}{\sum_{j=1}^{n} x_j \left(\sum_{p=1}^{ng} v_n^j\right)}$$ $$\tau_{p,m} = exp\left[-\frac{A_{p,m}}{T}\right]$$	- Coordination number, Z=10 - Group volume parameter, R_k - Group surface parameter, Q_k - Binary group interaction parameters $A_{p,m}$, $A_{m,p}$

Continuation Table A3-1. *UNIFAC Activity coefficient equations.*

Model	Equations	Parameters
UNIFAC 1993	$ln\,\gamma_i\,(T,x) = ln\,\gamma_i^{C} + ln\,\gamma_i^{R}$ Combinatorial contribution, $\ln \gamma_i^{C}$ $ln\,\gamma_i^{C} = ln\frac{\omega_i}{x_i} + \left(1-\frac{\omega_i}{x_i}\right) + \frac{Zq_i}{2}\left(1-\frac{\phi_i}{\theta_i} + ln\frac{\phi_i}{\theta_i}\right)$ $\omega_i = \frac{x_i r_i^{3/4}}{\sum_{j=1}^{n} x_j r_J^{3/4}}$ *(5.14)* $r_i = \sum_{k=1}^{ng} v_k^i R_k$ *(5.6)* $q_i = \sum_{k=1}^{ng} v_k^i Q_k$ *(5.7)* Residual contribution, $\ln \gamma_i^{R}$ $ln\,\gamma_i^{R} = \sum_{k=1}^{ng} v_k^i \left(ln\,\Gamma_k - ln\,\Gamma_k^i\right)$ *(5.8)* $ln\,\Gamma_k = Q_k\left[1 - ln\left(\sum_{m=1}^{ng}\Theta_m\tau_{m,k}\right) - \sum_{m=1}^{ng}\frac{\Theta_m\tau_{k,m}}{\sum_{p=1}^{ng}\Theta_p\tau_{p,m}}\right]$ $\Theta_m = \frac{Q_m X_m}{\sum_{p=1}^{ng} Q_p X_p}$ $X_m = \frac{\sum_{j=1}^{n} v_m^j x_j}{\sum_{j=1}^{n} x_j \left(\sum_{p=1}^{ng} v_n^j\right)}$ $\tau_{p,m} = exp\left[-\frac{a_{p,m} + b_{p,m}T + c_{p,m}T^2}{T}\right]$	- Coordination number, $Z=10$ - Group volume parameter, R_k - Group surface parameter, Q_k - Binary group interaction parameters $a_{p,m}$, $a_{m,p}$, $b_{m,p}$, $b_{m,p}$, $c_{m,p}$, $c_{m,p}$

Tableau A3-2. *UNIFAC Volume and surface parameters for the groups present in the system ethyl lactate–ethanol–water. Information available in Simulis® thermodynamics package.*

Group	UNIFAC 1975		UNIFAC 1993	
	R_i	Q_i	R_i	Q_i
CH_2				
CH_3	0.9011	0.8480	0.6325	1.0608
CH_2	0.6744	0.5400	0.6325	0.7081
CH	0.4469	0.2280	0.6325	0.3554
OH				
OH(p)	1.0000	1.2000	1.2303	0.8927
OH(s)	1.0000	1.2000	1.0630	0.8663
H_2O				
H_2O	0.9200	1.4000	1.7334	2.4561
COO				
COO	1.3800	1.2000	1.6000	0.9000

Table A3-3. *UNIFAC binary interaction parameters for the groups present in the system ethyl lactate–ethanol–water. The values for subgroups CH_3, CH_2, CH and OH(p) (primary), OH(s) (secondary), belonging to a main group, CH_2 and OH respectively, are identical. Information available in Simulis® thermodynamics package.*

Main group i	Main group j	UNIFAC 1975			UNIFAC 1993				
		A_{ij}	A_{ji}	a_{ij}	a_{ji}	b_{ij}	b_{ji}	c_{ij}	c_{ji}
CH_2 (CH_3,CH_2,CH)	OH	9.8650×10^{2}	1.5640×10^{2}	2.7770×10^{3}	1.6060×10^{3}	-4.6740×10^{0}	-4.7460×10^{0}	1.5510×10^{-3}	9.1810×10^{-4}
	H_2O	1.3180×10^{3}	3.0000×10^{2}	1.3913×10^{3}	-1.7253×10^{1}	-3.6156×10^{0}	8.3890×10^{-1}	1.1440×10^{-3}	9.0210×10^{-4}
	COO	3.8710×10^{2}	5.2900×10^{2}	1.3120×10^{3}	-3.1460×10^{2}	-3.6430×10^{0}	1.2870×10^{0}	-	-
OH (OH(p), OH(s))	H_2O	3.5350×10^{2}	-2.2910×10^{2}	-8.0190×10^{2}	1.4600×10^{3}	3.8240×10^{0}	-8.6730×10^{0}	-7.5140×10^{-3}	1.6410×10^{-2}
	COO	1.9030×10^{2}	8.8630×10^{1}	4.0380×10^{2}	7.0340×10^{2}	-9.3460×10^{-1}	-1.3830×10^{0}	-	-
H_2O	COO	-1.9750×10^{2}	2.8440×10^{1}	6.7600×10^{2}	8.0840×10^{2}	-9.9090×10^{-1}	-2.9290×10^{0}	-	-

Table A3-4. *COSMO-SAC Activity coefficient equations.*

Model	Equations	Parameters
COSMO-SAC 2002	$ln\,\gamma_i(T,x) = ln\,\gamma_i^C + ln\,\gamma_i^R$ Combinatorial contribution, ln γ_i^C Staverman-Guggenheim term $ln\,\gamma_i^C = ln\frac{\phi_i}{x_i} + \frac{Z}{2}q_i\,ln\frac{\theta_i}{\phi_i} + l_i - \frac{\phi_i}{x_i}\sum_{j=1}^{n} x_j l_j$ $l_i = \frac{Z}{2}(r_i - q_i) - (r_i - 1)$ $\varphi_i = \frac{r_i x_i}{\sum_{j=1}^{n} r_j x_j}$ $\theta_i = \frac{q_i x_i}{\sum_{j=1}^{n} q_j x_j}$ $r_i = \frac{V_i}{r}$ $q_i = \frac{S_i}{q}$ Residual contribution, ln γ_i^R $ln\,\gamma_i^R = \sum_{\sigma_m} \frac{S_i}{a_{eff}} p_i(\sigma_m)\{ln[\Gamma_S(\sigma_m)] - ln[\Gamma_i(\sigma_m)]\}$ $ln\,\Gamma_L(\sigma_m) = -\,ln\left\{\sum_{\sigma_n} p_L(\sigma_n)\Gamma_i(\sigma_n)\,exp\left[\frac{-\Delta W(\sigma_m,\sigma_n)}{RT}\right]\right\}$ $\Delta W(\sigma_m,\sigma_n) = \frac{\alpha'}{2}(\sigma_m+\sigma_n)^2 + c_{hb}\,max[0,\sigma_{acc}-\sigma_{hb}]\,min[0,\sigma_{don}+\sigma_{hb}]$ $\sigma_{acc} = max[\sigma_m,\sigma_n]\,;\sigma_{don} = min[\sigma_m,\sigma_n]$ Calculation of sigma profiles $p_i(\sigma_m) = \frac{S_i(\sigma_m)}{S_i}$ $p_S(\sigma) = \frac{\sum_i x_i S_i p_i(\sigma)}{\sum_i x_i S_i}$ Averaging procedure of surface charges $\sigma_v = \frac{\sum_u \sigma_u^* \frac{r_u^2 r_{eff}^2}{r_u^2+r_{eff}^2} exp\left(-f_{decay}\frac{d_{uv}^2}{r_u^2+r_{eff}^2}\right)}{\sum_u \frac{r_u^2 r_{eff}^2}{r_u^2+r_{eff}^2} exp\left(-f_{decay}\frac{d_{uv}^2}{r_u^2+r_{eff}^2}\right)}$ $r_u = \left(\frac{a_u}{\pi}\right)^{1/2}$ $r_{eff} = \left(\frac{a_{eff}}{\pi}\right)^{1/2}$	- Coordination number, Z=10 - Molecular volume, V_i from quantum calculations - Molecular surface, A_i from quantum calculations - Sigma-profile, $p(\sigma_m)$ from quantum calculations - Standard volume, r = 6.669×10^{-2} nm^3 - Standard surface area, q = 7.953×10^{-1} nm^2 - Effective standard segment surface area, a_{eff} = 7.5×10^{-2} nm^2 - Misfit energy constant, α' = 1.646598 kcal·nm^4·e^{-2}·mol^{-1} - Hydrogen-bonding energy constant, c_{hb} = 8.558 kcal·nm^4·e^{-2}·mol^{-1} - Sigma-value cutoff for hydrogen-bonding interactions, σ_{hb} = 8.4×10^{-1} e.nm^{-2} - Empirical parameter used to balance the unit, f_{decay}=3.57
COSMO-SAC 2006	$ln\,\gamma_i(T,x) = ln\,\gamma_i^C + ln\,\gamma_i^R$ Combinatorial contribution, ln γ_i^C Same equations of the 2002 version Residual contribution, ln γ_i^R Same equations of the 2002 version Calculation of sigma profiles Same equations of the 2002 version Averaging procedure of surface charges $\sigma_v = \frac{\sum_u \sigma_u^* \frac{r_u^2 r_{av}^2}{r_u^2+r_{av}^2} exp\left(-\frac{d_{uv}^2}{r_u^2+r_{av}^2}\right)}{\sum_u \frac{r_u^2 r_{av}^2}{r_u^2+r_{av}^2} exp\left(-\frac{d_{uv}^2}{r_u^2+r_{av}^2}\right)}$	Same parameters of the 2002 version, except for: - Averaging segment radius, r_{av} = 8.1764×10^{-2} nm. - Misfit energy constant, α' = 9.03497×10^{-1} kcal·nm^4·e^{-2}·mol^{-1}.

Continuation table A3-4. *COSMO-SAC Activity coefficient equations.*

Model	Equations	Parameters
COSMO-SAC 2010	$\ln \gamma_i(T,x) = \ln \gamma_i^C + \ln \gamma_i^R$ Combinatorial contribution, $\ln \gamma_i^C$ Same equations of the 2002 version Residual contribution, $\ln \gamma_i^R$ $\ln \gamma_i^R = \frac{S_i}{a_{eff}} \sum_s^{nhb,hb} \sum_m p_i^s(\sigma_m^s)\{\ln[\Gamma_S^s(\sigma_m^s)] - \ln[\Gamma_i^s(\sigma_m^s)]\}$ $\ln \Gamma_L^s(\sigma_m^t) = -\ln\left\{\sum_s^{nhb,hb} \sum_{\sigma_n} p_i^t(\sigma_m^t) \exp\left[\frac{-\Delta W(\sigma_m^t,\sigma_m^s)}{kT}\right]\right\}$ $\Delta W(\sigma_m^t,\sigma_m^s) = c_{ES}(\sigma_m^t+\sigma_m^s)^2 - c_{hb}(\sigma_m^t,\sigma_m^s)(\sigma_m^t-\sigma_m^s)^2$ $c_{ES} = A_{ES} + \frac{B_{ES}}{T^2}$ $c_{hb}(\sigma_m^t,\sigma_m^s) = \begin{cases} C_{OH\text{-}OH} & If\ s=OH, t=OH,\ \sigma_m^t\sigma_m^s<0 \\ C_{OT\text{-}OT} & If\ s=OT, t=OT,\ \sigma_m^t\sigma_m^s<0 \\ C_{OH\text{-}OT} & If\ s=OH, t=OT,\ \sigma_m^t\sigma_m^s<0 \\ 0 & Otherwise \end{cases}$ Calculation of sigma profiles $p_i(\sigma) = p_i^{hb}(\sigma) + p_i^{nhb}(\sigma)$ Hydrogen bonding sigma-profile $p_i^{hb}(\sigma) = p_i^{OH}(\sigma) + p_i^{OT}(\sigma)$ $p_i^{OH}(\sigma) = \frac{A_i^{OH}(\sigma)}{A_i} P^{HB}(\sigma)$ $p_i^{OT}(\sigma) = \frac{A_i^{OT}(\sigma)}{A_i} P^{HB}(\sigma)$ Non-hydrogen bonding sigma-profile $p_i^{nhb}(\sigma) = \frac{A_i^{nhb}(\sigma)}{A_i} + \frac{A_i^{hb}(\sigma)\left[1-P^{HB}(\sigma)\right]}{A_i}$ $P^{HB}(\sigma) = 1 - \exp\left(\frac{\sigma^2}{2\sigma_0^2}\right)$ Averaging procedure of surface charges Same equations of the 2002 version,	Same parameters of the 2002 version, except for: - Effective surface area of a segment, a_{eff} = 7.25×10^{-2} nm^2 - Reference charge density, σ_0 = 7.0×10^{-1} e.nm^{-2} - Constants of the electrostatic interaction parameter, A_{ES} = 6.52569×10^{-1} kcal·nm^4·e^{-2}·mol^{-1}, B_{ES} = 1.4859×10^4 kcal·nm^4·e^{-2}·mol^{-1}·K^2 - Hydrogen-bonding interaction energies, $C_{OH\text{-}OH}$ = 4.01378×10^{-1} kcal·nm^4·e^{-2}·mol^{-1}, $C_{OT\text{-}OT}$ = 9.32310×10^{-2} kcal·nm^4·e^{-2}·mol^{-1} and $C_{OH\text{-}OT}$ = 3.01643×10^{-1} kcal·nm^4·e^{-2}·mol^{-1}
COSMO-SAC 2014	$\ln \gamma_i(T,x) = \ln \gamma_i^C + \ln \gamma_i^R + \ln \gamma_i^{dsp}$ Combinatorial contribution, $\ln \gamma_i^C$ Same equations of the 2002 version Residual contribution, $\ln \gamma_i^R$ Same equations of the 2010 version Dispersive contribution, $\ln \gamma_i^{dsp}$ $\ln \gamma_i^{dsp} = \sum_{j>i} \Lambda_{ij} \frac{\partial x_j x_i}{\partial x_i}$ $\Lambda_{ij} = w\left[\frac{1}{2}(\varepsilon_i+\varepsilon_j) - (\varepsilon_i\varepsilon_j)^{1/2}\right]$ $\varepsilon_i = \frac{1}{M_{atom}} \sum_{k=1}^{m} \varepsilon_k M_{ki}$ Calculation of sigma profiles Same equations of the 2010 version Averaging procedure of surface charges Same equations of the 2002 version	Same parameters of the 2010 version, except for: - Atomic dispersion parameter, ε_k, adjustable value (table A3-5) - Universal scaling factor, w = ±0.27027 according to the chemical nature of the system

Table A3-5. *Values of atomic dispersion parameters of the COSMO-SAC 2014 model. k_B is the Boltzmann constant (k_B = 1.38064852·10^{-23} J·K^{-1}).*

Atom type k	ε_k/k_B /K
C (sp^3)	1.157023×10^2
C (sp^2)	1.174650·10^2
C (sp)	6.606910×10^1
-O-	9.561840×10^1
=O	-1.105490×10^1
H (OH)	1.934770×10^1
H (NH)	1.411709×10^1
H (Water/COOH)	5.833010×10^1

université PARIS-SACLAY
ÉCOLE DOCTORALE
Agriculture, alimentation, biologie, environnement, santé (ABIES)

Titre : Modélisation des équilibres entre phases et simulation de la distillation des eaux-de-vie en vue d'une meilleure compréhension du comportement des composés volatils d'arôme.

Mots clefs : Distillation des eaux-de-vie, composés volatils d'arôme, simulation, équilibres entre phases, identification de modèle, réconciliation de données.

Résumé : La qualité des eaux-de-vie est un paramètre associé à la composition en composés volatils d'arôme. Cette composition résulte de la combinaison de différents facteurs dont la nature et le traitement des matières premières, mais surtout des transformations ayant lieu lors des phases de fermentation, distillation et, dans la plupart de cas, vieillissement.

La distillation est une opération de séparation pratiquée depuis des millénaires, avec une technologie assez mature. Cependant, dans le domaine des eaux-de-vie, elle s'appuie essentiellement sur des connaissances empiriques. L'objectif de ce doctorat fut de contribuer à une meilleure compréhension du comportement des composés volatils d'arôme au cours de différents modes de distillation et de fournir des bases scientifiques à la conduite des unités par le biais de modules de simulation. L'attention a été portée sur la distillation d'Armagnac et de Calvados dans des colonnes multiétagées en régime stationnaire.

Les modules de simulation ont été construits avec le logiciel ProSimPlus®. La première partie des travaux a été consacrée à l'acquisition de données d'équilibre liquide-vapeur des composés volatils d'arôme en milieu hydroalcoolique pour l'identification du modèle NRTL, en suivant trois approches complémentaires : recherche dans la littérature, détermination expérimentale et prédiction théorique avec les modèles UNIFAC et COSMO. Grâce à la connaissance acquise sur les volatilités relatives par rapport à l'éthanol et à l'eau, les composés volatils d'arôme ont pu être classés en trois groupes : composés légers, composés intermédiaires et composés lourds. La deuxième partie des travaux a porté sur la construction et la validation des modules de simulation, après réconciliation des données issues de la caractérisation expérimentale des unités de distillation. Cette investigation démontre que la simulation est un outil d'ingénierie performant dans le domaine des eaux-de-vie. Les résultats de la simulation ont permis d'affiner la classification des composés intermédiaires en trois catégories supplémentaires selon leur profil de concentration dans la colonne et leur taux de récupération dans le distillat. Enfin, cet outil a mis en évidence que certains paramètres opératoires, notamment l'augmentation de la teneur en éthanol du distillat ainsi que l'extraction de queues, favorisent la séparation préférentielle de certaines espèces de volatilité faible ou intermédiaire par rapport à l'éthanol.

Title: Modeling of phase equilibria and simulation of spirits distillation for a better understanding of volatile aroma compounds behavior.

Keywords: Spirits distillation, volatile aroma compound, simulation, phase equilibria, model identification, data reconciliation.

Abstract: The quality of spirits is a parameter related to the composition of volatile aroma compounds. This composition results from the combined production process of raw material extraction, subsequent fermentation, distillation and, in many cases, ageing.

Distillation is a very old and the most important industrial separation technology. However, in spirits production, this operation relies essentially on empirical knowledge. The aim of this PhD was to contribute to a better understanding of the volatile aroma compounds behaviour in spirits distillation and to provide a scientific basis for the process through computer simulation. The study was focused on Armagnac and Calvados production by continuous multistage distillation.

The simulation modules were built using the software ProSimPlus®. The first part of this research was dedicated to the acquisition of vapor-liquid equilibrium data of the volatile aroma compounds in ethanol-water solutions, in order to estimate the binary interaction parameters of the NRTL model.

Three complementary approaches of data acquisition were used: literature compilation, experimental measurements and predictions with UNIFAC and COSMO models.

According to their relative volatilities with respect to ethanol and water, the volatile aroma compounds can be classified in three groups: light compounds, intermediary compounds and heavy compounds. The second part of this research dealt with the creation and validation of simulation modules, by using reconciled experimental data from the distillation units. The results prove that simulation is a powerful tool in spirits distillation. The simulation data enables a more precise classification of the intermediary compounds in three categories, by considering their composition profiles in the distillation column and their recovery ratios from feed to distillate. Finally, the analysis of some operating parameters, including ethanol concentration in the distillate as well as tails extractions, demonstrates that the distillate composition can be modified by virtue of a selective separation of intermediary and heavy compounds with respect to ethanol.

Université Paris-Saclay
Espace Technologique / Immeuble Discovery
Route de l'Orme aux Merisiers RD 128 / 91190 Saint-Aubin, France